UNIVERSIDAD DE GRANADA
PROGRAMA DE DOCTORADO DE BIOMEDICINA REGENERATIVA

INSTITUTO DE PARASITOLOGÍA Y BIOMEDICINA "LÓPEZ-NEYRA", CSIC

Analysis of LRRK2 towards understanding the pathogenic mechanisms underlying Parkinson´s disease: deregulated autophagy and endocytosis

Patricia María Gómez Suaga

Tesis doctoral

2014

Editor: Universidad de Granada. Tesis Doctorales
Autora: Patricia María Gómez Suaga
ISBN: 978-84-9163-126-2
URI: http://hdl.handle.net/10481/45093

La doctoranda P atricia Marí a G ómez Suaga y la dir ectora de la tesis Sabine Hilfiker gar antizamos, al firm ar esta tesis doct oral, que el tr abajo ha sido realizado por el doctorando ba jo la dir ección de los dir ectores de la tes is y ha sta donde nuestro c onocimiento alc anza, en la realización del tr abajo, se h an respetado los der echos de otros aut ores a ser ci tados, cuand o se ha n utiliz ado sus resultados o publicaciones.

Granada, 14 de Marzo de 2014

Director/es de la Tesis Doctorando

Fdo.: Fdo.:

Sabine Nicole Navarro Hilfiker Patricia María Gómez Suaga

ACKNOWLEDGEMENTS/AGRADECIMIENTOS

My sincere thanks to Dr Sabine Hilfiker for giving me the opportunity to work in her lab. I am very grateful for your constant encouragement, patience and helping me through this time. I have learnt many things from you, for example, how to really enjoy doing science without ever losing the enthusiasm!

Many thanks to Dr.Philip Woodman and Dr.Francesco Cecconi, for allowing me to spend some months in their respective labs. I really had good experiences in Manchester and Rome, thank you both for your kindness and support. I specially thank Phil for being my referee and helping me in the next step in my career in London.

A mis amig@s, mis chaperonas, por los buenos ratos que hemos compartido durante esta tesis y los que vendrán (¡os espero en Londres!). A Mariascen y Belén, gracias por vuestra amistad, comprensión y cariño todos estos años de compañeras de pasillo. A Jaime, Elo, Jose, Fati, Marisa, Laura, Valen, Almu, … gracias!

Gracias a mis compañeras del 114. A Berta, porque tu amistad y apoyo fue decisivo, sin ti todo hubiera sido aún más difícil. A Mar y a Marian, gracias por vuestro optimismo contagioso, habéis sido mi energía a pesar de las veces que os mandé a callar durante la escritura de esta tesis, (especialmente). A Ele, Belén, Jesús y Pilar (la heredera), gracias por vuestro compañerismo y buenos ratos.

Thanks to my mates in Manchester, especially Ling, I have fond good memories of the “snow day”, thanks! Thanks also to my mates in Rome, especially July and Meysam, I was lucky to meet you both. Thanks for your help inside the lab and also visiting the beautiful Rome, it was a wonderful experience.

Gracias a mis tíos y tías, Miguel, Carmen, Diego, Antonia, Manoli, Manolín, Mercedes, Paco, Viqui, Pili y Javi, también gracias por vuestro espíritu de sacrificio y vuestra generosidad, sois un modelo a seguir, (sobre todo ellas, que son unas guerreras!). También a mis ti@s “políticos”, que aunque no os mencione de forma individualizada, me acuerdo mucho de vosotros.

A mis primos, primas (que son mis hermanas), (y al que inventó el wasap), por hacerme sentir tan cerca y acompañada de vosotras, a pesar de la distancia, durante todos estos años.

Gracias Manuel, por tu ayuda, por escucharme, por tu paciencia, por tu generosidad. Tu amor me hace feliz cada día.

Finalmente, quiero agradecer y co-dedicar este trabajo a mis padres, Juan y Angélica. Por vuestro cariño, confianza, entereza, esfuerzo, ejemplo, amor y sobre todo buenos consejos (y buenos genes) para poder dedicarme a aquello que me apasiona. Sin vuestro apoyo esta tesis no se habría realizado. ¡¡Gracias!!

Gracias a los donantes que generosamente ceden sus órganos o células para investigación.

Gracias a LRRK2, porque sus interrogantes han sido un aliciente diario.

Quiero dedicar esta tesis a mis abuelos:

A Manuela Oliva Marín y Manuel Suaga González
A María Lucía García García y a Francisco Gómez López

Gracias por vuestro amor.

I. RESUMEN/SUMMARY

Resumen

La Enfermedad de Parkinson (EP) se presenta de forma esporádica (idiopática) en la mayoría de los pacientes. Sin embargo, en los casos en que la enfermedad está determinada genéticamente, la identificación y el estudio de las mutaciones responsables proporciona una valiosa información sobre los mecanismos moleculares implicados en la muerte neuronal.

Se ha descrito la asociación de EP, tanto familiar como esporádica, con mutaciones en el gen que codifica LRRK2 (leucine-rich repeat kinase 2). LRRK2 es una proteína que contiene varios dominios, entre los que se encuentran los dominios quinasa y GTPasa, donde suelen aparecer mutaciones patogénicas. Existe una clara correlación entre el grado de actividad catalítica de LRRK2 y su citotoxicidad; sin embargo, los efectos de LRRK2 sobre los procesos celulares tempranos que en última instancia causan la muerte celular aún no han sido analizados en profundidad. Aunque se ha descrito tanto *in vitro* como *in vivo* que LRRK2 está involucrada en el tráfico endosomal y autofágico, los mecanismos exactos en los que participa aún se desconocen.

Esta tesis analiza los mecanismos patogénicos de la EP en los que está implicada LRRK2, haciendo especial énfasis en los procesos de endocitosis y autofagia. En primer lugar, hemos descrito que mutaciones patogénicas en LRRK2 causan un bloqueo del flujo autofágico a través de una ruta que implica canales sensibles a NAADP (nicotinic acid adenine dinucleotide phosphate) localizados sobre estructuras endosomales tardías y lisosomas. Asimismo, observamos que estas mutaciones provocan un incremento parcial del pH lisosomal, así como una disminución de la supervivencia celular en la presencia de estrés debido a agregación proteíca.

Puesto que el lisosoma es la estructura final para las rutas de autofagia y endocitosis, se estudió el efecto de las mutaciones patogénicas en LRRK2 sobre la endocitosis. En este trabajo demostramos que mutaciones patogénicas en LRRK2 producen deficiencias, tanto en eventos tempranos como tardíos, en la endocitosis mediada por receptor. Este déficit provoca un retraso en el tráfico del receptor a nivel del endosoma tardío y, como consecuencia, su acumulación en estructuras anormalmente alargadas.

Rab7 es una GTPasa pequeña implicada en varios eventos del tráfico endosomal, tales como el tráfico endosoma tardío-lisosoma y el tráfico retrómero entre endosoma tardío y la cara trans del aparato de Golgi. Los efectos provocados por mutaciones

patogénicas en LRRK2 sobre el tráfico del receptor pudieron ser revertidos por la sobreexpresión de la forma constitutivamente activa de Rab7 o Rab7L1, así como por proteínas que interaccionan con Rab7, como dynamin2/CIN85. Estas proteínas se localizan en endosomas tardíos y son cruciales en la regulación de la degradación de receptores de membrana.

Nuestros resultados demuestran además que la expresión de mutaciones patogénicas en LRRK2 está asociada a un descenso de la actividad de Rab7.

En definitiva, el presente estudio pone de manifiesto la importante contribución de mutaciones patogénicas en LRRK2 en la alteración de varios mecanismos regulatorios de tráfico endo-lisosomal, dando luz sobre los procesos celulares tempranos implicados en la patogénesis de la EP.

Although the majority of PD cases are idiopathic, the identification of disease-causing mutations helps in our understanding of the molecular mechanisms involved in neuronal demise. Mutations in LRRK2 (leucine-rich repeat kinase 2) are found associated with both sporadic and familial Parkinson´s disease (PD). LRRK2 is a multidomain protein characterised by kinase and GTPase activities, with pathogenic mutations localized to both catalytic domains. There is a significant body of evidence correlating altered catalytic activity with cytotoxicity. However, early cellular LRRK2-mediated events which eventually lead to cellular demise remain poorly understood. LRRK2 has been implicated in autophagic and endosomal trafficking pathways *in vitro* and *in vivo*, even though the mechanism(s) remain unclear.

This thesis describes work towards addressing how pathogenic LRRK2 may cause cellular dysfunction linked to PD pathogenesis, with emphasis on autophagy and endosomal trafficking deficits. First, mutant LRRK2 was found to cause a block in autophagic flux through a pathway involving NAADP (nicotinic acid adenine dinucleotide phosphate)-sensitive channels in acidic late endosomal/lysosomal structures. Pathogenic LRRK2 was found to cause a partial increase in lysosomal pH, and decreased cell survival in the presence of protein aggregation-induced stress.

Since autophagy and endocytosis share late endosomes/lysosomes as common end-points, the effect of mutant LRRK2 on endocytosis was evaluated. Pathogenic LRRK2 was found to cause deficits in both early and late events of receptor-mediated endocytosis, including a delay in receptor trafficking out of late endosomes, which become aberrantly elongated.

Rab7 is a small GTPase involved in various endosomal trafficking processes, including late endosomal-lysosomal trafficking and retromer-mediated trafficking between late endosomes and the trans-Golgi network. The effects on receptor trafficking could be rescued when overexpressing constitutively active Rab7 or Rab7L1, as well as the Rab7-interacting proteins dynamin2/CIN85, which localize to late endosomes and regulate degradative receptor trafficking. Pathogenic LRRK2 expression was associated with a decrease in Rab7 activity.

Alltogether, the present results highlight an important role for pathogenic LRRK2 in deregulating several endolysosomal membrane trafficking events, which may underlie early cellular pathogenesis in PD.

II. ABBREVIATIONS

AMP- adenosine monophosphate

AMPK- adenosine monophosphate-activated protein kinase

BAC- bacterial artificial chromosome

CaMKK- calcium/calmodulin-dependent protein kinase kinase

CIN85- cbl-interacting protein of 85 kDa

CMA- chaperone-mediated autophagy

COR- C-terminal of ROC

DA- Dopamindergic

ER- endoplasmic reticulum

EGFR- epidermal growth factor receptor

GAP- GTPase-activating protein

GDP- guanosine diphosphate

GEF- guanine nucleotide exchange factor

GST- glutatione S-transferase

GTP- Guanosine-triphosphate

IP3- inositol 1,4,5-trisphosphate

IP3R- inositol 1,4,5-trisphosphate receptor

MAPK- Mitogen-activated protein kinase

mTOR- The mammalian target of rapamycin

LN- Lewy neurite

LAMP2- Lysosomal-associated membrane protein 2

LB- lewy body

LRRK2- Leucine-rich repeat kinase 2

LTR- LysoTracker Red DND99

PBS- Phosphate buffered saline

PCR- Polymerase chain reaction

PD- Parkinson's disease

ROC- Ras of complex

ROS- Reactive oxygen species

SDS-PAGE- Sodium dodecyl sulfate–polyacrylamide gel electrophoresis

TGN- trans-Golgi netword

ULK- UNC-51-like kinase

Wt -Wild-type

III. INTRODUCTION

1. PARKINSON'S DISEASE

The British physician James Parkinson (1755-1824) first described the disease in 1817 in his publication "An Essay on the Shaking Palsy". Parkinson's disease (PD) (OMIM 168600) is a progressive and chronic disorder of the central nervous system that mainly affects control of voluntary movement [1]. It is the second most common neurodegenerative disease. The prevalence of PD is increasing from 1 % at the age of 65 to 5 % by the age of 85, affecting up to 10 million people worldwide according to the World Health Organization [2]. The most prominent risk factor in PD is age [3], and due to the increase in life expectancy, the number of affected individuals in industrialized countries is estimated to double by 2030 [4].

1.1 Clinical symptoms

Four motor symptoms are considered cardinal in PD: tremor (involuntary shaking), rigidity (increased resistance to passive movement), bradykinesia (slowness of movement), and postural instability [5]. Tremor is characterized by shaking of hands, arms, legs, jaw and face, and represents the most well-known symptom. Rigidity is caused by increased muscle tone and muscle contraction, and may be associated with joint pain, being a frequent early manifestation of the disease. Bradykinesia, as well as akinesia (difficulty at initiating movement) and hypokinesia (movement amplitude reduction), are manifested as a variety of symptoms, including micrographia (decreased size of handwriting), hypomimia (paucity of normal facial expression), hypophonia (decreased voice volume), and decreased stride length during walking.

Motor symptoms occur along with non-motoric symptoms, such as cognition abnormalities and neuropsychiatric problems (including mood and behavioral alterations). Some of the earliest changes in PD include olfactory dysfunction, cardiac sympathetic denervation and sleep difficulties [6]. PD progression has been shown to occur in distinct stages, and is quantified in stages according to the restrictive effects that are placed along a patient's life [7]. It has been estimated that disease progression takes around 14 years from initial onset to reach a wheelchair-bound state [2, 8, 9].

1.2 Pathology

PD is characterized by the progressive degeneration of dopaminergic (DA) neurons in the *pars compacta* of the *substantia nigra* (SNpc), together with the presence of intraneuronal inclusions called Lewy bodies (LBs) and abnormal dystrophic neuronal processes called Lewy neurites (LN) in surviving neurons [10]. Late in the disease process, LB pathology is prominent throughout the brain stem and also in cortical areas. Whilst it is generally considered that cell death in PD is rather specific to DA neurons, loss of other types of neurons can be observed as well. For example, cell loss in the *locus coeruleus* (noradrenergic system), the dorsal motor nuclei of the vagus and nucleus basalis of Meynert (cholinergic system), raphe nuclei (serotonergic system) and some other catecholaminergic brain stem structures, including the ventrotegmental area, have been reported [7, 11]. This has important implications for our mechanistic understanding of cell death associated with PD (see below).

In the SNpc of PD patients, as DA neurons containing the pigment neuromelanin die, macroscopic changes are visible in the form of depigmentation [12], (see figure 1). The SNpc contains neurons involved in the nigrostriatal pathway, a descending pathway that is afferent to the striatum and constitutes the main input to the basal ganglia. Loss of these neurons causes a depletion of dopamine in the striatum, and the lack of DA input into the striatum explains most of the motor symptoms. The onset of clinical motor symptoms occur when 60-80 % of DA neurons have died, attesting to the plasticity and possible compensatory mechanisms of this complex circuitry [13][14].

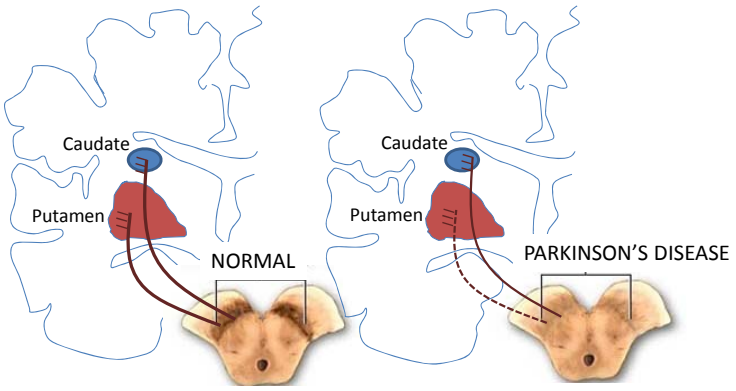

Figure 1 Schematic representation of the normal and disease nigrostriatal pathway
DA neurons project from the SNpc (where the cell bodies are located) to the caudate nucleus and putamen (collectively called the striatum). In PD there is a loss of DA neurons in the SNpc, (thereby depigmentation) and consequently a depletion of dopamine in the striatum. Figure adapted from "Substantia Nigra and Parkinson's Disease." A.D.A.M. Editorial Team.

As mentioned above, apart from DA cell loss, LBs and LN are observed in surviving neurons in all PD-affected brain regions. They are comprised of α-synuclein and a variety of ubiquitinated proteins, implicating α-synuclein and abnormal protein ubiquitylation/degradation in the mechanism underlying disease (see below). LB pathology is characteristic for PD, even though it can be observed in select other disease states such as dementia with LBs (DLB). Conversely, some autosomal recessive and autosomal dominant forms of PD may not present with LBs [15, 16]. Whilst LBs have been proposed to be toxic to neurons by interfering with normal cellular processes, the latter observation indicates that they may not be causal to cell death, but rather protect neurons by sequestering harmful protein aggregates [13].

1.3 Current treatment options

There is no cure for PD, and treatment is directed towards alleviating some of the symptoms. Treatment involves dopamine replacement strategies, which include levodopa (the precursor of dopamine) or dopamine receptor agonists. Inhibitors of monoamine oxidase B which metabolizes dopamine in the brain, and catechol O-methyltransferase, which breaks down levodopa, are used as well.

Despite the fact that the effect of levodopa is robust and currently the most effective form of oral symptomatic treatment for motor symptoms, prolonged treatment has been associated with the development of motor fluctuations and the occurrence of levodopa-induced dyskinesias, thereby increasing involuntary movements. Even though levodopa has dramatically improved the quality of life for PD patients, most patients suffer considerable levodopa-associated motor disabilities, and treatment has to be halted several years later [14]. Dopamine receptor agonists, which stimulate presynaptic and postsynaptic dopamine receptors, can be used as an adjunct therapy in advanced stages of PD. Also, several surgical procedures exist such as deep brain stimulation which helps in the management of the motor symptoms [15].

Currently, there are no proven neuroprotective or disease-modifying treatments for PD. Slowing the rate of loss of nigral DA neurons would improve the quality of life for PD patients. However, this requires considerable knowledge about disease mechanism(s), approaches able to modify disease course, and the existence of biomarkers able to predict disease onset. Thus, to develop neuroprotective therapies, a

detailed understanding of the key molecular events that provoke neurodegeneration is imperative.

1.4 Etiology

The exact pathological mechanisms underlying PD remain largely unclear, with most cases (called sporadic or idiopathic cases) having no apparent familial heritage nor relation to a defined environmental cause. Importantly, the first evidence for environmental causes underlying the disease was made in 1983, when heroin users came to the clinic with irreversible PD symptoms, which subsequently were found to be due to 1-methyl-4-phenyl-1,2,3,6-tetrahydropyridine (MPTP), a contaminant in the synthetic heroin preparations they had used [16]. Further studies over the years also identified additional toxic compounds such as a herbicide (paraquat) and an insecticide (rotenone). All three compounds induce DA degeneration by inhibiting respiratory chain complex I activity of mitochondria [17], and have led to the proposal that oxidative stress and mitochondrial dysfunction may be key to causing the disease, (see also below). Apart from environmental toxins, aging constitutes the most relevant risk factor for PD, and it has become clear that a combination between environmental and genetic factors influence PD development.

Familial PD is due to mutations in a set of genes, some of which remain to be identified (see Table 1). The discovery of such monogenic forms has significantly advanced our understanding of the molecular mechanisms involved in PD, as it allows for the generation of cellular and animal models carrying the mutant gene. This permits to define pathological pathways and provides definable targets for therapeutic strategies.

Mutations in five genes have been unequivocally shown to cause familial parkinsonism with two of them (*α-SYNUCLEIN* and the leucine-rich repeat kinase 2 (*LRRK2))* causing autosomal-dominant PD, and the other three (*PARKIN, PINK1* and *DJ-1*) causing autosomal-recessive forms of the disease. Mutations in various other genes are likely causing the disease as well, even though this is difficult to prove at times due to the infrequent nature of the mutation. For example, genetic studies have revealed genes such as Ubiquitin C-terminal esterase L1 (*UCHL1*) [18], Growth-factor-receptor-bound protein 10-interanting GYF protein 2 (*GIGYF2*), Vacuolar protein sorting 35 (*VPS35*), Nuclear receptor subfamily 4 (*NR4A2*), synphilin 1, or Omi/HtrA2, a calcium-independent phospholipase A2 (*PLA2G6*) [19].

PARK loci	Gene	Chromosomic location	Inheritance
PARK1/ PARK4	SNCA	4q21	Dominant, Rarely sporadic
PARK2	PARKIN	6q25-q27	Recessive, sporadic
PARK6	PINK1	1p35-p36	Recessive
PARK7	DJ-1	1p36	Recessive
PARK8	LRRK2	12q12	Dominant, sporadic

TABLE 1 Loci involved in genetic PD, chromosomic location, gene name and inheritance.

Indeed, recent genomic research using genome-wide association studies (GWAS) (examining many common genetic variants in different individuals to see association with PD) has revealed the complexity of PD genetics. GWAS studies have changed the PD field generating a new hypothesis whereby genetic variants with individual effects which are not strong enough to give rise to Mendelian PD may constitute high-risk loci for PD, having a direct role in disease etiology. These findings have made it clear that there is a more prominent genetic component to the disease than previously thought [20]. Thus, some genes contribute to both familial and sporadic disease mechanisms, causing inherited PD, and contributing to the risk of sporadic PD, such as for example the G2385R and R1628P variants in the LRRK2 gene [21] as well as SNP variations in *SNCA*. Another case is the Gaucher's disease-associated β-Glucocerebrosidase (*GBA)* gene, the most common PD risk factor. Loss of one allele of *GBA* increases risk of PD about 5-fold [22]. In addition, mutations in the same gene can be involved both in familial PD and can represent risk factors for sporadic PD, providing a clue as to possible shared mechanisms [23].

Other variations which are considered risk factors have been described in other genes, as the N-acetyltransferase 2 gene (*NAT2)*, inducible NO synthase 2 (*INOS2A)*, Cyclin G-associated kinase (*GAK*) and *HLA-DRA* genes [24, 25]. Interestingly,

polymorphic variations in the microtubule associated protein tau gene (*MAPT*) [26] and in the *APOE* gene [27], two Alzheimer's disease-related genes, have been related to PD. Specifically variations in the *MAPT* gene have been proposed to be significantly associated with age of PD disease onset with mutations in LRRK2 [28], linking both neurodegenerative diseases genetically. Interestingly, several GWAS studies have reported variations in several PARK-designated genes such as the PARK16 locus, containing the *RAB7L1* gene (a retromer-linked gene as further explained below) associated with risk for PD in different populations [28].

1.4.1 Autosomal dominant forms of PD

α- Synuclein

In 1997, a mutation in the *α-SYNUCLEIN* gene was identified to be responsible for autosomal dominantly-inherited Parkinsonism [29]. This gene was the first one to be identified as a causative factor for PD; however, mutations in this gene are a very rare cause of the disease [30].

Point mutations and genomic multiplications of the complete gene have been linked to familial PD and there is a direct relation between gene dosage and disease age-of-onset and phenotypic severity and disease progression [31]. In addition, genetic variability at the *α-SYNUCLEIN* locus contributes to the etiology of sporadic PD[32]. α-Synuclein is a 140 aminoacid lipid-binding protein which is abundantly expressed in the mammalian brain and comprises a major component of LBs, suggesting some mechanistic link to the disease [33].

α-Synuclein aggregation is preceded by its oligomerization and oligomers undergo transition to a fibrilar state which is toxic [34]. However, aggregates have proposed to not necessarily lead to cell death, possibly representing a protective mechanism [35]. Post-translational modifications such as phosphorylation and nitration of α-synuclein result in increased oligomerization and eventual accumulation of the protein as the major insoluble fibrillar component which can subsequently cause the degeneration of DA neurons [36]. Impaired clearance of α-Synuclein may also be responsible for its accumulation. Although proteasomes degrade α-Synuclein, the lysosome is the major site of degradation accessed through multiple routes, such as the endolysosomal pathway, macroautophagy and chaperone-mediated autophagy (CMA).

Interestingly, clearance via CMA is modulated by various factors, including LRRK2 (see below)[37].

LRRK2

In 2004, two independent groups identified mutations in the LRRK2 gene which co-segregated with PD in several PARK8-linked pedigrees [38, 39]. The LRRK2 gene is located on human chromosome 12 (12p11.2-q13.1) and has 51 exons, encoding for a large protein of 286 kDa. Autosomal-dominant mutations in LRRK2 are the most common genetic cause of late-onset PD. Approximately 5-8 % of European individuals with a first-degree relative with PD carry mutations in LRRK2 [40].

Importantly, variations in *LRRK2* increase PD risk, indicating that LRRK2 is an important player for both genetic and sporadic forms of the disease [41, 42]. GWAS studies relate noncoding variants with higher risk for PD as well, revealing the possible importance of expression and splicing of *LRRK2* [43, 44].

LRRK2-associated parkinsonism is clinically largely indistinguishable from idiophathic PD, being characterized by LBs and Lewy neurites in most cases [45, 46]. The clinical progression of PD in cases due to LRRK2 mutations is also similar to sporadic PD. However, pathological variability exists, with some patients showing nigral degeneration without LBs or even tau pathology [47, 48].

1.4.2 Autosomal recesive forms of PD

PARKIN

Exon deletions in the *PRKN* gene were first discovered in two Japanese families with recessive juvenile Parkinsonism in 1998 [49]. Homozygous *PARKIN* mutations are associated with early onset PD (between age 20 and 50). In addition, heterozygous *PARKIN* mutations have been found in sporadic cases of PD [49, 50].

Cell loss in the SNpc in *PARKIN*-associated PD appears to be caused by loss of function of the parkin protein, therefore overexpression of parkin was demonstrated to be neuropotective. Many mutations in this gene reported to date appear to alter the cellular localization of wild-type parkin, its solubility and/or aggregation properties to either reduce or abolish enzymatic function [51]. The parkin protein, predominantly cytoplasmic, is a ubiquitin E3 ligase that targets specific substrates for degradation such as the mitofusins, other mitochondrial proteins (e.g. the voltage-dependent anion

channel) [52] and PARIS (ZNF746) (a transcriptional repressor) [35]. There is some evidence that parkin may regulate Lys^{48}-linked polyubiquitination, thereby regulating proteasome-dependent cellular processes [53], as well as Lys^{63}-linked ubiquitination, involved in other processes such as endocytosis and autophagy [54]. In addition, parkin has been demonstrated to regulate mitochondrial dynamics and target damaged mitochondria for degradation (mitophagy). In this pathway, parkin translocates from the cytosol to the outer mitochondrial membrane and where it ubiquitinates specific substrates, leading to mitochondrial degradation [55-57].

PINK1

Mutations in the *PINK1* gene were identified in three families with early-onset autosomal-recessive PD previously linked to the *PARK6* locus. Mutations in this gene are the second most common cause of autosomal recessive Parkinsonism after mutations in the *PARKIN* gene [58]. *PINK1* variants include point mutations, as well as insertions and deletions that lead to frame shifts and subsequent truncation of the protein, compromising its kinase activity or interfering with its stability [59, 60].

PINK1 is a protein kinase with an N-terminal mitochondrial targeting sequence. Overexpression of PINK1 is neuroprotective [61] and knockdown of PINK1 induces mitochondrial fragmentation and mitophagy [62, 63]. Several mechanisms have been proposed to explain the function of PINK1, including effects on mitochondrial bioenergetics and calcium homeostasis [64]. In addition, there is evidence to indicate that PINK1 and PARKIN interact genetically to prevent oxidative stress by regulating mitochondrial homeostasis and mitophagy [65-68].

1.5 LRRK2

1.5.1 LRRK2 structure

LRRK2 is a large (2527 amino acids) multi-domain containing protein belonging to the ROCO family of proteins [69], characterized by the presence of two conserved domains: a Ras of complex (ROC) GTPase domain followed by a C-terminal of ROC (COR) domain. In addition, LRRK2 also contains a kinase domain situated C-teminal of the COR domain, and multiple protein-protein interaction domains flanking the enzymatic core [70]. The protein-protein interaction domains include LRRK2-specific, ankyrin and leucine-rich repeat motifs, as well as WD40 repeats. These

domains are thought to participate in the assembly of protein complexes, similar to MAPK scaffolding proteins [71], although at present few of the proposed LRRK2 interactors have been mapped to the distinct interaction domains.

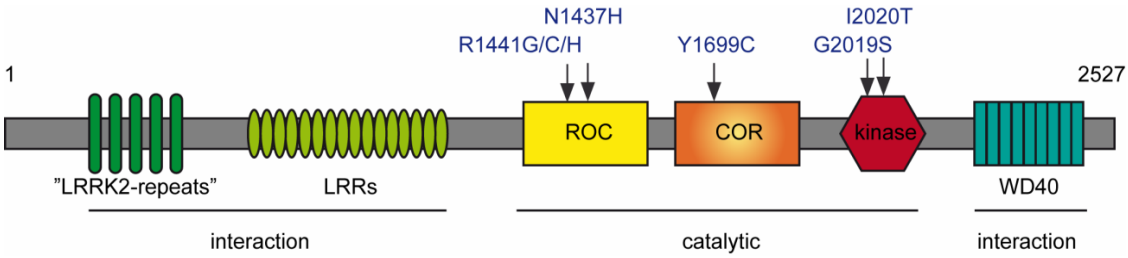

Figure 2 Domain structure and PD mutations of LRRK2

Schematic representation of the LRRK2 protein and its known functional domains and pathogenic mutations. The central region of the LRRK2 protein contains a GTPase domain (ROC), a COR domain and a kinase domain, flanked on either side by multiple protein-protein interaction domains. Disease-segregating mutations are indicated and map around the catalytic domains of LRRK2. LRR, leucine-rich repeats. Figure adapted from [72].

LRRK2: KINASE

Much attention has focused on the kinase domain of LRRK2, since kinase activity is an attractive PD therapeutic target. Indeed, inhibition of kinase activity has been shown to be protective in both *in vitro* and *in vivo* models of LRRK2-mediated cytotoxicity [73-75]. From a phylogenetic analysis, the LRRK2 kinase domain belongs to the tyrosine-like kinase (TKL) family, possessing highest sequence and predicted structure homology to the mixed lineage kinase (MLK) proteins and to the receptor-interacting protein kinases, subfamilies within the TKL [76]. LRRK2 is a serine/threonine kinase, even though the inherent kinase activity of LRRK2 is very low. Putative LRRK2 substrates suggested to date will be further described.

Mutations inactivating LRRK2 kinase activity have been artificially generated. D1994N mutation (a predicted proton acceptor) abolishes the active site, inhibiting kinase activity through mutation of the conserved aspartic acid residue found in all known kinase proteins [73]. K1906A/M (an ATP-binding site) abolishes ATP-binding [77], and DY2017-2018AL alters the predicted DYG kinase active conserved motif.

The K1906M mutation has been shown to to be reasonably stable, displaying similar levels of overexpression as compared to wild-type LRRK2, whilst other kinase-inactivating mutations are less stable [77, 78].

As mentioned before, the LRRK2 kinase activity has been proposed as a potential pharmacological target. Drugs targeting LRRK2 kinase may also be used as valuable tools to better understand the pathophysiological roles of LRRK2 [79]. Indeed, pharmacological inhibition of LRRK2 kinase activity may represent an important therapeutic strategy for PD, as LRRK2 is linked to both sporadic and familiar PD. [79]. To date, several specific compounds have been described as LRRK2 inhibitors, some of which even cross the blood-brain barrier, but further studies are necessary to evaluate their therapeutic potential and potential liability issues associated with continuous LRRK2 kinase activity inhibition [80-83]. Indeed, knockout studies of LRRK2 in mice and rats suggest that peripheral organs may become affected when inhibiting LRRK2, which would make kinase-inhibitor based therapeutic strategies less promising [84, 85].

LRRK2: GTPase

To date, little is known about the GTPase activity of LRRK2. The GTPase domain shares homology to members of the Rab GTPase family [86]. LRRK2 can bind GTP via its guanine nucleotide phosphate-biding motif and can hydrolyze bound GTP *in vitro*, although with low activity. In fact, the GTPase activity of LRRK2 is weak and difficult to quantify and, although values have been reported in some studies, negative results have been also reported [78, 86-89].

At present, it is unclear how the GTPase activity of LRRK2 is regulated. As described below for Rabs, GEFs promote the exchange of GDP for GTP, whereas GAPs promote the hydrolysis of protein-bound GTP. A GAP, GCS1, has been reported as a suppressor of LRRK2 catalytic core toxicity in yeast [90]. The mammalian homologue, ADP ribosylation factor GTPase activating protein 1 (ARFGAP1), has been shown to accelerate the GTPase activity of LRRK2 approximately 2–3-fold *in vitro* [91, 92]. In addition, a putative GEF for LRRK2, ARHGEF7, has been identified as well [93]. Alternatively, LRRK2 may function as a dimeric GAD [94, 95] whereby dimerization is induced by GTP binding, and this may eliminate the need for regulation of LRRK2 by GAPs and GEFs.

LRRK2: DIMER

Indeed, biochemical studies show that LRRK2 exists as a dimer, where the ROC domain contributes to dimerization, although sequences outside of the ROC-COR bi-domain are also required for dimer formation [88, 96]. Dimeric LRRK2 displays enhanced kinase activity, and dimerization may also be important for the GTPase activity [97-99]. Notably, there is some evidence to suggest that LRRK2 additionally forms higher-order structures consistent with homomultimerization [97].

LRRK2: KINASE AND/OR GTPase?

A mutual crosstalk between kinase and GTPase activities has been proposed. This is supported by the observation that LRRK2 autophosphorylates the ROC domain at several sites and regulates its activity (more details in LRRK2 substrates section) [100, 101]. Phosphomimetic mutant versions of two different autophosphorylated residues in the ROC domain (T1491D and T1503D) show impaired GTP binding [101, 102], whilst the data for another phosphomimetic construct (T1410D) are controversial [102, 103].

Given the homology of LRRK2 kinase domain with the MLK subfamily, comprised of kinases which are regulated by small GTPases, it was proposed that the GTPase activity may regulate the kinase activity in an intrinsic manner (reviewed in [104]). Adding non-hydrolysable GTP analogues was shown to increase kinase activity [74, 78], although this finding could not be reproduced in subsequent studies [105]. Recently, it was found that the GTP binding capacity of LRRK2 is necessary for kinase activity, whilst activity is independent of GDP or GTP binding to ROC, proposing that there may be an upstream guanine nucleotide binding protein which may activate LRRK2 in a GTP-dependent manner [106]. In this context, the LRRK2 kinase domain may not be the direct effector of the LRRK2 ROC domain. Another possibility is that the dimeric ROC or ROC-COR domains may regulate kinase activity through induction of self-association of the kinase domains and allowing for autophosphorylation and successive activation [88, 94, 107].

Indeed, results from a prokaryotic ROCO family homolog of LRRK2 suggest a possible regulation of dimerization by guanine nucleotides [94].

1.5.2 PD-associated mutations of LRRK2

Conceptually, mutations can decrease ("loss-of-function") or increase ("gain-of-function") protein function. Gain-of-function mutations can either increase the normal function of the protein or confer a novel function. Usually, recessive mutations act via a loss-of-function, whereas dominantly inherited mutations act via a gain-of-function mechanism. A third class of mutations is called "dominant-negative mutations". These are dominantly inherited mutations that impair the function of the remaining wild-type protein present. There is some evidence that LRRK2 pathology is related with a gain-of-function mechanism: all pathogenic LRRK2 mutations are dominantly inherited and no deletions or mutations causing premature stop codons in LRRK2-related PD have been described thus far; the PD-related mutation G2019S is known to increase kinase activity and kinase inhibition is reported to block neurotoxicity both *in vitro* and *in vivo*; and homozygous human LRRK2 patients have neither earlier onset nor faster progression of PD. In addition, several independently generated and distinct LRRK2 transgenic mouse models develop some PD-like phenotypes whilst knockout mice do not, and overexpression of pathogenic LRRK2 versus knockout of LRRK2 has opposite effects on neurite outgrowth [108].

A large number of LRRK2 mutations have been described as putative causes of PD, and several of those are clearly pathogenic (G2019S, R1441C, R1441G, R1441H, N1437H, Y1699C and I2020T) based on disease segregation in large genetic and functional studies [109].

The disease-segregating mutations in LRRK2 map to the central region comprised of the two catalytic domains. Whilst the most frequent genetic cause of PD, LRRK2 mutations display an incomplete and age-dependent penetrance, suggesting the existence of genetic modifiers [110]. G2019S is predominantly linked to a late-onset PD phenotype and it is the most frequent pathogenic LRRK2 mutation, affecting up to 40 % of familial PD cases depending on ethnicity and having been detected in sporadic PD cases as well [9, 41-43]. The highest known frequencies of G2019S are reported in people of Ashkenazi or North African descent.

The G2019S substitution maps to the N-terminal hinge region of the activation segment of the kinase domain, and has been consistently shown to enhance kinase activity (by 3-5 fold) [111], possibly due to the novel serine residue resulting in a more rigid conformation with persistence of the active state [112]. The small side chain of

glycine allows maximum flexibility and thus motion of the activation loop, whilst the serine residue, with a negatively charged hydroxy-containing side chain and less conformational flexibility, might "lock" the kinase in an active conformation. In fact, Luzón-Toro *et al.* (2007) reported that substitution of alanine for glycine in that site on autophosphorylation-negative mutant protein restores autophosphorylation to wild-type levels [112].

The position R1441 in the GTPase domains is the second most common spot of pathogenic LRRK2 mutations. The R1441 residue is mutated to either glycine, cysteine or histidine (that is, R1441G/C/H) in families with PD [38, 113-116] The R1441 residue sits at the interface between two monomers in the dimeric LRRK2 structure, and the Y1699 residue in the COR domain at the ROC-COR interface [117]. These mutations are thought to change dimer interactions and decrease GTPase activity, suggesting that the GTP-bound state is associated with disease [87, 117-119].

1.5.3 Expression and localization of LRRK2

LRRK2 is expressed in virtually all tissues examined, with comparably high levels in peripheral organs such as kidney, lung, spleen, liver, heart and peripheral blood mononuclear cells [120]. In the brain, LRRK2 is expressed at comparably low levels [120]. LRRK2 protein can be observed in distinct areas, with highest expression in cortex and hippocampus as well as striatum, and very low levels in the SNpc [121]. The protein is expressed in neurons, astrocytes and microglia [120]. Together, such broad and varied expression indicates that LRRK2 may play a role in a cellular process shared amongst most cells.

Some LRRK2 protein has been detected in LBs of sporadic PD [122] and in LN [123], even though the specificity of antibodies used is controversial, and generally it is assumed that LRRK2 is not a major component of LB or LN. Similarly, the low levels of LRRK2 present in neurons have made the exact determination of the intracellular localizations of the protein somewhat difficult.

Overexpressed as well as endogenous LRRK2 has been found in the cytoplasm as well as associated to specific membranes including endo-lysosomal structures in neuronal and non-neuronal cells [124-126], the Golgi complex, mitochondrial outer membrane, plasma membrane and endoplasmic reticulum (ER) [125]. In addition,

LRRK2 also is found located to lipid rafts, specific microdomains within membranous structures [127].

The membrane association of LRRK2 has been proposed to be important for LRRK2 dimerization [99]. The membrane-associated fraction of LRRK2 possesses greater kinase activity and binds GTP more efficiently than cytosolic LRRK2 such that activity may be tightly linked to localization [99].

In addition, it is suggested that the phosphorylation status of LRRK2 may affect cellular localization by modifiyng its interaction with 14-3-3 proteins [128]. The phospho-sites within LRRK2 to which 14-3-3 proteins bind are not autophosphorylation sites, suggesting that upstream kinases may regulate the cytosolic (and possibly membrane-bound) amounts of active LRRK2 [128, 129].

1.5.4 Putative LRRK2 kinase substrates

One general complexity in studying the physiological function of LRRK2 is the fact that there are no consistently identified substrates for its kinase activity, neither functional output for its GTPase activity. Therefore, methods to assess *in vitro* LRRK2 kinase activity are limited to assays employing autophosphorylation [111, 130], or the phosphorylation of LRRK2-specific peptides such as LRRKtide or Nictide [83, 131].

LRRK2 clearly phosphorylates itself on multiple sites, which may change its GTPase activity and/or interactions with a variety of proteins. LRRK2 is also subject to so-called cellular phosphorylation by upstream kinases, which include PKA [128, 129, 132, 133].

A series of substrates for LRRK2 have been proposed [131, 134-139] but the large majority await independent verification or have been shown not to be physiologically relevant in follow-up studies [140]. Some may be regulated by LRRK2, without being direct substrates [141, 142]. In sum, LRRK2 kinase substrate identification approaches have yet to reveal a good target for the kinase activity of LRRK2.

1.5.5 LRRK2 interactors

Additional large research efforts are attempting to systematically study the LRRK2 interactome. As a result, LRRK2 has been reported to interact with a whole

array of proteins, and this somewhat complicates establishing coherent hypotheses about the molecular mechanism(s) by which LRRK2 acts. However, these protein interactions may happen in a cell-type dependent manner, may be subcellular compartment-specific, or reflect distinct protein complexes LRRK2 can engage in [18].

LRRK2 can bind 14-3-3 proteins when phosphorylated on several cellular phosphorylation sites [106, 128, 129, 132, 143, 144]. 14-3-3 proteins are characterised by binding to partner proteins and alter their subcellular localization [145]. In addition, LRRK2 interactions with others proteins involved in chaperone-mediated pathways including Hsp90//p50cdc37, Hsp60, Hsp70, and the C-terminal Hsp70 interacting protein (CHIP) have been described [146, 147]. These chaperone proteins may serve to maintain the accurate folding and activation state of LRRK2, and disruption of the interaction may lead to proteasomal degradation [146, 148].

Possibly due to its homology with other kinases such as MLKs and RIPs, LRRK2 has also been found to interact with MKKs, and may be involved in various kinase signalling pathways [138, 149, 150]. Interestingly, various non-biased *in vitro* interaction assays reported interactions of LRRK2 with actin, actin-binding proteins, tubulin and microtubule-interacting proteins, as well as proteins involved in vesicle exo- and endocytosis and intracellular membrane trafficking pathways related to endocytic-lysosomal trafficking and retromer-mediated trafficking, (see below) [134, 151-155]. These interactions help to formulate molecular models as to how LRRK2 may function in cells.

1.5.6 Animal and cell models

Animal models

The classical intoxication PD models are based on relatively selective killing of DA neurons, but in a very rapid and pronounced manner which does not recapitulate the degenerative process of PD. The possibility to generate animal models carrying a mutant gene causing PD to uncover the fundamental biology and pathobiology of the encoded protein associated with the disease has proven very useful to study a cellular process in the context of functional neuronal circuits.

Several animal model systems have been developed to better understand the pathobiology of *LRRK2* disease-associated mutations. It is important to notice that

whilst the *LRRK2* gene is conserved across higher eukaryotic species, *Danio rerio* (zebrafish), *Caenorhabditis elegans* and *Drosophila melanogaster* possess only one *LRRK* ortholog whose function may be somewhat distinct from mammalian LRRK2. However, these models have a short lifespan, are genetically easily manipulable, show overt phenotypes, and are very useful for *in vivo* compound screening approaches.

YEAST

The yeast *S.cerevisae*, a eukaryotic single-cell organism, does not contain an obvious LRRK2 ortholog. Expression of truncated human LRRK2 was found to decrease yeast viability in a GTPase domain-dependent but kinase activity- and disease-associated mutation-independent manner [90]. The lack of effect of kinase activity or pathogenic mutations on yeast toxicity induced by truncated human LRRK2 expression indicates that full-length protein may be required to observe effects, or that kinase-dependent and mutation-dependent LRRK2-induced toxicity may require a cellular context other than that provided by the yeast system. Interestingly, the expression of truncated LRRK2 GTPase variant has been shown to induce defects in endocytic and autophagic trafficking, and genetic modifier screens identified the GAP which seems to regulate LRRK2 GTPase activity [90].

WORMS

The invertebrate model *Caenorhabditis elegans* possesses a human LRRK ortholog termed LRK-1. LRK-1 deletion studies have implicated it in determining polarized sorting of synaptic vesicle proteins to axons by excluding these proteins from the dendrite-specific transport machinery in the Golgi [156]. Furthermore, the *C. elegans* knockout for the LRK-1 gene displays hypersensitivity to the ER stressor tunycamicin [157]. Expression of human LRRK2 wild type, R1441C and G2019S mutants in nematode DA neurons causes age-dependent neurodegeneration, behavioral deficits and motor activity deficits that are accompanied by a reduction of dopamine levels *in vivo,* with pathogenic mutations having a stronger effect than the wild-type protein. Importantly, LRRK2 kinase inhibition has been demonstrated to be effective in rescuing the degeneration of DA neurons in transgenic R1441C and G2019S *C. elegans,* suggesting that the LRRK2 kinase may represent a promising target [158, 159].

FLIES

Drosophila melanogaster represents a good model organism for studying neurodegenerative diseases, as there exists a high degree of conservation of disease-related loci between flies and humans [160]. *Drosophila* contains one LRRK ortholog [161], dLRRK, which is present at synapses [162] and critical for the synaptic morphology and integrity of DA neurons [162]. dLRRK loss-of-function mutants exhibit synaptic overgrowth [139, 163], whereas overexpression of human *LRRK2* has opposite effects [163]. Wild-type and mutant G2019S LRRK2 expression induces loss of DA neurons and motor dysfunction [164, 165], with G2019S LRRK2 causing a more severe parkinsonism-like phenotype than wild-type [166], even though reported phenotypes are variable [167]. Furthermore, non-autonomous cellular dysfunction has also been observed in flies expressing LRRK2-G2019S in DA neurons, including elevated autophagy, apoptosis and mitochondrial disorganization in photoreceptors, causing a deterioration of vision [168].

The Drosophila model is a valuable tool to rapidly screen for pharmacologic intervention in PD. Indeed, LRRK2 kinase inhibitors attenuate neurodegeneration in this model system as well [159]. Furthermore, several LRRK2 interactors and substrates have been described in this model system [134, 169], as described above.

MICE

A whole variety of transgenic animal models for LRRK2 have been generated [170]. Overexpression levels are very different amongst the transgenic lines, which may explain some apparent discrepancies in phenotypes. In other words, it remains possible that the presence or absence of a phenotype simply correlates with the levels of transgene expression.

Bacterial artificial chromosome (BAC) – mediated transgenesis has been used by several groups, and overexpression of wildtype or mutant human or mouse LRRK2 has generally failed to recapitulate the loss of DA cells observed in PD. However, some neurochemical and behavioural deficits are common features in various LRRK2 mouse models, and may represent some of the earliest neuronal dysfunctions set in motion by pathogenic LRRK2 mutations [75, 171-175].

Neither the R1441C LRRK2 homozygous knockin mice, in which the R1441C mutation is expressed under the control of endogenous regulatory elements [172], nor

the R1441C LRRK2 BAC transgenic mice [171], display DA neurodegeneration. However, they show impaired dopamine neurotransmission, axonal pathology and motor deficits.

Similarly, several G2019S LRRK2 BAC transgenic mice have been reported to display abnormal dopamine neurotransmission, as evidenced by a decrease in extracellular dopamine levels and increased striatal tau immunoreactivity without DA neuron loss in the SNpc [173, 175]. Degeneration of the nigrostriatal pathway has been reported in two transgenic mouse models expressing G2019S mutant LRRK2 [176, 177], with loss of DA neurons in an age-dependent manner. In addition, one of the studies reported autophagic and mitochondrial abnormalities in the brains of aged G2019S LRRK2 mice and markedly reduced neurite complexity of cultured DA neurons derived from these animals [177].

In contrast to the mutants, wild-type LRRK2 BAC transgenic mice have minimal evidence of neurodegeneration and the phenotypes described to date are controversial, with either enhanced or impaired DA transmission [173, 175].

Finally, mouse and rat LRRK2 knockout (LRRK2 KO) models have been generated to study the normal physiological function of LRRK2 [178, 179]. These models are also useful for evaluating potential safety liabilities of LRRK2 kinase inhibitor therapeutics for treating PD, (see above). Knockout animals have no signs of PD-pertinent phenotypes, and do not show a significant difference in their susceptibility to MPTP [180]. However, there are striking phenotypes in peripheral organs, especially kidney, lung and liver. For example, the kidneys of knockout mice develop an age-dependent accumulation and aggregation of α-synuclein and ubiquitinated proteins [85], implicating LRRK2 in autophagic-lysosomal defects [84], as further explained in detail below.

Cellular models

In cellular models, the molecular function of proteins can be dissected in a relatively fast and reproducible manner by using molecular, biochemical and pharmacological approaches. Importantly, these features also offer the possibility to implement high-throughput screening approaches for drug candidates. The availability and, at least in some cases, unlimited proliferation capacity are a major advantage of such models. They also offer a controlled environment, even though they are missing

the natural neuronal network in which disease states develop. Consequently, it is necessary to be cautious in the interpretation of cellular studies, as they cannot accurately model the environment of a postmitotic midbrain neuron in the intact brain.

Several tissue-culture models have been used for studding LRRK2-related biological effects. Immortalized cell lines, either in a proliferating or differentiated state, are commonly used. Human neuroblastoma or carcinoma cell lines such as SH-SY5Y cells, or PC12 cells derived from a pheochromocytoma of the rat adrenal medulla, which are all DA in nature, are commonly used to study the effects of LRRK2 on neurite outgrowth or serve as *in vitro* model systems for drug discovery. Non-neuronal cell lines such as human embryonic kidney (HEK-293) or HeLa cells have also been widely used because they are efficiently transfected, achieving high overexpression levels [92, 127, 132, 148, 181-183]. Primary DA neurons derived from animal models comprise helpful cellular systems for investigating PD pathogenesis, even though few cells can be obtained and they are tedious to culture [184]. Finally, cells from patients are important cellular model systems, as they contain the pathogenic mutations which cause the disease, even though the genetic variability between patients means that cellular readouts may be more variable than what is observed in homogenous cell lines or cells derived from background-controlled transgenic animals [185]. Generally, studies using human cells are performed in primary dermal skin fibroblasts from age- and sex-matched control and LRRK2 mutant patients. Cells can also be modified towards induced pluripotent stem cells (iPSCs), and these can be differentiated into DA neurons [37, 185-190]. However, this is a lengthy and very costly process. Other primary patient-specific cells include lymphoblastoid cells.

All types of cellular systems for the study of LRRK2 have been employed, and interestingly, some common denominators have been found in all cell systems mentioned, including altered autophagy, which attests to the validity of the more simple, transient expression systems for studying LRRK2 function [37, 124, 177, 191-194].

1.5.7 Biological effects of LRRK2

Up to date, various cell biological effects of LRRK2 have been reported. Some have been only robustly observed under overexpression conditions, whilst others are also detected when LRRK2 is present at physiological levels, and those are the most relevant. In addition, knockout or RNAi approaches, as well as LRRK2 kinase

inhibition with specific inhibitors highlight roles for LRRK2 in various cellular processes, as outlined below.

Cytotoxicity

PD-associated mutations in LRRK2 have been robustly reported to cause cell toxicity when overexpressed in multiple cell lines, including primary neurons in culture, while overexpression of wild-type LRRK2 does not seem to significantly decrease cell viability under the assay conditions employed [73, 74, 195, 196]. Cell death is also evident upon viral vector-mediated expression of mutant LRRK2 *in vivo* [75, 197].

Kinase as well as GTPase activities seem to mediate cytotoxicity [73-75, 90, 194] and in some cases isolated domain fragments (e.g. kinase domain) have been shown to have effects as well [196]. In overexpression studies, toxicity starts to be evident 72 hours after transfection [130], indicating that cellular alterations mediated by LRRK2 take time to manifest themselves in terms of viability. This opens up a window during which LRRK2-mediated cellular effects can be studied before events related to apoptosis take over.

In transgenic mice overexpressing G2019S LRRK2, proliferation of newly generated cells is significantly decreased and survival of newly generated neurons is also severely impaired in two neurogenic regions [174, 198]. In contrast, iPSC-derived DA neurons from mutant LRRK2 carriers do not show enhanced cell death, but they do display increased susceptibility to death upon different stressors related to oxidative stress or disruption of the autophagy-lysosomal pathway and UPS [186, 188]. Generally, phenotypes in those cells take longer to develop, and are often only seen upon prolonged culture conditions [198] suggesting that overexpression of pathogenic LRRK2 may shorten the time to observe LRRK2-mediated cellular events [187, 189, 199, 200].

The mechanism of LRRK2-mediated cell death seems to involve an apoptotic pathway. Indeed, pathogenic LRRK2 mutants were reported to show enhanced binding to the death adaptor Fas-associated protein at the death domain (FADD) and promote caspase-8-dependent apoptosis in a kinase activity-dependent manner [201].

Neurite outgrowth and synaptic alterations

Both human patients and primate models of PD display deficits in DA transmission and alterations in synaptic terminals in the striatum which seem to occur prior to neuron loss in the SNpc [202]. Thus, the earliest pathogenic alterations

underlying PD may arise at the synapse. Interestingly, neurite shortening represents a consistent phenotype associated with mutant LRRK2 expression both in primary culture and *in vivo* [92, 155, 157, 174, 177, 187, 194, 196, 203]. Reduced dendritic arborization and fewer spines have also been reported in transgenic mice expressing G2019S mutant LRRK2 [174]. Where investigated, this phenotype seems kinase activity-dependent and mediated by macroautophagy [157, 174, 177, 194, 196]. A recent study in mouse cortical neurons expressing either G2019S or R1441C LRRK2 mutations has shown that the observed dendrite shortening is mediated by mitophagy, and due to alterations in calcium homeostasis [190]. Conversely, silencing or knockout of LRRK2 seems to cause opposite effects on neurite outgrowth and arborization, even though this has been controversial [155, 196, 204, 205]. Interestingly, the silencing of LRRK2 in cortical neurons has been reported to increase the mobility of synaptic vesicles, which may indicate a role for LRRK2 in SV trafficking [206].

The precise mechanism(s) by which LRRK2 regulates neurite morphology remains unclear, but may involve presynaptic and/or postsynaptic events [207] including effects on SV trafficking or cytoskeletal organization and dynamics [134, 156, 174, 204, 205, 208-210]. Notably, the effects of G2019S LRRK2 on neurite morphology can be rescued *in vitro* by overexpression of Rac1 [155] and *in vitro* and *in vivo* by Rab7L (involved in retromer-mediated trafficking between late endosomes (LEs) and the Golgi) [152]. Thus, the LRRK2-mediated effects on neurite outgrowth and synaptic dysfunction may be due to alterations in one or more intracellular membrane trafficking pathways in a cytoskeleton-mediated manner.

Cytoskeleton

Actin and microtubule dynamics are crucial for proper neuronal network formation, regulating elementary processes such as axonal guidance and synaptogenesis [211]. Furthermore, the cytoskeleton plays a critical role in various cellular processes including cell motility, division, intracellular organization, and organelle and vesicle transport. As a typical SNpc DA neuron has extremely long axonal projections [212], there is a larger need for synaptic membrane trafficking, and its dysfunction may potentially contribute to the axonal pathology seen in PD patients.

Various independent studies have shown that LRRK2 can interact with numerous cytoskeletal proteins including actin, moesin, ezrin and radixin-(ERM) family members, myosin and myosin-related proteins, α- and β-tubulins and microtubule-

bound tau [135, 136, 141, 203]. Thus, LRRK2 may be closely related with microtubule-related processes and actin dynamics with concomitant effects on neurite outgrowth and/or cellular trafficking (reviewed in [213]).

With respect to actin-mediated events, neurons from G2019S mutant LRRK2 mice display an increase in the number of phospho-ERM and F-actin-enriched filopodia, which correlates with retarded neurite outgrowth, whilst the reverse is observed in LRRK2 knockout neurons [214]. LRRK2 has also been reported to interact with the Rho GTPase Rac1, which binds to a complex that regulates actin filament formation, neurite outgrowth and endocytosis [155].

Both wildtype and pathogenic mutant LRRK2 can interact with α/β tubulin heterodimers and microtubules [141, 215]. It may enhance tubulin polymerization by direct or indirect phosphorylation of brain-derived β-tubulin isoforms [135]. Tubulin phosphorylation during neurite outgrowth is known to stabilize the microtubule cytoskeleton, and G2019S LRRK2 transgenic mice display microtubule assembly consistent with enhanced tubulin polymerization [215]. In addition, the levels of soluble β-tubulin are dramatically decreased in brains of LRRK2 expressing mice [215] and are significantly increased in the brains of LRRK2 KO mice [135].

A role for LRRK2 in the modulation of microtubule dynamics is also suggested by reports that it directly or indirectly regulates the phosphorylation of microtubule-bound tau [136, 173, 203]. Tau is a microtubule-associated protein present mainly in neuronal axons and drives neurite outgrowth by promoting the assembly of microtubules [216]. Pathogenic LRRK2 has been reported to increase tau phosphorylation, resulting in concomitant microtubule destabilization by reducing the ability of phosphorylated tau to bind to tubulin [203]. In rodent models overexpressing pathogenic LRRK2, hyperphosphorylation of tau is associated with abnormal processing or accumulation of tau and motor deficits [171, 173, 197, 216]. Collectively, these data may suggest that LRRK2 may modulate microtubule dynamics by controlling the phosphorylation status of tau. Alterations in microtubule dynamics have also been observed in the context of endogenous levels of LRRK2. For example, primary fibroblasts derived from LRRK2 patients were shown to contain a reduced microtubule mass, a higher fraction of unpolymerized tubulin, and resulting changes in cell morphology and cell migration [141, 217].

The reported roles of LRRK2 in regulating microtubule and actin dynamics may cause the observed membrane-related membrane trafficking deficits (see below), as intracellular membrane trafficking is largely cytoskeleton-dependent. However, whether LRRK2 affects microtubule dynamics directly, or whether these events occur secondarily to some other upstream event(s) remains to be determined.

Autophagy and endocytosis

There are indications that LRRK2 plays an important role in autophagy [37, 84, 85, 124, 177, 191, 194, 196]. Indeed, an accumulation of autophagic vacuoles is a consistent neuropathological feature in PD, and may reflect a dysfunction in the autophagic-lysosomal protein degradation system [218]. Initial studies had shown accumulation of autophagic vacuoles in neurons or in DA SH-SY5Y cells overexpressing G2019S mutant LRRK2 [194, 196], and such autophagic alterations were accompanied by a reduction in neurite outgrowth. Changes were also observed when expressing R1441C mutant LRRK2 in HEK293 cells, such as accumulation of abnormal MVBs [124]. However, the mechanism by which pathogenic LRRK2 alters autophagy, and whether it induces or blocks autophagic flux, had remained largely unclear. Similarly, whilst overexpression of mutant LRRK2 in mammalian cells had been shown to affect endocytosis [134, 154, 219], the mechanism(s) underlying such effects had been unclear.

1.6 PD Pathogenesis

While the exact molecular mechanisms of neurodegeneration in PD remain unknown, impairment in a number of cellular processes have been suggested to underlie PD, including protein accumulation and aggregation, impairments in autophagy, oxidative stress, mitochondrial defects, calcium homeostasis dysregulation and neuroinflammation. The pathogenic factors exposed are not mutually exclusive, and the aim of current research is to elucidate mechanisms underlying PD associated with mutations in LRRK2.

1.6.1 Protein aggregation and lysosome-dependent pathways.

The presence of LBs in DA neurons as a hallmark of PD suggests that protein misfolding and aggregation are central features of PD pathophysiology [220]. Indeed, PD as well as other neurodegenerative diseases are often referred to as ‘protein

misfolding diseases' [221]. The accumulation of misfolded proteins in these diseases suggests a common pathological mechanism possibly underlying clinically distinct neurological states. Genetic mutations, environmental factors, oxidative damage and dysfunction in protein degradation mechanisms may result in protein misfolding and subsequent accumulation [222]. As explained above, largely natively unfolded proteins such as α-synuclein tend to be prone to aggregation into smaller and larger oligomeric structures, which can impair cell function and viability. When misfolded proteins form oligomers, they become inaccessible to the proteasome and can only be degraded by autophagy-lysosome-related pathways. As mentioned previously, the importance of lysosomal function has also become apparent from the discovery that mutations in GBA, a gene which codifies for a housekeeping enzyme crucial for lysosomal degradation comprises the most common risk factor for sporadic PD (see above) [22, 223, 224].

Along with ubiquitinated protein aggregates, an increased number of autophagic structures have been found in PD patients, animal and cellular models of PD [72]. Another piece of evidence linking autophagy to PD comes from the reported effect of α-Synuclein overexpression blocking macroautophagy [225]. In addition, α-Synuclein and UCHL-1 mutants have been reported to block CMA, another type of protein degradation (see below) [226, 227]. Conversely, pharmacological activation of macroautophagy has been shown to alleviate the toxicity associated with mutant α-Synuclein *in vitro* and *in vivo* [228, 229]. Other PD-related proteins have been related to altered autophagic flux as well. For example, the absence of DJ-1, PINK1 or Parkin impairs basal autophagic flux, causes accumulation of autophagic markers, mitochondrial fragmentation and depolarization in human DA cells [230-232], and LRRK2 has been closely related with macroautophagy as well (see above).

1.6.2 Mitochondrial damage and oxidative stress

Neurons use a considerable amount of energy, and thus are highly equipped with mitochondria and extremely sensitive to mitochondrial dysfunction [233]. There is chemical and genetic evidence for the involvement of mitochondrial damage in PD (see above). The idea that MPTP, rotenone, and paraquat inhibit complex I is widely accepted. In addition, studies on different cell types from idiopathic PD patients confirm the important role of mitochondria in the pathogenesis of PD.

Additional evidence for mitochondrial involvement comes from the study of PD-related genes (*PARKIN*, *PINK1*, and *DJ-1),* where PD-linked mutations cause deficits in mitochondrial homeostasis [55-57, 65, 66, 68, 230, 231]. Furthermore, overexpression of mutant LRRK2 or α-Synuclein increase ROS levels and cause defects in the morphology and dynamics of mitochondria, which compromises neuronal survival [234, 235]. In *Drosophila*, LRRK2 mutations have also been shown to increase susceptibility to complex I inhibition [165].

Mitochondria are one of the major cellular producers of ROS [236]. Oxidative damage has been reported in mitochondria and other cellular components, such as DNA, proteins, and lipids, in the SNpc of PD brains [237]. Oxidative stress is not just a consequence of mitochondrial dysfunction, but may also comprise a pathogenic factor on its own. The link between oxidative stress and PD is based on the observation that oxidation of cytosolic dopamine and its metabolites leads to the production of cytotoxic free radicals in DA neurons [238]. Whilst this theory may explain the selective vulnerability of DA neurons, other neurons die in PD as well (see above), and thus oxidative stress may be an important, but not the principal culprit for the disease [239].

1.6.3 Altered calcium homeostasis

Currently, one of the mechanisms believed to be implicated in the selective degeneration of DA neurons in PD relates to perturbations in calcium homeostasis [240]. Adult SNpc DA neurons are autonomously active, generating action potentials in the absence of synaptic input, as many others neurons [241]. However, whilst most neurons use exclusively monovalent cation channels to drive this pacemaking activity, SNpc DA neurons also employ L-type calcium channels that allow calcium to enter the cytoplasm [242].

Since the spatiotemporal pattern of calcium signalling is crucial for the specificity of cellular responses, calcium must be under a tight homeostatic control that requires energy. Therefore, calcium must be extruded by ATP-dependent processes: it needs to be pumped out or rapidly sequestered by intracellular organelles, including the ER and lysosomes. Both processes are mediated by ATP-dependent pumps and exchangers [243, 244]. This additional energy requirement and energy production via mitochondria can generate oxidative stress and production of reactive oxygen species. In addition, the increase in calcium uptake by mitochondria from the endoplasmic

reticulum (ER) through inositol trisphosphate receptor receptors (IP_3R) leads to an increase in the basal generation of oxidant stress in the mitochondria of SNc DA neurons, increasing SNc DA neuron vulnerability [239, 242, 245].

Interestingly, as mentioned previously, non-DA neurons degenerate in PD as well, and these neurons also possess autonomous or spontaneous activity which can open NMDA receptors, which can become permeable to calcium, thus increasing intracellular calcium load [240].

1.6.4 Neuroinflammation

Even though the brain has been classically considered to be free from immune reactions since it is protected by the blood–brain-barrier, recent findings have revealed that immune responses may occur in the brain, especially due to the activation of microglia. In classical toxin-induced PD models, inflammation and resultant oxidant stress are important modulators of cell loss.

Chronically activated microglia and astrocytes may contribute to PD; indeed, microglial activation, T-cell infiltration and astrocyte accumulation are observed in the later stages in the nigro-striatum of PD brains [246]. Activation of microglia causes inflammatory responses which activates inducible nitric oxide synthase (iNOS) and contributes to oxidative stress in the affected areas [45]. In addition, microglial activation has been shown to upregulate and release pro-inflammatory cytokines and decrease the levels of neurotrophins, the latter of which seem to be neuroprotective [247].

2. THE AUTOPHAGIC AND ENDOCYTIC PATHWAYS

Endocytosis is responsible for internalization of a wide range of cell surface receptors, which are either recycled via distinct pathways or targeted to the lysosome for degradation. Autophagy likewise targets proteins, protein aggregates or entire organelles for lysosome-mediated degradation. Thus, both trafficking events share lysosomes as common endpoint [48]. They intersect at other stages as well; biochemical and morphological studies have shown that autophagosomes can fuse with endosomes, mainly late endosomes (LEs), generating amphisomes, pinpointing towards another convergence of these two pathways [248]. Both routes also employ common proteins such as Ras-like small guanosine triphosphatases (Rab GTPases), as further detailed below.

2.1 Autophagy

2.1.1 Function and forms

Autophagy is an evolutionarily conserved catabolic process. It is important for balancing sources of energy at critical times in development, in response to nutrient stress, and plays a key role in the homeostatic clearance of old or damaged organelles, proteins and protein aggregates [249, 250]. Autophagy normally proceeds at a low basal rate, but basal autophagy is especially high in neurons, and disrupting basal autophagic degradation causes neurodegeneration in mice [251, 252].

There are at least three types of autophagy, depending on the delivery route of the material for degradation to the lysosomal lumen: chaperone-mediated autophagy, microautophagy, and macroautophagy [253, 254].

1. Chaperone-mediated autophagy (CMA) is a selective mechanism responsible for the lysosomal degradation of soluble cytosolic proteins targeted with a consensus motif. These proteins are translocated across the lysosomal membrane in a complex with chaperone proteins that are recognized by the CMA-receptor lysosome-associated membrane protein (LAMP) 2A (LAMP2A), resulting in their unfolding and degradation. Defective CMA has been described in different pathologies including lysosomal storage diseases and familial forms of PD [255].
2. Microautophagy is a mechanism by which a portion of cytoplasm is directly taken up by the lysosome itself through invagination of the lysosomal membrane.

3. Macroautophagy (hereafter referred to as autophagy) is a process by which cytosolic constituents, including damaged organelles and aggregated proteins, are engulfed within specialized double-membrane vesicles called autophagosomes. Autophagosomes fuse with LEs first, or directly with lysosomes, followed by the hydrolytic degradation of products in lysosomes and reformation of these organelles to maintain cellular degradative capacity. Disrupting any part of this process impairs autophagic flux, accompanied by the accumulation of autophagic substrates.

2.1.2 Signalling pathways

The signalling mechanisms leading to the activation of autophagy under nutrient starvation conditions have been extensively investigated [256]. However, these circumstances are rare under physiological conditions. Nevertheless, as mentioned previously, autophagy plays an essential role in the maintenance of normal homeostasis at both a cellular and organismal level, and can also be induced by several cellular stresses under normal nutritional conditions. Under normal non-starved conditions, autophagy is regulated by a wide array of extracellular factors including growth factors, cytokines and chemokines, suggesting that there is a mutual exclusive regulation of cell growth and autophagy [257].

The best known canonical autophagy regulator is the mammalian TOR kinase (mTOR), specifically complex1 (mTORC1, comprised of by mTOR, RAPTOR, GβL/mLst8, PRAS40 and DEPTOR) [256]. Therefore, autophagy signalling has been divided into mTOR-dependent and –independent pathways.

mTOR-dependent autophagy

mTOR is a serine/threonine protein kinase that belongs to the phosphatidylinositol kinase-related kinase (PIKK) family. mTOR regulates the balance between anabolic (cell growth) and catabolic (autophagic degradation) processes and has recently been shown to be an important player in neurodegeneration [258].

The mTORC1 complex is positively regulated by the small GTPase Rheb, which can be inactivated by the GTPase activating protein (GAP) formed by the heterodimer regulator tuberous sclerosis 1 and 2 (TSC1/TSC2). In response to amino acids, mTORC1 has been reported to be recruited to the lysosomal surface by Rag GTPases [259]. Such lysosomal localization seems to be required for activation of the complex

by Rheb [260]. The active mTORC1 complex promotes cell growth and inhibits autophagy by phosphorylating the mammalian Atg1 orthologous ULK1 and ULK2 (ULK1/2) and ATG13L subunits (see figure 3) [261]. mTOR can be inhibited indirectly by another autophagy-related kinase, adenosine monophosphate-activated protein kinase (AMPK).

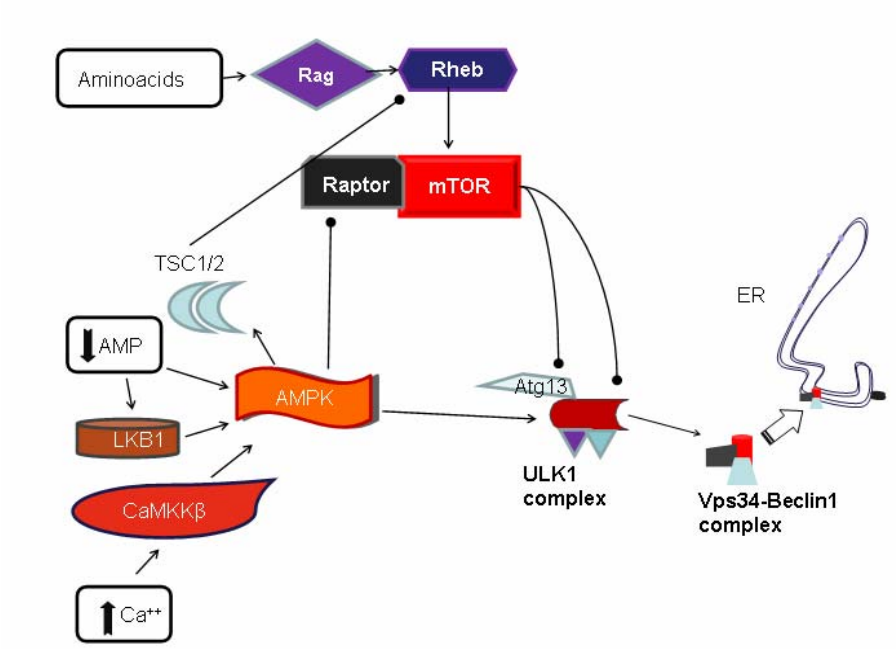

FIGURE 3 Signalling pathways in autophagy.

The ULK1/2 complex integrates upstream mTOR and AMPK signalling to coordinate the induction of autophagy. The mTOR complex inhibits the induction of autophagy through phosphorylation of ULK1/2 complex, which undergoes dephosphorylation upon starvation. AMPK may promote autophagy through inhibition of mTOR and through phosphorylation of the ULK1/2 complex as well. Dot-end arrows indicate events that inhibit autophagy, while normal arrows indicate events that are inducing autophagy. Figure adapted from [262].

mTOR-independent autophagy

Autophagy can be also controlled by several additional pathways, independently of mTOR. Direct induction of autophagy can be mediated by the activation of AMPK in response to energy loss (an increase in AMP levels), through LKB1 or through an increase in cytosolic calcium levels and activation of CaMKKβ [263, 264]. Thereby, activated AMPK phosphorylates the ULK1/2 complex and induces autophagosome formation directly [265, 266] .

Intracellular calcium has been proposed to be a regulator of autophagy, even though it is unclear whether there is positive [267, 268] or negative [269, 270] regulation. Releasing calcium from the ER by thapsigargin (an ER ATPase inhibitor) has been shown to block autophagic flux [269]. L-type calcium channel agonists have been proposed to inhibit autophagy at the level of autophagosome biogenesis [270]. On the other hand, calcium release from the ER has been shown to activate the CaMKKβ/AMPK-mediated suppression of mTOR, thus causing induction of autophagosome formation [268]. Finally, constitutive IP_3R calcium transfer from ER to mitochondria inhibits autophagy under normal nutritional conditions. In the absence of such calcium transfer, AMPK is activated due to a decrease in mitochondrial ATP production and concomitant increase in AMP levels, causing mTOR-independent autophagy induction [271]. These complex findings indicate that it is important to consider the precise intraorganellar location of calcium, and the role calcium plays at these organelles in the context of autophagosome biogenesis, autophagosome-lysosome or endosome-lysosome fusion, respectively [272].

ULK1/2-Atg13-Atg101-FIP200 complex

There is a significant body of evidence indicating that all above-mentioned signalling pathways converge onto the mammalian Atg1 orthologues ULK1 and ULK2 (ULK1/2). ULK1/2 is a direct target of multiple kinases that affect its function and localization in multiple ways. mTORC1 and AMPK are able to oppositely regulate ULK1/2 kinase activity by direct phosphorylation [261, 273, 274], (see figure 3). ULK1/2 activation then leads to autophosphorylation and phosphorylation of both FIP200 and Atg13, which causes translocation of the entire complex to the pre-autophagosomal membrane and autophagy induction.

2.1.3 Molecular components of mammalian autophagy

A crucial element in the autophagic pathway downstream of the ULK1/2 complex is the class III phosphatidylinositol-3 kinase vacuolar protein sorting 34 (Vps34). Vps34 is involved in several membrane-sorting processes such as autophagy, endocytosis and cytokinesis, but is selectively involved in autophagy when complexed to Beclin1, and this complex is crucial for autophagosome initiation [275]. The protein AMBRA1 has been proposed as the link between ULK1/2 and the Vps34-Beclin1 complex [276]. The ULK1-dependent phosphorylation of AMBRA1 might lead to the

release of the Beclin1 complex from the dynein motor complex to allow translocation of the core complex to the autophagosome formation-related region [276]. In addition, other proteins, such as UVRAG, BIF-1, and Atg14L associate with the complex to enhance autophagy [277, 278], whilst others, such as Rubicon or Bcl-2, associate with the complex to inhibit autophagy [279, 280]. Importantly, Bcl-2 seems to provide a link between apoptosis and autophagy, playing a dual role in determining cell viability, maybe depending upon its subcellular localization [280].

Autophagic steps

The autophagic pathway is comprised of four steps: initiation, autophagosome formation, trafficking and recycling of macromolecules [281].

Early studies provide evidence that the autophagosome membrane is largely derived from ER membranes [282, 283]. More recently, mitochondria [284, 285], plasma membrane [286], recycling endosomes [287], and the trans-Golgi network (TGN) [288, 289] have all been shown to be cellular sources for autophagosome formation. However, it remains unclear how much of the autophagosome membrane comes from such distinct sources, and under which conditions, and it is generally accepted that the ER membrane provides the major source of autophagosome membrane.

The transient association of the complex Vps34-Beclin1-Vps15, together with other different modulatory proteins, is a requirement for the initiation of the isolation membrane [290]. The lipid phosphatidylinositol-3-phosphate (PI3P) seems to be important for the initiation of the autophagosome membrane: PI3P-enriched membranes recruit and activate effector proteins containing FYVE or PX PI3P-binding domains [291].

The isolation membrane subsequently elongates, sequestering the cargo for degradation, and finally closes off to form a double-membraned vesicle, the autophagosome. The elongation process is regulated by two ubiquitination-like reactions, the Atg12/Atg5 conjugation and the conjugation of microtubule-associated protein 1 light chain 3 (LC3) to the lipid anchor phosphatidylethanolamine (the autophagosome-associated LC3-II form) [281]. The action of those two ubiquitin-like conjugation systems is modulated by Atg7. The Atg5/12 complex is further associated with Atg16L and LC3, but dissociates from the vesicle once it is fully formed [292]. In contrast, LC3, which is diffuse in the cytoplasm under normal conditions (LC3I), is

bound to autophagic membranes (LC3II) upon the mentioned conjugation and is classically used as a marker of autophagy, (see figure 4).

Autophagosomes are then transported on microtubules from the cell periphery to the perinuclear region towards the microtubule-organizing center in a dynein/dynactin-dependent manner (reviewed in [293]). During maturation, the outer membrane of the autophagosome fuses with late endosomes, generating a hybrid organelle called the amphisome, or directly fuses with lysosomes to form an autolysosome, (see figure 4). Fusion events during autophagic maturation are similar to endosome-lysosome fusion events, where kiss-and-run, complete fusions or fusion mediated through tubules have been described [294]. Several protein complexes and signalling pathways are involved in the maturation of autophagosomes and their delivery to and fusion with lysosomes.

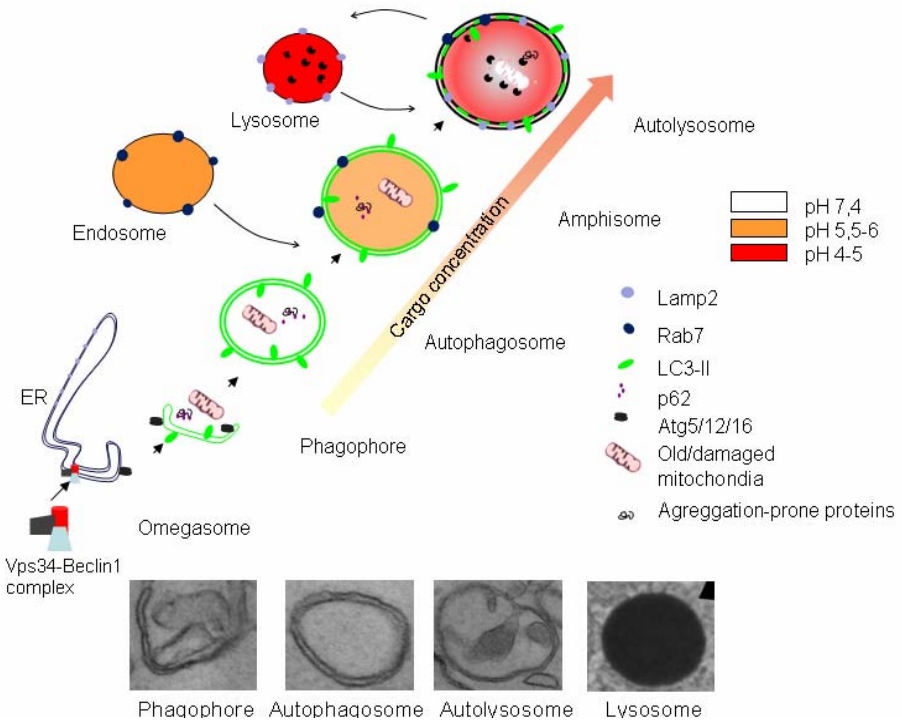

FIGURE 4. An overview of autophagy.

Autophagy is initiated by the formation of phagophores which engulf the autophagic cargo (non-specific or specific substrates such as p62, aggregation-prone proteins or mitochondria) inside a double-membrane. Once formed, the autophagosome fuses with endosomes (to form amphisomes) or lysosomes (to form autolysosomes), a process which involves several lysosomal proteins such as LAMPs and Rab7. Degraded products are translocated to the cytoplasm and the autolysosome is recycled back to lysosome by lysosomal reformation.

Autophagic compartments become progressively acidified during this trafficking route. Figure adapted from [295].

Finally, lysosomal hydrolases degrade the content and the inner membrane of the autophagosome/amphisome. After this process, lysosomal function is restored again by formation of proto-lysosomes budding off from tubules emanating from the autolysosomes. These proto-lysosomes have been reported to be non-acidic and LAMP1 positive [296]. Interestingly, mTOR may potentially regulate lysosomal reformation through Rab7, because inhibiton of mTOR by rapamycin impaired the dissociation of Rab7 from distended autolysosomes [296].

2.2 Endocytosis

2.2.1 Function and forms

Endocytosis is the mechanism by which cells control signalling pathways and interact with their environment. It consists of an active transport of molecules from the extracellular space and the plasma membrane to the interior of the cell, requires adenosine triphosphate (ATP) and involves the *de novo* production of internal membranes from the plasma membrane lipid bilayer.

Endocytosis can be separated into distinct categories based on cargo and intracellular mechanisms involved in vesicle formation and scission from the plasma membrane. In addition, dependent on cell type, the same endocytic cargo may be internalized by different mechanisms, and even a switch of one pathway to another within the same cell type may be possible under different conditions [297].

The most prominent and well-characterized pathway is clathrin-mediated endocytosis (CME), and it is mainly responsible for the internalization of nutrients, pathogens, antigens, growth factors and receptors [298]. In CME, coated pits invaginate, pinch off and are subsequently endocytosed via coated vesicles, which are encapsulated by a polygonal clathrin coat (CCVs). When CCVs are uncoated, they fuse with the early endosome [299]. CCVs are involved in several transport steps such as receptor-mediated endocytosis, but also in transport from the TGN to endosomes [300].

2.2.2 Endocytic compartments

Despite the great plasticity and dynamics of the endocytic system, four classes of endocytic compartments are typically distinguished: early endosomes (EEs), late endosomes (LEs), recycling vesicles (RVs), and lysosomes. These different vesicular organelles are differentiated by their morphological appearance, different protein and/or lipid composition, association with Rab GTPases and by different luminal pH [298].

Early endocytic compartments

The biogenesis of early endosomes (EEs) is not entirely clear, but they might be mainly derived from primary endocytic vesicles that fuse with each other [301]. Normally, an EE fuses with incoming vesicles and, while most membrane and fluids are rapidly recycled, some of the received cargo accumulates. During this period, EEs recruit specific proteins from the cytosol to their cytosolic membrane surface [297, 299].

Functionally, EEs serve as a key control point for cargo sorting. Basically, there are two routes a cargo can take when exiting the EE: 1) it can enter the late endosomal pathway for degradation; or 2) it can be transferred to the endocytic recycling compartment (Rab11/Rab4-positive recycling endosomes) and shuttled back to the plasma membrane [302, 303].

Individual EEs have a complex structure with tubular and vacuolar domains, which differ in composition and function [301]. EEs undergo homotypic fusion as well as fission events in a manner requiring specific cytosolic and membrane-associated protein factors, including Rabs [304, 305].

Rabs are Ras-like small GTPases, and like other GTPases, they cycle between an inactive GDP-bound form in a complex with the GDP dissociation inhibitor (GDI) in the cytoplasm, and a membrane-associated GTP-bound active form. To be activated, they need to be recruited to membranes, where GDI is removed and GDP replaced by GTP. A GDI-displacement factor (GDF) can recruit the Rab-GDP to the membrane, whereas a guanine nucleotide exchange factor (GEF) facilities the exchange of nucleotides and activates the Rab, (see figure 5). Active Rabs interact with downstream effectors to exert their biological functions. Rab-inactivation finally requires a GTPase-activating protein (GAP) to catalyse efficient nucleotide hydrolysis [306]. These Rab regulatory proteins can be phosphorylated in response to different signalling pathways, thereby modulating Rab activity [307].

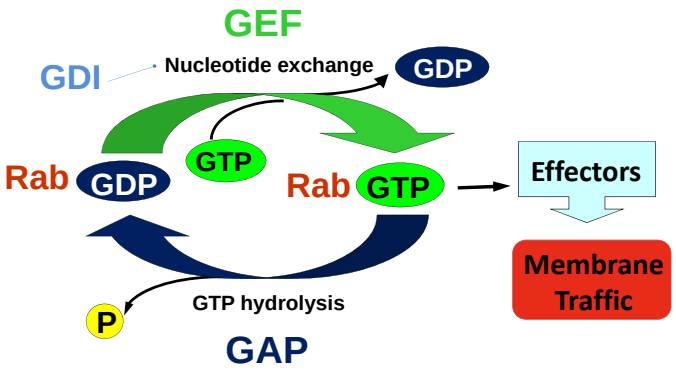

Figure 5. GTPase cycle

Conversion of the GDP-bound Rab into the GTP-bound form occurs through the exchange of GDP for GTP. This step is catalysed by a guanine nucleotide exchange factor (GEF). The GTP-bound 'active' conformation is recognized by multiple effector proteins and is converted back to the GDP-bound 'inactive' form through hydrolysis of GTP, which is stimulated by a GTPase-activating protein (GAP) and releases an inorganic phosphate (P). The GDP-bound Rab is recognized by Rab GDP dissociation inhibitor (GDI), which regulates the membrane cycle of the Rab. Figure adapted from [308].

Canonically defined EEs contain Rab5 and its protein effectors Early Endosome Antigen1 (EEA1) and Vps34/p150. Rab5 regulates the fusion of primary endocytic vesicles with pre-existing EEs as well as homotypic EE fusion [305]. Another early endosomal characteristic is the only slightly acidic pH [309].

The recruitment of Rab5 to endosomes initiates the subsequent binding and activation of effector molecules such as Vps34/p150, which by producing PI3P further increases the binding of Rab5 and more effector molecules, resulting in a strong positive feedback loop in terms of activation of Rab5 [310].

Endocytic recycling compartments

Recycling components are rapidly removed prior to the transition of early to late endosomes. Endocytic recycling is the main way for the cell to maintain constituents of the plasma membrane, for example to maintain the abundance of receptors and transporters on the cell surface after bound ligands dissociate from receptors in the slightly acidic lumen of early endosomes [304].

The recycling compartment is composed of vesiculo-tubular membrane structures often associated with microtubules and concentrated predominantly in a perinuclear area [311]. Recycling from the early endosome back to the plasma membrane can be facilitated by a route via Rab11-positive or Rab4-positive recycling endosomes. Rab11 is also involved in the regulation of membrane traffic between the TGN and recycling endosomes, and the recycling of the transferrin receptor back to the cell surface [312].

Late endocytic compartments: endosomal maturation

During endosomal maturation, EEs are moving towards the perinuclear region along microtubules [298]. E*n route,* they acquire newly synthesized lysosomal hydrolases, form additional intraluminal vesicles, change morphology, drop lumenal pH and switch membrane components [313], as described in detail below:

Rab switch

EE to LE maturation involves a conversion from Rab5 to Rab7. During this endocytic maturation process, Rab5 and Rab7 work sequentially and dynamically.

Lipid composition switch

Apart from the protein switch, the lipid composition changes during endosomal maturation, mediated by various protein complexes. PI3P synthesis serves to recruit proteins with PI3P recognition motifs such as the phosphatidylinositol 3-phosphate 5-kinase PIKfyve, which generates PI(3,5)P(2), as well as myotubularin lipid phosphatases to control endosomal levels of PI3P. PIKfyve is also involved in the formation of intraluminal vesicles [137].

Intraluminal vesicles (ILV)

The formation of intraluminal vesicles is an important process in LE biogenesis because these structures are critical for the selective sorting of membrane-associated cargo towards degradation. The main players in intraluminal vesicle biogenesis are the endosomal sorting complex required for transport complexes (ESCRT-0, -I, II, -III) and accessory proteins such as the AAA-type ATPase VPS4 and Alix. These complexes bind cargo, deform the membrane, and pinch off vesicles as they form from the limiting membrane of the endosome [153].

Changes in luminal ionic environment

Another important feature of the endosomal system is the progressive drop in pH, which goes down from around 6.0 in early endosomes to 5.0-5.5 after LE formation. The

vacuolar H+ ATPase (V-ATPase) generates the acidic lumen of endosomes and lysosomes. Chloride ions accompany the entry of protons so as to maintain electroneutrality in the endosomal lumen. An acidic lumen is also essential for the genesis of ILVs [137].

Fission from endosomes triggers endosomal maturation, as interfering with fission can block endosomal acidification, endosomal motility along microtubules, perinuclear localization, and lysosomal degradation [314].

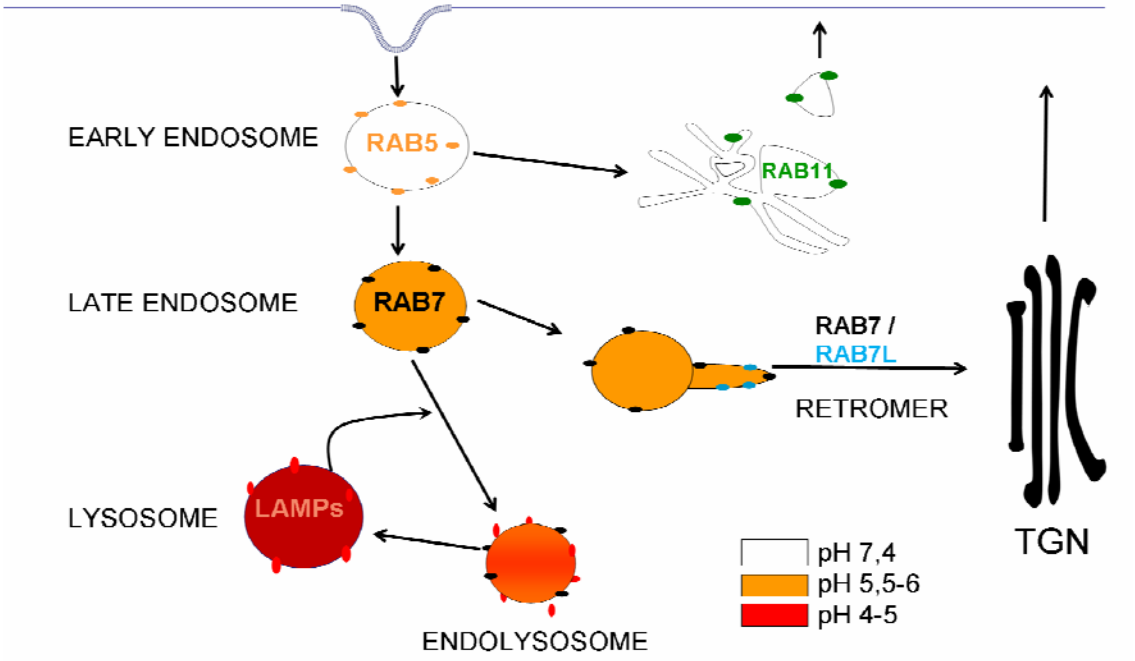

FIGURE 6. Endocytosis

General model of endocytosis and link to other membrane trafficking events. E*n route* endosomal compartments acquire a progressive drop in luminal pH and switch membrane components. Cargo entering by endocytosis can recycle back to the plasma membrane via Rab11-positive recycling endosomes from Rab5-positive sorting endosomes. Alternatively, endocytic cargo can take a degradative route of trafficking to Rab7-positive late endosomes. Then, late endosomes fuse with lysosomes (LAMP-positive) for degradation of contents. Degraded products translocate to the cytoplasm, and the autolysosome is recycled back to lysosome by lysosomal reformation. Various transmembrane receptors, such as the M6PR, are sorted back to the Golgi by retromer complex. Rab7 and Rab7L are important in this trafficking.

Rab7 is a "master" regulator of late endocytic membrane transport, protein sorting, endosomal maturation and autophagy, orquestrating the temporal and spatial regulation of different trafficking events [315]. A number of Rab7 effectors have been identified, including the VPS34/p150 complex, an α-proteasome subunit (XAPC7) [316], a modulator of endosomal acidification (Rab7-interacting ring-finger protein Rabring 7) [317], and modulators of microtubule-mediated transport of late endosomes Rab7-interacting lysosomal protein (RILP) [318] and FYCO [319].

Indeed, Rab7 is involved in microtubule-mediated transport to and from the cell periphery through its effectors. RILP is involved in the regulation of endo-lysosomal morphogenesis and microtubule (MT) minus-end directed transport through cooperation with Oxysterol-binding protein Related Protein 1 (ORP1L) [320], another Rab7 effector, to recruit the dynein/dynactin complex [321]. RILP may facilitate Rab7-regulated membrane fusion and MT minus-end directed vesicle movements towards the microtubule organizing center (MTOC). In contrast, a Rab7–FYCO1–kinesin interaction (with a possible involvement of LC3 and PI3P) has been proposed to regulate the MT plus-end directed transport of vesicles to the periphery as well. Since motility of endosomes depends on dynein and kinesin motors, providing opposing forces that move endosomes in opposite directions, Rab7 might act as master regulator in membrane trafficking, deciding the direction of the bidirectional transport on microtubules by its differential interaction with FYCO-kinesin or RILP-dynein-dynactin [322].

Rab7 also seems to be required for the recruitment of the retromer complex, suggesting that it participates in retrograde transport between endosomes and the Golgi apparatus [323]. The retromer is a multimeric complex that mediates retrograde transport of transmembrane proteins to the trans-Golgi network (TGN). For instance, the mannose 6-phosphate receptor (M6PR), which is involved in the delivery of acid hydrolases from the TGN to endosomes, is sorted back to the Golgi by retromer complex. It is composed of sorting nexins and other proteins (Vps26, Vps29 and Vps35) recruited to the cytosolic surface of EEs and maturing LEs [324, 325]. The Vps trimer (Vps26, Vps29 and Vps35) specifically binds to activated Rab7(-GTP) and localizes to Rab7-containing endosomal domains [324], (see figure 6).

Once LEs are in the perinuclear area they may fuse with other LEs or with lysosomes to become endolysosomes. By fusing with lysosomes, the LEs follow what is essentially a unidirectional, dead-end pathway. The core machinery of fusion includes cytosolic factors, such as N-ethylmaleimide-sensitive factor (NSF), soluble NSF-attachment proteins, Rab7, and HOPS proteins, the formation of a trans-SNARE complex, and a late requirement for calcium released from the lumen of the fusing organelles [272].

Alternatively to the degradative pathway, LEs can be transported to plasma membrane where they exocytose their digested material to the extracellular milieu as exosomes. Interestingly, a similar behaviour has been described as well for amphisomes [248]. Importantly, a role for exosomes in the progression of PD has been recently suggested via α-synuclein release and PD transmissibility [326].

Lysosomes

Lysosomes are the degradative organelles of higher eukaryotic cells. The lysosomal compartment can be defined as primary lysosomes, as well as lysosomes generated through fusion with endosomes, phagosomes, macropinosomes and autophagosomes. Lysosomes comprise the end point of the degradation process and act, in part, as storage vesicles for lysosomal components ready to be redistributed. These components include the hydrolases, the limiting membrane protected by a complex and substantial glycocalyx on its luminal leaflet, the heavily glycosylated integral membrane proteins LAMPs and other substances resistant to degradation. While the components of LEs are mainly degraded in the lysosomal environment, it has been suggested that some components such as MPR or tetraspanins may escape degradation through vesicle retrieval by the retromer complex, contributing to the maintenance and generation of lysosomes [324, 325].

2.2.3 Receptor-mediated endocytosis

Receptor-mediated endocytosis occurs via diverse vesicular uptake mechanisms, but the best-identified pathway is mediated by CCVs (see above) [327].

Epidermal Growth Factor Receptor (EGFR)

The Receptor Tyrosine Kinase (RTK) superfamily, of which EGFR is the prototypical member, controls the proliferation, differentiation, migration, adhesion and

cell survival of a wide range of cell types. EGFR is a 170 kDa transmembrane glycoprotein with kinase activity [328].

The binding of EGF induces dimerization of the receptor, which results in the activation of EGFR kinase and receptor trans-autophosphorylation on tyrosine residues in the cytoplasmic domain of the EGFR [328].

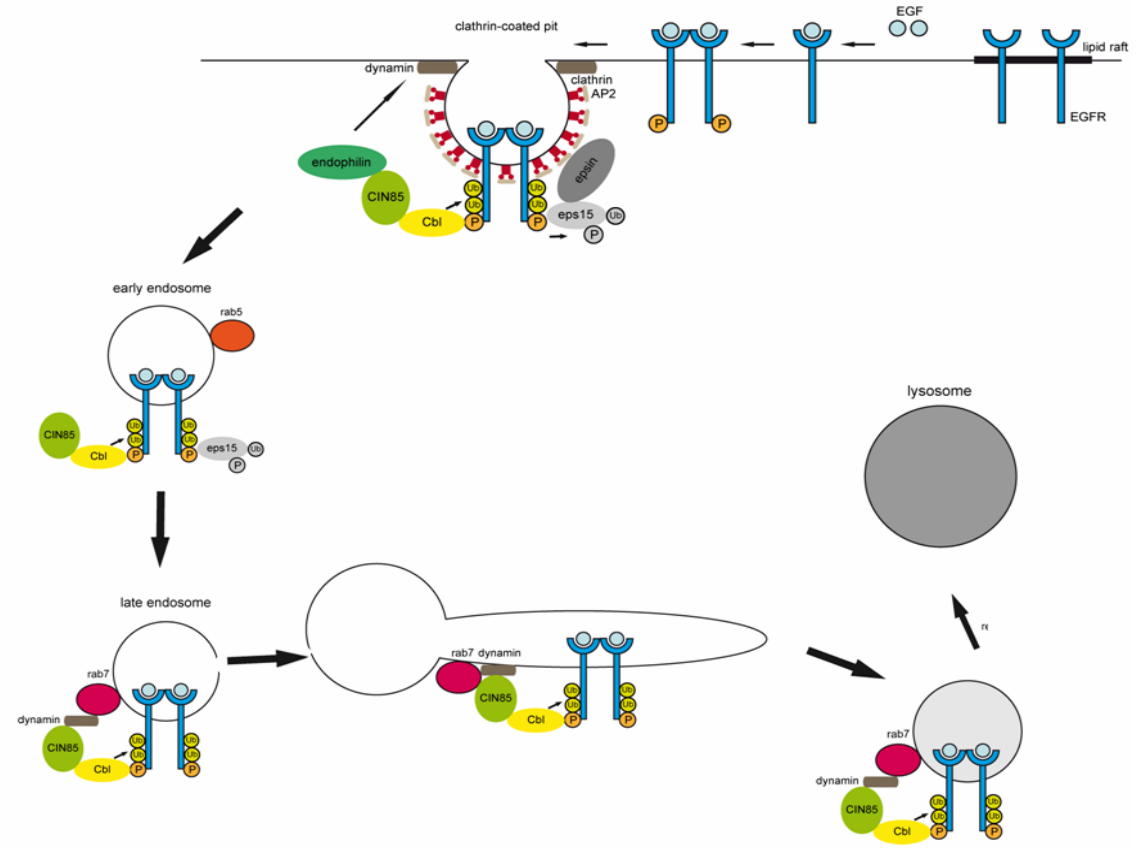

FIGURE 7. Trafficking of EGFR receptor Upon ligand binding, the EGFR dimerizes and is internalized through a coated pit pathway. The receptor moves through the endocytic compartments from early Rab5-positive to late Rab7-positive endosomes. The EGFR gets internalized into ILVs (not shown). The Cin85-Dyn2-Rab7 complex is necessary at the late compartment to pinch off late-endosomal vesicles, followed by degradation of the EGFR in lysosomes. Figure adapted from [329].

After pinching-off from the plasma membrane, the internalized receptor-ligand complexes commonly follow the degradative pathway through the endocytic compartments, (see figure 7).

Cbl-interacting protein of 85 kDa (CIN85) functions as an adaptor by binding to various endocytic proteins such as endophilin, clathrin adaptor protein (AP)-2 complex and the adaptor protein GRB2. These complexes regulate EGFR endocytosis by changing the curvature of the plasma membrane. In particular, endophilinA is mainly localized to the synaptic vesicle pool via interactions with rab3, but acts at the plasma membrane as a membrane-bending and curvature-sensing molecule to participate in clathrin-mediated endocytosis together with dynamin (reviewed in [330]). Dynamins are large GTPases that participate in vesicle scission as well. Generally, dynamin and CIN85 have been thought to play a role in regulation of EGFR internalization from the plasma membrane. [331]. However, they participate not only in the initial steps of EGFR internalization, but also in post-endocytic receptor trafficking and degradation at the level of the Rab7-positive late endosome, (see figure 7). Disruption of the dynamin2-CIN85 interaction results in a defect in vesicle budding from late endosomes, with a concomitant accumulation of the EGFR in this compartment [332].

Formation of receptor-signalling protein complexes initiates activation of several signalling pathways. Downstream signalling of EGFR is tightly regulated both spatially and temporally by controlling its internalization and degradation [333]. Signalling from endocytosed EGFR can be down-regulated by two different mechanisms: ESCRT-mediated sequestration on ILVs of endosomes before lysosomal delivery, and degradation and dephosphorylation by protein tyrosine phosphatases, such as protein tyrosine phosphatase 1B [334].

3. ACIDIC CALCIUM STORES

As mentioned previously, the spatiotemporal pattern of calcium signalling is crucial for the specificity of cellular responses. Changes in cytosolic calcium can be due to either entry from the extracellular space or release from intracellular calcium stores. The ER is the best characterized store of calcium within the cell. IP_3 and cyclic ADP ribose both mobilize calcium from ER through activation of IP_3 and ryanodine receptors, respectively [335, 336]. Mitochondria are also an important calcium store and their connection with the ER calcium store has shown to be crucial for cellular viability and mitochondrial dynamics [337].

Apart from the ER and mitochondria, a range of acidic organelles also serve as significant calcium stores in mammals [338].

3.1 The acidic calcium stores

Endosomes and lysosomes are considered calcium stores [338]. Endosomes pinching off from the plasma membrane are thought to contain high levels of calcium due to the elevated concentrations of this ion in the extracellular fluid [309] whilst only having a slightly acidic pH (pH 6.3–5,9) [309]. It has been proposed that the uptake of H+ into endosomes mediated by the proton-pumping ATPase must be balanced to maintain the electroneutrality, and that this may happen by calcium efflux via endosomal calcium channels [339].

Even though direct measurement of luminal calcium concentration of lysosomes is difficult, the average free calcium concentration in lysosomes has been reported to be in a similar range as that of the ER [340]. Calcium has an important regulatory function in homotypic and heterotypic fusions of LEs and lysosomes and during lysosomal reformation [341], analogous to the well-described role of calcium in regulated secretion [342]. Chelation of luminal calcium blocks fusion, suggesting that calcium release from the acidic calcium stores, and generally intraluminal calcium, may be required for the functioning of the degradative pathway [272, 343, 344].

Secretory vesicles and the Golgi complex

Whilst less acidic (pH~ 6.6), the Golgi apparatus also contains substantial levels of calcium and calcium release channels such as the IP_3R [345]. In addition, secretory

vesicles contain calcium and calcium release channels [346, 347] which is particularly interesting due the role of calcium for vesicle fusion [342].

3.2 Channels

Several calcium-permeable channels are present on acidic organelles. Although mainly located in the ER, IP_3 and ryanodine receptors are found to be also located on acidic calcium stores [348]. However, nicotinic acid adenine dinucleotide phosphate (NAADP) has been postulated to be the most powerful endogenous calcium-mobilizing messenger known to date and the major regulator of calcium release from endolysosomes [349-351].

Two different families of channels have been proposed to be intracellular NAADP targets:

1. Transient receptor potential (TRP) superfamily, particularly the mucolipins (TRPMLs), are found on acidic stores such as lysosomes and endosomes [352]. Mutations in the TRPMLs channels are responsible for several lysosomal-storage disorders [352]. There are three TRPMLs, displaying differential albeit partially overlapping localization within the endo-lysosomal compartment: TRPML1 localizes to LEs and lysosomes, TPRML2 to recycling endosomes, LEs, lysosomes and the plasma membrane, and TRPML3 is present throughout the endolysosomal system and at the plasma membrane [338]. TRPML1 has been proposed as the calcium channel responsible for the local release of calcium crucial for fusion within the endo-lysosomal system [353]. There is evidence that TPRML1 may be an NAADP target, whilst other studies indicate that $PI(3,5)P_2$, rather than NAADP, may regulate the channel [354, 355]. Interestingly, TRPML1 has been reported to co-immunoprecipitate with the other family of calcium channels, the two pore channels (TPCs) [356].

2. There have been several independent studies describing the TPCs as primary NAADP targets [338]. Controversy about the ionic specificity of the TPCs has been recently raised, as TPCs was shown to behave as a sodium-selective channel activated by $PI(3,5)P_2$, not by NAADP. In addition, mTOR has been shown to regulate TPCs during regulation of amino acid homeostasis [357]. Therefore, further studies will be necessary to resolve those discrepancies; however, at present, the vast majority of studies indicate that TPCs can conduct calcium [358, 359].

Two TPC isoforms are present in humans. TPC1 localizes to both endosomes and lysosomes, whereas TPC2 is predominantly lysosomal [360]. TPCs possess an unusual structure of two repeated, 6 TMD-containing domains and a putative pore-forming region between the predicted TMD5 and TMD6, and they form dimers [361]. Like other lysosomal proteins which have to be protected from the highly acidic lumen, TPCs are glycosylated.

Inhibition of the NAADP-mediated calcium response occurs upon downregulation of the TPCs, or when overexpressing TPCs with a mutation in the pore-forming region (L273P for TPC1, L265P for TPC2) [362]. Furthermore, NAADP-mediated calcium release can be abolished by different mechanisms, including inhibition of agonist-evoked calcium signals by self-inactivation of NAADP, the use of Ned-19, a selective membrane-permeable NAADP antagonist[363], and the use of lysosomotropic agents such as the cathepsinC substrate glycylphenylalanine-2-naphthylamide (GPN) and the V-type ATPase inhibitor bafilomycinA1 [364, 365].

Release of calcium from the endo-lysosomal compartment, triggered by NAADP, evokes cytosolic calcium signals which can by amplified through calcium-induced calcium release (CICR) from the ER [366], (see figure 8).

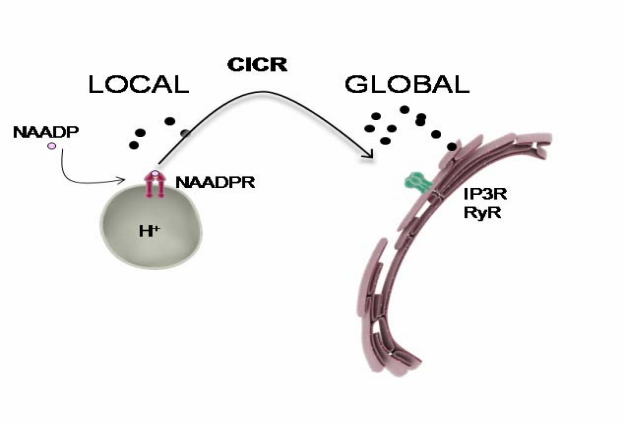

Figure 8. NAADP-mediated calcium signalling.

NAADP triggers its receptor and the resulting local calcium signal is then amplified by ER calcium release in a CICR manner to mediate a larger global calcium signal. Figure adapted from [367].

Membrane contact sites between ER and the endo-lysosomal system have been suggested to correspond to NAADP trigger zones [360]. This interaction has been

proposed to be similar or maybe shared with that which mediates cholesterol exchange between ER and LEs, and it is performed by the interaction of Rab7 and RILP on the LE and the VAMP-associated ER protein (VAP) through ORP1L [360].
Several cellular processes are regulated by acidic calcium store release. For example, NAADP-mediated calcium release has been related to cell differentiation and induction of neurite outgrowth [368]. NAADP has also been shown to increase the levels of autophagic markers in cultured astrocytes [368]. NAADP-mediated release of calcium from the endo-lysosomal compartment can cause a partial alkalinization of acidic stores and induce lipid accumulation [349]. The mechanism by which NAADP affects luminal pH remains unknown, but it has been proposed to be secondary to calcium release from acidic stores [349]. Given that the luminal pH is crucial for endo-lysosomal events including fusion and degradation activity, deregulation of endo-lysosomal calcium homeostasis has been proposed as a primary cause of the lysosomal-storage disorder Niemann Pick C1, where the reduced lysosomal calcium results in a block in endocytic trafficking to lysosomes [343].

As mentioned above, several studies indicate a possible role for LRRK2 in regulating autophagic and endocytic trafficking, even though the precise mechanism(s) underlying the effects have remained unclear. The present thesis attempted to study the implication of pathogenic LRRK2 in altered endomembrane trafficking, with a focus on autophagy and endocytosis.

IV. SPECIFIC AIMS

1. Determine whether pathogenic LRRK2 expression causes alterations in autophagy induction, and the signalling mechanism(s) involved.
2. Study whether LRRK2 expression causes alterations in lysosomal homeostasis which may affect autophagic flux.
3. Determine whether LRRK2 expression alters cell viability in the context of stressors which activate autophagic pathways.
4. Study the molecular mechanism(s) by which pathogenic LRRK2 may cause changes in autophagic flux and lysosomal degradation.
5. Evaluate whether LRRK2 expression causes alterations in receptor-mediated endocytosis.
6. Determine whether possible alterations in endocytosis occur early and/or late in the endocytic process.
7. Evaluate the effect of LRRK2 on the functioning/morphology of affected endocytic organelles.
8. Determine the pathway(s) by which LRRK2 may cause endocytic alterations.
9. Evaluate whether overexpression of a series of Rab proteins can rescue the effect of mutant LRRK2 on endocytosis, and whether LRRK2 alters Rab protein levels and/or activity.

V. Materials and Methods

1. Buffers and solutions

Where indicated, pre-made buffers were used, with a composition according to manufacturers. For all others buffers, components were purchased from SIGMA and were of molecular biology grade.

Cell lysis buffer. 1 % SDS in PBS containing 1 mM PMSF, 1 mM Na_3VO_4 and 5 mM NaF, pH 7.4.

Complete Dulbecco's Modified Eagle's Medium (DMEM). 1X DMEM (PAA) containing sodium pyruvate, phenol red, 1g/l or 4.5 g/l D-glucose and 4 mM L-glutamine supplemented with 10% (w/v) heat-inactivated Fetal Bovine Serum (FBS, Gibco), non-essential amino acids (Sigma, penicillin (100 units/ml) and streptomycin (100 units/ml) (Sigma).

IP buffer. 1% NP-40, 50 mM Tris/HCl, 150 mM NaCl, phosphatase inhibitor cocktails 2 and 3 (Sigma) and protease inhibitor cocktail (Roche), pH 7.4.

Hank's solution. 10 mM HEPES, 140 mM NaCl, 5 mM KCl, 1.3 mM $Mg_6Cl_2.H_2O$, 2 mM $CaCl_2.H_2O$, 1g/l D-glucose, pH 7.4.

Phosphate Buffered Saline (PBS). In tablet form. One tablet dissolved in 200 ml of deionized water yields 0.01 M phosphate buffer, 0.0027 M potassium chloride and 0.137 M sodium chloride, pH 7.4.

PBS-Triton 0.05%. 1X PBS, supplemented with 0.05% Triton X-100, pH 7.4.

Pull down buffer. 20 mM HEPES, 100 mM NaCl, 5 mM $MgCl_2$, 1 % Triton X-100 and c*O*mplete protease inhibitor tablets (Roche), pH 7.4.

Purification buffer. 25 mM Tris-HCl, 1 M NaCl, 0.5 mM EDTA, 1 mM DTT, 0.1% Triton X-100, c*O*mplete protease inhibitor tablets (Roche), pH 7.4.

Running Buffer. 25 mM Tris, 190 mM glycine, 0.1 % SDS, pH 8.6.

Sample buffer 5X. 250 mM Tris, 10 % SDS, 20 % Glycerol. Bromophenol blue.

Tris-buffered Saline (TBS). 25 mM Tris, 150 mM NaCl, 2mM KCl, pH 7.6.

TBS-Tween (PBST). 1X TBS, supplemented with 0.01% Tween-20, pH 7.4.

Transfer Buffer. 25 mM Tris, 192 mM glycine, 20% methanol, pH 8.3.

2. Molecular biology

2.1 Plasmid constructions

To generate the LRRK2 kinase domain-GFPemd construct (kinase-GFPemd), the human LRRK2 kinase domain (amino acids 1844–2143) was PCR amplified using full-length LRRK2 as template, with EcoRI/BamHI sites on either end. VAMP2-GFPemd [369] was digested with EcoRI/BamHI to release VAMP2, and the PCR-amplified kinase domain cloned in-frame with the GFPemd at the C-terminal end. To generate the LRRK2 kinase domain pCMV construct (pCMV-kinase), human LRRK2 kinase domain (amino acids 1844–2143) was PCR amplified using full-length LRRK2 as template, with SacI/BamHI sites on either end. pCMV-VAMP2 [369] was digested with SacI/BamHI to release VAMP2, and religated with the digested, PCR-amplified kinase domain.

To generate the full-length human LRRK2 pCMV vector (pCMV-flLRRK2), pGEMT-LRRK2 was digested with SacII/MluI to release fl-LRRK2. Quick Change Site Directed Mutagenesis was performed with the empty pCMV vector to introduce a SacII site 5′ to the MluI site, followed by digestion of the vector with SacII/MluI and introduction of flLRRK2.

K1906M and G2019S mutations were introduced into all respective vectors by Quick Change Site Directed Mutagenesis, and the identity of all constructs verified by direct sequencing of the entire coding regions.

The double-myc-tagged, full-length wild-type and mutant human LRRK2 constructs were kindly provided by Dr M. Cookson (NIH, Bethesda, USA), or obtained through Addgene. N-terminally myc-tagged constructs for wild-type, dominant-negative and constitutively active AMPKα1, as well as N-terminally myc-tagged constructs for wild-type and dominant-negative AMPKα2 were kindly provided by Dr. D. Carling (MRC, Imperial College London, UK). Bcl-2 and its organelle-specific mutants were kindly provided by Dr. M. Jaättelä (Institute of Cancer Biology, Danish Cancer Society, Denmark) and Dr. D.W. Andrews (McMaster University, Hamilton, Ontario, Canada). Human TPC1-mRFP, TPC1-L273P-mRFP and TPC2-mRFP have been previously described [362] and were obtained from Dr. S. Patel (University College London, London, UK). The L265P mutation in TPC2-mRFP was generated by Quick Change

Site Directed Mutagenesis and verified by direct sequencing. The tandem-tagged LC3 construct mCherry-EGFP-LC3B (human) was kindly provided by Dr. T. Johansen (University of Tromsø, Norway), and EGFP-LC3 (rat) was provided by Dr. T. Yoshimori (National Institute for Basic Biology, Okazaki, Japan) and Dr. J. Oliver (Institute of Parasitology and Biomedicine 'López-Neyra', CSIC, Granada, Spain). The G120A mutation was introduced into both tagged LC3 constructs by Quick Change Site-Directed Mutagenesis (Stratagene) and verified by direct sequencing. Myc-tagged VPS26, YFP-tagged VPS29 and HA-tagged vps35 constructs were kindly provided by Dr. J. Bonifacino (University of Berkeley, California, USA). YFP-tagged VPS29 was subcloned into a GFPemd-vector and verified by direct sequencing. For this purpose, VAMP2-GFPemd [369] was digested with EcoRI/BamHI to release VAMP2, and the VPS29 fragment PCR amplified with EcoRI/BamHI sites on either end, and ligated into the GFPemd vector. GFP-tagged Endophilin A2 construct was kindly provided by Dr. P. De Camilli (Yale School of Medicine, New Haven, USA) and EndophilinA1-HA and EndophilinA3-myc were provided by Dr. G. Auburger (Goethe University Medical School, Frankfurt am Main, Germany). The Rab7 binding domain of RILP (murine, amino acids 220-299) and myc-tagged TBC1D15 (murine) constructs were kindly provided by Dr. A. Edinger (University of California, California, USA). Full-length GFP-tagged RILP and dominant-negative RILP were provided by Dr. C. Bucci (Universitá del Salento, Lecce, Italy). FLAG-CIN85 wild-type and mutant (ACW-Y) constructs and FLAG-DYN2 were kindly provided by Dr. M. McNiven, and GFP-tagged Rab29/Rab7L construct was provided by Dr. J. Galán (Yale University School of Medicine, New Haven, USA).

2.2 Plasmid purification

Clones were picked and grown overnight in 100 ml LB broth with the appropriate antibiotic. For LRRK2 plasmid purifications, cultures of 500 ml were grown at 28 ºC. DNA was purified using Promega midiprep kit according to manufacturer's instructions. Before transfections, a sample of all purified LRRK2 plasmids were digested with EcoRI for 2 h at 37 ºC and run in 2 % agarose gels prepared in TAE buffer to assure no DNA rearrangements/recombination events had occurred.

3. Cell culture

3.1 Cell lines and primary cells

For autophagy studies, HEK293 (Human Embryonic Kidney 293) cells were used. HeLa cells (a human cell line derived from cervical cancer) were mainly used for endocytosis studies. Both cell lines have been used previously to transiently overexpress LRRK2, and both express reasonable levels of endogenous LRRK2.

To study effects of endogenous mutant LRRK2, primary human dermal fibroblasts were employed. Age- and sex-matched control and G2019S mutant LRRK2 fibroblasts were provided by Dr. A. López de Munain (Biodonostia, San Sebastian, Spain).

3.1.1 Culture and transfection of cell lines

HEK293 and HeLa cells were cultured in 100 mm dishes and grown at 37 °C in 5 % CO_2 in complete DMEM medium with low or high glucose (1 g/l or 4.5 g/l for HEK293 or HELA, respectively) supplimented with 10% heat-inactivated fetal bovine serum (Invitrogen), penicillin (100 units/ml) and streptomycin (100 units/ml) and non-essential amino acids (Sigma),. Confluent cells were harvested using 0.05 % trypsin, 0.02 mM EDTA in PBS and subcultured at a ratio of 1:4 to 1:6. Cells were plated onto 6well plates and the following day, at 70–80 % confluency, were transfected using Lipofectamine 2000 (Invitrogen) according to manufacturer's specifications for 4 h in DMEM, followed by addition of fresh full medium.

Single transfections were performed using 3.5 μg of plasmid of interest and 10 μl of Lipofectamine 2000. For double-transfections, 2.5 μg of each plasmid was used, and for triple-transfections, 1.7 μg of each plasmid was employed. The DNA ratio for co-transfections in the case of full-length LRRK2 constructs was 1:5, using a total of 1 μg of DNA . Transfected cells were re-plated the next day at a 1:3 ratio onto coverslips in 6-well plates.

LRRK2 was expressed for 48 h unless otherwise indicated. Various proteins involved in endolysosomal trafficking were only expressed for 24 h, due to the observation that overexpression of these proteins can result in abnormal endocytic/lysosomal structures.

3.1.3 Primary fibroblast culture

Skin samples had been obtained from five PD patients (G2019S) and five healthy control individuals who had undergone plastic surgery. All subjects had given informed consent using forms approved by the Ethical Committee on the Use of Human Subjects in Research (Hospital Donosti, San Sebastian, Spain). PD patients had been diagnosed with familial PD at the Movement Disorders Unit of Donosti Hospital, and had been sequenced and found to have a G2019S mutation. Fibroblasts were obtained at passage 1 or 2, and were cultured in IMDM (Iscove's Modified Dulbecco's Medium) medium (Gibco), containing 10 % FBS (Invitrogen) and antibiotics where necessary. The medium was changed every two days. Cells were harvested using 0.25 % trypsin, 0.2 g/l EDTA (SIGMA) and subcultured at a ratio of 1:2. Cells were subcultured at a ratio of 1:2, and seeded at equal densities on coverslips. Cells were seeded to coverslips in 24-well dishes for cell biological experiments (13 mm diameter coverslips). For all experiments, comparison between control and G2019S LRRK2 mutant fibroblasts were performed in a passages *in vitr*o. All analyses were carried out on passages 4-12, and no passage-dependent differences were observed.

3.2 Reagents

LRRK2-IN-1, TAE684 and CZC25146 were obtained through the Michael J. Fox Foundation (USA), and GSK2578215A was from Tocris Bioscience (Missouri, USA). NAADP-AM and NED-19 were synthesized as previously described (54,65), and obtained from Dr. G. Churchill (Oxford University, Oxford, UK). Torin was a generous gift of Dr. D. Sabatini (Whitehead Institute for Biomedical Research, Cambridge, USA). 3-MA (3-methyladenine), NH_4Cl, bafilomycin A1, E-64d, pepstatin A, nigericin, trichostatin A, dantrolene, puromycin and ionomycin were from Sigma. STO-609 (7-oxo-7H-benzimidazo[2,1-a]benz[de]isoquinoline-3-carboxylic acid) and L690,440 (1-[(4-hydroxyphenoxy)ethylidene] bis [[phosphinylidyne bis(oxymethylene)] -2,2-dimethylpropanoate) were from Tocris Bioscience (Missouri, USA). Compound C, cycloheximide and MG-132 were from Calbiochem. BAPTA-AM was from Invitrogen, rapamycin was from LC Laboratories (Woburn, USA) and chloroquine was a generous gift from L. Ruiz Pérez (Institute of Parasitology and Biomedicine 'López-Neyra', CSIC, Granada, Spain).

3.4 Cell biology methods

3.4.1 Immunofluorescence staining

Immunofluorescence staining protocols were optimized depending on the antibody and/or cell type employed during this thesis. Fixation/permeabilization protocols, antibody dilutions, incubation times and detection systems were developed individually for each antibody to obtain optimal results.

General protocol: Cells on coverslips were fixed with 4% paraformaldehyde (PFA) in PBS for 20 min at room temperature. Cells were permeabilized in 0.5 % Triton X-100 in PBS (3 × 5 min) and preincubated in blocking buffer (10 % goat serum; Vector Laboratories) in 0.5 % Triton X-100 in PBS for 1 h at room temperature, followed by exposure to primary antibody diluted in blocking buffer for 1 h at room temperature. Cells were washed in 0.5 % Triton X-100 in PBS and incubated with goat anti-rabbit or anti-mouse AlexaFluor-488- or 594-conjugated secondary antibody (1:1000, Invitrogen), dependent on application, in 0.5 % Triton X-100 in PBS for 1 h at room temperature, followed by washes in 0.5 % Triton X-100 in PBS, PBS, H_2O and a rinse in 70% ethanol. Fixed cells were mounted using mounting medium containing DAPI (Vector Laboratories).

Whilst this protocol was successful for most antibodies, staining protocols had to be optimized for the following antibodies and cells:

Rab antibodies (HEK293 and fibroblasts): Cells on coverslips were fixed with 2% PFA in PBS for 10 min at room temperature. Cells were permeabilized in 0.05 % saponin in PBS for 3 min, and preincubated in blocking buffer (2% goat serum in 0.05 % saponin in PBS) for 1 h at room temperature, followed by exposure to primary antibody diluted in blocking buffer for 1 h at room temperature temperature (anti-Rab5B (A-20) 1:50, Santa Cruz and anti-Rab7 (R4779) 1:50, Sigma). Cells were washed in PBS (3 × 5 min washes) and incubated with goat anti-rabbit or anti-mouse AlexaFluor-488 or 555-conjugated secondary antibody (1:1000, Invitrogen) diluted in PBS, for 1 h at room temperature, followed by washes in PBS. Fixed cells were mounted using mounting medium containing DAPI (Vector Laboratories).

LAMP antibodies (fibroblasts): Cells on coverslips were fixed with 4% PFA (in PBS) for 1 hour at room temperature. Cells were incubated in blocking buffer with

detergent (1% goat serum in 0.05 % saponin in PBS) for 2 h at room temperature, followed by exposure to primary antibody diluted in blocking buffer for 1 h at room temperature (anti-LAMP1 (L1418) 1:50, Sigma). Cells were washed in 0.05 % saponin in PBS (3 × 5 min washes) and incubated with goat anti-rabbit AlexaFluor-488-conjugated secondary antibody (1:1000, Invitrogen) diluted in PBS for 1 h at room temperature, followed by washes in PBS. Fixed cells were mounted using mounting medium containing DAPI (Vector Laboratories).

LC3 and p62 (HEK293 and fibroblasts): Cells on coverslips were fixed with 4% PFA (in PBS) for 20 min at room temperature. Cells were washed with PBS three timens and incubated in blocking buffer (50 mM glycine in 50 mM TRIS, pH 7.4) for 15 min at room temperature, followed by permeabilization in 0.1 % SDS for 3 min and washing three times in PBS. Then cells were incubated with the primary antibody diluted in PBS for 1 h at room temperature (anti-LC3B (2775) 1:100, Cell Signaling and anti-P62 (610832) 1:50, BD). Cells were washed in PBS (3 × 5 min washes) and incubated with goat anti-rabbit or mouse AlexaFluor-488-conjugated secondary antibody (1:1000, Invitrogen) diluted in PBS for 1 h at room temperature, followed by washes in PBS. Fixed cells were mounted using mounting medium containing DAPI (Vector Laboratories).

Rhodamine phallodin staining: for determining the morphology of fibroblasts, cells were stained with rhodamine phalloidin (Molecular Probes) after immunostaining. Incubations with rhodamine phalloidin (Invitrogen) were performed at a final concentration of 82.5 nM (in PBS) for 15 min at room temperature. Cells were washed in PBS and mounted for analysis as described above. The stained actin cytoskeleton was imaged by 543 nm HeNe Laser line and a 580–650 nm emission band pass.

3.4.2 Acidic organelle-selective pH indicators

Weakly basic amines selectively accumulate in cellular compartments with low internal pH and can be used to investigate the biosynthesis and pathogenesis of lysosomes [370]. LysoTracker and Lysosensor probes (Invitrogen) are fluorescent acidotropic probes for labeling and tracing acidic organelles in live cells, as well as in fixed cells in the case of Lysotracker probes. Lysotracker Red DND-26 and Lysosensor Green DND-167 were used according to manufacter's specifications. Lysotracker Red DND-26 was tested in fixed and living cells, and behaved identically. It was used for

experiments where fixation was needed. For this purpose, cells on coverslips were incubated in prewarmed probe–containing full medium , (500 nM Lysotracker Red DND-26) for 10 min at 37ºC, the loading solution was replaced with fresh medium, and fixation and immunostaining performed as described above. For live cell imaging, cells were plated on microwell dishes containing 35 mm diameter glass bottom (IBIDI) coated with poly-L-lysine hydrobromide. Cells were incubated in prewarmed probe–containing medium (1 μM Lysosensor Green DND-167 for 10 min at 37ºC in full medium), the loading solution was washed off twice with PBS and cells observed by confocal microscopy in PBS.

3.4.3 Lipid staining

Cells on coverslips were carefully rinsed in PBS, then fixed with 4 % PFA (in PBS) for 10 min at room temperature. Cells were washed with PBS, followed by incubation in 2 μM BODIPY 493/503 (Invitrogen) in PBS for 5 min, followed by three washes in PBS. Cells were mounted as indicated above.

3.4.4 Assessment of cell viability

Cell survival was determined in fixed cells mounted in mounting medium containing DAPI by counting cells on a Zeiss microscope using a ×100 oil-immersion objective. For each experiment, an average of 100 cells from several random fields were quantified, and condensed or fragmented nuclei were scored as apoptotic cells. Occasionally, apoptotic cells were also quantified using the DeadEnd Fluorometric TUNEL System (Promega) according to manufacturer's specifications.

3.4.5 Assesment of autophagy flux

Autophagic activity was evaluated by quantifying the average number of GFP–LC3 punctae per cell. For this purpose, z-stacks of random fields of cells were captured at ×100 magnification on a Leica confocal microscope. The number of GFP–LC3 punctae per cell was either obtained by manual counts performed by an observer blinded to condition, or more regularly using an NIH ImageJ macro called GFP–LC3 [194] Alternatively, random fields of transfected cells were imaged on a Zeiss microscope using a ×100 oil-immersion objective by an individual blinded to the experimental conditions, and the number of GFP–LC3 punctae per cell counted manually. Whilst the decreased resolution results in identification of overlapping or

clustered punctae as a single large puncta, and thus will underestimate the number of GFP–LC3 punctae per cell, the relative changes observed using this determination were similar to those using the high-resolution analysis described above. For all determinations of LC3–GFP punctae per cell, between 30 and 50 randomly chosen transfected cells were analysed per experiment and condition. For quantification of yellow and red mCherry-EGFP–LC3 (td-tag-LC3) punctae, pictures were captured at ×100 magnification on a confocal microscope, and the number of yellow and red punctae analysed as described above from 40 randomly chosen transfected cells per experiment and condition.

3.4.6 Assesment of endocytic trafficking

Alexa555-EGF binding and uptake assays: HeLa cells were co-transfected with 4 μg of LRRK2 constructs (or empty pCMV vector) and 1 μg of GFP, Rab5-, Rab7- or LAMP1-GFP constructs using Lipofectamine 2000 (Invitrogen, 10 μl per well of a 6-well plate) in serum-free medium for 4 h as indicated by manufacturer's instructions, followed by replacement of fresh full medium. After a further 24 h, cells were re-seeded onto coverslips in 24-well plates and then serum-starved for 16 h. The following day, after 48 h of DNA overexpression, serum-free medium was replaced by 4 ºC fresh serum-free medium containing 100 ng/ml EGF-555 (Invitrogen, E35350) and cells were incubated for 30 min at 4 ºC. Cells were then washed twice in ice-cold PBS and transferred to pre-warmed serum-free media for the indicated periods of time to allow uptake of the bound fluorescent EGF. At the assay endpoint, cells were fixed (4 % PFA in PBS, 15 min, room temperature) and softly permeabilized (0.5 % Triton-X100/PBS for 3 min). . To confirm that labelled EGF was only surface-bound, control cells were washed twice with PBS, followed by acid stripping (0.5 M NaCl, 0.2 M acetic acid, pH 2.5) for 3 min at 4ºC. Cells were then stained for the presence of LRRK2 (anti-myc) or other constructs as indicated and described above, using AlexaFluor 488 as secondary.

Quantification of EGF dots was preformed by using ImageJ by an observer blinded to condition, as indicated below.

Rhodamine-EGF uptake and in vivo imaging: For live-cell fluorescence microscopy, co-transfected cells were reseeded onto 35-mm glass-bottom dishes (IBIDI Biosciences) the following day, and serum-starved for 16 h. Medium was replaced by phenol-free, serum-free DMEM (GIBCO), and cells were incubated with Rhoadmine-

EGF (Rh-EGF, 200 ng/ml, Invitrogen) for 90 min at 37 ºC before imaging as previously described (35). Time-lapse images were acquired on a Leica TCS-SP5 confocal microscope using a 100X 1.4 NA oil UV objective (HCX PLAPO CS). Images were taken every 1.4 sec over a total time of 86 sec for each movie (total 60 frames) with pinhole 1.22 airy. During imaging, cells were maintained at 5 % CO2 and at 37 ºC. The length GFP-Rab7-positive tubules were quantified using Leica Applied Systems (LAS AF6000) image acquisition software. GFP-rab7-positive structures were scored over the entire imaging period as late endosomal tubules if they were RhEGF-positive and > 900 nm. 7-15 cells were quantified per condition per each experiment.

3.4.7 General confocal microscopy and analysis.

Images were acquired on a Leica TCS-SP5 confocal microscope using a ×60 HCX PL APO CS 1.4 oil UV objective. Images were collected using single excitation for each wavelength separately [488 nm Argon Laser line and a 500–545 nm emission band pass; 543 nm HeNe Laser line and a 556–673 nm emission band pass; 405 nm UV diode and a 422–466 nm emission band pass (12.5% intensity)] . Ten to fifteen image sections of selected areas were acquired with a step size of 0.4 μm, and z-stack images analysed and processed using Leica Applied Systems (LAS AF6000) image acquisition software. For quantifications, all images were taken at the same exposure time and setting and analysed using ImageJ.

The JACoP pluggin of ImageJ was used for the quantification of colocalization of GFP-Rab5- or GFP-Rab7-positive compartments with Alexa555-EGF. After image thresholding, the percentage of colocalization was obtained by calculating the Mander´s coefficients (M1 for red channel (Alexa555-EGF)), and percentage of colocalization was obtained by multiplying M1 by 100

The colocalization of TPCs with lysosomal markers was performed using Leica Applied Systems (LAS AF6000) image acquisition software, adjusting thresholds to 28% for each channel, and quantifying colocalization as described above.

To measure total number of EGF-555 structures in a single cell, cells co-expressing GFP-tagged constructs were circled and a modified NIH ImageJ macro (GFP–LC3 macro) was employed. For each condition, 20 independent cells were analysed.

3.4.8 Electron microscopy

All electron microscopy experiments were performed in Dr. P. Woodman's laboratory during my stay at the Faculty of Life Sciences, Manchester University, Manchester, UK. Transfected cells were collected, resuspended in HEPES-buffered media and filtered through a 50 μm filter before FACS sorting. Sorted cells were fixed with 4% PFA, 0.1 % glutaraldehyde in 0.1 M cacodylate buffer containing 3 μM $CaCl_2$ and 7.5 % sucrose for 15 min at room temperature. Fixed cells were washed and pelleted, then cell pellets were cut into small cubes and mixed to randomize the sample. Samples were stained with reduced osmium tetraoxide, dehydrated and embedded in resin. Sections (~80 nm) were examined with an FEI TECNAI BioTWIN electron microscope. Random cells were imaged. To calculate relative volume densities, Photoshop software was used to combine separate images to obtain a complete view of each cell. Autophagic structures were recognized according to their morphological characteristics. A counting grid was superimposed on images at a random offset and intersections were scored according to the underlying structures, using the ImageJ plug-ins Grids and Cell Counter (NIH, Bethesda, MD, USA). The relative volume density of each structure was calculated by dividing the number of intersections counted for each category by the number counted for the whole cell.

4. Biochemical assays

4.1 Western blotting

Cells were rinsed once in ice-cold PBS, followed by resuspension in 1 ml of cell lysis buffer per 100 mm dish (160 μl of lysis buffer per well of a 6-well plate) (1 % SDS in PBS containing 1 mM PMSF, 1 mM Na_3VO_4 and 5 mM NaF).

Fibroblasts and HeLa cells were trypsinized, then blocked with full media and centrifugated before washing with PBS and processed for lysis.

Extracts were boiled for 5 min, sonicated and centrifuged at 13 500 rpm for 10 min at 4 °C. Protein concentrations of supernatants were estimated using the BCA assay (Pierce). Whenever possible, extracts were immediately resolved by SDS–PAGE without repeated freeze-thaws, as the latter was found to decrease detection of some phosphorylated proteins.

Antibodies used for immunoblotting included a mouse monoclonal anti-LAMP2 antibody (1:50; Santa Cruz Biotechnology), a mouse monoclonal anti-p62 antibody

(1:50; BD Transduction Laboratories), a mouse monoclonal anti-myc antibody (1:1000, Sigma) and a rabbit polyclonal anti-GFP antibody (1:1000; Abcam), a rabbit polyclonal anti-GFP antibody (1:2000, Abcam), a mouse monoclonal anti-flag antibody (1:1000, Sigma), a mouse monoclonal anti-tubulin antibody (clone DM1A, 1:10´000, Sigma), a rabbit polyclonal anti-Rab7 antibody (1:1000, Sigma) a mouse monoclonal anti-Rab7L1 antibody (1:1000, Abcam), and a rabbit polyclonal anti-EGFR antibody (1:500, Cell Signaling).

EGFR degradation assays: For EGFR degradation assays, we employed HEK293T cells, as overexpression and transfection efficiencies were much higher than in HeLa cells. Cells were transfected overnight in p-100 plates using LipoD293 (SignaGen Laboratories) with 12 μg of LRRK2 constructs or empty pCMV vector according to the manufacturer's instructions. Transfected cells were re-plated into 8 wells into a 6-well plate the following day. 48 h after transfection, cells were serum-starved for 1 h in the presence of cycloheximide (1μg/ml, Calbiochem) to block new protein synthesis [371] and subsequently stimulated with non-labeled EGF (Invitrogen, 100 ng/ml) for the indicated time points. Total cell lysates were collected in 1 % SDS cell lysis buffer (see above), and equal protein amounts per sample subjected to Western blot analysis. Densitometric quantitation of bands was performed on non-saturated films using QuantityOne software (Biorad).

Human tissues and sample preparation: Freshly frozen brain samples from deceased human subjects were collected at autopsy following informed consent from the next of kin under a protocol approved by the local ethics committee. Brain regions from healthy control and genotyped LRRK2 G2019S mutant PD patients analyzed included cortex, cerebellum and caudate. For all samples, patient age, gender, time to postmortem tissue collection and postmortem pathological analysis was known. Sample preparation and analysis was performed as previously described.

4.2 Co-Immunoprecipitation

Transfected HEK293 cells were washed in chilled PBS and pelleted by centrifugation. Pellets were resuspended in IP (immunoprecipitation) buffer (1 ml/10 cm dish) containing 1% NP-40, 50 mM Tris/HCl, pH 7.4, 150 mM NaCl, phosphatase inhibitor cocktails 2 and 3 (Sigma) and protease inhibitor cocktail (Roche) and lysates centrifuged at 13 500 rpm for 10 min at 4 ºC. Protein concentration of supernatants was

estimated using a BCA assay, and 1mg total protein was subjected to immunoprecipitation with either anti-GFP (5 µg, Abcam) or anti-LRRK2 (10 µg, N138/6, NeuroMab, UCDavis, USA) antibodies. For immunoprecipitations, lysates were incubated with antibodies for 1 h at 4 ºC, followed by addition of protein G- or protein A-Sepharose beads and overnight incubation at 4 ºC. Beads were washed five times with IP buffer, followed by elution with SDS sample buffer (2x) and 1% β-mercaptoethanol and heating at 50 ºC for 3 min prior to separation by SDS-PAGE.

4.3 GST-RILP pull-down assay

The GST-RILP vector, or an empty GST-containing vector were transformed into *E.coli* strain BL21. 250 ml of LB was inoculated with 1 ml of an overnight culture and grown at 37 °C to an OD of 0.6 to 0.8. Isopropyl-1-thio-β-d-galactopyranoside (EMD Biosciences) was then added to a final concentration of 0.5 mM to induce protein production. The 250 ml culture was incubated for additional 3–4 h at 30 °C, after which the bacteria were spun down, washed with cold PBS and frozen down if necessary. Then, the pellet was resuspended in 5 ml of cold purification buffer (25 mM Tris-HCl, 1 M NaCl, 0.5 mM EDTA, 1 mM dithiothreitol, 0.1% Triton X-100, with protease inhibitor cocktail (Roche), pH 7.4) and sonicated 10 times, 30 second each in ice. The bacterial lysates were cleared by centrifugation, and 5 ml of cold lysis buffer was added to the supernatant. GST-RILP was purified by adding 300 µl of a pre-equilibrated 50 % slurry of glutathione-Sepharose 4B beads (GE Healthcare) in purification buffer to the lysate. Beads were incubated with the bacterial lysates for 1 h at 4 ºC, washed with purification buffer, resuspended as a 50 % slurry, and kept at 4 ºC. 5 µl of the sample was separated by SDS-PAGE and analyzed by Coomassie brilliant blue staining to determine protein purity, and protein concentration estimated by a BCA assay.

Transfected HeLa cells were washed in chilled PBS and pelleted by centrifugation. Pellets were resuspended in pull-down buffer (20 mM HEPES, 100 mM NaCl, 5 mM $MgCl_2$, 1 % TritonX-100 and protease inhibitor cocktail (Roche), pH 7.4) and lysates centrifuged at 13 500 rpm for 10 min at 4 ºC. Protein concentration of supernatants was estimated using a BCA assay. Each pull-down was performed in 1 ml with 300 µg of cell lysate and 30 µg of beads pre-equilibrated in pull-down buffer. Beads were rocked overnight at 4 °C, washed twice with cold pull-down buffer, and

bound proteins eluted by adding 2×Sample buffer/β-mercaptoethanol and incubating at 72 °C for 10 min prior to separation by SDS-PAGE.

5. Statistical analysis

Data are expressed as means +/- S.E.M., and the significance of differences was assessed using Student´s t-test or ANOVA followed by Tukey´s HSD post hoc analysis. Differences were accepted as significant at the 95% level ($P < 0.05$).

VI. RESULTS

1. Leucine-rich repeat kinase 2 regulates autophagy through a calcium-dependent pathway involving NAADP

HMG Advance Access published November 1, 2011

Human Molecular Genetics, 2011 **1–15**
doi:10.1093/hmg/ddr481

Leucine-rich repeat kinase 2 regulates autophagy through a calcium-dependent pathway involving NAADP

Patricia Gómez-Suaga[1], Berta Luzón-Toro[1], Dev Churamani[2], Ling Zhang[3], Duncan Bloor-Young[4], Sandip Patel[2], Philip G. Woodman[3], Grant C. Churchill[4] and Sabine Hilfiker[1,*]

[1]Institute of Parasitology and Biomedicine 'López-Neyra', Consejo Superior de Investigaciones Científicas (CSIC), Avda del Conocimiento s/n, 18100 Granada, Spain, [2]Department of Cell and Developmental Biology, University College London, London, UK, [3]Faculty of Life Sciences, University of Manchester, Manchester, UK and [4]Department of Pharmacology, University of Oxford, Oxford, UK

Received July 21, 2011; Revised and Accepted October 14, 2011

Mutations in the leucine-rich repeat kinase-2 (LRRK2) gene cause late-onset Parkinson's disease, but its physiological function has remained largely unknown. Here we report that LRRK2 activates a calcium-dependent protein kinase kinase-β (CaMKK-β)/adenosine monophosphate (AMP)-activated protein kinase (AMPK) pathway which is followed by a persistent increase in autophagosome formation. Simultaneously, LRKR2 overexpression increases the levels of the autophagy receptor p62 in a protein synthesis-dependent manner, and decreases the number of acidic lysosomes. The LRRK2-mediated effects result in increased sensitivity of cells to stressors associated with abnormal protein degradation. These effects can be mimicked by the lysosomal Ca^{2+}-mobilizing messenger nicotinic acid adenine dinucleotide phosphate (NAADP) and can be reverted by an NAADP receptor antagonist or expression of dominant-negative receptor constructs. Collectively, our data indicate a molecular mechanism for LRRK2 deregulation of autophagy and reveal previously unidentified therapeutic targets.

INTRODUCTION

Autosomal-dominant mutations in leucine-rich repeat kinase 2 (LRRK2) cause late-onset familial Parkinson's disease (PD) (1,2) which is symptomatically and neurochemically indistinguishable from sporadic PD. In addition, pathogenic mutations contribute to sporadic PD and variations increase risk for PD, suggesting that LRRK2 may be an important factor for idiopathic disease progression as well (3). The most prominent pathogenic LRRK2 mutation (G2019S), located within the kinase domain, has been consistently shown to enhance kinase activity *in vitro* (4–7), suggesting that it may display a dominant, gain-of-function phenotype. Overexpression of LRRK2 harbouring this disease-segregating mutation leads to neurotoxicity *in vivo*, and such neurotoxicity is linked to the kinase activity of LRRK2 (8–11). Thus, the pathogenic role of mutant LRRK2 seems to be dependent on catalytic activity.

Overexpression of G2019S-mutant LRRK2 in neuronal cells decreases neurite process length with a concomitant accumulation of autophagic structures (12–14), and an impaired autophagic balance is also observed upon overexpression of LRRK2 in non-neuronal and yeast cells (15,16). This is in agreement with the findings that a significant portion of endogenous LRRK2 is localized to membranous structures including ER and endosomal–lysosomal compartments (17), and implicates LRRK2 as an important regulator of macroautophagy.

Macroautophagy (hereafter referred to as autophagy) is a process whereby cytoplasmic constituents are engulfed within specialized double-membrane vesicles called autophagosomes,

*To whom correspondence should be addressed. Tel: +34 958181654; Fax: +34 958181632; Email: sabine.hilfiker@ipb.csic.es

© *The Author 2011. Published by Oxford University Press.*
This is an Open Access article distributed under the terms of the Creative Commons Attribution Non-Commercial License (http://creativecommons.org/licenses/by-nc/3.0), which permits unrestricted non-commercial use, distribution, and reproduction in any medium, provided the original work is properly cited.

Downloaded from http://hmg.oxfordjournals.org/ at CSIC on March 9, 2014

and subsequently delivered to the lysosome for degradation. Autophagy normally proceeds at a low, basal rate, which plays a key role in the homeostatic clearance of old or damaged organelles and proteins (18,19). Basal autophagy is especially high in neuronal cells, and neurons undergo degeneration when basal autophagic degradation is disrupted (20,21). Autophagic failure seems to underlie a variety of neurodegenerative diseases (22), and deregulation of autophagy is evident in the brains of PD patients (23).

Despite the findings linking LRRK2 to deregulated autophagy, the exact mechanisms underlying such deregulation have not been characterized. In this work, we find that overexpression of LRRK2 causes an increase in autophagy induction through Ca^{2+}-dependent activation of a CaMKK/adenosine monophosphate (AMP)-activated protein kinase (AMPK) pathway, which can be inhibited by calcium chelation or ectopic Bcl-2. At the same time, LRRK2 causes a partial increase in lysosomal pH and a decrease of cell survival in the presence of protein aggregation-induced stress. The LRRK2-mediated effects involve activation of nicotinic acid adenine dinucleotide phosphate (NAADP)-sensitive two-pore channels (TPCs) located on acidic stores, and can be blocked by a specific antagonist. Together, our data indicate a molecular mechanism by which LRRK2 may act to regulate lysosomal Ca^{2+} homeostasis, with downstream effects on autophagy as well as other Ca^{2+}-dependent cellular events.

RESULTS

LRRK2 overexpression causes autophagy induction

To study the effect of LRRK2 on basal autophagy, we selected a variety of constructs including full-length LRRK2 (fl-kinase) and variants bearing the pathogenic G2019S mutation (fl-G2019S) or the kinase-inactivating K1906M mutation (fl-K1906M), respectively. To evaluate whether effects are due to the kinase domain and activity of LRRK2 (12), we also used the kinase domain (kinase) or variants therof (G2019S, K1906M) on their own, respectively. Overexpressed proteins were mostly cytosolic, wild-type (WT) and mutant proteins displayed similar overexpression levels, and no cellular toxicity was apparent 24 or 48 h upon transfection, as previously described (10) (Supplementary Material, Fig. S1).

We next addressed the effects of LRRK2 overexpression on autophagosome formation. LC3 is the mammalian homologue of the yeast Atg8 protein, which is covalently modified and re-distributes to autophagic vacuoles during induction of autophagy (23). This process can be followed by the appearance of LC3 puncta or ring-like structures and by a mobility shift from LC3I to LC3II by SDS–PAGE. Cells transiently transfected with LC3–GFP alone, or co-transfected with empty vector and analysed 48 h after transfection, display few cytoplasmic LC3–GFP punctae (Fig. 1A and B). An increase in LC3–GFP punctae was observed when co-transfecting with full-length wild-type as well as with G2019S-mutant LRRK2, but not with the inactive K1906M mutant (Fig. 1B). A similar increase in LC3–GFP punctae was observed with wild-type or G2019S-mutant, but not K1906M-mutant kinase domain only (Fig. 1A and B), indicating that the effects on autophagy are, at least in part, due to the kinase domain and activity of LRRK2. Wild-type and G2019S-mutant full-length LRRK2 increased autophagosome numbers to a similar degree and comparable with that of wild-type or G2019S-mutant kinase domain only (Fig. 1B), possibly due to saturating levels of overexpression of the various active constructs with respect to downstream targets.

As a positive control, inhibition of the mammalian target of rapamycin (mTOR) protein kinase by rapamycin was found to induce autophagy to a similar degree (Fig. 1B). The phosphatidylinositol 3-kinase inhibitor 3-methyladenine (3-MA) is thought to suppress autophagy by inhibiting the production of phosphatidylinositol-3-phosphate required for autophagosome formation (24), and was found to block the increase in autophagosome numbers mediated by rapamycin, but not by LRRK2 overexpression (Fig. 1B). Such differential 3-MA sensitivity has previously been described (13), and points towards a possible mechanistic difference between mTOR- and LRRK2-mediated autophagy induction. An increase in autophagosome numbers was further reflected by an increase in the level of endogenous LC3II (Fig. 1C), and transmission electron microscopy confirmed that the induction of LC3-positive vesicles by LRRK2 overexpression correlated with an increase in the number of autophagic structures (Fig. 1D and E).

We next used a pH-sensitive tagged LC3 construct consisting of a tandem fusion of the red, acid-insensitive mCherry ($pK_a < 4.5$) and the acid-sensitive GFP (pK_a 6.0) (td-tag-LC3) (25,26). Td-tag-LC3 will emit yellow (green merged with red) fluorescence in non-acidic structures, but appear as red only in autolysosomes due to the quenching of GFP in these acidic structures (25,26). Indeed, td-tag-LC3 was found to faithfully track autophagosome maturation in transfected cells, thus allowing for the identification of possible deficits in autophagic maturation (Supplementary Material, Fig. S2). Co-transfection of td-tag-LC3 with G2019S-mutant LRRK2 kinase domain increased both early and late autophagic structures (Fig. 2A and B). Such increase in both yellow and red punctae was also observed with wild-type kinase domain or with full-length LRRK2, but not with the catalytically inactive K1906M mutant (Fig. 2B). As a positive control for blocking autophagosome maturation, we used trichostatin A, an inhibitor of histone deacetylases (HDACs) known to be required for the fusion of autophagosomes with lysosomes (27). Indeed, trichostatin A treatment significantly increased the percentage of yellow punctae (and decreased the number of red punctae), in contrast to LRRK2 expression or autophagy induction by rapamycin (Fig. 2C and D). These data indicate that LRRK2 overexpression enhances autophagosome numbers and at least the initial steps of autophagosome maturation in a manner dependent on kinase activity.

LRRK2 overexpression activates the Ca^{2+}/CaMKK/AMPK pathway

The increase in autophagosome numbers probably results from cytosolic events regulated by LRRK2. As recent studies imply an important role for AMPK in basal autophagy regulation (28), we evaluated the effects of LRRK2 on AMPK activity. Expression of wild-type and G2019S-mutant LRRK2 kinase domain, but not its inactive mutant, increased AMPK activity (Fig. 3A and B). This was not accompanied by inhibition of

Downloaded from http://hmg.oxfordjournals.org/ at CSIC on March 9, 2014

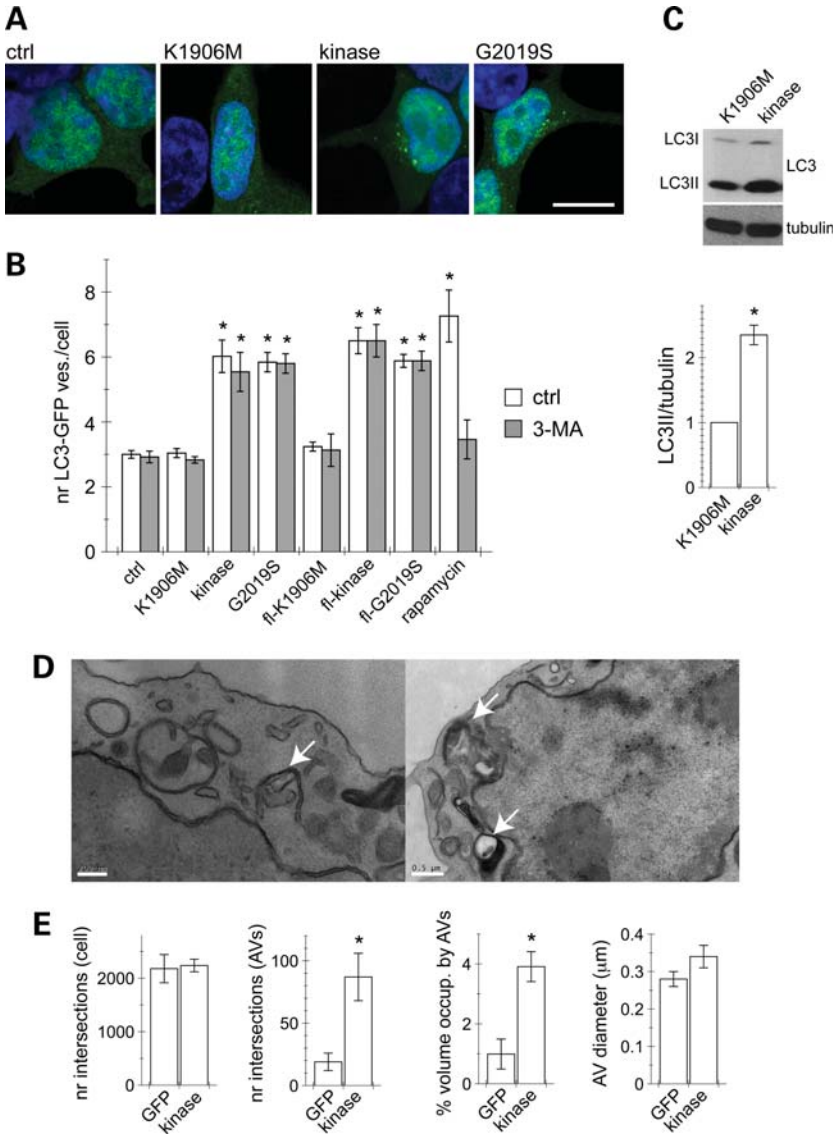

Figure 1. Effects of LRRK2 overexpression on autophagosome formation. (**A**) Example of HEK293T cells transfected with LC3–GFP and either empty vector (ctrl), catalytically inactive K1906M-mutant LRRK2 kinase domain (K1906M), wild-type LRRK2-kinase domain (kinase) or catalytically hyperactive G2019S-mutant LRRK2 kinase domain (G2019S). LC3–GFP fluorescence (green) and nuclear DAPI staining (blue). Scale bar, 10 μm. (**B**) Quantification of the number of LC3–GFP punctae per cell in the absence (white bars) or the presence of 3-MA (5 mM, 24 h) (grey bars). Cells were co-transfected with LC3–GFP and the indicated constructs, and LC3–GFP punctae quantified 48 h after transfection. Rapamycin (100 nM, 12 h) was used as positive control. Bars represent mean ± s.e.m. ($n = 4$); $^*P < 0.001$. (**C**) Top: cells were transfected with either K1906M or kinase constructs, and extracts analysed for endogenous LC3I and LC3II blotting with an anti-LC3 antibody (Cell Signalling). Bottom: quantification of LC3II/tubulin from different experiments (mean ± s.e.m. ($n = 3$); $^*P < 0.05$. (**D**) Representative electron micrographs of cells expressing LRRK2 kinase domain. Arrows point to distinct autophagic structures [scale bar 200 nm (left) or 500 nm (right)]. (**E**) Cells were co-transfected with EGFP and empty vector (GFP) or kinase domain (kinase), and FACS sorted before processing for electron microscopy. Stereological analysis of the number of intersections per cell, number of intersections per autophagic structures (AVs), percentage of cellular volume occupied by AVs and AV diameter were quantified from three individual cells per condition. $^*P < 0.05$.

mTORC1 activity when compared with rapamycin or torin treatment (Fig. 3C and D and Supplementary Material, Fig. S3) (29). Accordingly, inhibition of AMPK by a pharmacological inhibitor (compound C) (30) attenuated the increase in autophagosome numbers induced by LRRK2 kinase domain overexpression (Fig. 3E). Compound C also attenuated the increase in autophagosome numbers observed with ionomycin and ATP, two treatments previously shown to activate AMPK (31), but was without effect on autophagosome numbers induced by rapamycin (Fig. 3E).

Further evidence for an involvement of AMPK was gained by expressing wild-type, dominant-negative and constitutively active forms of this kinase (32). Wild-type and mutant AMPKα1 forms were overexpressed to similar degrees and without effect on cellular viability, with AMPKα2 forms expressed to a lesser degree and displaying cellular toxicity (Supplementary Material, Fig. S4). Expression of wild-type and constitutively active, but not dominant-negative, AMPKα1 induced an increase in autophagosome numbers (Fig. 4A). Importantly, the dominant-negative AMPKα1

Downloaded from http://hmg.oxfordjournals.org/ at CSIC on March 9, 2014

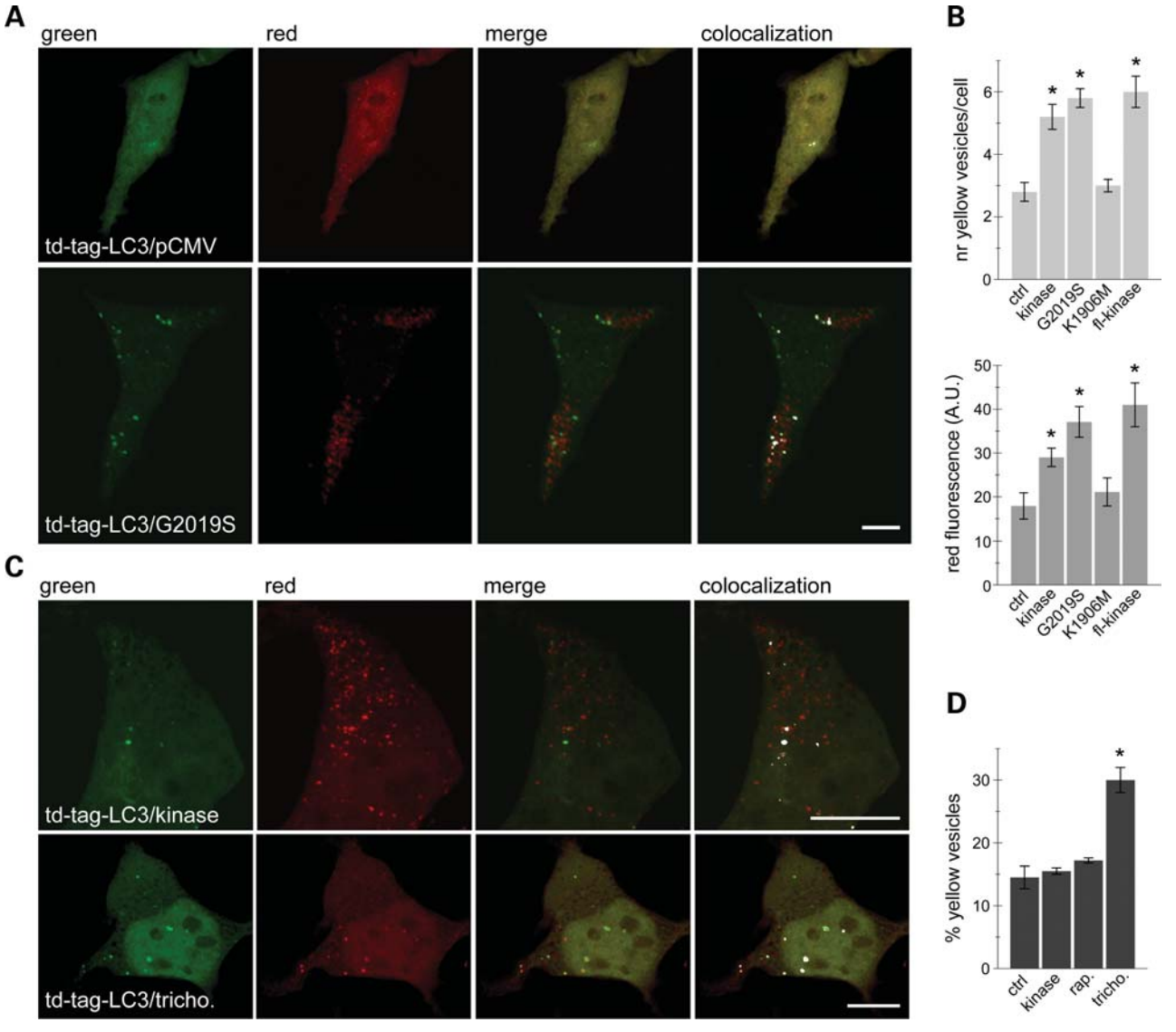

Figure 2. Effects of LRRK2 overexpression on autophagosome maturation. (**A**) Example of HEK293T cells co-transfected with tandem-tagged-LC3 (td-tag-LC3) and either empty vector (pCMV) or G2019S-mutant LRRK2 kinase domain. White: co-localization mask to highlight yellow punctae. Scale bar, 10 μm. (**B**) Quantification of the number of early, yellow-only td-tag-LC3 punctae per cell (top), or the overall fluorescence from late, red-only td-tag-LC3 punctae per cell (bottom). Cells were co-transfected with td-tag-LC3 and either empty pCMV vector (ctrl), wild-type or mutant kinase or full-length LRRK2 kinase (fl-kinase) constructs as indicated, and quantified 48 h after transfection. Bars represent mean ± s.e.m. ($n = 3$); $^{*}P < 0.05$. (**C**) Example of cells co-transfected with td-tag-LC3 and LRRK2 kinase domain, or transfected with td-tag-LC3 and treated with trichostatin A (300 nM, 4 h). White: co-localization mask to highlight yellow punctae. Scale bar, 10 μm. (**D**) Quantification of the percentage of early, yellow td-tag-LC3 punctae per cell. Cells were co-transfected with td-tag-LC3 and either kinase or empty vector. The latter were either left untreated (ctrl), or treated with rapamycin (rap.; 100 nM, 4 h) or trichostatin A (tricho.; 300 nM, 4 h) prior to fixation. Note that the percentage of yellow punctae in trichostatin-treated cells is increased because of the decrease in the number of red punctae. Bars represent mean ± s.e.m. ($n = 2$); $^{*}P < 0.05$.

construct was able to inhibit the increase in autophagosome numbers observed upon active LRRK2 kinase domain co-expression (Fig. 4B). Such inhibition was not observed when autophagic on-rate was increased by distinct means, indicating a specific involvement of the AMPK pathway in the LRRK2-mediated process (Supplementary Material, Fig. S4).

AMPK can be activated by CaMKK-β in response to an increase in the cytosolic-free calcium $[Ca^{2+}]_c$ (31). In order to test whether LRRK2 expression regulates the Ca^{2+}/CamKK-β/AMPK pathway, we first treated cells with a CaMKK-α/β inhibitor (STO-609) (33). This compound attenuated the increase in autophagosome formation induced by LRRK2 kinase domain (Fig. 4C). Such inhibition was similar to that observed when cells were treated with two stimuli which increase $[Ca^{2+}]_c$ by distinct means: ATP, which acts on P2 purinoreceptors to generate inositol 1,4,5-triphosphate (IP_3) that triggers the release of Ca^{2+} from the ER through IP_3 receptor-regulated channels, or ionomycin, a Ca^{2+} ionophore that serves as a mobile Ca^{2+} carrier to equilibrate Ca^{2+} levels across biological membranes, including plasma and ER membranes (31,34,35) (Fig. 4C). In contrast, the CaMKK-α/β inhibitor had no effect on

Downloaded from http://hmg.oxfordjournals.org/ at CSIC on March 9, 2014

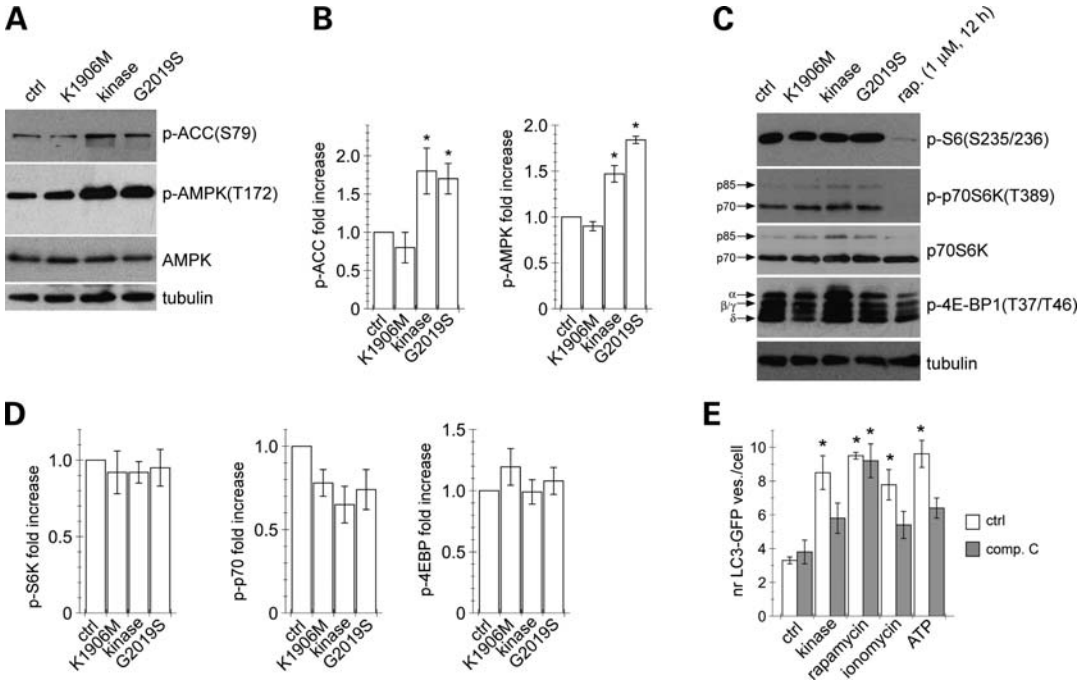

Figure 3. Effects of LRRK2 overexpression on AMPK and TORC1 signalling. (**A**) HEK293T cells were transfected with either empty vector (ctrl) or indicated constructs, and cell extracts analysed for phospho-ACC, phospho-AMPK and AMPK. (**B**) Quantification of the type of experiments depicted in (A). Bars represent mean ± s.e.m. ($n = 3$); $^*P < 0.05$. (**C**) As in (A), but extracts analysed for the indicated TORC1 substrates. (**D**) Quantification of the type of experiments depicted in (C). Bars represent mean ± s.e.m. ($n = 3$). (**E**) Cells were co-transfected with LC3−GFP and either empty vector (ctrl) or LRRK2 kinase domain, and control-transfected cells were treated with rapamycin (100 nM, 12 h), ionomycin (2.5 μM, 12 h) or ATP (100 μM, 12 h) where indicated. Cells were incubated in the absence (white bars) or the presence (grey bars) of compound C (5 μM, 24 h), and LC3−GFP punctae quantified 48 h after transfection. Bars represent mean ± s.e.m. ($n = 3$); $^*P < 0.05$.

autophagosome numbers elicited by rapamycin treatment (Fig. 4C). Remarkably, addition of the intracellular Ca^{2+} chelator BAPTA-AM (bis-(*O*-aminophenoxy)-ethane-*N*,*N*,*N*,*N*′-tetraacetic acid/tetra(acetoxymethyl)-ester) to LRRK2 kinase domain or full-length LRRK2-transfected cells for the last 2 hours completely abolished the increase in autophagosome numbers (Fig. 4D). BAPTA-AM was further able to block the ionomycin-mediated, but not the rapamycin-mediated, increase in autophagosome numbers (Supplementary Material, Fig. S4). Thus, a Ca^{2+}/CaMKK/AMPK pathway seems to be required for the increased formation of autophagosomes in response to active LRRK2 overexpression.

ER-localized Bcl-2 inhibits LRRK2-mediated autophagy induction

Bcl-2 has been reported to regulate cellular Ca^{2+} handling and Ca^{2+}/CaMKK/AMPK-induced autophagy (31,36). Thus, we tested whether expression of bcl-2 could inhibit the LRRK2-mediated increase in autophagosome numbers via its effects on Ca^{2+} homeostasis. For this purpose, we expressed wild-type bcl-2 (Bcl-WT), which is mostly mitochondrial (36,37), or mutants in which the C-terminal hydrophobic sequence has been either removed (Bcl-cyt), resulting in cytosolic expression, or exchanged to a corresponding membrane anchor from an ER-specific isoform of cytochrome b5 (Bcl-ER) or *L. monocytogenes* ActA (Bcl-mito), resulting in distinct subcellular localizations (31,38). Western blot analysis confirmed equal expression levels, and only slight effects on cytotoxicity were observed when overexpressing Bcl-wt or Bcl-mito, but not Bcl-cyto or Bcl-ER, respectively (Supplementary Material, Fig. S4). Importantly, only Bcl-ER was able to fully inhibit the LRRK2 kinase domain-mediated increase in autophagosome numbers (Fig. 4E). ER-localized Bcl-2 has previously been demonstrated to lower $[Ca^{2+}]_{ER}$ and agonist-induced Ca^{2+} leak from the ER (39). Together with the inhibitory effect of BAPTA-AM and inhibition of CaMKK on the LRRK2-mediated increase in autophagosome numbers, these results indicate that active LRRK2 may increase $[Ca^{2+}]_c$ by directly or indirectly inducing Ca^{2+} release from the ER. This release is likely mediated by IP_3 receptors, as the increase in autophagosome numbers upon LRRK2 expression could not be blocked by dantrolene, a ryanodine receptor antagonist (Supplementary Material, Fig. S4).

LRRK2 alkalinizes a subpopulation of lysosomes

Overexpression of LRRK2 has previously been shown to lead to accumulation of multi-vesicular bodies and autophagosomes containing incompletely degraded material and p62 (15), a classical macroautophagy substrate (40), indicating possible defects in autophagic degradation. Indeed, overexpression of wild-type or G2019S-mutant, but not inactive K1906M-mutant, kinase domain led to a significant increase in p62 levels and p62-positive structures (Fig. 5A–C).

Downloaded from http://hmg.oxfordjournals.org/ at CSIC on March 9, 2014

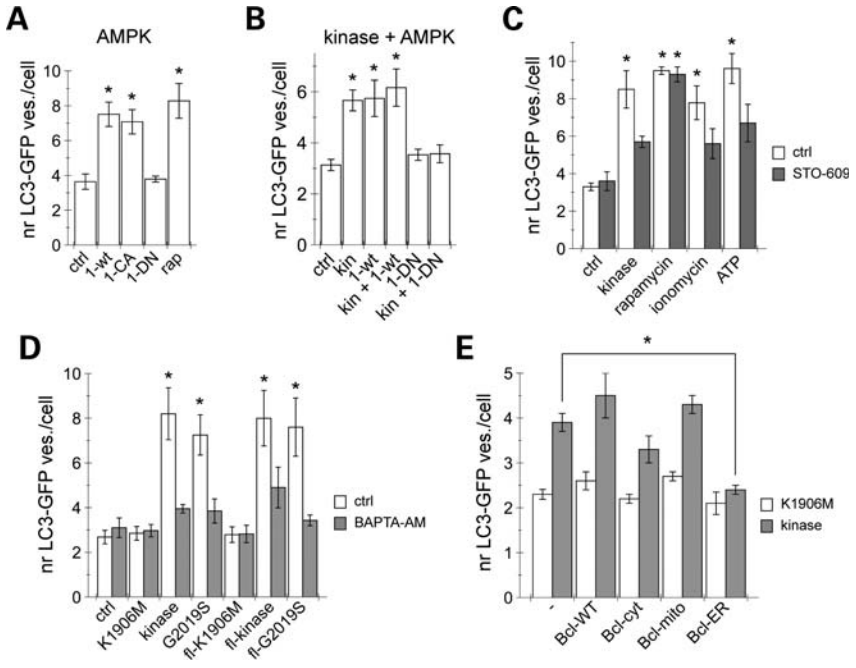

Figure 4. Effects of LRRK2 overexpression on AMPK and intracellular calcium. (**A**) HEK293T cells were co-transfected with LC3–GFP and either empty vector (ctrl), human wild-type AMPKα1 (1-wt), dominant-negative (1-DN) or constitutively active (1-CA) AMPKα1, and LC3–GFP punctae quantified 48 h after transfection. Rapamycin (100 nM, 12 h) (rap.) was used as control. Bars represent mean ± s.e.m. ($n = 3$); $^*P < 0.05$. (**B**) Cells were transfected with LC3–GFP along with either empty vector (ctrl), or LRRK2 kinase domain (kin) in the presence or in the absence of wild-type (1-wt) or dominant-negative (1-DN) AMPKα1 constructs as indicated, and LC3–GFP punctae quantified 48 h after transfection. Bars represent mean ± s.e.m. ($n = 3$); $^*P < 0.01$. (**C**) Cells were co-transfected with LC3–GFP and either empty vector (ctrl) or LRRK2 kinase domain (kinase), and control-transfected cells were treated with rapamycin (100 nM, 12 h), ionomycin (2.5 μM, 12 h) or ATP (100 μM, 12 h) where indicated. Cells were incubated in the absence (white bars) or in the presence (grey bars) of STO-609 (20 μM, 24 h), a CaMKKβ inhibitor and LC3–GFP punctae quantified 48 h after transfection. Bars represent mean ± s.e.m. ($n = 3$); $^*P < 0.05$. (**D**) Cells were co-transfected with LC3–GFP and either empty vector (ctrl) or the indicated wild-type or mutant kinase domain or full-length (fl) constructs, and either left untreated (white bars) or treated with BAPTA-AM (5 μM, 2 h) (grey bars) prior to analysis for LC3–GFP punctae 48 h after transfection. Bars represent mean ± s.e.m. ($n = 3$); $^*P < 0.05$. (**E**) Cells were transfected with LC3–GFP along with either K1906M mutant (white bars) or wild-type (grey bars) LRRK2 kinase domain and either control empty vector (−) or the indicated chimeric Bcl constructs, and LC3–GFP punctae analysed 24 h after transfection. Bars represent mean ± s.e.m. ($n = 3$); $^*P < 0.05$.

However, the LRRK2-mediated increase in p62 levels could be blocked by protein synthesis inhibitors (Fig. 5D), indicating that it was not reflecting changes in autophagic flux. Identical results were obtained when using ionomycin or thapsigargin (Supplementary Material, Fig. S5), suggesting that the LRRK2-mediated effects on p62 levels may be due to Ca^{2+}-dependent changes in protein synthesis (41).

A possible defect in lysosomal homeostasis, however, became apparent when employing lipid staining with BODIPY 493/503 (42), which revealed an increase in lipid droplet numbers in cells overexpressing LRRK2 kinase domain (Fig. 6A and B). In addition, lysotracker DND-99 or Lysosensor staining to determine lysosomal pH indicated a decrease in the number of positive punctae in cells overexpressing active LRRK2 kinase domain (Fig. 6C and D). This was not due to a decrease in lysosomal content (43), as no change in the levels of LAMP1 or LAMP2 were observed (Supplementary Material, Fig. S6). Interestingly, quantification of the percent colocalization of LAMP2 and lysotracker showed an increase in the number of structures positive for LAMP2, but negative for lysotracker, suggesting that LRRK2 increases pH in a subpopulation of lysosomes, without affecting the processing of lysosomal hydrolases (Fig. 6E and Supplementary Material, Fig. S6).

LRRK2 acts through NAADP receptors

There is considerable evidence that acidic organelles such as endosomes and lysosomes are significant stores of Ca^{2+} that can be released by the Ca^{2+} mobilizing messenger NAADP (44,45). NAADP-evoked cytosolic Ca^{2+} signals are accompanied by partial alkalinization of acidic stores (46) and amplification by ER Ca^{2+} stores (47), and lysosomal Ca^{2+} depletion causes lipid accumulation (48). That LRRK2 increases lipid droplet numbers (Fig. 6), causes an increase in lysosomal pH (Fig. 6) and regulates Ca^{2+}-dependent events in the cytosol which likely also involve the ER (Figs. 4 and 5) prompted us to consider the involvement of the NAADP pathway in mediating the effects of LRRK2.

Application of NAADP-AM was found to increase autophagosome numbers (Fig. 6F). This increase was abolished at higher NAADP concentrations, in agreement with the notion that NAADP-induced Ca^{2+} release desensitizes at high ligand concentrations (49,50). The effect of NAADP on autophagosome formation could be blocked by BAPTA-AM (Fig. 6F) and was accompanied by an increase in AMPK activity (Supplementary Material, Fig. S6). The autophagy induction observed with NAADP could be inhibited by Bcl-ER (Fig. 6G), similar to starvation-induced autophagy (36,37),

Downloaded from http://hmg.oxfordjournals.org/ at CSIC on March 9, 2014

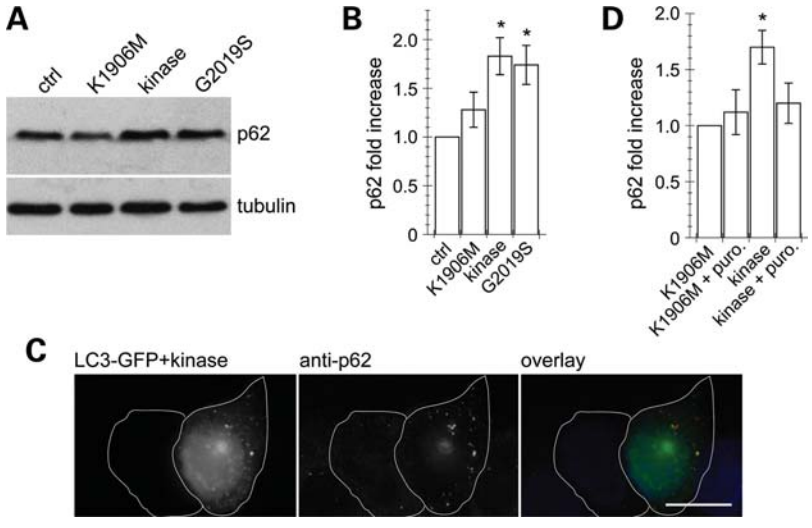

Figure 5. Effects of LRRK2 overexpression on p62 levels. (**A**) HEK293T cells were transfected with either control empty vector (ctrl) or wild-type or mutant kinase domain constructs as indicated, and extracts analysed for endogenous p62 levels. (**B**) Quantification of the type of experiments as depicted in (A). Bars represent mean ± s.e.m. ($n = 3$); $^{*}P < 0.05$. (**C**) Example of cells co-transfected with LC3–GFP (green, left) and LRRK2 kinase domain and co-stained with anti-p62 (red, middle). Scale bar, 10 μm. (**D**) Cells were transfected with indicated constructs, and treated with puromycin (1 μM, 6 h) where indicated before analysis and quantification of p62 levels. Bars represent mean ± s.e.m. ($n = 3$); $^{*}P < 0.05$.

but distinct from autophagy induced by rapamycin or torin treatment (Fig. 6G). In addition, the autophagy induced by NAADP was insensitive to 3-MA, in contrast to TORC1-dependent autophagy inducers (Fig. 6H). Furthermore, NAADP caused an increase in LC3II levels (Fig. 6I), a protein synthesis-dependent increase in p62 levels (Fig. 6J), increased lipid droplet numbers (Fig. 6K) and increased lysosomal pH (Fig. 6L), thus fully mimicking the effects of LRRK2 expression.

TPCs have recently emerged as the likely targets for NAADP, with TPC1 localized to both endosomes and lysosomes, and TPC2 mainly to lysosomes (50,51). Point mutants in the putative helix of the pore-forming regions have been described, which seem to largely abolish Ca^{2+} conductance and uncover dominant-negative effects with respect to NAADP-mediated Ca^{2+} signals (51,52). Thus, we evaluated whether co-expressing wild-type or mutant TPCs may interfere with LRRK2-mediated autophagosome formation. Expression of mRFP-tagged TPC constructs indicated that wild-type and mutant versions were similarly overexpressed and localized to intracellular compartments, with TPC2 partially co-localizing with the lysosomal marker LAMP2, as previously described (51). None of the TPC constructs displayed cytotoxicity at 24 h upon overexpression, but TPC1 and its mutant were found to increase autophagosome formation (Supplementary Material, Fig. S7). Whilst consistent with the involvement of TPC1 in endolysosomal trafficking (53), this finding precluded further analysis of a possible reversal of the LRRK2-mediated increase in autophagosome numbers by TPC1 constructs. In contrast, TPC2 and its mutant did not display effects on autophagosome numbers when expressed on their own (Fig. 7A). Importantly, mutant but not wild-type TPC2 was able to block the effect of LRRK2 kinase domain on autophagosome numbers (Fig. 7A).

We next evaluated whether NED-19, a newly described NAADP antagonist (54), could reverse the LRRK2-mediated effects on autophagic flux. NED-19 on its own was without effect on autophagosome numbers, but could block the increase in autophagosome numbers mediated by active kinase domain or full-length LRRK2 (Fig. 7B). This was accompanied largely by a reversal in the LRRK2-mediated changes on AMPK activity (Supplementary Material, Fig. S7), p62 levels, LC3II levels and lysotracker-positive structures (Fig. 7C–E). Finally, when probing for an interaction between endogenous LRRK2 and GFP–TPC2, LRRK2 was found to co-immunoprecipitate with GFP–TPC2 and vice versa (Fig. 7F and Supplementary Material, Fig. S7). Together, these data indicate that NAADP mimicks the effects of active LRRK2, whilst NED-19 application can revert those effects, and suggest that NAADP receptors may be direct targets for regulation by LRRK2.

LRRK2 sensitizes cells to cell death induced by proteasome inhibition

As the observed LRRK2-mediated effects were not cytotoxic *per se*, we next wondered whether they would sensitize cells towards cell death under certain conditions (55). When cells were treated with the proteasomal inhibitor MG-132, cell death was markedly accelerated in cells overexpressing active, but not inactive, LRRK2 kinase domain (Fig. 8A). The increased cell death in the presence of MG-132 in LRRK2 kinase domain-expressing cells could be blocked by NED-19 (Fig. 8B), supporting the involvement of the NAADP pathway in this process. Interestingly, application of rapamycin or torin, two specific TORC1 inhibitors, reverted the LRRK2-mediated effects on cell death in the presence of MG-132, whilst L690,440, a TORC1-independent autophagy-enhancing compound (56), was unable to do so (Fig. 8A and C). Rapamycin and torin also largely reversed the effects of LRRK2 on p62 accumulation and on the decrease in lysotracker staining (Fig. 8D and E). Measurements

Downloaded from http://hmg.oxfordjournals.org/ at CSIC on March 9, 2014

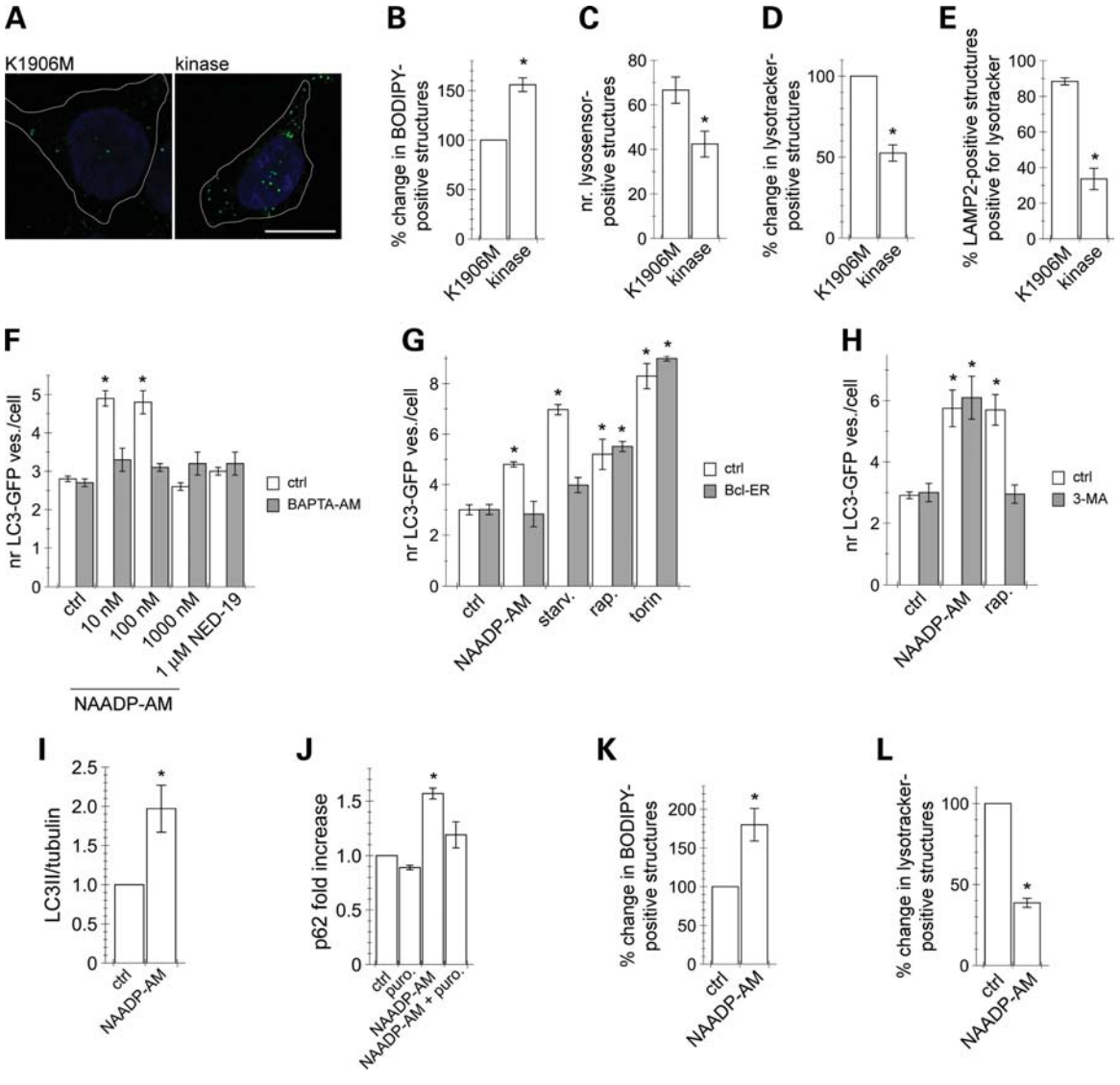

Figure 6. Effects of LRRK2 on lipid accumulation and lysosomal pH, and effects of NAADP. (**A**) Example of HEK293T cells co-transfected with mCherry and either K1906M-mutant or wild-type LRRK2 kinase domain, and stained with BODIPY 493/503 (green). Scale bar, 10 μm. (**B**) Percentage change in the number of lipid droplets quantified from experiments as in (A). Bars represent mean ± s.e.m. ($n = 3$); $^*P < 0.005$. (**C**) The number of lysosensor-positive structures in cells expressing K1906M or kinase domain. Bars represent mean ± s.e.m. ($n = 4$); $^*P < 0.05$. (**D**) Percentage change in the number of lysotracker-positive structures in cells co-transfected with EGFP and either K1906M or kinase domain constructs. Bars represent mean ± s.e.m. ($n = 3$); $^*P < 0.005$. (**E**) Quantification of LAMP2-positive structures positive for lysotracker in K1906M or kinase-expressing cells. Ten random cells were analysed per condition per experiment. Bars represent mean ± s.e.m. ($n = 2$); $^*P < 0.05$. (**F**) Cells were transfected with LC3–GFP and either left untreated, or treated with the indicated concentrations of NAADP-AM or with 1 μM NED-19 for 12 h, in the absence (white bars) or in the presence (grey bars) of BAPTA-AM (5 μM, 2 h), and LC3–GFP punctae quantified 48 h after transfection. Bars represent mean ± s.e.m. ($n = 3$); $^*P < 0.005$. (**G**) Cells were co-transfected with LC3–GFP and either control empty vector (white bars) or bcl-ER (grey bars), and either left untreated (ctrl), treated with NAADP-AM (100 nM, 4 h), starvation (Earle's salt solution, 4 h), rapamycin (200 nM, 4 h) or torin (50 nM, 4 h) as indicated, and LC3–GFP punctae analysed 24 h after transfection. Bars represent mean ± s.e.m. ($n = 3$); $^*P < 0.05$. (**H**) Cells were transfected with LC3–GFP and either left untreated (ctrl), or treated with NAADP-AM (100 nM, 12 h) or rapamycin (100 nM, 12 h) as indicated in the presence or in the absence of 3-MA (5 mM, 24 h) (grey bars). Bars represent mean ± s.e.m. ($n = 3$); $^*P < 0.05$. (**I**) Cells were either left untreated, or treated with NAADP-AM (100 nM, 12 h) as indicated, and cell extracts analysed and quantified for endogenous LC3. Bars represent mean ± s.e.m. ($n = 2$); $^*P < 0.05$. (**J**) Cells were left untreated or treated with NAADP-AM (100 nM, 12 h) or puromycin (1 μM, 6 h) as indicated, and extracts analysed and quantified for p62 levels. Bars represent mean ± s.e.m. ($n = 3$); $^*P < 0.05$. (**K**) Non-treated or NAADP-AM-treated cells were stained with BODIPY 493/503 and analysed for the percentage change in the number of lipid droplets. Bars represent mean ± s.e.m. ($n = 3$); $^*P < 0.01$. (**L**) Non-treated or NAADP-AM-treated cells were stained with lysotracker and the percentage change quantified. Bars represent mean ± s.e.m. ($n = 3$); $^*P < 0.005$.

in dopaminergic neuroendocrine PC12 cells yielded similar results. The NAADP-receptor antagonist NED-19 was able to revert the LRRK2-mediated increase in autophagosome numbers, the LRRK2-mediated decrease in lysosensor-positive structures and the LRRK2-mediated increase in cell death in the presence of MG-132 (Supplementary Material, Fig. S8). Together, these data indicate that additional interference with proteasomal degradation is detrimental to cells over-expressing catalytically active LRRK2, and that blocking NAADP-mediated signalling, or enhancing autophagic flux

Downloaded from http://hmg.oxfordjournals.org/ at CSIC on March 9, 2014

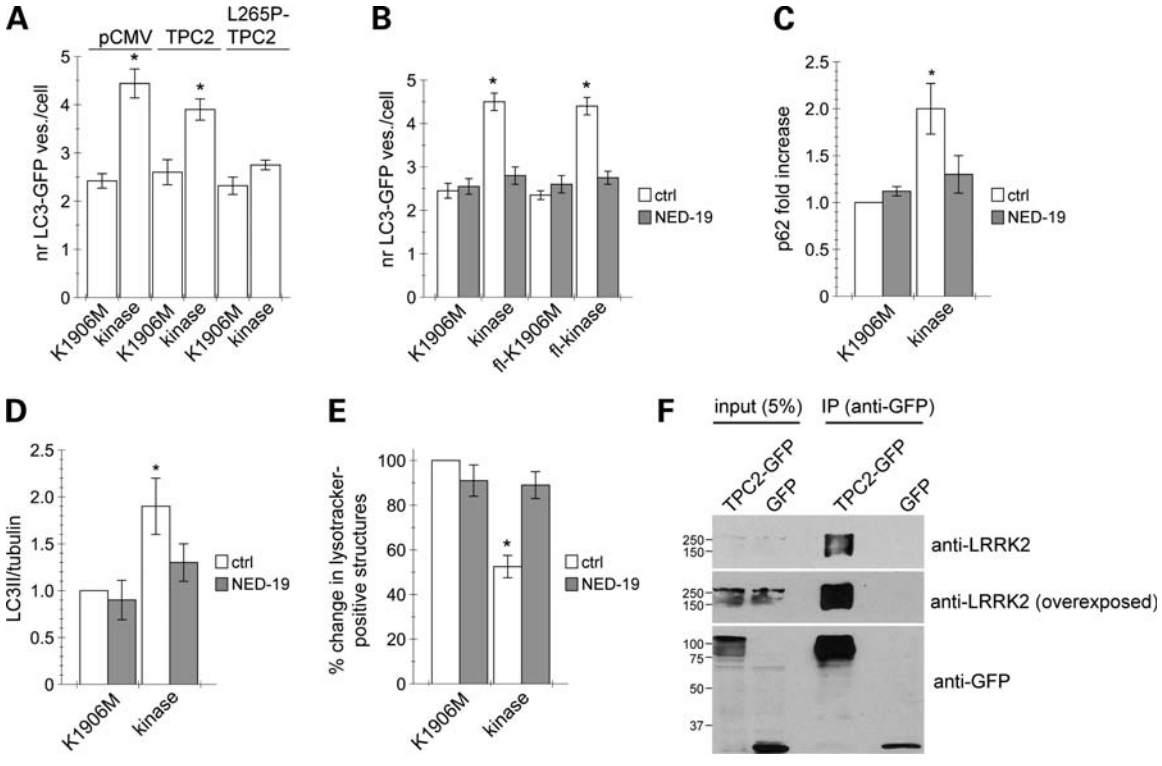

Figure 7. A link between LRRK2 and NAADP-sensitive receptors. (**A**) HEK 293T cells were transfected with LC3–GFP along with K1906M-mutant or wild-type kinase domain and either empty vector (pCMV), TPC2 or mutant TPC2 as indicated, and LC3–GFP punctae quantified 24 h after transfection. Bars represent mean ± s.e.m. ($n = 5$); $^{*}P < 0.005$. (**B**) Cells were co-transfected with LC3–GFP and the indicated kinase domain or full-length (fl) LRRK2 constructs, and either left untreated (white bars) or treated with NED-19 (1 μM, 12 h) (grey bars), followed by quantification of LC3–GFP punctae 48 h after transfection. Bars represent mean ± s.e.m. ($n = 3$); $^{*}P < 0.005$. (**C**) Transfected cells were treated with NED-19 (1 μM, 12 h) where indicated before analysis for p62 levels. Bars represent mean ± s.e.m. ($n = 3$); $^{*}P < 0.05$. (**D**) As in (C), but extracts analysed and quantified for LC3II levels. Bars represent mean ± s.e.m. ($n = 3$); $^{*}P < 0.05$. (**E**) Transfected cells were treated with NED-19 (1 μM, 12 h) where indicated before staining with lysotracker. Bars represent mean ± s.e.m. ($n = 4$); $^{*}P < 0.05$. (**F**) Cells were transfected with TPC2–GFP or GFP vector, and extracts (1 mg) subjected to immunoprecipitation with an anti-GFP antibody. Note that TPC2–GFP runs as distinct bands corresponding to core glycosylated and mature fully glycosylated versions, respectively (67). Co-immunoprecipitated endogenous LRRK2 was detected using an anti-LRRK2 antibody (MJFF2, Epitomics). Note the additional presence of lower molecular-weight bands, which are likely distinct degradation products of endogenous LRRK2. Inputs (5%) were run along-side the immunoprecipitates. Representative of a total of seven independent experiments.

and/or suppressing protein synthesis or affecting lysosomal homeostasis through a TORC1-dependent pathway can overcome the enhanced susceptibility to cell death induced by LRRK2 in non-neuronal as well as neuroendocrine cells.

DISCUSSION

Mutations in LRRK2 are the most common genetic cause of PD, but the function of the protein remains unknown. Our study provides insight into the molecular mechanism of LRRK2 action. We have shown that LRRK2 kinase activity exerts a previously unknown regulatory role on macroautophagy that seems to involve Ca^{2+} release from lysosomes and the Ca^{2+}/CaMKK/AMPK pathway. These events seem to be mediated by activation of NAADP receptors, which causes Ca^{2+} efflux from acidic stores and is accompanied by a partial alkalinization of lysosomal store pH (Fig. 9).

In our experimental conditions, wild-type LRRK2 had a significant effect similar to pathogenic G2019S-mutant LRRK2. As mutations in LRRK2 cause PD in an autosomal-dominant manner, we overexpressed the protein to mimic a gain-of-function phenotype. It is feasible that the pathogenic mechanism of LRRK2 depends on exceeding a threshold level of activity, also supported by the finding that homo- and heterozygous carriers of LRRK2 mutations are clinically indistinguishable (3). In this context, overexpressing both wild-type or G2019S-mutant LRRK2 may reach the threshold level required for LRRK2 function and/or activity to become pathogenic. Alternatively, we may have missed a small but biologically important difference in effect, which nevertheless may have important consequences when present over many years. Finally, it remains possible that the effects described here are a wild-type function of LRRK2 unrelated to PD, even though other studies describing an impaired autophagic balance with G2019S-mutant, but not wild-type LRRK2 (12–16), are consistent with the idea of a threshold effect.

Previous studies have indicated that enhanced autophagy may mediate neurite shortening induced by G2019S LRRK2 expression, as molecular inhibition of autophagy reversed, and pharmacological activation of autophagy potentiated the effects of LRRK2 on neurite shortening (12,13). Whilst our data are consistent with the notion that LRRK2 expression causes autophagy induction, we find that pharmacological

Downloaded from http://hmg.oxfordjournals.org/ at CSIC on March 9, 2014

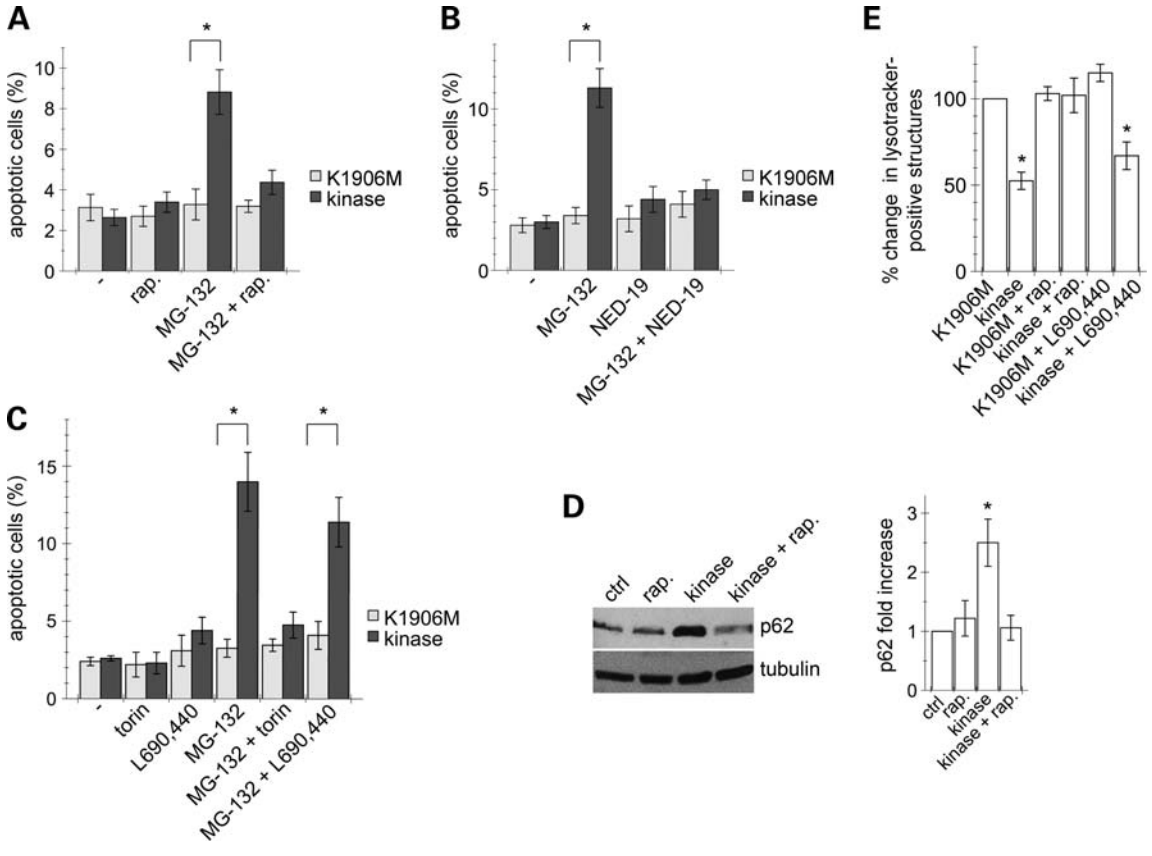

Figure 8. Effects of LRRK2 expression on cellular viability in the presence of proteasomal inhibitor. (**A**) HEK293T cells were co-transfected with GFP and K1906M or kinase domain constructs as indicated and either left untreated (−), treated with rapamycin (100 nM, 4 h), MG-132 (500 nM, 12 h) or both as indicated. Cells were analysed for cell death 48 h after transfection using Hoechst staining. Bars represent mean ± s.e.m. ($n = 3$); $^*P < 0.005$. (**B**) As in (A), but cells treated with NED-19 (1 μM, 12 h) as indicated. Bars represent mean ± s.e.m. ($n = 3$); $^*P < 0.005$. (**C**) As in (A), but cells treated with torin (500 nM, 4 h) or L690,440 (10 μM, 4 h) as indicated. Bars represent mean ± s.e.m. ($n = 3$); $^*P < 0.005$. (**D**) Left: cells were transfected with either empty vector or kinase domain construct, and treated with rapamycin (200 nM, 12 h) where indicated before analysis for p62 levels. Right: quantification of experiments where bars represent mean ± s.e.m. ($n = 3$); $^*P < 0.05$. (**E**) Transfected cells were treated as indicated before staining with lysotracker. Bars represent mean ± s.e.m. ($n = 3$); $^*P < 0.05$.

activation of autophagy is beneficial to cell survival, contradictory to the aggravating effects of rapamycin on neurite length (13). However, the micromolar, but not nanomolar, concentrations of rapamycin employed in this study (13) leave open the possibility of secondary effects unrelated to TORC1 inhibition. In addition, even though neurite length and complexity may be relevant readouts for the cellular effects of LRRK2, enhanced stress sensitivity and cell death are equally informative for our understanding of LRRK2 function in cultured cells (55). The observed effects of LRRK2 are not sufficient to cause cell death, but increase the susceptibility of cells to further insults related to protein degradation-mediated stress, reminiscent of data obtained with LRRK2/α-synuclein double-transgenic mice (57). In addition, transgenic mice expressing G2019S-mutant LRRK2 display progressive age-dependent degeneration of dopaminergic neurons *in vivo*, accompanied by the accumulation of autophagic structures (14). These data imply an important regulatory role for LRRK2 in autophagic balance, which leads to eventual cell death in the presence of an additional trigger.

LRRK2 overexpression induces the formation of autophagosomes through a Ca^{2+}/CaMKK/AMPK pathway. Contradictory data have emerged as to the role of cytosolic Ca^{2+} and autophagy, with both stimulatory (31) and inhibitory (56) effects on autophagy. Our data indicate that Ca^{2+} displays complex effects at different stages of the pathway, and is required in distinct intracellular locations. In this context, it is interesting to note that LRRK2 or reagents which increase intracellular Ca^{2+} were both found to increase p62 protein synthesis, indicating that, apart from regulation of autophagy, the LRRK2-mediated change in cytosolic Ca^{2+} may, at least in part, underlie some of the protein synthesis-mediated events proposed for LRRK2 (58,59).

The effects of LRRK2 on autophagy induction were found to be TORC1 independent, in agreement with recent findings that autophagy under normal nutritional conditions is TORC1 independent and regulated by AMPK and $InsP_3$-R-mediated Ca^{2+} signalling from the ER (28,56,60). Furthermore, the LRRK2-mediated sensitization to cell death in the presence of proteasomal inhibition could be reversed by TORC1 inhibitors. Such reversal may be due to an increase in degradative capacity as autophagic flux is enhanced, a decrease in protein synthesis, an effect on lysosomal homeostasis (61) or a combination thereof. Indeed, evidence for all three

Downloaded from http://hmg.oxfordjournals.org/ at CSIC on March 9, 2014

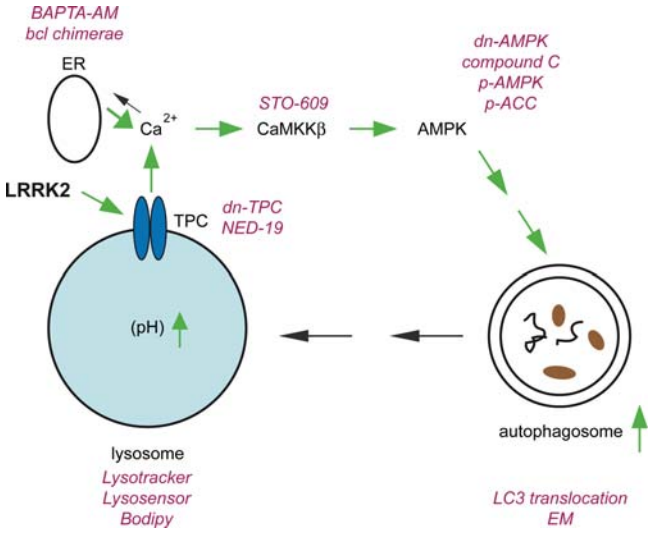

Figure 9. Model for the LRRK2-mediated events identified in this study. It is proposed that LRRK2 directly or indirectly activates NAADP-receptors (such as TPC2), resulting in an increase in cytosolic Ca^{2+}. Ca^{2+} efflux from acidic stores may lead to a concomitant increase in lysosomal pH. The cytosolic increase in Ca^{2+} may result in Ca^{2+}-induced Ca^{2+} release from ER stores, and activation of CaMKKβ, followed by activation of AMPK and an increase in autophagosome numbers. These LRRK2-mediated events seem to sensitize cells to cell death in the presence of additional compounds interfering with proteasomal degradation. Detection methods and/or tools used in this study to analyse and modulate the indicated events are depicted in red. dn, dominant-negative.

events were found with rapamyin. In either case, these data suggest that TORC1 inhibitors may prove beneficial in treating neurodegenerative events related to LRRK2.

LRRK2-expressing cells display a decrease in the number of lysosomes with acidic pH. Given that acidic pH is only lost in a fraction of lysosomes, further studies are warranted to elucidate whether there exists a correlation between the affected lysosomal subpopulation and the localization of endogenous NAADP receptors. In either case, the LRRK2-mediated effects on lysosomal pH are mild and do not result in a lysosomal proteolysis phenotype (62,63), and under basal conditions and in the absence of additional protein aggregation stress, these LRRK2-mediated effects do not affect cell survival.

NAADP is the most powerful endogenous Ca^{2+} mobilizing compound known to date. It seems to invoke an initial trigger release from acidic stores which is then amplified by Ca^{2+}-induced Ca^{2+} release from the ER mediated by Ins_3P receptors (47). TPCs are the likely target receptors for NAADP. Whilst still poorly characterized ion channels, they display a broad tissue distribution, indicating that they might play a general role in the mobilization of acidic Ca^{2+} stores. The observation that a specific NAADP antagonist blocks all LRRK2-mediated effects analysed here, together with the observed interaction between LRRK2 and TPC2, suggests a molecular mechanism for LRRK2 function involving TPC2 on acidic stores. In this context, LRRK2 may regulate TPC2 channel behaviour, even though additional effects at the level of NAADP generation cannot be excluded. To our knowledge, this is the first report which links the effects of LRRK2 through an effect on NAADP receptors. Thus, NAADP receptors may represent possible new targets for interventions for familial and sporadic PD linked to abnormal LRRK2 activity.

MATERIALS AND METHODS

Plasmid constructions

To generate the LRRK2 kinase domain-GFPemd construct (kinase-GFPemd), the human LRRK2 kinase domain (aa 1844–2143) was PCR amplified using full-length LRRK2 as template, with *Eco*RI/*Bam*HI sites on either end. VAMP2-GFPemd (64) was digested with *Eco*RI/*Bam*HI to release VAMP2, and the PCR-amplified kinase domain cloned in-frame with the GFPemd at the C-terminal end.

To generate the LRRK2 kinase domain pCMV construct (pCMV-kinase), human LRRK2 kinase domain (amino acid 1844–2143) was PCR amplified using full-length LRRK2 as template, with *Sac*I/*Bam*HI sites on either end. pCMV-VAMP2 (64) was digested with *Sac*I/*Bam*HI to release VAMP2, and religated with the digested, PCR-amplified kinase domain.

To generate the full-length human LRRK2 pCMV vector (pCMV-flLRRK2), pGEMT-LRRK2 was digested with *Sac*II/*Mlu*I to release fl-LRRK2. Quick Change Site Directed Mutagenesis was performed with the empty pCMV vector to introduce a *Sac*II site 5′ to the *Mlu*I site, followed by digestion of the vector with *Sac*II/*Mlu*I and introduction of flLRRK2.

K1906M and G2019S mutations were introduced into all respective vectors by Quick Change Site Directed Mutagenesis, and the identity of all constructs verified by direct sequencing of the entire coding regions.

The double-myc-tagged, full-length wild-type and mutant human LRRK2 constructs were kindly provided by M. Cookson (NIH, Bethesda, USA). Full-length constructs were transformed in Stbl3 *E. coli*, and DNA prepared using the BACMAX DNA Purification Kit (Epicentre Biotechnologies, Madison, USA).

N-terminally myc-tagged constructs for wild-type, dominant-negative and constitutively active AMPKα1, as well as N-terminally myc-tagged constructs for wild-type and dominant-negative AMPKα2 were kindly provided by D. Carling (MRC, Imperial College London, UK). Bcl-2 and its organelle-specific mutants were kindly provided by M. Jäättelä (Institute of Cancer Biology, Danish Cancer Society, Denmark) and D.W. Andrews (McMaster University, Hamilton, Ontario, Canada). Human TPC1-mRFP, TPC1-L273P-mRFP and TPC2-mRFP have been previously described. The L265P mutation in TPC2-mRFP was generated by Quick Change Site Directed Mutagenesis and verified by direct sequencing.

The tandem-tagged LC3 construct mCherry-EGFP-LC3B (human) was kindly provided by T. Johansen (University of Tromsø, Norway), and EGFP-LC3 (rat) was provided by T. Yoshimori (National Institute for Basic Biology, Okazaki, Japan) and J. Oliver (Institute of Parasitology and Biomedicine 'López-Neyra', CSIC, Granada, Spain). The G120A mutation was introduced into both tagged LC3 constructs by Quick Change Site-Directed Mutagenesis (Stratagene) and verified by direct sequencing.

Downloaded from http://hmg.oxfordjournals.org/ at CSIC on March 9, 2014

Reagents

NAADP-AM and NED-19 were synthesized as previously described (54,65). Torin was a generous gift of D. Sabatini (Whitehead Institute for Biomedical Research, Cambridge, USA). 3-MA (3-methyladenine), NH_4Cl, bafilomycin A1, E-64d, pepstatin A, nigericin, trichostatin A, dantrolene, puromycin and ionomycin were from Sigma. STO-609 (7-oxo-7H-benzimidazo[2,1-a]benz[de]isoquinoline-3-carboxylic acid) and L690,440 (1-[(4-hydroxyphenoxy)ethylidene]bis [[phosphinylidyne bis(oxymethylene)]-2,2-dimethylpropanoate) were from Tocris Bioscience (Missouri, USA). Compound C, cycloheximide and MG-132 were from Calbiochem. BAPTA-AM was from Invitrogen, rapamycin was from LC Laboratories (Woburn, USA) and chloroquine was a generous gift from L. Ruiz Pérez (Institute of Parasitology and Biomedicine 'López-Neyra', CSIC, Granada, Spain).

Cell culture, transfection and cell lysis

Unless otherwise indicated, experiments were performed in HEK293T cells, which were cultured as previously described (66). Where indicated, experiments were also performed in neuroendocrine PC12 cells, which were cultured and transfected as previously described (64). Cells at 70–80% confluency were transfected using Lipofectamine 2000 (Invitrogen) according to manufacturer's specifications for 4 h, followed by addition of fresh medium. Single transfections were performed using 3.5 μg of plasmid of interest and 10 μl of Lipofectamine 2000. For double-transfections, 2.5 μg of each plasmid was used, and for triple-transfections, 1.7 μg of each plasmid was employed. The DNA ratio for co-transfections in the case of full-length LRRK2 constructs was 1:5, using a total of 10 μg of DNA.

Cells were treated with the indicated concentrations of compounds and for the indicated times, and cell extracts prepared 24 or 48 h after transfection. Cells were rinsed once in ice-cold PBS, followed by resuspension in 1 ml of lysis buffer per 100 mm dish (160 μl of lysis buffer per well of a 6-well plate) (1% SDS in PBS containing 1 mM PMSF, 1 mM Na_3VO_4 and 5 mM NaF). Extracts were boiled for 5 min, sonicated and centrifuged at 13 500 rpm for 10 min at 4°C. Protein concentrations of supernatants were estimated using the BCA assay (Pierce). Whenever possible, extracts were immediately resolved by SDS–PAGE without repeated freeze-thaws, as the latter was found to decrease detection of some phosphorylated proteins.

Immunofluorescence staining and confocal microscopy

Transfected cells were re-plated at a 1:3 ratio onto coverslips and processed for immunocytochemistry 24 or 48 h after transfection. Lysotracker DND-99, LysoSensor Green DND-189 and Bodipy 493/503 dyes were used essentially according to manufacturer's instructions (Invitrogen). Fixed cells were mounted using ProLong Gold AntiFade mounting medium (Invitrogen), and images acquired on a Leica TCS-SP5 confocal microscope using a ×100 HCX PL APO CS 1.4 oil UV objective. Images were collected using single excitation for each wavelength separately [488 nm Argon Laser line and a 500–545 nm emission band pass; 543 nm HeNe Laser line and a 556–673 nm emission band pass; 405 nm UV diode and a 422–466 nm emission band pass (12.5% intensity)]. Ten to fifteen image sections of selected areas were acquired with a step size of 0.3 μm, and z-stack images analysed and processed using Leica Applied Systems (LAS AF6000) image acquisition software. The same laser intensity was used for image acquisition of individual experiments. Co-localization analysis was performed using Leica Applied Systems (LAS AF6000) image acquisition software, adjusting thresholds to 28% for each channel.

Primary antibodies included a mouse monoclonal anti-LAMP2 antibody (1:50; Santa Cruz Biotechnology), a mouse monoclonal anti-p62 antibody (1:50; BD Transduction Laboratories), a mouse monoclonal anti-myc antibody (1:10 000, Sigma) and a rabbit polyclonal anti-GFP antibody (1:1000; Abcam). Secondary antibodies included goat anti-rabbit or goat anti-mouse AlexaFluor-405-conjugated secondary antibody (1:100; Invitrogen), AlexaFluor-488-conjugated secondary antibody (1:1000; Invitrogen) or AlexaFluor-555-conjugated secondary antibody (1:1000; Invitrogen).

For detection of apoptosis, fixed cells were mounted using mounting medium containing DAPI (Vector Laboratories) and visualized on a Zeiss microscope using a ×100 oil-immersion objective. For each experiment, an average of 100 cells from random fields was quantified, and condensed or fragmented nuclei scored as apoptotic cells. Occasionally, apoptotic cells were also quantified using the DeadEnd Fluorometric TUNEL System (Promega) according to manufacturer's specifications (Promega).

Quantitative image analysis

Autophagic activity was evaluated by quantifying the average number of GFP–LC3 punctae per cell. For this purpose, z-stacks of random fields of cells were captured at ×100 magnification on a confocal microscope. The number of GFP–LC3 punctae per cell was either obtained by manual counts performed by an observer blinded to condition, or more regularly using an NIH ImageJ macro called GFP–LC3 (13). Alternatively, random fields of transfected cells were imaged on a Zeiss microscope using a ×100 oil-immersion objective by an individual blinded to the experimental conditions, and the number of GFP–LC3 punctae per cell counted manually. Whilst the decreased resolution results in identification of overlapping or clustered punctae as a single large puncta, and thus will underestimate the number of GFP–LC3 punctae per cell, the relative changes observed using this determination were similar to those using the high-resolution analysis described above. For all determinations of LC3–GFP punctae per cell, between 30 and 50 randomly chosen transfected cells were analysed per experiment and condition. For quantification of yellow and red mCherry-EGFP–LC3 (td-tag-LC3) punctae, pictures were captured at ×100 magnification on a confocal microscope, and the number of yellow and red punctae analysed as described above from 40 randomly chosen transfected cells per experiment and condition.

Downloaded from http://hmg.oxfordjournals.org/ at CSIC on March 9, 2014

Electron microscopy

Transfected cells were collected, resuspended in HEPES-buffered media and filtered through a 50 μm filter before FACS sorting. Sorted cells were fixed with 4% paraformaldehyde, 0.1% glutaraldehyde in 0.1 M cacodylate buffer containing 3 μM $CaCl_2$ and 7.5% sucrose for 15 min at room temperature. Fixed cells were washed and pelleted, then cell pellets were cut into small cubes and mixed to randomize the sample. Samples were stained with reduced osmium tetraoxide, dehydrated and embedded in resin. Sections (~80 nm) were examined with an FEI TECNAI BioTWIN electron microscope. Random cells were imaged.

To calculate relative volume densities, Photoshop software was used to combine separate images to obtain a complete view of each cell. Autophagic structures were recognized according to their morphological characteristics. A counting grid was superimposed on images at a random offset and intersections were scored according to the underlying structures, using the ImageJ plug-ins Grids and Cell Counter (NIH, Bethesda, MD, USA). The relative volume density of each structure was calculated by dividing the number of intersections counted for each category by the number counted for the whole cell.

Western blotting

Proteins were resolved by SDS–PAGE, transferred onto polyvinylidene difluoride membranes (Hybond, GEHealthcare) and probed with primary antibodies overnight at 4°C. The following antibodies were employed: a rabbit polyclonal anti-phospho-ACC (Ser79), a rabbit monoclonal anti-phospho-AMPKα (Thr172) (40H9), a rabbit monoclonal anti-AMPKα, a rabbit polyclonal phospho-S6 (S235/236), a rabbit polyclonal phospho-p70 S6 kinase (Thr389), a rabbit polyclonal p70 S6 kinase, a rabbit monoclonal phospho-4E-BP1 (T37/46) (236B4) and a rabbit polyclonal 4E-BP1. All those antibodies were from Cell Signaling Technology, and used at a dilution of 1:500. Additional antibodies included a mouse monoclonal anti-p62 (1:500; BD Transduction Laboratories), a mouse monoclonal anti-LAMP2 (H4B4) (1:200; Santa Cruz Biotechnology), a mouse monoclonal anti-LAMP1 (H4A3) (1:200; Santa Cruz Biotechnology), a goat polyclonal anti-cathepsin D antibody (1:100; Santa Cruz Biotechnology), a mouse monoclonal anti-cathepsin L antibody (1:100; BD Biosciences), a mouse monoclonal anti-LC3 (1:500; MBL, Japan), a rabbit polyclonal anti-LC3 (1:500; Cell Signaling Technology), a rabbit polyclonal anti-GFP (ab6556) (1:500; Abcam), a monoclonal anti-bcl antibody (ab694) (1:10000; Abcam), a monoclonal anti-tubulin antibody (clone DM1A) (1:5000; Sigma), a rabbit polyclonal anti-pan-14-3-3 antibody (K-19) (1:500; Santa Cruz Biotechnology), a rabbit monoclonal anti-LRRK2 antibody (MJFF2, 1:500; Epitomics) or a mouse monoclonal C-terminal anti-LRRK2 antibody (N241A/34, NeuroMab, UCDavis, USA). Membranes were washed and incubated with secondary antibodies [anti-rabbit HRP-conjugated antibody (1:2000) or anti-mouse HRP-conjugated antibody (1:2000) (Dako Cytomation)] for 90 min at room temperature, followed by detection using ECL reagents (Roche). Unless otherwise indicated, 50 μg of cell extracts were resolved on MiniProtean Gels (BioRad Laboratories), whilst for phospho-p70 S6 kinase, phospho-4E-BP1, LC3 and p62, 150 μg of cell extracts were resolved on large PROTEAN II gels (BioRad Laboratories), and westerns developed with enhanced ECL reagents (Roche). Upon chemiluminescence detection, a series of timed exposures were undertaken to ensure that densitometric analyses were performed at exposures within the linear range. Films were scanned, and QuantityOne (Biorad) was employed for densitometric analysis.

Immunoprecipitation

Transfected cells were washed in chilled PBS and pelleted by centrifugation. Pellets were resuspended in IP buffer (1 ml/10 cm dish) containing 1% NP-40, 50 mM Tris/HCl, pH 7.4, 150 mM NaCl, phosphatase inhibitor cocktails 2 and 3 (Sigma) and protease inhibitor cocktail (Roche) and lysates centrifuged at 13 500 rpm for 10 min at 4°C. Protein concentration of supernatants was estimated using a BCA assay, and 1 mg total protein was subjected to immunoprecipitation with either anti-GFP (5 μg, Abcam) or anti-LRRK2 (10 μg, N138/6, NeuroMab, UCDavis, USA) antibodies. For immunoprecipitations, lysates were incubated with antibodies for 1 h at 4°C, followed by addition of protein G or protein A Sepharose beads and incubation overnight. Beads were washed five times with IP buffer followed by elution with SDS sample buffer and heating at 50°C for 3 min prior to separation by SDS-PAGE.

Statistical analysis

Data are expressed as means ± s.e.m., and the significance of differences was assessed using unpaired *t*-tests. Differences were accepted as significant at the 95% level ($P < 0.05$).

SUPPLEMENTARY MATERIAL

Supplementary Material is available at *HMG* online.

ACKNOWLEDGEMENTS

We thank M. Cookson, D. Carling, M. Jäättelä, D. Andrews, T. Johansen, T. Yoshimori and J. Oliver for constructs, D. Sabatini and L. Ruiz Pérez for reagents, the Electron Microscopy Facility at Manchester University and J.G. Castaño for helpful comments.

Conflict of Interest statement. None declared.

FUNDING

This work was supported by FEDER, the Spanish Ministry of Science and Innovation (grant numbers SAF2009-11292, intramural project number 200920I126, BFU2011-29899 and CEI-GREIB (GREIB.PT_2011_19)), the Fondo de Investigación Sanitaria (grant number FIS-PI040262), the Junta de Andalucia (grant number CTS 6816), and a Research Prize from the Federación Española de Parkinson (FEP). P.G-S. is funded by a JAE-pre studentship from the CSIC. Work in the laboratory of S.P. was supported by grant BB/G013721 from the

Downloaded from http://hmg.oxfordjournals.org/ at CSIC on March 9, 2014

Biotechnology and Biological Sciences Research Council and grants from the Alzheimer's Research Trust and Research into Ageing (UK). Funding to pay the Open Access publication charges for this article was provided by the Junta de Andalucia (grant number CTS 6816).

REFERENCES

1. Zimprich, A., Biskup, S., Leitner, P., Lichtner, P., Farrer, M., Lincoln, S., Kachergus, J., Hulihan, M., Uitti, R.J., Calne, D.B. *et al.* (2004) Mutations in LRRK2 cause autosomal-dominant parkinsonism with pleomorphic pathology. *Neuron*, **44**, 601–607.
2. Paisán-Ruíz, C., Jain, S., Evans, E.W., Gilks, W.P., Simón, J., van der Brug, M., López de Munain, A., Aparicio, S., Gil, A.M., Khan, N. *et al.* (2004) Cloning of the gene containing mutations that cause PARK8-linked Parkinson's disease. *Neuron*, **44**, 595–600.
3. Hardy, J. (2010) Genetic analysis of pathways to Parkinson disease. *Neuron*, **68**, 201–206.
4. West, A.B., Moore, D.J., Biskup, S., Bugayenko, A., Smith, W.W., Ross, C.A., Dawson, V.L. and Dawson, T.M. (2005) Parkinson's disease-assocated mutations in leucine-rich repeat kinase 2 augment kinase activity. *Proc. Natl Acad. Sci. USA*, **102**, 16842–16847.
5. Guo, L., Gandhi, P.N., Wang, W., Petersen, R.B., Wilson-Delfosse, A.L. and Chen, S.G. (2007) The Parkinson's disease-associated protein, leucine-rich repeat kinase 2 (LRRK2), is an authentic GTPase that stimulates kinase activity. *Exp. Cell Res.*, **313**, 3658–3670.
6. Jaleel, M., Nichols, R.J., Deak, M., Campbell, D.G., Gillardon, F., Knebel, A. and Alessi, D.R. (2007) LRRK2 phosphorylates moesin at threonine-558: characterization of how Parkinson's disease mutants affect kinase activity. *Biochem. J.*, **405**, 307–317.
7. Luzón-Toro, B., Rubio de la Torre, E., Delgado, A., Perez-Tur, J. and Hilfiker, S. (2007) Mechanistic insight into the dominant mode of the Parkinson's disease-associated G2019S LRRK2 mutation. *Hum. Mol. Genet.*, **16**, 2031–2039.
8. Smith, W.W., Pei, Z., Jiang, H., Dawson, V.L., Dawson, T.M. and Ross, C.A. (2006) Kinase activity of mutant LRRK2 mediates neuronal toxicity. *Nat. Neurosci.*, **9**, 1231–1233.
9. Greggio, E., Jain, S., Kingsbury, A., Bandopadhyay, R., Lewis, P., Kaganovich, A., van der Brug, M.P., Beilina, A., Blackinton, J., Thomas, K.J. *et al.* (2006) Kinase activity is required for the toxic effects of mutant LRRK2/dardarin. *Neurobiol. Dis.*, **23**, 329–341.
10. West, A.B., Moore, D.J., Choi, C., Andrabi, S.A., Li, X., Dikeman, D., Biskup, S., Zhang, Z., Lim, K.L., Dawson, V.L. and Dawson, T.M. (2007) Parkinson's disease-associated mutations in LRRK2 link enhanced GTP-binding and kinase activities to neuronal toxicity. *Hum. Mol. Genet.*, **16**, 223–232.
11. Lee, B.D., Shin, J.H., Vankampen, J., Petrucellli, L., West, A.B., Ko, H.S., Lee, Y.I., Maguire-Zeiss, K.A., Bowers, W.J., Federoff, H.J. *et al.* (2010) Inhibitors of leucine-rich repeat kinase-2 protect against models of Parkinson's disease. *Nat. Med.*, **16**, 998–1000.
12. Macleod, D., Dowman, J., Hammond, R., Leete, T., Inoue, K. and Abeliovich, A. (2006) The familial Parkinsonism gene LRRK2 regulates neurite process morphology. *Neuron*, **52**, 587–593.
13. Plowey, E.D., Cherra, S.J. III, Liu, Y.J. and Chu, C.T. (2008) Role of autophagy in G2019S-LRRK2-associated neurite shortening in differentiated SH-SY5Y cells. *J. Neurochem.*, **105**, 1048–1056.
14. Ramonet, D., Daher, J.P., Lin, B.M., Stafa, K., Kim, J., Banerjee, R., Westerlund, M., Pletnikova, O., Glauser, L., Yang, L. *et al.* (2011) Dopaminergic neuronal loss, reduced neurite complexity and autophagic abnormalities in transgenic mice expressing G2019S mutant LRRK2. *PLoS One*, **6**, e18568.
15. Alegre-Abarrategui, J., Christian, H., Lufino, M.M., Mutihac, R., Venda, L.L., Ansorge, O. and Wade-Martins, R. (2009) LRRK2 regulates autophagic activity and localizes to specific membrane microdomains in a novel human genomic reporter cellular model. *Hum. Mol. Genet.*, **18**, 4022–4034.
16. Xiong, Y., Coombes, C.E., Kilaru, A., Li, X., Gitler, A.D., Bowers, W.J., Dawson, V.L., Dawson, T.M. and Moore, D.J. (2010) GTPase activity plays a key role in the pathobiology of LRRK2. *PloS Genet.*, **6**, e1000902.
17. Biskup, S., Moore, D.J., Celsi, F., Higashi, S., West, A.B., Andrabi, S.A., Kurkinen, K., Yu, S.W., Savitt, J.M., Waldvogel, H.J. *et al.* (2006) Localization of LRRK2 to membranous and vesicular structures in mammalian brain. *Ann. Neurol.*, **60**, 557–569.
18. Levine, B. and Kroemer, G. (2008) Autophagy in the pathogenesis of disease. *Cell*, **132**, 27–41.
19. Yang, Z. and Klionsky, D.J. (2010) Mammalian autophagy: core molecular machinery and signaling regulation. *Curr. Opin. Cell Biol.*, **22**, 124–131.
20. Hara, T., Nakamura, K., Matsui, M., Yamamoto, A., Nakahara, Y., Suzuki-Migishima, R., Yokoyama, M., Mishima, D., Saito, I., Okano, H. and Mizushima, N. (2006) Suppression of basal autophagy in neural cells causes neurodegenerative disease in mice. *Nature*, **441**, 885–889.
21. Komatsu, M., Waguri, S., Chiba, T., Murata, S., Iwata, J., Tanida, I., Ueno, T., Koike, M., Uchiyama, Y., Kominami, E. and Tanaka, K. (2006) Loss of autophagy in the central nervous system causes neurodegeneration in mice. *Nature*, **441**, 880–884.
22. Wong, E. and Cuervo, A.M. (2010) Autophagy gone awry in neurodegenerative diseases. *Nat. Neurosci.*, **13**, 805–811.
23. Anglade, P., Vyas, S., Javoy-Agid, F., Herrero, M.T., Michel, P.P., Marquez, J., Mouatt-Prigent, A., Ruberg, M., Hirsch, E.C. and Agid, Y. (1997) Apoptosis and autophagy in nigral neurons of patients with Parkinson's disease. *Histol. Histopathol.*, **12**, 25–31.
24. Simonsen, A. and Tooze, S.A. (2009) Coordination of membrane events during autophagy by multiple class III PI3-kinase complexes. *J. Cell. Biol.*, **186**, 773–782.
25. Pankiv, S., Clausen, T.H., Lamark, T., Brech, A., Bruun, J.A., Outzen, H., Øvervatn, A., Bjørkøy, G. and Johansen, T. (2007) P62/SQSTM1 binds directly to Atg8/LC3 to facilitate degradation of ubiquitinated protein aggregates by autophagy. *J. Biol. Chem.*, **282**, 24131–24145.
26. Kimura, S., Noda, T. and Yoshimori, T. (2007) Dissection of the autophagosome maturation process by a novel reporter protein, tandem fluorescent-tagged LC3. *Autophagy*, **3**, 452–460.
27. Lee, J.Y., Koga, H., Kawaguchi, Y., Tang, W., Wong, E., Gao, Y.S., Pandey, U.B., Kaushik, S., Tresse, E., Lu, J. *et al.* (2010) HDAC6 controls autophagosome maturation essential for ubiquitin-selective quality-control autophagy. *EMBO J.*, **29**, 969–980.
28. Behrends, C., Sowa, M.E., Gygi, S.P. and Harper, J.W. (2010) Network organization of the human autophagy system. *Nature*, **466**, 68–76.
29. Thoreen, C.C., Kang, S.A., Chang, J.W., Liu, Q., Zhang, J., Gao, Y., Reichling, L.J., Sim, T., Sabatini, D.M. and Gray, N.S. (2009) An ATP-competitive mammalian target of rapamycin inhibitor reveals rapamycin-resistant functions of mTORC1. *J. Biol. Chem.*, **284**, 8023–8032.
30. Zhou, G., Myers, R., Li, Y., Chen, Y., Shen, X., Fenyk-Melody, J., Wu, M., Ventre, J., Doebber, T., Fujii, N. *et al.* (2001) Role of AMP-activated protein kinase in mechanism of metformin action. *J. Clin. Invest.*, **108**, 1167–1174.
31. Høyer-Hansen, M., Bastholm, L., Szyniarowski, P., Campanella, M., Szabadkai, G., Farkas, T., Bianchi, K., Fehrenbacher, N., Elling, F., Rizzuto, R. *et al.* (2007) Control of macroautophagy by calcium, calmodulin-dependent kinase kinase-β, and bcl-2. *Mol. Cell*, **25**, 193–205.
32. Woods, A., Azzout-Marniche, D., Foretz, M., Stein, S.C., Lemarchand, P., Ferré, P., Foufelle, F. and Carling, D. (2000) Characterization of the role of AMP-activated protein kinase in the regulation of glucose-activated gene expression using constitutively active and dominant negative forms of the kinase. *Mol. Cell. Biol.*, **20**, 6704–6711.
33. Tokumitsu, H., Inuzuka, H., Ishikawa, Y., Ikeda, M., Saji, I. and Kobayashi, R. (2002) STO-609, a specific inhibitor of the Ca^{2+}/calmodulin-dependent protein kinase kinase. *J. Biol. Chem.*, **277**, 15813–15818.
34. Dixon, C.J., Bowler, W.B., Fleetwood, P., Ginty, A.F., Gallagher, J.A. and Carron, J.A. (1997) Extracellular nucleotides stimulate proliferation in MCF-7 breast cancer cells via P2-purinoreceptors. *Br. J. Cancer*, **75**, 34–39.
35. Ferrari, D., Pinton, P., Szabadkai, G., Chami, M., Campanella, M., Pozzan, T. and Rizzuto, R. (2002) Endoplasmic reticulum, Bcl-2 and Ca^{2+} handling in apoptosis. *Cell Calcium*, **32**, 413–420.
36. Pattingre, S., Tassa, A., Qu, X., Garuti, R., Liang, X.H., Mizushima, N., Packer, M., Schneider, M.D. and Levine, B. (2005) Bcl-2 antiapoptotic proteins inhibit beclin 1-dependent autophagy. *Cell*, **122**, 927–939.
37. Criollo, A., Maiuri, M.C., Tasdemir, E., Vitale, I., Fiebig, A.A., Andrews, D., Molgo, J., Díaz, J., Lavandero, S., Harper, F. *et al.* (2007) Regulation

Downloaded from http://hmg.oxfordjournals.org/ at CSIC on March 9, 2014

of autophagy by the inositol trisphosphate receptor. *Cell Death Diff.*, **14**, 1029–1039.
38. Zhu, W., Cowie, A., Wasfy, G.W., Penn, L.Z., Leber, B. and Andrews, D.W. (1996) Bcl-2 mutants with restricted subcellular location reveal spatially distinct pathways for apoptosis in different cell types. *EMBO J.*, **15**, 4130–4141.
39. Palmer, A.E., Jin, C., Reed, J.C. and Tsien, R. (2004) Bcl-2-mediated alterations in endoplasmic reticulum Ca^{2+} analyzed with an improved genetically encoded fluorescent sensor. *Proc. Natl Acad. Sci. USA*, **101**, 17404–17409.
40. Bjørkøy, G., Lamark, T., Pankiv, S., Øvervatn, A., Brech, A. and Johansen, T. (2009) Monitoring autophagic degradation of p62/SQSTM1. *Meth. Enzymol.*, **452**, 181–197.
41. Lee, Y.H., Ko, J., Joung, I., Kim, J.H. and Shin, J. (1998) Immediate early response of the p62 gene encoding a non-proteasomal multiubiquitin chain binding protein. *FEBS Lett.*, **438**, 297–300.
42. Singh, R., Kaushik, S., Wang, Y., Xiang, Y., Novak, I., Komatsu, M., Tanaka, K., Cuervo, A.M. and Czaja, M.J. (2009) Autophagy regulates lipid metabolism. *Nature*, **458**, 1131–1135.
43. Dehay, B., Bové, J., Rodríguez-Muela, N., Perier, C., Recasens, A., Boya, P. and Vila, M. (2010) Pathogenic lysosomal depletion in Parkinson's disease. *J. Neurosci.*, **30**, 12535–12544.
44. Churchill, G.C., Okada, Y., Thomas, J.M., Genazzani, A.A., Patel, S. and Galione, A. (2002) NAADP mobilizes Ca^{2+} from reserve granules, lysosome-related organelles, in sea urchin eggs. *Cell*, **111**, 703–708.
45. Patel, S. and Docampo, R. (2010) Acidic calcium stores open for business: expanding the potential for intracellular Ca^{2+} signaling. *Trends Cell. Biol.*, **20**, 277–286.
46. Morgan, A.J. and Galione, A. (2007) NAADP induces pH changes in the lumen of acidic Ca^{2+} stores. *Biochem. J.*, **402**, 301–310.
47. Guse, A.H. and Lee, H.C. (2008) NAADP: a universal Ca^{2+} trigger. *Sci. Signal.*, **1**, re10.
48. Lloyd-Evans, E., Morgan, A.J., He, X., Smith, D.A., Elliot-Smith, E., Sillence, D.J., Churchill, G.C., Schuchman, E.H., Galione, A. and Platt, F.M. (2008) Niemann–Pick disease type C1 is a sphingosine storage disease that causes deregulation of lysosomal calcium. *Nat. Med.*, **14**, 1247–1255.
49. Cancela, J.M., Churchill, G.C. and Galione, A. (1999) Coordination of agonist-induced Ca^{2+}-signalling patterns by NAADP in pancreatic acinar cells. *Nature*, **398**, 74–76.
50. Calcraft, P.J., Ruas, M., Pan, Z., Cheng, X., Arredouani, A., Hao, X., Tang, J., Rietdorf, K., Teboul, L., Chuang, K.T. *et al.* (2009) NAADP mobilizes calcium from acidic organelles through two-pore channels. *Nature*, **459**, 596–600.
51. Brailoiu, E., Churamani, D., Cai, X., Schrlau, M.G., Brailoiu, C., Gao, X., Hooper, R., Boulware, M.J., Dun, N.J., Marchant, J.S. and Patel, S. (2009) Essential requirement for two-pore channel 1 in NAADP-mediated calcium signaling. *J. Cell Biol.*, **186**, 201–209.
52. Brailoiu, E., Rahman, T., Churamani, D., Prole, D.L., Brailoiu, G.C., Hooper, R., Taylor, C.W. and Patel, S. (2010) An NAADP-gated two-pore channel targeted to the plasma membrane uncouples triggering from amplifying Ca^{2+} signals. *J. Biol. Chem.*, **285**, 38511–38516.
53. Ruas, M., Rietdorf, K., Arredouani, A., Davis, L.C., Lloyd-Evans, E., Koegel, H., Funnell, T.M., Morgan, A.J., Ward, J.A., Watanabe, K. *et al.* (2010) Purified TPC isoforms form NAADP receptors with distinct roles for Ca^{2+} signaling and endolysosomal trafficking. *Curr. Biol.*, **20**, 703–709.
54. Naylor, E., Arredouani, A., Vasudevan, S.R., Lewis, A.M., Parkesh, R., Mizote, A., Rosen, D., Thomas, J.M., Izumi, M., Ganesan, A. *et al.* (2009) Identification of a chemical probe for NAADP by virtual screening. *Nat. Chem. Biol.*, **5**, 220–226.
55. Nguyen, H.N., Byers, B., Cord, B., Shcheglovitov, A., Byrne, J., Gujar, P., Kee, K., Schuele, B., Dolmetsch, R.E., Langston, W. *et al.* (2011) LRRK2 mutant iPSC-derived DA neurons demonstrate increased susceptibility to oxidative stress. *Cell Stem Cell*, **8**, 267–280.
56. Williams, A., Sarkar, S., Cuddon, P., Ttofi, E.K., Saiki, S., Siddiqi, F.H., Jahreiss, L., Fleming, A., Pask, D., Goldsmith, P. *et al.* (2008) Novel targets for Huntington's disease in an mTOR-independent autophagy pathway. *Nat. Chem. Biol.*, **4**, 295–305.
57. Lin, X., Parisiadou, L., Gu, X.L., Wang, L., Shim, H., Sun, L., Xie, C., Long, C.X., Yang, W.J., Ding, J. *et al.* (2009) Leucine-rich repeat kinase 2 regulates the progression of neuropathology induced by Parkinson's-disease-related mutant α-synuclein. *Neuron*, **64**, 807–827.
58. Imai, Y., Gehrke, S., Wang, H.Q., Takahashi, R., Hasegawa, K., Oota, E. and Lu, B. (2008) Phosphorylation of 4E-BP by LRRK2 affects the maintenance of dopaminergic neurons in *Drosophila*. *EMBO J.*, **27**, 2432–2443.
59. Gehrke, S., Imai, Y., Sokol, N. and Lu, B. (2010) Pathogenic LRRK2 negatively regulates microRNA-mediated translational repression. *Nature*, **466**, 637–641.
60. Cárdenas, C., Miller, R.A., Smith, I., Bui, T., Molgó, J., Müller, M., Vais, H., Cheung, K.H., Yang, J., Parker, I. *et al.* (2010) Essential regulation of cell bioenergetics by constitutive $InsP_3$ receptor Ca^{2+} transfer to mitochondria. *Cell*, **142**, 270–283.
61. Yu, L., McPhee, C.K., Zheng, L., Mardones, G.A., Rong, Y., Peng, J., Mi, N., Zhao, Y., Liu, Z., Wan, F. *et al.* (2010) Termination of autophagy and reformation of lysosomes regulated by mTOR. *Nature*, **465**, 942–946.
62. Lee, J.H., Yu, W.H., Kumar, A., Lee, S., Mohan, P.S., Peterhoff, C.M., Wolfe, D.M., Martinez-Vicente, M., Massey, A.C., Sovak, G. *et al.* (2010) Lysosomal proteolysis and autophagy require presenilin 1 and are disrupted by Alzheimer-related PS1 mutations. *Cell*, **141**, 1146–1158.
63. Mazzulli, J.R., Xu, Y.H., Sun, Y., Knight, A.L., McLean, P.J., Caldwell, G.A., Sidransky, E., Grabowski, G.A. and Krainc, D. (2011) Gaucher disease glucocerebrosidase and α-synuclein form a bidirectional pathogenic loop in synucleinopathies. *Cell*, **146**, 37–52.
64. Fdez, E., Martínez-Salvador, M., Beard, M., Woodman, P. and Hilfiker, S. (2010) Transmembrane-domain determinants for SNARE-mediated membrane fusion. *J. Cell Sci.*, **123**, 2473–2480.
65. Parkesh, R., Lewis, A.M., Aley, P.K., Arredouani, A., Rossi, S., Tavares, R., Vasudevan, S.R., Rosen, D., Galione, A., Dowden, J. and Churchill, G.C. (2008) Cell-permeant NAADP: a novel chemical tool enabling the study of Ca^{2+} signalling in intact cells. *Cell Calcium*, **43**, 531–538.
66. Rubio de la Torre, E., Luzón-Toro, B., Forte-Lago, I., Minguez-Castellanos, A., Ferrer, I. and Hilfiker, S. (2009) Combined kinase inhibition modulates parkin inactivation. *Hum. Mol. Genet.*, **18**, 809–823.
67. Hooper, R., Churamani, D., Brailoiu, E., Taylor, C.W. and Patel, S. (2011) Membrane topology of NAADP-sensitive two-pore channels and their regulation by N-linked glycosylation. *J. Biol. Chem.*, **286**, 9141–9149.

Downloaded from http://hmg.oxfordjournals.org/ at CSIC on March 9, 2014

SUPPLEMENTARY MATERIAL

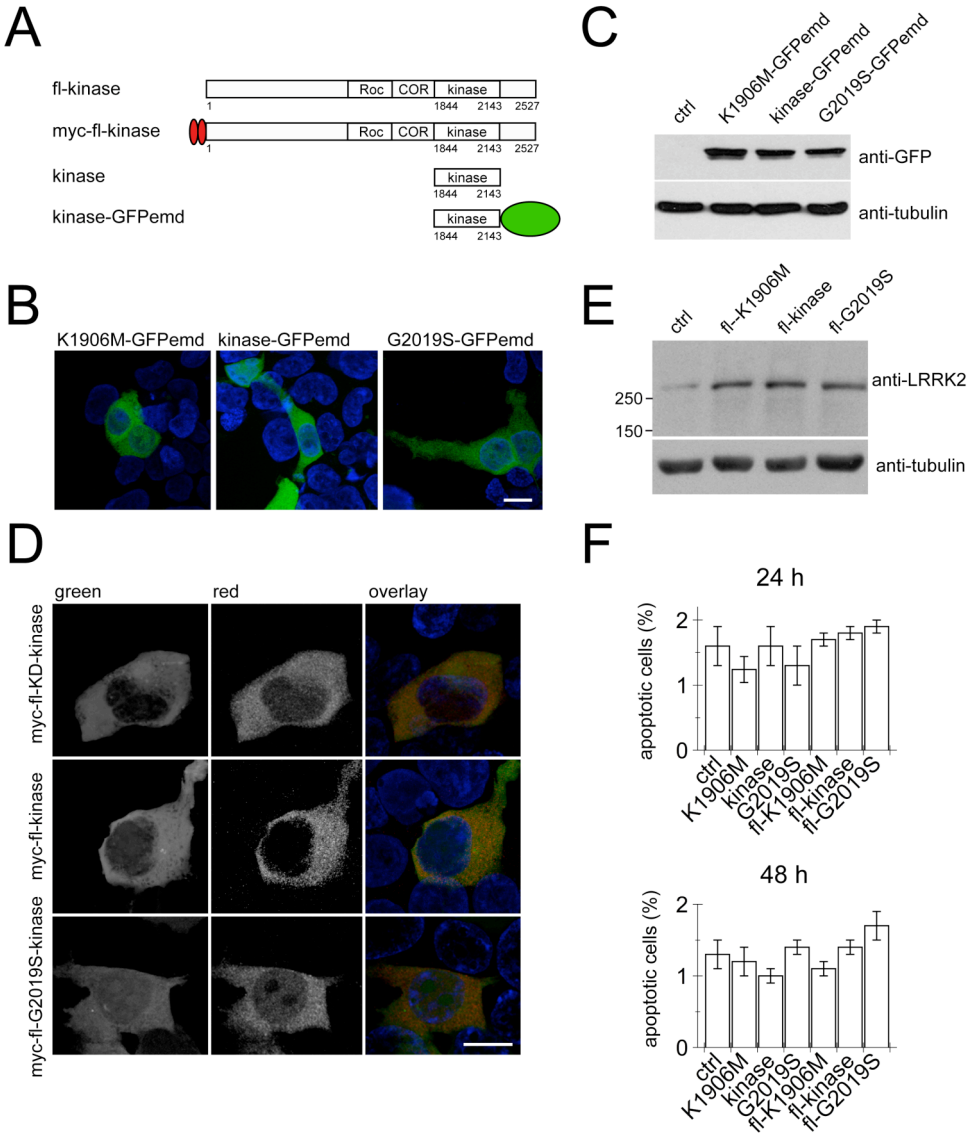

Figure S1 (related to Figure 1) Overexpression of LRRK2 constructs and effects on cell death. (**A**) Schematic representation of myc-tagged full-length LRRK2 (myc-fl-kinase) and non-tagged full-length LRRK2 (fl-kinase), as well as C-terminally tagged or non-tagged kinase domain (kinase) constructs employed, with domains and amino acids indicated. (**B**) Representative maximum-intensity projection of confocal images of cells transfected with GFP-tagged catalytically inactive K1906M-mutant kinase, wildtype kinase or G2019S-hyperactive kinase domain constructs as indicated, and processed 48

h after transfection. Scale bar, 10 μm. (**C**) As in (**B**), but cell extracts prepared and analyzed for levels of overexpression using a GFP antibody, and using a tubulin antibody to correct for differences in protein loading. (**D**) Representative maximum-intensity projection of confocal images of cells co-transfected with GFP (green) and myc-tagged full-length wildtype (myc-fl-kinase) or mutant LRRK2 constructs (G2019S or catalytically dead (KD)) as indicated, fixed 48 h after transfection and stained with an anti-myc antibody (red). Scale bar, 10 μm. (**E**) Cells were transfected with non-tagged, full-length wildtype or mutant LRRK2 constructs as indicated, and cell extracts prepared and analyzed with an anti-LRRK2 antibody (MJFF2, Epitomics) 48 h after transfection for levels of overexpression, and with a tubulin antibody to correct for differences in protein loading. (**F**) Cells were co-transfected with mCherry and with either empty vector (ctrl) or with the indicated kinase or full-length (fl) kinase constructs, and cell death analyzed either 24 h (top) or 48 h (bottom) after transfection using Hoechst staining. Bars represent mean ± s.e.m. (n=3).

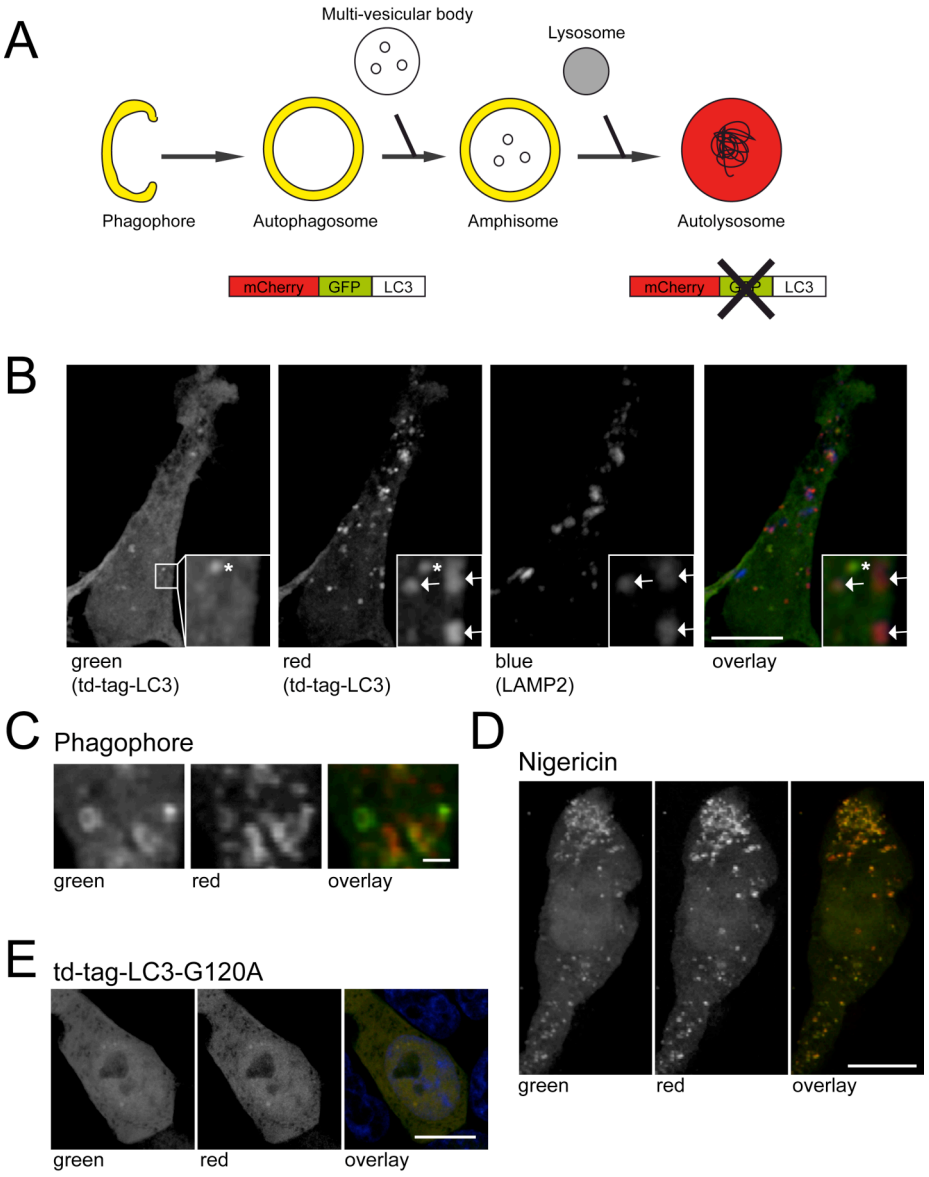

Figure S2 (related to Figure 2) Characterization of td-tag-LC3 labeling. (**A**) The tandem-tagged (td-tag) LC3 protein emits yellow (green merged with red) fluorescence in non-acidic structures, but appears as red only in autolysosomes due to the quenching of the GFP in the acidic environment. (**B**) Confocal image of a cell transfected with td-tag-LC3 and co-stained with LAMP2 (blue). Scale bar, 10 μm. Inset: Example of yellow, early autophagic structures negative for LAMP2 (asterisk) and red-only, late autophagic structures positive for LAMP2 (arrows). (**C**) Detection of a phagophore with td-tag-LC3. Scale bar, 1 μm. (**D**) Confocal image of a cell transfected with td-tag-LC3

and treated with nigericin (25 μM, 5 min), a H^+/K^+ ionophore which increases lysosomal pH, thus allowing visualization of both early and late autophagic structures as yellow punctae. Scale bar, 10 μm. (**E**) Confocal image of a cell transfected with G120A-mutant td-tag-LC3, which cannot be processed and conjugated to the autophagosomal membrane, and thus appears only as cytosolic fluorescence. Scale bar, 10 μm.

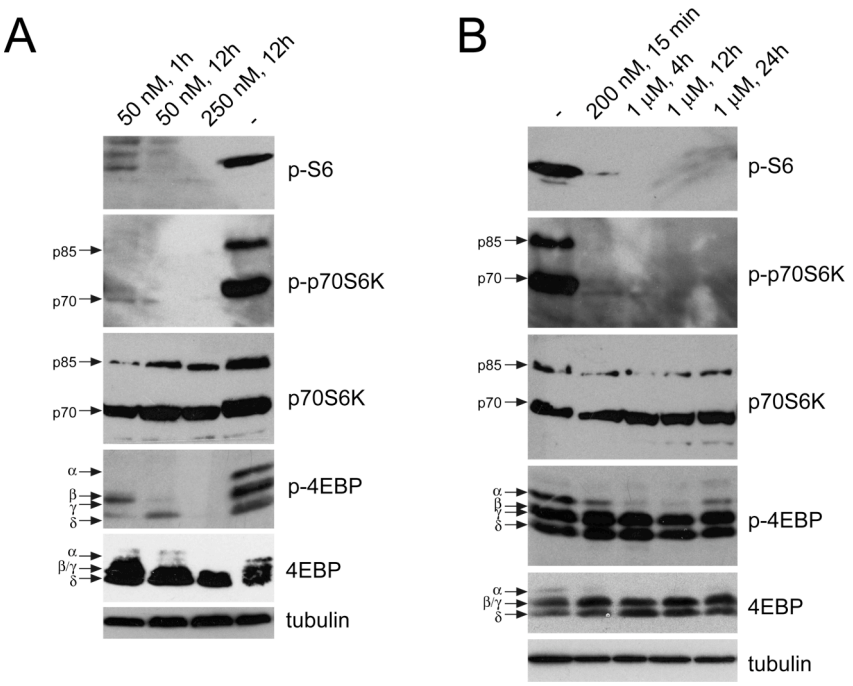

Figure S3 (related to Figure 3) Positive controls for regulation of TORC1 signaling. (**A**) Example of an experiment where cells were either left untreated (-), or treated for the indicated times with the indicated concentrations of torin, followed by analysis of cell extracts for the various substrates related to TORC1 activity. (**B**), as in (**A**), but cells treated with rapamycin as indicated, and cell extracts analyzed for the indicated TORC1 substrates. As previously described, both rapamycin and torin block TORC1-dependent phosphorylation of p70S6K, which in turn blocks phosphorylation of S6K. In contrast, only torin is able to suppress the TORC1-dependent but rapamycin-resistant phosphorylation of 4E-BP1. Experiments of this type were performed two times with similar results.

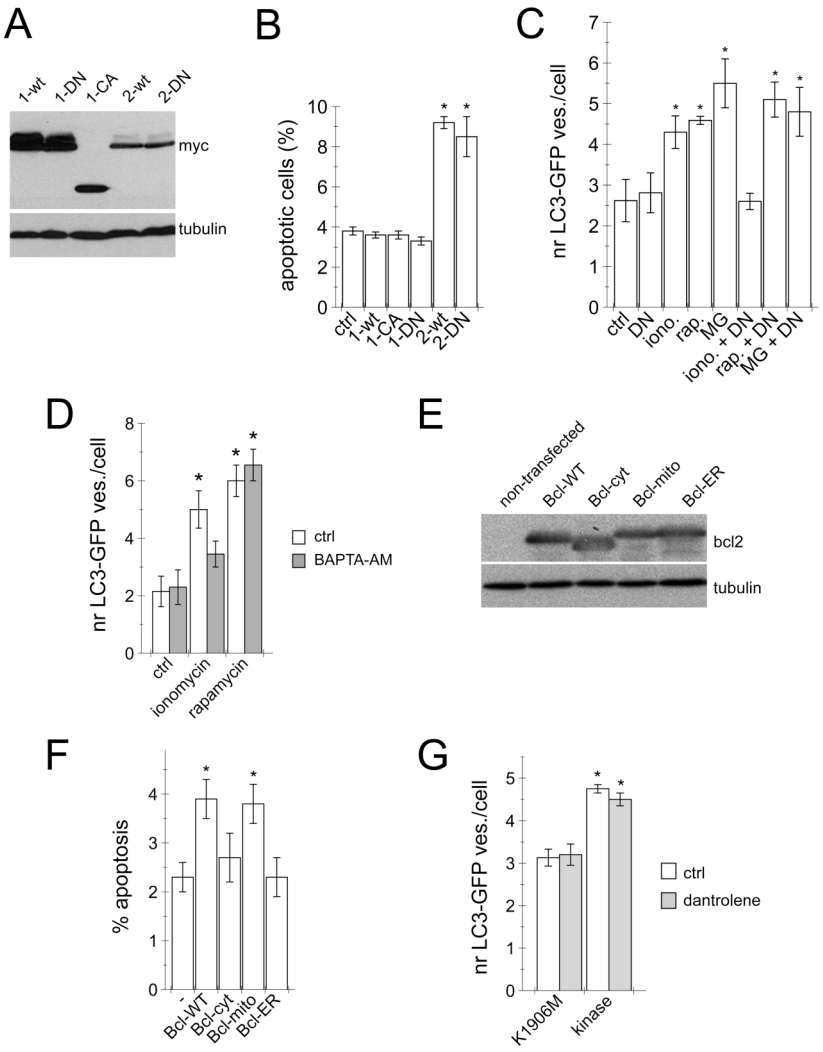

Figure S4 (related to Figure 4) Effects of LRRK2 overexpression on AMPK and intracellular calcium. (**A**) Cells were transfected with N-terminally myc-tagged human wildtype (1-wt), dominant-negative (1-DN) or constitutively active (1-CA) AMPKα1, or with wildtype (2-wt) or dominant-negative (2-DN) AMPKα2, and cell extracts analysed for expression with an anti-myc antibody 48 h after transfection. (**B**) Cells were transfected with the indicated AMPK constructs, and analyzed for cell death using Hoechst staining 48 h after transfection. Bars represent mean ± s.e.m. (n=3); *, $p < 0.005$. (**C**) Cells were co-transfected with LC3-GFP and either empty vector or dominant-negative AMPKα1 (DN) as indicated, and treated with ionomycin (2.5 μM,

12 h) (iono.), rapamycin (100 nM, 12 h) (rap.) or MG-132 (500 nM, 12 h) (MG) as indicated, and LC3-GFP punctae quantified 48 h after transfection. Bars represent mean ± s.e.m. (n=3); *, $p < 0.05$. (**D**) Cells were transfected with LC3-GFP and either left untreated (ctrl) or treated with ionomycin (2.5 μM, 12 h) or rapamycin (100 nM, 12 h) as indicated, and either left untreated (white bars) or treated with BAPTA-AM (5 μM, 2 h) (grey bars) prior to analysis for LC3-GFP punctae 48 h after transfection. Bars represent mean ± s.e.m. (n=3); *, $p < 0.05$. (**E**) Cells were transfected with the indicated bcl chimerae, and extracts analyzed for overexpression levels 24 h after transfection with an anti-bcl antibody. (**F**) Cells were transfected with either empty vector (-) or the indicated Bcl chimerae, and analyzed for cell death using Hoechst staining 24 h after transfection. Bars represent mean ± s.e.m. (n=3); *, $p < 0.05$. (**G**) Cells were co-transfected with LC3-GFP and either K1906M or kinase domain constructs, and either left untreated (white bars) or treated with dantrolene (1 μM, 2 h) (grey bars) prior to analysis for LC3-GFP punctae 48 h after transfection. Bars represent mean ± s.e.m. (n=3); *, $p < 0.05$.

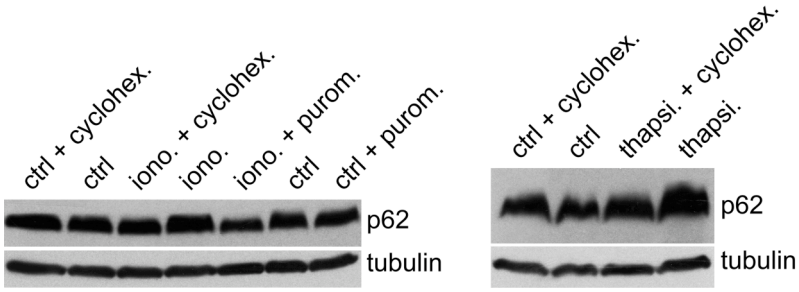

Figure S5 (related to Figure 5) Effects of intracellular calcium on p62 levels. Representative experiment where cells were either left untreated (ctrl), or incubated with ionomycin (2.5 μM, 6h) or thapsigargin (100 nM, 6h) to increase cytosolic calcium levels. Where indicated, cells were treated with puromycin (1 μM, 6h) or cycloheximide (350 nM, 6h) before analysis of p62 levels by Western blotting. The experiment was repeated once with similar results.

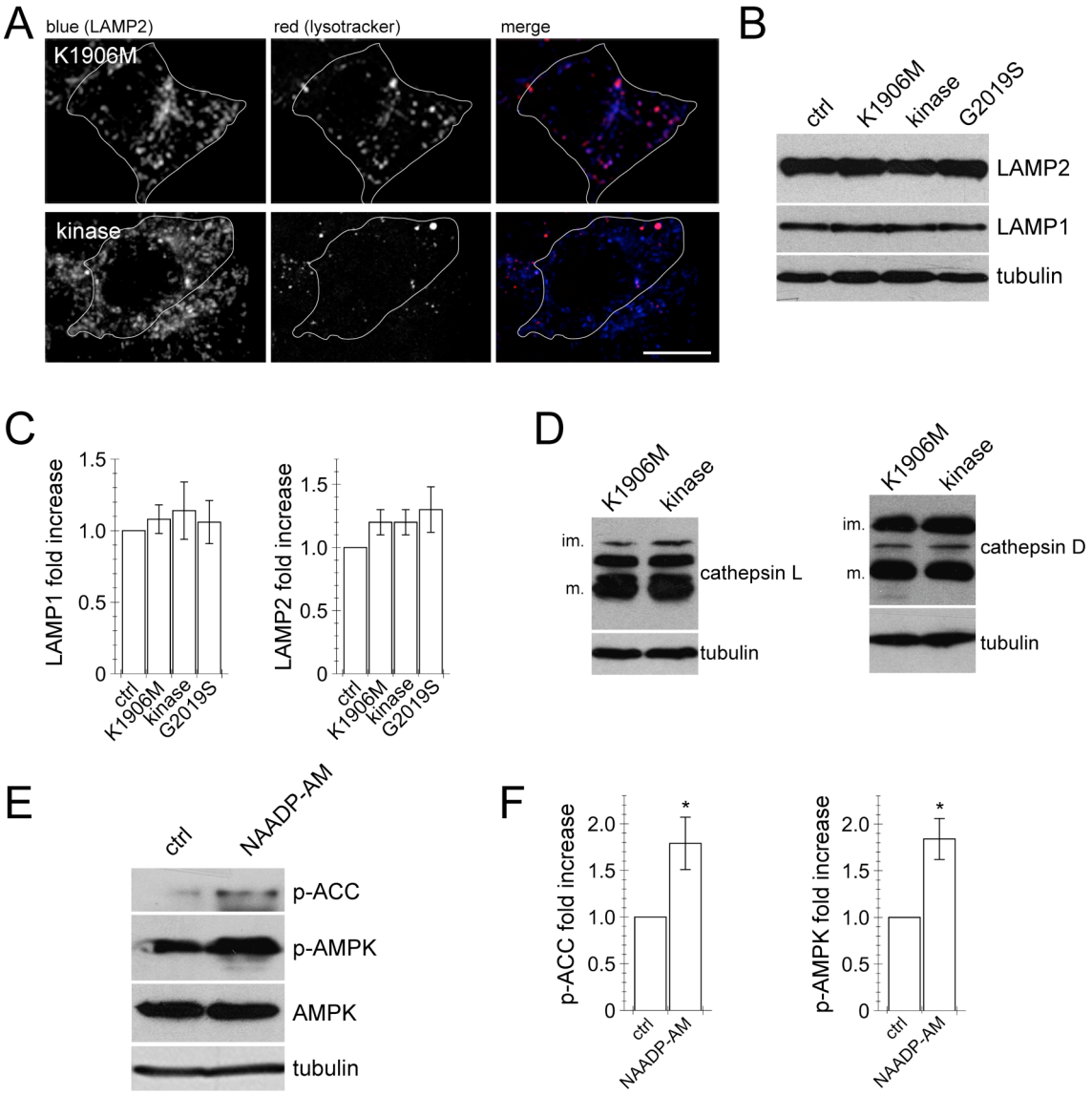

Figure S6 (related to Figure 6) Effects of LRRK2 on lipid accumulation and lysosomal pH, and effects of NAADP-AM. (**A**) Example of cells co-transfected with EGFP and either K1906M or kinase domain constructs, and stained with anti-LAMP2 (blue) and lysotracker (red). Scale bar, 10 μm. (**B**) Cells were transfected with empty vector (ctrl) or the indicated constructs, and extracts analyzed for levels of LAMP1 and LAMP2 by Western blotting. (**C**) Quantification of experiments as in B, where bars represent mean ± s.e.m. (n=3). (**D**) Cells were transfected with the indicated constructs and analyzed for the processing of cathepsin L (left) or cathepsin D (right). (**E**) Cells

were treated with NAADP-AM (100 nM, 12 h) before analysis for levels of p-ACC and p-AMPK as indicated. (**F**) Quantification of experiments as in E, where bars represent mean ± s.e.m. (n=3); *, $p < 0.05$.

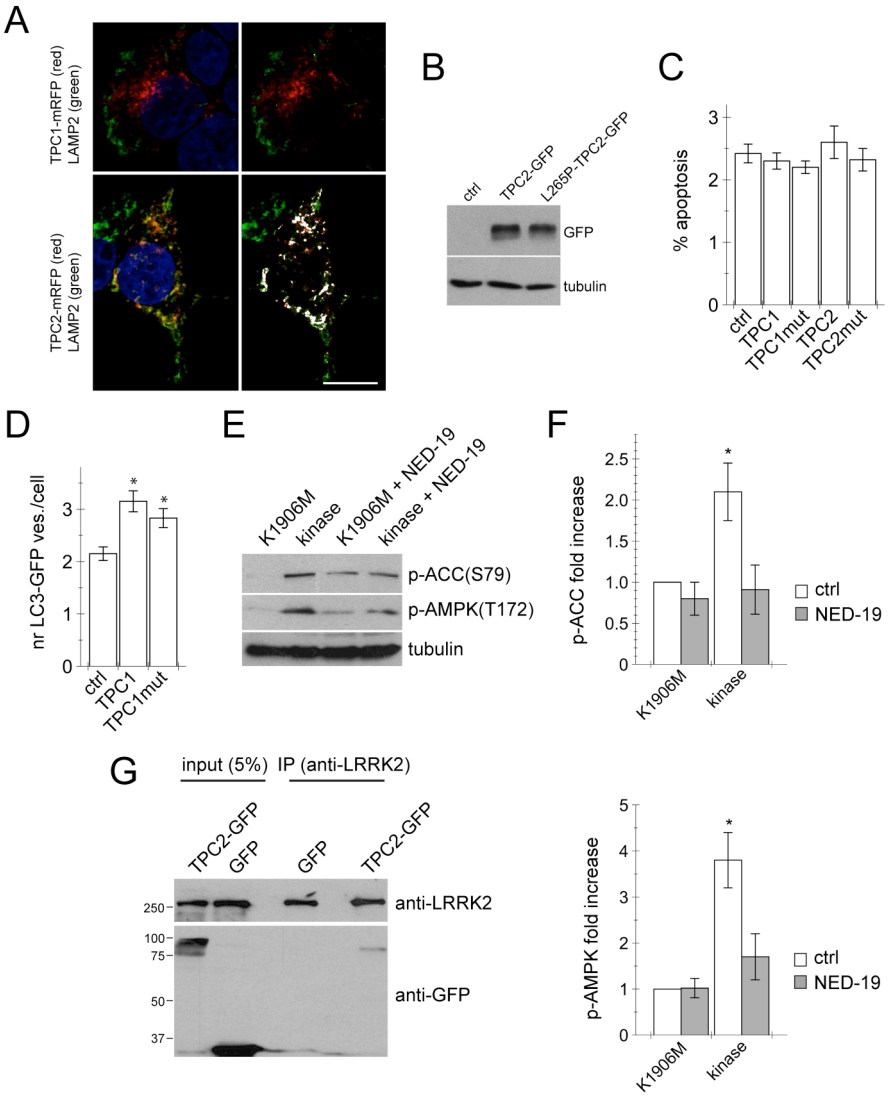

Figure S7 (related to Figure 7) A link between LRRK2 and NAADP-sensitive receptors. (**A**) Cells were transfected with the indicated RFP-tagged TPC constructs and stained for LAMP2 (green) and DAPI (blue). White: colocalization mask. Scale bar, 10 μm. (**B**) Cells were transfected with empty vector (ctrl) or the indicated GFP-tagged TPC2 constructs, and extracts analyzed for differences in overexpression using an anti-GFP antibody. (**C**) Cells were transfected with either empty vector (ctrl) or the indicated constructs, and analyzed for cell death using Hoechst staining 24 h after transfection. Bars represent mean ± s.e.m. (n=3). (**D**) Cells were co-transfected with LC3-GFP and

either empty vector (ctrl) or wildtype or mutant TPC1, and LC3-GFP punctae analyzed 24 h after transfection. Bars represent mean ± s.e.m. (n=4); *, $p < 0.05$. (**E**) Cells were transfected with either K1906M or wildtype LRRK2 kinase domain constructs, and treated with NED-19 (1 μM, 12 h) where indicated before analysis for p-ACC and p-AMPK. (**F**) Quantification of experiments as in E, where bars represent mean ± s.e.m. (n=3); *, $p < 0.05$. (**G**) Cells were transfected with TPC2-GFP or GFP vector, and extracts (1 mg) subjected to immunoprecipitation of endogenous LRRK2 with an anti-LRRK2 antibody (N138/6, NeuroMab, UCDavis, USA). Co-immunoprecipitated TPC2-GFP was detected using an anti-GFP antibody, and inputs (5%) were run along-side the immunoprecipitates. Representative of a total of four independent experiments. Note that TPC2-GFP runs as distinct bands corresponding to core glycosylated and mature fully glycosylated versions, respectively (67).

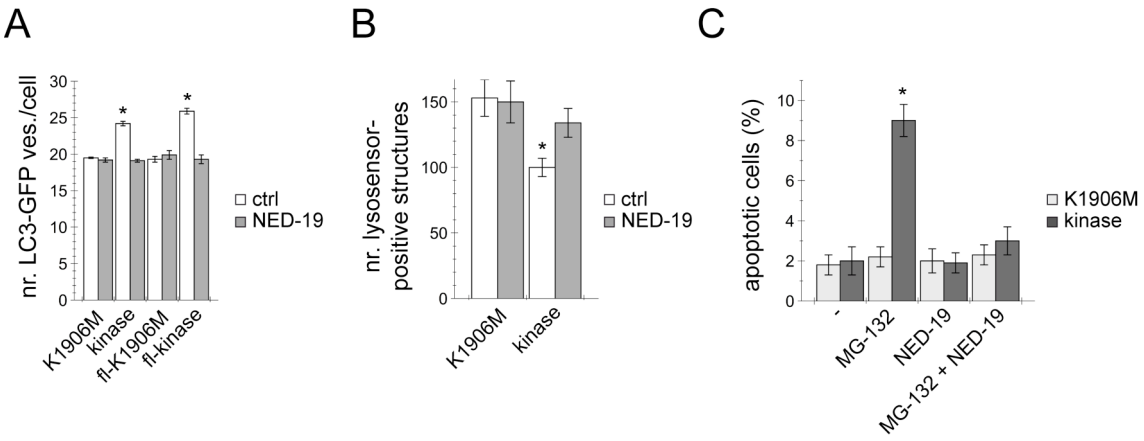

Figure S8 (related to Figure 8) Effects of LRRK2 expression on autophagy induction, lysosomal pH and cellular viability in the presence of proteasomal inhibitors in dopaminergic neuroendocrine PC12 cells. (**A**) Neuroendocrine PC12 cells were co-transfected with LC3-GFP and the indicated kinase domain or full-length LRRK2 (fl-kinase) constructs, and either left untreated (white bars) or treated with NED-19 (1 μM, 12 h) (grey bars), followed by quantification of LC3-GFP punctae 48 h after transfection. Bars represent mean ± s.e.m. (n=3); *, $p < 0.005$. (**B**) Transfected PC12 cells were treated with NED-19 (1 μM, 12 h) where indicated before staining with lysotracker. Bars represent mean ± s.e.m. (n=3); *, $p < 0.05$. (**C**) PC12 ells were co-transfected with GFP and K1906M or kinase domain constructs as indicated and either left untreated (-), treated with MG-132 (500 nM, 12 h), NED-19 (1 μM, 12 h) or both as indicated. Cells were analysed for cell death 48 h after transfection using Hoechst staining. Bars represent mean ± s.e.m. (n=3); *, $p < 0.005$.

2. LRRK2 as a modulator of lysosomal calcium homeostasis with downstream effects on autophagy

Autophagy 8:4, 692–693; April 2012; © 2012 Landes Bioscience

LRRK2 as a modulator of lysosomal calcium homeostasis with downstream effects on autophagy

Patricia Gómez-Suaga and Sabine Hilfiker*
Institute of Parasitology and Biomedicine "López-Neyra"; Consejo Superior de Investigaciones Cientificas (CSIC); Granada, Spain

Alterations in autophagy are thought to underlie various neurodegenerative diseases including Parkinson disease (PD). Previous studies have indicated that the PD gene leucine rich repeat kinase 2 (*LRRK2*) is involved in this process, but its mechanism of action has remained unknown. Our recent work describes how LRRK2 acts through calcium-mediated events originating from acidic stores to regulate autophagy and cell survival, which may give rise to novel therapeutic strategies.

Keywords: LRRK2, Parkinson disease, autophagy, calcium, NAADP, two-pore channel, lysosome

Submitted: 12/22/11

Revised: 01/09/12

Accepted: 01/09/12

http://dx.doi.org/10.4161/auto.19305

*Correspondence to: Sabine Hilfiker;
Email: sabine.hilfiker@ipb.csic.es

Punctum to: Gómez-Suaga P, Luzón-Toro B, Churamani D, Zhang L, Bloor-Young D, Patel S, et al. Leucine-rich repeat kinase 2 regulates autophagy through a calcium-dependent pathway involving NAADP. Hum Mol Genet 2011; 21:511–25; PMID:22012985; http://dx.doi.org/10.1093/hmg/ddr481

Mutations in the gene encoding *LRRK2* cause autosomal-dominant PD and represent the strongest risk factor for the development of idiopathic PD. Thus, understanding LRRK2 function may be relevant for our understanding of the more common sporadic form of the disease as well. LRRK2 is a large protein, and its catalytic GTPase and kinase activities implicate an important role for this protein in cellular signaling events. However, the normal cellular function of LRRK2 and how this function is altered by pathogenic mutations are currently unknown. Several previous studies had implicated LRRK2 as an important regulator of macroautophagy (hereafter referred to as autophagy), and our recent studies indicate a possible molecular mechanism of action (**Fig. 1**). Using a transient overexpression approach in various cell lines, including dopaminergic neuroendocrine cells, we found that LRRK2 causes an increase in autophagosome numbers. Such an increase in basal autophagy induction is mTORC1-independent, but dependent on the kinase activity of LRRK2, as overexpression of a catalytically inactive mutant LRRK2 is without effect. The LRRK2-mediated increase in autophagosome numbers occurs through activation of a calcium-dependent protein kinase kinase-β (CaMKK-β)/adenosine monophosphate (AMP)-activated protein kinase (AMPK) pathway and can be inhibited by calcium chelation or by expressing a BCL-2 chimera targeted to the endoplasmic reticulum (ER) and known to lower ER calcium concentrations. At the same time, LRRK2 overexpression was found to cause an increase in the pH of a population of lysosomes. Such change in pH is not sufficient to cause a complete lysosomal proteolysis phenotype, but correlates with an increase in lipid droplet numbers and with a decrease in cell survival in the presence of protein aggregation-induced stress.

Endosomes, lysosomes and lysosome-related organelles have recently emerged as important intracellular calcium storage compartments. Release can be triggered by the calcium mobilizing messenger nicotinic acid adenine dinucleotide phosphate (NAADP), with further increases in cytosolic calcium through amplification by ER calcium stores. In addition, the NAADP-mediated calcium release is accompanied by a partial alkalinization of acidic stores, and lysosomal calcium depletion can cause lipid accumulation. Application of the membrane-permeable NAADP-AM mimics, while Ned-19, a recently described NAADP antagonist, reverses the effects of LRRK2, indicating that the NAADP pathway may be involved in mediating the effects of LRRK2.

Two-pore channels (TPCs), a novel family of endolysosomal calcium channel proteins, are the likely receptors for

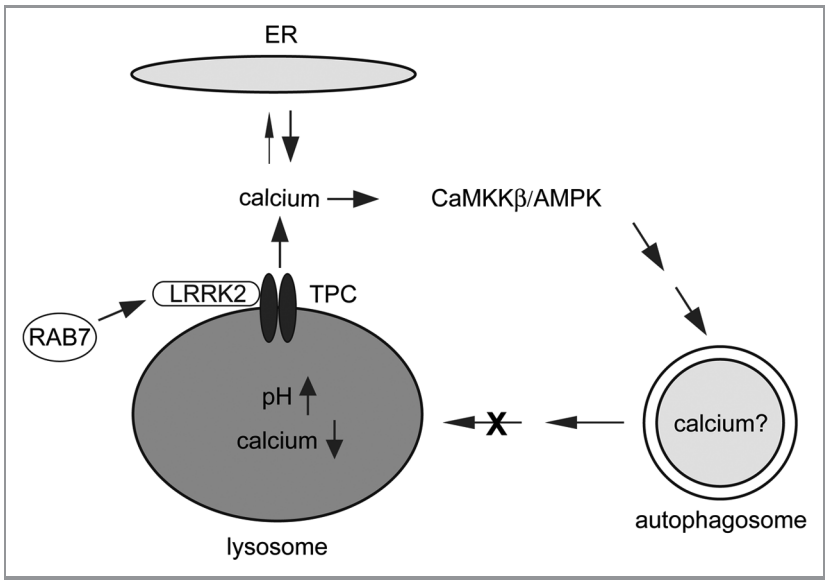

Figure 1. Diagram illustrating the proposed mechanism by which LRRK2 regulates autophagy. LRRK2 localizes to late endosomes and lysosomes, where it regulates calcium release through two-pore channels (TPCs). Calcium-induced calcium release from the ER further amplifies cytosolic calcium signals, leading to the activation of a CaMKKβ/AMPK cascade resulting in increased autophagosome numbers. Autophagosomes may display a decreased fusion efficiency if the intralumenal calcium levels are decreased in either autophagosomes or lysosomes, respectively, which would lead to a decrease in autophagic flux. Apart from regulating TPC-mediated calcium release, LRRK2 has also been reported to interact with RAB7 to negatively regulate the perinuclear localization of lysosomes in a microtubule-dependent manner, which would further limit autophagic flux.

NAADP. They are widely expressed channel proteins, with TPC1 localized to endosomes and lysosomes, and TPC2 mainly localized to lysosomes. Point mutants in the putative helix of the pore-forming regions of those channel proteins have been described, which abolish calcium conductance and display dominant-negative effects with respect to NAADP-mediated calcium signals. Co-expression of a dominant-negative version of TPC2 blocks the effects of LRRK2 on autophagosome numbers, and TPC2 and LRRK2 are found to interact upon co-expression and immunoprecipitation. Together, our data indicate that a lysosomal NAADP receptor such as TPC2 may be a target for LRRK2, causing calcium release from lysosomes, followed by calcium-induced calcium release from the ER and activation of a CaMKK/AMPK pathway to induce autophagy, while simultaneously alkalinizing lysosomal pH and causing an accumulation of lipids. These events are not detrimental to the cell under basal conditions, but cause enhanced cell death in the presence of additional stress associated with abnormal protein degradation.

Calcium is an important regulator of autophagy, even though its precise subcellular site(s) of action, or indeed whether it stimulates or inhibits autophagy have remained unclear. Several homotypic and heterotypic fusion events between organelles within the endolysosomal system are dependent on lumenal calcium. Thus, a decrease in lysosomal calcium levels would be predicted to cause a block in autophagosome-lysosome fusion and a concomitant accumulation of autophagosomes. Other scenarios by which calcium may regulate autophagosomal trafficking and/or fusion events with lysosomes have recently emerged as well. For example, thapsigargin was recently shown to inhibit autophagic flux by preventing the recruitment of RAB7 to autophagosomes. While the potential calcium-mediated event in this case remains unclear, it may be due to the importance of intralumenal autophagosomal calcium for the recruitment of RAB7 and/or for their fusion with lysosomes. Finally, a recent study indicates that the Drosophila LRRK2 homolog localizes to late endosomes and lysosomes where it interacts with RAB7 to negatively regulate the RAB7-dependent perinuclear localization of lysosomes. Interfering with lysosomal clustering in a perinuclear position prevents the efficient degradation of autophagosomes, causing their accumulation and an overall reduction of flux through the autophagosome-lysosome pathway. It will be interesting to determine whether the interaction between LRRK2 and RAB7 or TPC2 is calcium-dependent. In either case, our model provides a possible mechanism linking the distinct LRRK2-mediated phenomena as well as suggesting possible ways of intervention.

Acknowledgments

The work was supported by FEDER, the Spanish Ministry of Science and Innovation, the Junta de Andalucia and a JAE-pre studentship from the CSIC (to P.G.-S.).

3. A link between LRRK2, autophagy and NAADP-mediated endolysosomal calcium signalling

Biochemical Society TRANSACTIONS

www.biochemsoctrans.org

Biochemical Society Transactions

A link between LRRK2, autophagy and NAADP-mediated endolysosomal calcium signalling

Patricia Gómez-Suaga*, Grant C. Churchill†, Sandip Patel‡ and Sabine Hilfiker*[1]

*Institute of Parasitology and Biomedicine 'López-Neyra', Consejo Superior de Investigaciones Científicas (CSIC), Avda del Conocimiento s/n, 18100 Granada, Spain, †Department of Pharmacology, University of Oxford, Mansfield Road, Oxford OX1 3QT, U.K., and ‡Department of Cell and Developmental Biology, University College London, Gower Street, London WC1E 6BT, U.K.

Abstract

Mutations in LRRK2 (leucine-rich repeat kinase 2) represent a significant component of both sporadic and familial PD (Parkinson's disease). Pathogenic mutations cluster in the enzymatic domains of LRRK2, and kinase activity seems to correlate with cytotoxicity, suggesting the possibility of kinase-based therapeutic strategies for LRRK2-associated PD. Apart from cytotoxicity, changes in autophagy have consistently been observed upon overexpression of mutant, or knockdown of endogenous, LRRK2. However, delineating the precise mechanism(s) by which LRRK2 regulates autophagy has been difficult. Recent data suggest a mechanism involving late steps in autophagic–lysosomal clearance in a manner dependent on NAADP (nicotinic acid–adenine dinucleotide phosphate)-sensitive lysosomal Ca^{2+} channels. In the present paper, we review our current knowledge of the link between LRRK2 and autophagic–lysosomal clearance, including regulation of Ca^{2+}-dependent events involving NAADP.

Introduction

PD (Parkinson's disease) is a common age-related neurodegenerative disorder, and recent studies have revealed an important genetic component. Mutations in the gene encoding LRRK2 (leucine-rich repeat kinase 2) comprise the most common single genetic cause of familial PD [1,2], and variations increase the risk of sporadic PD [3–5]. These findings indicate that both forms of PD may share common pathological mechanisms related to LRRK2, and highlight the possibility that targeting LRRK2 may be beneficial in both cases [6]. However, this requires a detailed knowledge of the normal and pathological function(s) of LRRK2 at the molecular, cellular and systems levels.

The LRRK2 protein displays a complex multidomain structure with a central region comprising three independent domains, including a ROC (Ras of complex proteins), COR (C-terminal of ROC) and kinase domain. All six verified pathogenic mutations map to those three domains, indicating that altered enzymatic activity may be mediating the pathogenic effects of LRRK2 (Figure 1). However, whereas LRRK2 displays GTPase and kinase activity *in vitro*, only G2019S, the most prominent pathogenic LRRK2 mutation, has been consistently shown to augment kinase activity (reviewed in [7,8]). The effect of the other pathogenic mutations is less clear, as is the possible mutual regulation between the two enzymatic domains, or indeed the relevant pathogenic output of the protein (GTPase compared with kinase activity) [6–8]. Moreover, the true physiological target(s) of kinase activity are largely unknown, and other studies indicate that the function of LRRK2 may be rather mediated via a scaffolding role as a protein–protein interaction hub [9].

Although the molecular mechanism(s) of LRRK2 function remain unclear, at the cellular level, certain phenotypes have been consistently observed. At least under conditions of high-level expression *in vitro*, the pathogenic mutant forms of LRRK2 seem to be acutely toxic [10–13]. Similarly, there is evidence for cell death *in vivo* upon viral vector-mediated expression of mutant LRRK2 [14,15]. Importantly, toxicity seems dependent on the kinase activity of mutant LRRK2 [10,11,14]. In cellular models where cell death is not apparent, neurite shortening has also been reported to be a consistent phenotype associated with mutant LRRK2 [16–23]. Overexpression of wild-type and especially G2019S mutant LRRK2 in primary cortical neurons or neuronal cell lines leads to a reduction in neurite length, whereas ablation of endogenous LRRK2 oppositely enhances neurite length [16,17,23]. Likewise, upon long-term culture conditions, dopaminergic neurons differentiated from induced pluripotent stem cells from familial PD patients with the G2019S mutation display reduced numbers of neurites and neurite arborization [24]. Where evaluated, the effect of G2019S mutant LRRK2 on neurite morphology seems to be dependent on kinase activity and mediated by macroautophagy [16,17,23,24]. Since all mutations tested

Key words: calcium signalling, endolysosome, leucine-rich repeat kinase 2 (LRRK2), nicotinic acid–adenine dinucleotide phosphate (NAADP), Parkinson's disease, Rab protein.

Abbreviations used: COR, C-terminal of Ras of complex proteins; ER, endoplasmic reticulum; HEK, human embryonic kidney; LC3, light chain 3; LRRK2, leucine-rich repeat kinase 2; mTOR, mammalian target of rapamycin; NAADP, nicotinic acid–adenine dinucleotide phosphate; PD, Parkinson's disease; ROC, Ras of complex proteins; TPC, two-pore channel.

[1]To whom correspondence should be addressed (email sabine.hilfiker@ipb.csic.es).

©The Authors Journal compilation ©2012 Biochemical Society

Figure 1 | **Domain structure and PD mutations of LRRK2**

The central region of LRRK2 contains a GTPase domain also called ROC, a COR domain of unknown function and a kinase domain, flanked on either side by multiple protein–protein interaction domains. Clearly causative pathogenic mutations are indicated, and are clustered around the catalytic domains of LRRK2. Only the G2019S mutation consistently augments kinase activity. ANK, ankyrin repeat domain; LRR, leucine-rich repeats.

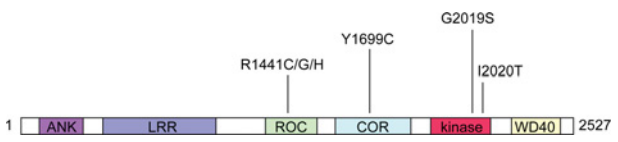

to date have at least one of these effects in cells, neurite shortening via changes in macroautophagy and eventual cell toxicity may reflect common cellular outputs of the same signalling pathways regulated by mutant LRRK2 [6]. In the present paper, we review the current knowledge of LRRK2's role in macroautophagy and how this may be related to endolysosomal Ca^{2+} signalling.

LRRK2 and autophagy: the good, the bad or the ugly?

Macroautophagy (hereinafter named autophagy) has been consistently shown to play important roles for determining neurite length (reviewed in [25]). Autophagy has recently gained much attention for its potential contribution to the pathogenesis of several neurodegenerative diseases including PD [26,27], and this link is supported further by the increase in autophagic vacuoles in the substantia nigra of PD brains [28]. Autophagy is a tightly regulated process by which cytosolic constituents, including damaged organelles and aggregated proteins, are engulfed within specialized double-membraned vesicles called autophagosomes, which are subsequently delivered to the lysosome for degradation [29,30]. Any disruption along the process, such as affecting autophagosome formation, fusion of autophagosomes with amphisomes or lysosomes, hydrolytic degradation or the re-formation of lysosomes can impair autophagic flux, concomitant with the accumulation of autophagy substrates and autophagic structures [29,30]. Furthermore, a close relationship exists between autophagy and endocytosis, with both sharing lysosomes as their common end-point [31]. Given this complexity, it has been difficult to assign a precise positive or negative role for normal or mutant LRRK2 in autophagic–lysosomal clearance.

To study the normal function of LRRK2, various lines of knockout mice have been generated. In LRRK2-deficient kidney, an increase in the number and size of secondary lysosomes and autolysosome-like structures has been consistently observed [32–34]. This is accompanied by the accumulation of lipofuscin granules, composed of highly oxidized and cross-linked proteins and lipids which cannot be properly degraded, and of p62, an autophagy substrate [32–34]. Such abnormal accumulation of undigested material indicates an impairment in the autophagy–lysosomal degradation system in the absence of LRRK2. To determine the possible defect along the autophagic pathway, the levels of LC3 (light chain 3)-I and LC3-II have been analysed. LC3-II, the lipidated form of LC3-I, is bound to the autophagosomal membrane, and its amount tends to be a reliable indicator of autophagic activity [35]. However, studies of this type have yielded a complex picture, with either no change [34] or a biphasic change reflecting an initial induction of autophagy at a young age, followed by a decrease in flux over time [32,33]. The continuous induction of autophagy caused by the absence of LRRK2 *in vivo* has been suggested to cause an eventual deficiency in the clearance or recycling of autophagic components/autolysosomes [33]. However, it remains to be seen whether such clearance/recycling represents a rate-limiting step, or whether other mechanism(s) may account for the observed age-dependent biphasic effects on autophagy.

In HEK (human embryonic kidney)-293 cells, RNAi (RNA interference)-mediated knockdown of LRRK2 resulted in increased LC3 turnover under starvation conditions. Unfortunately, equivalent flux experiments, or indeed an ultrastructural analysis, were not performed under nutrient rich conditions in the knockdown cells [36]. Conversely, in the same cellular model, overexpression of R1441C mutant LRRK2 was reported to cause impaired autophagic balance, as was evident by the accumulation of multivesicular bodies and large autophagosomes containing incompletely degraded material and increased levels of p62 [36]. Similarly, we detected improper autophagic–lysosomal clearance (indicated by an increase in lysosomal pH, accumulation of autophagic structures and lipid droplets) in HEK-293 cells overexpressing wild-type or G2019S mutant LRRK2 [37,38]. Thus it seems plausible that, at least in the kidney, the normal function of LRRK2 may be to negatively regulate autophagic clearance/lysosomal homoeostasis. In this setting, the presence of extra (or mutant hyperactive) LRRK2 would block, whereas the absence of LRRK2 would enhance, autophagic flux, with enhanced flux eventually overloading the lysosomal clearance/recycling system, such that both too much or too little LRRK2 activity may be detrimental to the proper functioning of this pathway *in vivo*.

LRRK2 and autophagy: universal or tissue-specific?

What about LRRK2-dependent autophagic–lysosomal clearance in the brain? Disappointingly, no accumulation of autophagic or lysosome-related structures has been reported in the brains of aged mice lacking LRRK2 [32–34]. This may indicate that LRRK2 performs distinct roles in distinct tissues [39]. Alternatively, LRRK1, a homologue of LRRK2, may functionally compensate for the loss of LRRK2 in the brain, but not in kidney, which suffers the biggest loss of LRRK compared with other organs [40,41]. The generation of double-knockout lines will be necessary to determine

©The Authors Journal compilation ©2012 Biochemical Society

whether complete loss of LRRK in neurons results in age-related changes in autophagy similar to those described in the kidney. Apart from compensatory events mediated by LRRK1, the levels of LRRK2 among different tissues may predetermine the presence and/or magnitude of a possible phenotype upon knockout and/or overexpression. For example, as LRRK2 levels are very high in the kidney [40,41], a knockout strategy may most pronouncedly uncover the (normal) role of LRRK2 in autophagic–lysosomal clearance in this organ. In contrast, given the low levels of LRRK2 in brain, a transgenic overexpression approach (of mutant hyperactive LRRK2) may be more effective, at least in the context of determining an autophagic–lysosomal clearance phenotype.

Alternatively, LRRK2 may affect a conserved pathway present in all cell types, but the same pathogenic mutation may give rise to different degrees of pathology depending on the cellular milieu in which it is operating [39]. As basal autophagy is very high in the kidney, deregulation of this pathway would be expected to be very pronounced in this organ, but should nevertheless also be detectable in other tissues such as brain. Indeed, overexpression of G2019S mutant LRRK2 has been reported to cause abnormal accumulation of autophagic and lysosomal structures in primary cortical neurons and neuronal cell lines in culture [16,17]. Similarly, an accumulation of autophagic vacuoles, including early and late autophagosomes, has been described in the soma and processes in the cortex and striatum from G2019S and, to a lesser degree, R1441C transgenic mice with advanced age [22]. Thus, both *in vitro* and *in vivo*, overexpression of mutant LRRK2 causes impaired autophagic–lysosomal clearance in neurons as well. In addition, bone-marrow-derived macrophages from mutant LRRK2 mice display a decrease in LC3-II levels, possibly highlighting an autophagic phenotype in those cells as well [42]. A decrease in autophagic flux, concomitant with an increase in p62 levels, autophagosomes and lipid droplets has recently also been described in human dopaminergic neurons derived from induced pluripotent stem cells from G2019S mutant LRRK2, but not control patients, after long-term culture [24], suggesting that endogenous levels of mutant LRRK2 are sufficient to induce an autophagic–lysosomal phenotype in dopaminergic neurons with time. Finally, and consistent with a role in autophagic–lysosomal clearance, overexpressed as well as endogenous LRRK2 has been reported to localize to specific membrane subdomains including endolysosomal structures in neuronal and non-neuronal cells [36,43,44]. Altogether, the data currently suggest that LRRK2 regulates autophagic–lysosomal clearance in a variety of cell types.

LRRK2 and autophagy: how?

The effects of LRRK2 on autophagic–lysosomal clearance may reflect its primary mechanism of action, or may occur secondarily, elicited as a response to some upstream event(s). Even if rather direct, many distinct scenarios are possible, as autophagy intersects with both the secretory and endocytic pathways at several points [45]. For example, LRRK2 has been shown to interact with the GTPase Rab5b, a regulator of endocytic vesicle trafficking [46]. Interestingly, both overexpression and knockdown of LRRK2 cause a decrease in presynaptic vesicle endocytosis rates, again indicating that both too much and too little LRRK2 adversely alters homoeostatic mechanisms, in this case controlling endocytosis [46]. Similarly, both overexpression or knockdown of LRRK2 induce defects in vesicle endocytosis upon depolarization of primary neuronal cultures [47,48], even though the possible effect of LRRK2 on the GTPase activity of Rab5b remains unclear.

Rab5b is a key regulator of the early endocytic pathway in mammalian cells [49], and recent studies indicate that it may play an additional positive role in autophagy by regulating an early step of autophagosome formation in a TORC1 (target of rapamycin complex 1)-independent manner [50]. In addition, endocytosis enables the formation of distinct signal transduction complexes which define specialized endosomal–lysosomal signalling platforms [51], such that LRRK2-mediated changes in endocytosis may modulate the formation of intracellular complexes to regulate signalling cascades including Wnt or MAPK (mitogen-activated protein kinase) cascades [51], both of which have been shown to be affected by LRRK2 [52].

Other mechanisms by which LRRK2 may regulate autophagy are possible as well. Fusion of both autophagosomes and endosomes with lysosomes requires Rab7, as does the process of lysosome re-formation [31,53–55], such that interfering with Rab7 function would affect autophagic–lysosomal clearance. Indeed, a recent study has shown that the *Drosophila* LRRK2 homologue interacts with Rab7 on late endosomes and lysosomes to negatively regulate Rab7-dependent perinuclear lysosomal positioning required for the efficient degradation of autophagosomes [56]. Finally, a recent study in *Caenorhabditis elegans* expressing human wild-type or mutant LRRK2, together with mutant tau as a source of proteostatic stress, revealed increased expression of numerous proteins including a subunit of the V-type proton ATPase [57,58]. Moreover, the behavioural motor deficits observed in these double-transgenic nematodes could be reverted by increasing autophagic flux using a rapamycin analogue. These data are consistent with our findings that mutant LRRK2 may increase lysosomal pH and concomitantly decrease lysosomal clearance, a process reversed by rapamycin, but not by other compounds which increase autophagy in an mTOR (mammalian target of rapamycin)-independent manner [37]. It will be interesting to determine whether the beneficial effect of the rapamycin analogue on motor output is related to an mTOR-dependent increase in degradative capacity as autophagic flux is enhanced, a decrease in protein synthesis, an effect on lysosomal homoeostasis or a combination thereof. In either case, a picture is starting to emerge whereby LRRK2 may regulate both early and late steps of autophagic–lysosomal clearance in a manner dependent on Rab proteins (Figure 2).

©The Authors Journal compilation ©2012 Biochemical Society

Figure 2 | Possible mechanisms by which LRRK2 may regulate events related to endolysosomal function

LRRK2 may regulate Rab5 function to cause changes in endocytosis and autophagosome formation. Altered endocytosis can further modulate signalling events occurring either at the plasma membrane or on intracellular organelles. Through its interaction with Rab7, LRRK2 may also regulate the fusion of autophagosomes or endosomes with lysosomes or lysosome re-formation, which in all cases would alter autophagic–lysosomal clearance. Finally, most of the above-mentioned membrane fusion/re-formation steps require intraluminal Ca^{2+}, and LRRK2 has been proposed to regulate endolysosomal function by modulating Ca^{2+} channels located on lysosomes. The increasing intraluminal Ca^{2+} concentrations along the endocytic–lysosomal pathway are indicated by the progressively darkened grey colour. Ligand binding to receptors, followed by endocytosis and interaction with signalling complexes, are indicated schematically. AV, autophagosome; EE, early endosome; LE/MVB, late endosome/multivesicular body; LYS, lysosome. For further details and references, see the text.

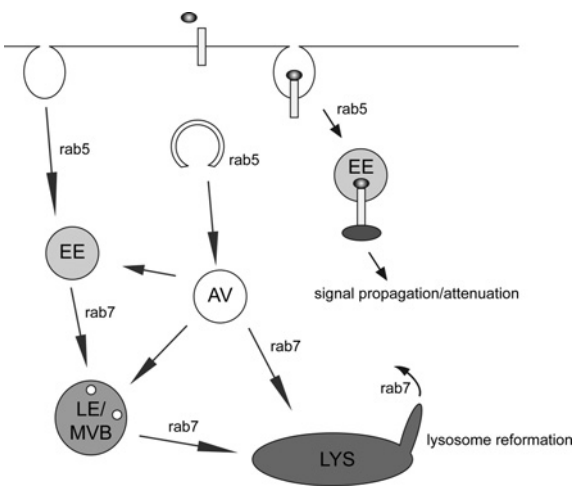

LRRK2 regulation of autophagy via NAADP (nicotinic acid–adenine dinucleotide phosphate)-mediated endolysosomal Ca^{2+} signalling

Changes in the concentration of cytosolic Ca^{2+} regulate a multitude of cellular events [59]. These changes result from both Ca^{2+} influx across the plasma membrane and the Ca^{2+} release from intracellular stores [60]. There is a growing appreciation of the importance of organelles of the endolysosomal system as mobilizable Ca^{2+} stores [61,62]. Indeed, release of Ca^{2+} from these stores has important implications for both endolysosomal trafficking [54] and intracellular Ca^{2+} signalling by the potent agonist-generated second messenger NAADP [61,63]. In many cell types, NAADP triggers complex Ca^{2+} signals that initiate from acidic Ca^{2+} stores, but which are subsequently amplified by ER (endoplasmic reticulum) Ca^{2+}-release channels [64,65]. Recent work has identified the endolysosomal TPC (two-pore channel) proteins TPC1 [66] and TPC2 [67] as the most likely primary targets for NAADP [68].

In our recent studies, we found an increase in autophagosome numbers upon transient overexpression of both wild-type and G2019S mutant, but not kinase-dead, LRRK2 in various cell lines, including dopaminergic neuroendocrine cells [37]. Importantly, we found that these effects were inhibited by the Ca^{2+} chelator BAPTA [1,2-bis-(*o*-aminophenoxy)ethane-*N*,*N*,*N*′,*N*′-tetra-acetic acid], suggesting that they were Ca^{2+}-dependent. The effects of LRRK2 overexpression were also blocked by overexpression of ER-targeted bcl2 (to deplete ER Ca^{2+} stores) and associated with an increase in the pH of a population of lysosomes and an increase in lipid droplet numbers. That NAADP evokes cytosolic Ca^{2+} signals which can be amplified by ER Ca^{2+} stores, and causes partial alkalinization of acidic stores and induces lipid accumulation [64,69,70], prompted us to test the role of NAADP in LRRK2 action.

Accordingly, we found that elevation of cellular NAADP levels using a cell-permeant NAADP analogue [NAADP-AM (NAADP acetoxymethyl ester)] [71] increased autophagosome numbers, lysosomal pH and lipid droplet numbers, thus largely mimicking the effects observed upon LRRK2 overexpression [37]. Conversely, the NAADP antagonist NED19 identified by virtual screening methods [72] reversed the effects of LRRK2. The increase in autophagosome number could also be blocked by overexpression of TPC2 mutated within the pore region [73]. This inactive mutant probably acts in a dominant manner similar to TPC1 in which the corresponding residue is mutated [66,74]. Taken together, these data uncover a hitherto unknown link between NAADP and LRRK2 function (Figure 3).

Outlook

Although the importance of LRRK2 in regulating autophagy is becoming increasingly clear, the underlying mechanisms are not fully understood. As discussed above, potential roles for Rab proteins and Ca^{2+} are emerging and not necessarily mutually exclusive. Moreover, the impact of Ca^{2+} on autophagy has been appreciated for some time and appears complex, with both positive and negative effects reported. Such dual effects may depend on the precise intraorganellar location at which Ca^{2+} is required for autophagosome–lysosome or endosome–lysosome fusion respectively [31,53].

Are the effects of LRRK2 on TPCs direct or indirect? It is tempting to speculate that TPCs may be kinase substrates. Recent evidence suggests that TPCs probably bind NAADP indirectly through associated low-molecular-mass binding proteins [75]. Although the precise identity of these proteins remains to be elucidated, might these be potential LRRK2 substrates? Although the NAADP pathway is implicated in LRRK2-mediated autophagy, the role of LRRK2 in regulation of cytosolic Ca^{2+} levels remains to be established. Future work will thus be necessary to delineate the precise molecular links between LRRK2, autophagy, NAADP and Ca^{2+}.

©The Authors Journal compilation ©2012 Biochemical Society

Figure 3 | Schematic diagram of proposed mechanism(s) by which LRRK2 regulates autophagy via modulation of NAADP-dependent Ca^{2+} channel (TPCs) on lysosomes

LRRK2 localizes to late endosomes and lysosomes and regulates Ca^{2+} release through TPCs. Whether this regulation is direct or mediated through interactions with Rab7 or NAADP receptor proteins (NAADP-R) remains to be determined. Ca^{2+}-induced Ca^{2+} release from the ER amplifies cytosolic Ca^{2+} signals, which leads to the activation of a Ca^{2+}-dependent cascade to increase autophagosome numbers. Simultaneously, diminished luminal Ca^{2+} may cause a decrease in autophagosome–lysosome fusion, and increased pH may have additional effects in impairing lysosomal proteolysis, leading to the observed autophagic–lysosomal clearance phenotype. For simplicity, additional Rab7- and Ca^{2+}-regulated events which may be subject to LRRK2 modulation in a TPC-dependent or -independent manner are not depicted.

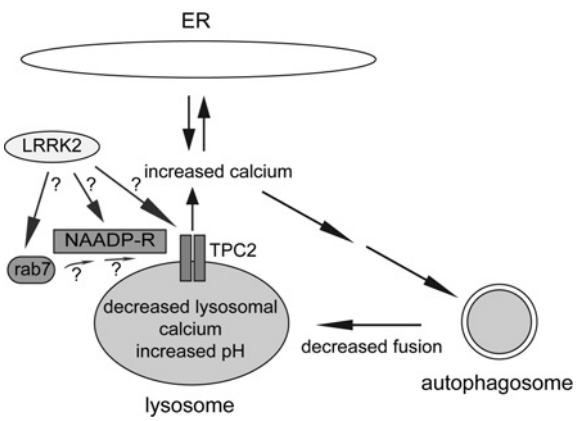

Funding

Our work is supported by the Spanish Ministry of Economy and Competitiveness [grant number BFU2011-29899], the Junta de Andalucía [grant number CTS 6816] and the Michael J. Fox Foundation.

References

1 Paisán-Ruiz, C., Jain, S., Evans, E.W., Gilks, W.P., Simón, J., van der Brug, M., López de Munain, A., Aparicio, S., Gil, A.M., Khan, N. et al. (2004) Cloning of the gene containing mutations that cause *PARK8*-linked Parkinson's disease. Neuron **44**, 595–600
2 Zimprich, A., Biskup, S., Leitner, P., Lichtner, P., Farrer, M., Lincoln, S., Kachergus, J., Hulihan, M., Uitti, R.J., Calne, D.B. et al. (2004) Mutations in *LRRK2* cause autosomal-dominant parkinsonism with pleomorphic pathology. Neuron **44**, 601–607
3 Satake, W., Nakabayashi, Y., Mizuta, I., Hirota, Y., Ito, C., Kubo, M., Kawaguchi, T., Tsunoda, T., Watanabe, M., Takeda, A. et al. (2009) Genome-wide association study identifies common variants at four loci as genetic risk factors for Parkinson's disease. Nat. Genet. **41**, 1303–1307
4 Simón-Sánchez, J., Schulte, C., Bras, J.M., Sharma, M., Gibbs, J.R., Berg, D., Paisán-Ruiz, C., Lichtner, P., Scholz, S.W., Hernandez, D.G. et al. (2009) Genome-wide association study reveals genetic risk underlying Parkinson's disease. Nat. Genet. **41**, 1308–1312
5 Nalls, M.A., Plagnol, V., Hernandez, D.G., Sharma, M., Sheerin, U.M., Saad, M., Simón-Sánchez, J., Schulte, C., Lesage, S., Sveinbjörnsdóttir, S. et al. (2011) Imputation of sequence variants for identification of genetic risks for Parkinson's disease: a meta-analysis of genome-wide association studies. Lancet **377**, 641–649
6 Rudenko, I.N., Chia, R. and Cookson, M.R. (2012) Is inhibition of kinase activity the only therapeutic strategy for *LRRK2*-associated Parkinson's disease? BMC Med. **10**, 20
7 Cookson, M.R. (2010) The role of leucine-rich repeat kinase 2 (LRRK2) in Parkinson's disease. Nat. Rev. Neurosci. **11**, 791–797
8 Greggio, E. and Cookson, M.R. (2009) Leucine-rich repeat kinase 2 mutations and Parkinson's disease: three questions. ASN NEURO **1**, art:e00002.doi:10.1042/AN20090007
9 Berwick, D.C. and Harvey, K. (2011) LRRK2 signaling pathways: the key to unlocking neurodegeneration? Trends Cell Biol. **21**, 257–265
10 Greggio, E., Jain, S., Kingsbury, A., Bandopadhyay, R., Lewis, P., Kaganovich, A., van der Brug, M.P., Beilina, A., Blackinton, J., Thomas, K.J. et al. (2006) Kinase activity is required for the toxic effects of mutant LRRK2/dardarin. Neurobiol. Dis. **23**, 329–341
11 Smith, W.W., Pei, Z., Jiang, H., Dawson, V.L., Dawson, T.M. and Ross, C.A. (2006) Kinase activity of mutant LRRK2 mediates neuronal toxicity. Nat. Neurosci. **9**, 1231–1233
12 West, A.B., Moore, D.J., Choi, C., Andrabi, S.A., Li, X., Dikeman, D., Biskup, S., Zhang, Z., Lim, K.L., Dawson, V.L. and Dawson, T.M. (2007) Parkinson's disease-associated mutations in LRRK2 link enhanced GTP-binding and kinase activities to neuronal toxicity. Hum. Mol. Genet. **16**, 223–232
13 Iaccarino, C., Crosio, C., Vitale, C., Sanna, G., Carri, M.T. and Barone, P. (2007) Apoptotic mechanisms in mutant LRRK2-mediated cell death. Hum. Mol. Genet. **16**, 1319–1326
14 Lee, B.D., Shin, J.H., VanKampen, J., Petrucelli, L., West, A.B., Ko, H.S., Lee, Y.I., Maguire-Zeiss, K.A., Bowers, W.J., Federoff, H.J. et al. (2010) Inhibitors of leucine-rich repeat kinase-2 protect against models of Parkinson's disease. Nat. Med. **16**, 998–1000
15 Dusonchet, J., Kochubey, O., Stafa, K., Young, Jr, S.M., Zufferey, R., Moore, D.J., Schneider, B.L. and Aebischer, P. (2011) A rat model of progressive nigral neurodegeneration induced by the Parkinson's disease-associated G2019S mutation in LRRK2. J. Neurosci. **31**, 907–912
16 MacLeod, D., Dowman, J., Hammond, R., Leete, T., Inoue, K. and Abeliovich, A. (2006) The familial parkinsonism gene *LRRK2* regulates neurite process morphology. Neuron **52**, 587–593
17 Plowey, E.D., Cherra, 3rd, S.J., Liu, Y.J. and Chu, C.T. (2008) Role of autophagy in G2019S-LRRK2-associated neurite shortening in differentiated SH-SY5Y cells. J. Neurochem. **105**, 1048–1056
18 Saemann, J., Hegermann, J., von Gromoff, E., Eimer, S., Baumeister, R. and Schmidt, E. (2009) *Caenorhabditis elegans* LRK-1 and PINK-1 act antagonistically in stress response and neurite outgrowth. J. Biol. Chem. **284**, 16482–16491
19 Lin, C.H., Tasi, P.I., Wu, R.M. and Chien, C.T. (2010) LRRK2 G2019S mutation induces dendrite degeneration through mislocalization and phosphorylation of tau by recruiting autoactivated GSK3β. J. Neurosci. **30**, 13138–13149
20 Winner, B., Melrose, H.L., Zhao, C., Hinkle, K.M., Yue, M., Kent, C., Braithwaite, A.T., Ogholikhan, S., Aigner, R., Winkler, J. et al. (2011) Adult neurogenersis and neurite outgrowth are impaired in LRRK2 G2019S mice. Neurobiol. Dis. **41**, 706–716
21 Chan, D., Citro, A., Cordy, J.M., Shen, G.C. and Wolozin, B. (2011) Rac1 protein rescues neurite retraction caused by G2019S leucine-rich repeat kinase 2 (LRRK2). J. Biol. Chem. **286**, 16140–16149
22 Ramonet, D., Daher, J.P., Lin, B.M., Stafa, K., Kim, J., Banerjee, R., Westerlund, M., Pletnikova, O., Glauser, L., Yang, L. et al. (2011) Dopaminergic neuronal loss, reduced neurite complexity and autophagic abnormalities in transgenic mice expressing G2019S mutant LRRK2. PLoS ONE **6**, e18568
23 Stafa, K., Trancikova, A., Webber, P.J., Glauser, L., West, A.B. and Moore, D.J. (2012) GTPase activity and neuronal toxicity of Parkinson's disease-associated LRRK2 is regulated by ArfGAP1. PLoS Genet. **8**, e1002526
24 Sánchez-Danés, A., Richaud-Patin, Y., Carballo-Carbajal, I., Jiménez-Delgado, S., Caig, C., Mora, S., Di Guglielmo, C., Ezquerra, M., Patel, B., Giralt, A. et al. (2012) Disease-specific phenotypes in dopamine neurons from human iPS-based models of genetic and sporadic Parkinson's disease. EMBO Mol. Med. **4**, 380–395
25 Chu, C.T., Plowey, E.D., Dagda, R.K., Hickey, R.W., Cherra, 3rd, S.J. and Clark, R.S. (2009) Autophagy in neurite injury and neurodegeneration: *in vitro* and *in vivo* models. Methods Enzymol. **453**, 217–249
26 Menzies, F.M., Moreau, K. and Rubinsztein, D.C. (2011) Protein misfolding disorders and macroautophagy. Curr. Opin. Cell Biol. **23**, 190–197
27 Wong, E. and Cuervo, A.M. (2011) Autophagy gone awry in neurodegenerative diseases. Nat. Neurosci. **13**, 805–811

©The Authors Journal compilation ©2012 Biochemical Society

28 Anglade, P., Vyas, S., Javoy-Agid, F., Herrero, M.T., Michel, P.P., Marquez, J., Mouatt-Prigent, A., Ruberg, M., Hirsch, E.C. and Agid, Y. (1997) Apoptosis and autophagy in nigral neurons of patients with Parkinson's disease. Histol. Histopathol. **12**, 25–31
29 Yang, Z. and Klionsky, D.J. (2010) Eaten alive: a history of macroautophagy. Nat. Cell Biol. **12**, 814–822
30 Codogno, P., Mehrpour, M. and Proikas-Cezanne, T. (2012) Canonical and non-canonical autophagy: variations on a common theme of self-eating? Nat. Rev. Mol. Cell Biol. **13**, 7–12
31 Luzio, J.P., Gray, S.R. and Bright, N.A. (2010) Endosome–lysosome fusion. Biochem. Soc. Trans. **38**, 1413–1416
32 Tong, Y., Yamaguchi, H., Giaime, E., Boyle, S., Kopan, R., Kelleher, 3rd, R.J. and Shen, J. (2010) Loss of leucine-rich repeat kinase 2 causes impairment of protein degradation pathways, accumulation of α-synuclein, and apoptotic cell death in aged mice. Proc. Natl. Acad. Sci. U.S.A. **107**, 9879–9884
33 Tong, Y., Giaime, E., Yamaguchi, H., Ichimura, T., Liu, Y., Si, H., Cai, H., Bonventre, J.V. and Shen, J. (2012) Loss of leucine-rich repeat kinase 2 causes age-dependent bi-phasic alterations of the autophagy pathway. Mol. Neurodeg. **7**, 2
34 Herzig, M.C., Kolly, C., Persohn, E., Theil, D., Schweizer, T., Hafner, T., Stemmelen, C., Troxler, T.J., Schmid, P., Danner, S. et al. (2011) LRRK2 protein levels are determined by kinase function and are crucial for kidney and lung homeostasis in mice. Hum. Mol. Genet. **20**, 4209–4223
35 Klionsky, D.J., Abeliovich, H., Agostinis, P., Agrawal, D.K., Aliev, G., Askew, D.S., Baba, M., Baehrecke, E.H., Bahr, B.A., Ballabio, A. et al. (2008) Guidelines for the use and interpretation of assays for monitoring autophagy in higher eukaryotes. Autophagy **4**, 151–175
36 Alegre-Abarrategui, J., Christian, H., Lufino, M.M.P., Mutihac, R., Lourenco Vande, L., Ansorge, A. and Wade-Martins, R. (2009) LRRK2 regulates autophagic activity and localized to specific membrane microdomains in a novel human genomic reporter cellular model. Hum. Mol. Genet. **18**, 4022–4034
37 Gómez-Suaga, P., Luzón-Toro, B., Churamani, D., Zhang, L., Bloor-Young, D., Patel, S., Woodman, P.G., Churchill, G.C. and Hilfiker, S. (2012) Leucine-rich repeat kinase 2 regulates autophagy through a calcium-dependent pathway involving NAADP. Hum. Mol. Genet. **21**, 511–525
38 Gómez-Suaga, P. and Hilfiker, S. (2012) LRRK2 as a modulator of lysosomal calcium homeostasis with downstream effects on autophagy. Autophagy **8**, 692–693
39 Lewis, P.A. and Manzoni, C. (2012) LRRK2 and human disease: a complicated question or a question of complexes? Sci. Signaling **5**, pe2
40 Westerlund, M., Belin, A.C., Anvret, A., Bickford, P., Olson, L. and Galter, D. (2008) Developmental regulation of leucine-rich repeat kinase 1 and 2 expression in the brain and other rodent and human organs: implications for Parkinson's disease. Neuroscience **152**, 429–436
41 Biskup, S., Moore, D.J., Rea, A., Lorenz-Deperieux, B., Coombes, C.E., Dawson, V.L., Dawson, T.M. and West, A.B. (2007) Dynamic and redundant regulation of LRRK2 and LRRK1 expression. BMC Neurosci. **28**, 102
42 Hakimi, M., Selvanantham, T., Swinton, E., Padmore, R.F., Tong, Y., Kabbach, G., Venderova, K., Girardin, S.E., Bulman, D.E., Scherzer, C.R. et al. (2011) Parkinson's disease-linked LRRK2 is expressed in circulating and tissue immune cells and upregulated following recognition of microbial structures. J. Neural Transm. **118**, 795–808
43 Biskup, S., Moore, D.J., Celsi, F., Higashi, S., West, A.B., Andrabi, S.A., Kurkinen, K., Yu, S.W., Savitt, J.M., Waldvogel, H.J. et al. (2006) Localization of LRRK2 to membranous and vesicular structures in mammalian brain. Ann. Neurol. **60**, 557–569
44 Higashi, S., Moore, D.J., Yamamoto, R., Minegishi, M., Sato, K., Togo, T., Katsuse, O., Uchikado, H., Furukawa, Y., Hino, H. et al. (2009) Abnormal localization of leucine-rich repeat kinase 2 to the endosomal–lysosomal compartment in Lewy body disease. J. Neuropathol. Exp. Neurol. **68**, 994–1005
45 Orsi, A., Polson, H.E.J. and Tooze, S.A. (2010) Membrane trafficking events that partake in autophagy. Curr. Opin. Cell Biol. **22**, 150–156
46 Shin, N., Jeong, H., Kwon, J., Heo, H.Y., Kwon, J.J., Yun, H.J., Kim, C.H., Han, B.S., Tong, Y., Shen, J. et al. (2008) LRRK2 regulates synaptic vesicle endocytosis. Exp. Cell Res. **314**, 2055–2065
47 Xiong, Y., Coombes, C.E., Kilaru, A., Li, X., Gitler, A.D., Bowers, W.J., Dawson, V.L., Dawson, T.M. and Moore, D.J. (2010) GTPase activity plays a key role in the pathobiology of LRRK2. PLoS Genet. **6**, e1000902
48 Piccoli, G., Condliffe, S.B., Bauer, M., Giesert, F., Boldt, K., De Astis, S., Meixner, A., Sarioglu, H., Vogt-Weisenhorn, D.M., Wurst, W. et al. (2011) LRRK2 controls synaptic vesicle storage and mobilization within the recycling pool. J. Neurosci. **31**, 2225–2237
49 Bucci, C., Parton, R.G., Mather, I.H., Stunnenberg, H., Simons, K., Hoflack, B. and Zerial, M. (1992) The small GTPase rab5 functions as a regulatory factor in the early endocytic pathway. Cell **70**, 715–728
50 Ravikumar, B., Imarisio, S., Sarkar, S., O'Kane, C.J. and Rubinsztein, D.C. (2008) Rab5 modulates aggregation and toxicity of mutant huntingtin through macroautophagy in cell and fly models of Huntington disease. J. Cell Sci. **121**, 1649–1660
51 Platta, H.W. and Stenmark, H. (2011) Endocytosis and signaling. Curr. Opin. Cell Biol. **23**, 393–403
52 Berwick, D.C. and Harvey, K. (2011) LRRK2 signaling pathways: the key to unlocking neurodegeneration? Trends Cell Biol. **21**, 257–265
53 Ganley, I.G., Wong, P.M., Gammoh, N. and Jiang, X. (2011) Distinct autophagosomal–lysosomal fusion mechanism revealed by thapsigargin-induced autophagy arrest. Mol. Cell **42**, 731–743
54 Pyror, P.R., Mullock, B.M., Bright, N.A., Gray, S.R. and Luzio, J.P. (2000) The role of intraorganellar Ca^{2+} in late endosome–lysosome heterotypic fusion and in the reformation of lysosomes from hybrid organelles. J. Cell Biol. **149**, 1053–1062
55 Yu, L., McPhee, C.K., Zheng, L., Mardones, G.A., Rong, Y., Peng, J., Mi, N., Zhao, Y., Liu, Z., Wan, F. et al. (2010) Termination of autophagy and reformation of lysosomes regulated by mTOR. Nature **465**, 942–946
56 Dodson, M.W., Zhang, T., Jiang, C., Chen, S. and Guo, M. (2012) Roles of the *Drosophila* LRRK2 homolog in rab7-dependent lysosomal positioning. Hum. Mol. Genet. **21**, 1350–1363
57 Di Domenico, F., Sultana, R., Ferree, A., Smith, K., Barone, E., Perluigi, M., Coccia, R., Pierce, W., Cai, J., Mancuso, C. et al. (2012) Redox proteomics analyses of the influence of co-expression of wild-type or mutated LRRK2 and tau on *C. elegans* protein expression and oxidative modification: relevance to Parkinson disease. Antioxid. Redox Signaling, doi:10.1089/ars.2011.4312
58 Ferree, A., Guillily, M., Li, H., Smith, K., Takashima, A., Squillace, R., Weigele, M., Collins, J.J. and Wolozin, B. (2012) Regulation of physiologic actions of LRRK2: focus on autophagy. Neurodegener. Dis. **10**, 238–241
59 Berridge, M.J. (2012) Calcium signalling remodelling and disease. Biochem. Soc. Trans. **40**, 297–309
60 Clapham, D.E. (2007) Calcium signaling. Cell **131**, 1047–1058
61 Patel, S. and Docampo, R. (2010) Acidic calcium stores open for business: expanding the potential for intracellular Ca^{2+} signaling. Trends Cell Biol. **20**, 277–286
62 Scott, C.C. and Gruenberg, J. (2011) Ion flux and the function of endosomes and lysosomes: pH is just the start. BioEssays **33**, 103–110
63 Churchill, G.C., Okada, Y., Thomas, J.M., Genazzani, A.A., Patel, S. and Galione, A. (2002) NAADP mobilizes Ca^{2+} from reserve granules, lysosome-related organelles, in sea urchin eggs. Cell **111**, 703–708
64 Guse, A.H. and Lee, H.C. (2008) NAADP: a universal Ca^{2+} trigger. Sci. Signaling **1**, re10
65 Morgan, A.J., Platt, F.M., Lloyd-Evans, E. and Galione, A. (2011) Molecular mechanisms of endolysosomal Ca^{2+} signalling in health and disease. Biochem. J. **439**, 349–374
66 Brailoiu, E., Churamani, D., Cai, X., Schrlau, M.G., Brailoiu, G.C., Gao, X., Hooper, R., Boulware, M.J., Dun, N.J., Marchant, J.S. and Patel, S. (2009) Essential requirement for two-pore channel 1 in NAADP-mediated calcium signaling. J. Cell Biol. **186**, 201–209
67 Calcraft, P.J., Ruas, M., Pan, Z., Cheng, X., Arredouani, A., Hao, X., Tang, J., Rietdorf, K., Teboul, L., Chuang, K.T. et al. (2009) NAADP mobilizes calcium from acidic organelles through two-pore channels. Nature **459**, 596–600
68 Patel, S., Ramakrishnan, L., Rahman, T., Hamdoun, A., Marchant, J.S., Taylor, C.W. and Brailoiu, E. (2011) The endo-lysosomal system as an NAADP-sensitive acidic Ca^{2+} store: role for the two-pore channels. Cell Calcium **50**, 157–167
69 Morgan, A.J. and Galione, A. (2007) NAADP induces pH changes in the lumen of acidic Ca^{2+} stores. Biochem. J. **402**, 301–310
70 Lloyd-Evans, E., Morgan, A.J, He, X., Smith, D.A., Elliot-Smith, E., Sillence, D.J., Churchill, G.C., Schuchman, E.H., Galione, A. and Platt, F.M. (2008) Niemann–Pick disease type C1 is a sphingosine storage disease that causes deregulation of lysosomal calcium. Nat. Med. **14**, 1247–1255
71 Parkesh, R., Lewis, A.M., Aley, P.K., Arredouani, A., Rossi, S., Tavares, R., Vasudevan, S.R., Rosen, D., Galione, A., Dowden, J. and Churchill, G.C. (2008) Cell-permeant NAADP: a novel chemical tool enabling the study of Ca^{2+} signalling in intact cells. Cell Calcium **43**, 531–538
72 Naylor, E., Arredouani, A., Vasudevan, S.R., Lewis, A.M., Parkesh, R., Mizote, A., Rosen, D., Thomas, J.M., Izumi, M., Ganesan, A. et al. (2009) Identification of a chemical probe for NAADP by virtual screening. Nat. Chem. Biol. **5**, 220–226

©The Authors Journal compilation ©2012 Biochemical Society

73 Brailoiu, E., Rahman, T., Churamani, D., Prole, D.L., Brailoiu, G.C., Hooper, R., Taylor, C.W. and Patel, S. (2010) An NAADP-gated two-pore channel targeted to the plasma membrane uncouples triggering from amplifying Ca^{2+} signals. J. Biol. Chem. **285**, 38511–38516
74 Rybalchenko, V., Ahuja, M., Coblentz, J., Churamani, D., Patel, S., Kiselyov, K. and Muallem, S. (2012) Membrane potential regulates NAADP dependence of the pH and Ca^{2+} sensitive organellar two-pore channel TPC1. J. Biol. Chem. **287**, 20407–20416
75 Lin-Moshier, Y., Walseth, T.F., Churamani, D., Davidson, S.M., Slama, J.T., Hooper, R., Brailoiu, E., Patel, S. and Marchant, J.S. (2012) Photoaffinity labeling of nicotinic acid adenine dinucleotide phosphate (NAADP) targets in mammalian cells. J. Biol. Chem. **287**, 2296–2307

Received 6 June 2012
doi:10.1042/BST20120138

©The Authors Journal compilation ©2012 Biochemical Society

4. A Link between Autophagy and the Pathophysiology of LRRK2 in Parkinson's disease

Hindawi Publishing Corporation
Parkinson's Disease
Volume 2012, Article ID 324521, 9 pages
doi:10.1155/2012/324521

Review Article

A Link between Autophagy and the Pathophysiology of LRRK2 in Parkinson's Disease

Patricia Gómez-Suaga, Elena Fdez, Marian Blanca Ramírez, and Sabine Hilfiker

Instituto de Parasitología y Biomedicina (López-Neyra), Consejo Superior de Investigaciones Cientificas (CSIC), Granada, 18100 Armilla, Spain

Correspondence should be addressed to Sabine Hilfiker, sabine.hilfiker@ipb.csic.es

Received 19 August 2012; Accepted 1 November 2012

Academic Editor: Lydia Álvarez-Erviti

Copyright © 2012 Patricia Gómez-Suaga et al. This is an open access article distributed under the Creative Commons Attribution License, which permits unrestricted use, distribution, and reproduction in any medium, provided the original work is properly cited.

Parkinson's disease is a debilitating neurodegenerative disorder, and its molecular etiopathogenesis remains poorly understood. The discovery of monogenic forms has significantly advanced our understanding of the molecular mechanisms underlying PD, as it allows generation of cellular and animal models carrying the mutant gene to define pathological pathways. Mutations in leucine-rich repeat kinase 2 (LRRK2) cause dominantly inherited PD, and variations increase risk, indicating that LRRK2 is an important player in both genetic and sporadic forms of the disease. G2019S, the most prominent pathogenic mutation, maps to the kinase domain and enhances enzymatic activity of LRRK2, which in turn seems to correlate with cytotoxicity. Since kinases are druggable targets, this has raised great hopes that disease-modifying therapies may be developed around modifying LRRK2 enzymatic activity. Apart from cytotoxicity, changes in autophagy have been consistently reported in the context of G2019S mutant LRRK2. Here, we will discuss current knowledge about mechanism(s) by which mutant LRRK2 may regulate autophagy, which highlights additional putative therapeutic targets.

1. Introduction

Parkinson's disease (PD) is a common neurodegenerative disorder with symptoms including tremor, rigidity, and postural instability [1]. Autosomal-dominant mutations in leucine-rich repeat kinase 2 (LRRK2) comprise the most common monogenic form of PD [2–5]. LRRK2-associated PD is symptomatically and neurochemically largely indistinguishable from sporadic PD cases [6], even though the reported pleomorphic pathology of mutant LRRK2 carriers differs from the rather classical α-synuclein pathology associated with sporadic PD. Variations in LRRK2 have further been reported to increase risk for sporadic PD [7–9], which implicates LRRK2 in both sporadic and familial forms of the disease. The big advantage of studying the function of a mutated gene product as compared to a sporadic disease is that one can generate cellular and animal models carrying the mutant gene to define pathological pathways. In conjunction with the described enzymatic activity of LRRK2 which may be targeted by select kinase inhibitors [10, 11], this has propelled the protein into the limelight of PD research worldwide. However, to develop disease-modifying or neuroprotective therapies around LRRK2, a clear understanding of its normal and pathological function(s) is required. A link between LRRK2 and aberrant macroautophagy has been consistently observed, and here we review our current knowledge of LRRK2's role in autophagy and lysosomal homeostasis with implications for cell demise in PD.

2. LRRK2 Structure and Cellular Localization

LRRK2 is a large multidomain protein belonging to the ROCO family of proteins which are characterized by the presence of leucine-rich repeats, a Ras of complex (ROC) GTPase domain, a C terminal of ROC (COR) linker region, and a kinase domain [12]. Among the many putative pathogenic variants identified to date, six missense mutations in LRRK2 have been clearly shown to segregate

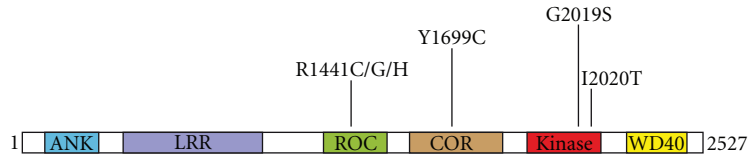

Figure 1: Domain structure and PD mutations of LRRK2. The central region of LRRK2 contains a GTPase domain also called (ROC), a C-terminal of ROC (COR) domain of unknown function, and a kinase domain, flanked on either side by protein-protein interaction domains including an ankyrin repeat domain (ANK), leucine-rich repeats (LRR) and a WD40 domain (WD40). Clearly causative pathogenic mutations are indicated and are clustered around the catalytic domains of LRRK2. Only the G2019S mutation consistently augments kinase activity.

with disease, and thus represent authentic disease-causing variants [13]. Importantly, these mutations all map to the central region comprised of the catalytic domains, indicating that a change in enzymatic activity (either GTPase or kinase) mediates the pathogenic effect(s) of LRRK2 (Figure 1). The G2019S mutation within the kinase domain (Figure 1) is the most frequent pathogenic LRRK2 mutation, having been identified in up to about 40% of familial PD cases dependent on ethnicity, and also detected in apparent sporadic PD cases [4, 5, 7–9]. This mutation has been consistently shown to augment catalytic activity [14], even though the inherent kinase activity of LRRK2 is very low. This may be, at least in part, due to the lack of currently identified and reproducible genuine kinase substrates. LRRK2 kinase is active towards itself [14], and autophosphorylation may represent a physiological readout. The effect of other pathogenic mutations on kinase activity is less clear. Intriguingly, a recent study indicates that the G2385R risk variant causes a partial loss of kinase activity, highlighting the possibility that both too much or too little LRRK2 kinase activity may be detrimental [15]. Mutations in the ROC and COR domain cause a decrease in GTPase, without gross changes in kinase activity [16, 17], suggesting that the GTPase activity may comprise the genuine physiological readout of LRRK2, which may be further modulated by kinase activity [11]. Finally, apart from the catalytic central domains, LRRK2 contains various protein-protein interaction domains including LRRK2-specific, ankyrin, and leucine-rich repeat motifs at the N-terminus, and WD40 repeats near the C-terminus of the protein (Figure 1). The existence of these domains indicates the possibility that it may act as a protein scaffold for the assembly of protein complexes [18]. Indeed, LRRK2 has been reported to interact with a whole array of proteins and may form distinct protein complexes in a cell-type or subcellular compartment-specific manner [19]. In this context, the enzymatic activities of LRRK2 may serve to change the affinity and/or composition of such complexes. Alternatively, a change in enzymatic activity may be the result of a change in protein complex interaction(s). Consistent with the latter possibility, LRRK2 has been reported to exist as a dimer, with dimerization enhancing kinase activity and causing relocalization to intracellular membranes [20–23], even though this has been disputed [24]. In either case, apart from being cytosolic, overexpressed, as well as endogenous, LRRK2 has been reported to localize to specific membrane subdomains including endolysosomal structures in neuronal and non-neuronal cells [25–27]. There, it may interact with and/or regulate distinct protein complexes. Such interactions may be controlled by the catalytic activity of LRRK2, either towards itself or currently unknown substrates. If correct, not only the catalytic activity of LRRK2, but also the modulation of distinct protein interactions should be considered possible targets for therapeutic strategies.

3. LRRK2 and the Regulation of Autophagy

The precise molecular mechanism(s) of LRRK2 function remain unclear. Certain phenotypes are robustly seen, such as the acutely toxic nature of pathogenic mutant forms of LRRK2 upon high-level overexpression in cultured cells [28–31]. Cell death is also evident upon viral vector-mediated expression of mutant LRRK2 *in vivo* [32, 33], and toxicity seems to depend on kinase activity [28, 29, 32]. In neuronal cellular models where cell death is not apparent, neurite shortening represents another consistent phenotype associated with mutant LRRK2 expression [34–42]. Where investigated, this also seems kinase activity-dependent and mediated by macroautophagy [34, 35, 41, 42]. All mutations tested to date have at least one of these effects on cells. Thus, the cellular pathway(s) underlying LRRK2 toxicity may involve altered macroautophagy, which in neurons may lead to neurite shortening and eventual cell demise. If so, elucidating the mechanism(s) by which LRRK2 alters macroautophagy becomes key.

Apart from playing an important role in determining neurite length [43], macroautophagy (thereafter named autophagy) has recently gained attention for its contribution to the pathogenesis of several neurodegenerative diseases including PD [44–46]. Autophagy is a process by which cytosolic constituents, including damaged organelles and aggregated proteins, are engulfed within specialized double-membraned vesicles called autophagosomes. Autophagosomes then fuse with amphisomes or lysosomes, followed by the hydrolytic degradation of products in lysosomes and reformation of these organelles to maintain cellular degradative capacity [47, 48]. Disrupting any part of this process impairs autophagic flux, accompanied by the accumulation of autophagic substrates and organelles [47, 48]. In addition, autophagy and endocytosis share lysosomes as their common end-point [49], such that it has been very difficult to define whether LRRK2 plays positive or negative roles in autophagic-lysosomal clearance.

A wealth of studies indicate that LRRK2 regulates autophagy. For example, various lines of knockout mice have been generated, which display an increase in the number and size of secondary lysosomes and autolysosome-like structures in the kidney [50–52]. An accumulation of lipofuscin granules, highly oxidized, and crosslinked proteins and lipids which cannot be properly degraded, and p62, an autophagy substrate, have also been observed [50–52]. Such abnormal accumulation of undigested material indicates an impairment in the autophagosomal-lysosomal degradation system. To determine a possible defect along the autophagic pathway, the levels of LC3I and LC3II have been analyzed. LC3II, the lipidated form of LC3I, becomes bound to the autophagosomal membrane and serves as a reliable indicator of autophagic activity [53]. Studies analyzing the levels of LC3II in the absence of LRRK2 in the kidney indicate either no change [52], or a biphasic change with an initial enhancement of flux at young age, followed by an impairment of flux over time [50, 51]. This block in flux has been interpreted to be due to an "overload" of the system, resulting in impaired clearance and/or recycling of autophagic components/autolysosomes [51]. Whilst an interesting hypothesis, it depends on assigning a rate-limiting step in the autophagy process, which will need further proof.

In agreement with the *in vivo* data of young animals, RNAi-mediated knockdown of LRRK2 has been found to result in increased autophagic flux under starvation conditions in a human embryonic kidney cell line (HEK293) [25]. Unfortunately, flux experiments were not performed under nutrient-rich conditions in these knockdown cells. Conversely, overexpression of R1441C mutant LRRK2 caused a block in autophagic flux, as evidenced by the accumulation of multivesicular bodies and large autophagosomes containing incompletely degraded material and increased levels of p62 [25]. Similarly, in our studies overexpressing wildtype and G2019S mutant LRRK2 in HEK293 cells, we found improper autophagic-lysosomal clearance, as indicated by an accumulation of autophagic structures and lipid droplets [54, 55]. Thus, at least in the kidney and in kidney-derived cell lines, the normal function of LRRK2 may be related to negatively regulating autophagic clearance and/or lysosomal homeostasis. Too much LRRK2 activity then would dampen, whilst too little activity would enhance autophagic flux. If the latter overloads the system with time, any deregulation of LRRK2 activity may be damaging to the proper functioning of the autophagic pathway *in vivo*.

4. Tissue-Specific versus Universal Regulation of Autophagy

In contrast to kidney, there has been no evidence for the accumulation of autophagic or lysosome-related structures in the brains of aged mice lacking LRRK2 [50–52]. Thus, LRRK2 may perform distinct roles in a tissue-specific manner, with an effect on autophagy in kidney, but not in brain. Alternatively, LRRK1 may functionally compensate for the loss of LRRK2 in the brain, but not in the kidney, the latter of which contains small amounts of LRRK1 versus LRRK2 and thus percentually suffers a much bigger loss of LRRK proteins [56, 57]. In addition, the homo- and heterodimerization of LRRK1 and LRRK2 proteins has been reported [58, 59], with LRRK1 involved in regulating endosomal trafficking [60, 61], consistent with a role for both proteins in recycling and degradation events. Generation of double-knockout lines will be required to delineate whether a complete loss of LRRK proteins in neurons results in age-related changes in autophagy similar to those observed in the kidney.

As another possibility, the overall levels of LRRK proteins present in different tissues may predetermine whether a phenotype is observed upon knockout versus overexpression conditions. For example, as LRRK levels are very high in kidney [56, 57], a knockout strategy may be more adequate to uncover the (normal) role of LRRK2 in autophagic-lysosomal clearance. Conversely, given the low levels of LRRK2 in the brain, an overexpression approach, especially of mutant, hyperactive LRRK2, may be more effective.

Apart from differences in the levels of LRRK proteins, the rate of basal autophagy also displays large differences across distinct tissues. Thus, the same pathogenic mutation of LRRK2 may give rise to different degrees of pathology depending on the cellular milieu in which it is operating [19]. As basal autophagy is very high in the kidney, a deregulation may be more pronounced in this organ as compared to other tissues. Nevertheless, if LRRK2 is a universal modulator of autophagic/lysosomal clearance, changes should also be detectable in other tissues such as brain, albeit possibly to a lesser degree or in an age-dependent manner difficult to track using rodent models. In agreement with a universal role in regulating autophagy, an overexpression approach using G2019S mutant LRRK2 has been reported to cause abnormal accumulation of autophagic and lysosomal structures in primary cortical neurons and neuronal cell lines in culture [34, 35]. Similarly, an accumulation of autophagic vacuoles, including early and late autophagosomes, has been described in the soma and processes in the cortex and striatum from G2019S, and to a lesser degree R1441C, transgenic mice with advanced age [40]. Thus, both *in vitro* and *in vivo*, overexpression of mutant LRRK2 seems to cause impaired autophagic-lysosomal clearance in neurons as well. A decrease in autophagic flux, concomitant with an increase in p62 levels, autophagosomes and lipid droplets has recently also been described in human dopaminergic neurons derived from induced pluripotent stem cells from G2019S mutant LRRK2, but not control patients, after long-term culture [42]. These data are important, as they indicate that endogenous levels of mutant LRRK2 are sufficient to induce an autophagic-lysosomal phenotype in dopaminergic neurons with time. In contrast, fibroblasts from those same patients do not reveal differences in autophagic clearance, consistent with their extremely low levels of basal autophagic activity [42]. However, the latter findings are in contrast to a recent report suggesting elevated levels of autophagic activity [62], and the precise role for mutant LRRK2 in autophagy regulation in fibroblasts remains to be determined. Finally, bone marrow-derived macrophages from mutant LRRK2 mice display a decrease in LC3II levels, possibly highlighting

an autophagic phenotype in those cells as well [63]. Alltogether, the currently available data indicate that LRRK2 can regulate autophagic-lysosomal clearance in neurons as well as a variety of other cell types, possibly in a manner dependent on the basal level of autophagy.

5. Mechanism of Autophagy Regulation by LRRK2

If LRRK2 indeed regulates autophagic clearance, understanding the mechanism of action becomes important to develop alternative and/or complementary treatment strategies. The effects of LRRK2 on autophagic-lysosomal clearance may reflect its primary mechanism of action or may occur secondarily, elicited as a response to some upstream event(s). Even if direct, many distinct scenarios remain possible, as autophagy intersects with both secretory and endocytic pathways at several points [64]. Given its heterodimerization with LRRK1 [58, 59], which has been reported to regulate trafficking events of the epidermal growth factor receptor (EGFR) between early and late endosomes, endosome motility and sorting of the epidermal growth factor receptor (EGFR) to the inner vesicles of multivesicular bodies [60, 61], one may speculate that LRRK2 regulates similar events, with consequences for autophagic pathways involving multivesicular bodies [65].

Apart from this mere analogy, LRRK2 has been shown to interact with the GTPase rab5b, a key regulator of early endocytic vesicle trafficking [66]. Overexpression or knockdown of LRRK2 cause a decrease in presynaptic vesicle endocytosis rates, again indicating that both too much and too little LRRK2 adversely alter the balance of homeostatic mechanisms, in this case controlling endocytosis [66]. Similarly, both overexpression or knockdown of LRRK2 induce defects in vesicle endocytosis upon depolarization of primary neuronal cultures [67, 68], which may involve interactions of LRRK2 with a series of endocytic proteins apart from rab5b [68], but further studies are needed to determine how LRRK2 may regulate the function of any of these proteins. Interestingly, rab5b, apart from regulating the endocytic pathway [69] has recently been shown to play an additional positive role in autophagy by regulating an early step of autophagosome formation in a TORC1-independent manner [70]. Thus, a LRRK2-mediated regulation of rab5b may rather directly impact upon autophagic flux. Indirect LRRK2-mediated regulation of autophagy via changes in endocytosis can be envisioned as well, as endocytosis enables the formation of distinct signal transduction complexes which define specialized endosomal-lysosomal signaling platforms [71]. LRRK2-mediated changes in endocytosis may modulate the formation of those intracellular complexes to regulate signalling cascades including Wnt or MAP kinase cascades [71], both of which have been shown to be affected by LRRK2 [18], and which then may modulate the function of downstream autophagic components.

Multiple data support the idea that LRRK2 also modulates late steps in the autophagic-lysosomal clearance pathway. The fusion of both autophagosomes and endosomes with lysosomes requires rab7, as does the process of lysosome reformation [49, 72–74], and interfering with rab7 function will thus affect autophagic-lysosomal clearance. Indeed, at least in Drosophila, the LRRK2 homolog seems to interact with rab7 on late endosomes and lysosomes to negatively regulate rab7-dependent perinuclear lysosomal positioning required for the efficient degradation of autophagosomes [75]. Another recent study in C. elegans expressing human wildtype or mutant LRRK2 in conjunction with proteostatic stress indicates increased expression of numerous proteins including a subunit of the V-type proton ATPase [76, 77], and the behavioural motor deficits observed in these double-transgenic worms can be reverted by increasing autophagic flux using a rapamycin analog. These data are consistent with our findings that mutant LRRK2 may increase lysosomal pH and concomitantly decrease lysosomal clearance, a process reverted by rapamycin, but not by other compounds which increase autophagy in an mTOR-independent manner [54]. It remains to be seen whether the beneficial effect of the rapamycin analog on motor output is related to an mTOR-dependent increase in degradative capacity as autophagic flux is enhanced, a decrease in protein synthesis, an effect on lysosomal homeostasis, or a combination thereof. Taken alltogether, a picture is emerging whereby LRRK2 may regulate both early and late steps of autophagic-lysosomal clearance in a rab protein-dependent manner (Figure 2).

6. A Link between LRRK2, Autophagy, and NAADP-Mediated Endolysosomal Calcium Signaling

In agreement with other reports, we also found an increase in autophagosome numbers upon transient overexpression of wildtype and G2019S-mutant, but not kinase-dead LRRK2 in various cell lines including dopaminergic neuroendocrine cells [54, 55]. Interestingly, we found that these effects were inhibited by the calcium chelator BAPTA, suggesting that they were calcium-dependent. The effects of LRRK2 overexpression on autophagosome numbers were also blocked when genetically depleting ER calcium stores and were accompanied by an increase in the pH of a population of lysosomes and an increase in the number of lipid droplets. This phenotype closely matches the one triggered by NAADP, which evokes cytosolic calcium signals that can be amplified by ER calcium stores, causes partial alkalinization of acidic stores, and induces lipid accumulation [78–80]. NAADP is a potent agonist-generated second messenger and capable of triggering complex calcium signals which are initiated from acidic stores and are being subsequently amplified by ER calcium release channels [81–83]. Targets for NAADP are likely comprised of the endolysosomal two-pore channels TPC1 and TPC2 [84–86], even though recent studies indicate that NAADP does not directly bind to TPCs, but rather indirectly through currently unidentified associated low-molecular weight binding proteins [87]. In either case, there is a growing appreciation of the importance of endolysosomal organelles as mobilizable calcium stores [81, 88], and intraluminal calcium seems required for endolysosomal

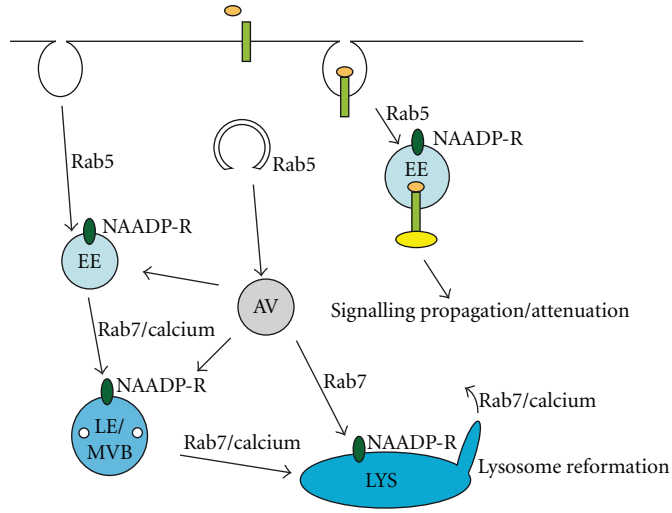

Figure 2: Possible mechanisms by which LRRK2 may regulate events related to endolysosomal and autophagic function. Modulation of rab5 function could cause changes in endocytosis and/or autophagosome formation. Altered endocytosis could also modulate signalling events occurring at the plasma membrane or on intracellular organelles, thereby, indirectly impacting upon autophagy through phosphorylation events of distinct proteins required for the process. At later stages, through modulating rab7 function, LRRK2 may alter the fusion of autophagosomes/endosomes with lysosomes or impair lysosome reformation, which would impact upon autophagic-lysosomal clearance in both cases. As most of the abovementioned membrane fusion/reformation steps require intraluminal calcium, LRRK2 may further regulate endolysosomal clearance by modulating NAADP-sensitive calcium channels (NAADP-R) located on endosomes and lysosomes. The increasing intraluminal calcium concentrations along the endocytic/lysosomal pathway are indicated by the progressively darkened blue color. Ligand binding to receptors, followed by endocytosis and interaction with signalling complexes are schematically indicated. EE: early endosome; AV: autophagosome; LE/MVB: late endosome/multivesicular body; LYS: lysosome. For further details and references, see text.

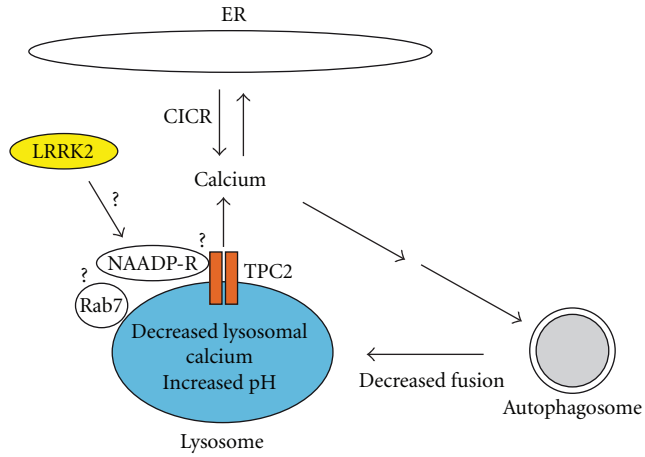

Figure 3: Diagram of proposed mechanism(s) by which LRRK2 regulates autophagy via modulation of NAADP-dependent calcium channels (NAADP-R) on lysosomes. LRRK2 localizes to lysosomes and regulates calcium release through two-pore channels (TPCs). Whether this is due to a direct interaction of LRRK2 with NAADP-R, an indirect interaction via rab7 or additional proteins, or whether it is mediated by a phosphorylation event remains to be determined. Calcium release from acidic organelles then causes calcium-induced calcium release (CICR) from the ER to amplify cytosolic calcium signals, which leads to the activation of a cascade to increase autophagosome numbers. Diminished luminal calcium will further cause a decrease in autophagosome-lysosome fusion, and increased pH may have additional effects on eventually impairing lysosomal proteolysis, leading to the observed autophagic-lysosomal clearance phenotype.

membrane fusion events, thus, directly impacting upon endosomal and autophagic trafficking events [73].

The analogy between the effects of LRRK2 overexpression and NAADP action prompted us to test the connection between NAADP and LRRK2 action. Accordingly, we found that elevation of cellular NAADP levels using a cell permeable NAADP analogue (NAADP-AM) [89] increases autophagosome numbers, lysosomal pH, and lipid droplet numbers, thus, largely mimicking the effects observed upon LRRK2 overexpression [54]. Conversely, the NAADP

antagonist NED19 recently identified by virtual screening methods [90] reverted the effects of LRRK2. The increase in autophagosome number could also be blocked by overexpression of TPC2 mutated within the pore region [91]. This inactive mutant likely acts in a dominant manner similar to TPC1 in which the corresponding residue is mutated [84, 92]. Together, these data uncover a hitherto unknown link between NAADP and LRRK2 function (Figure 3).

7. Summary

A wealth of recent data supports the idea that LRRK2 regulates autophagy. Another ROCO protein family member, death-associated protein kinase 1 (DAPK1), also seems to be an essential regulator of autophagy [93], and it will be interesting to determine whether other ROCO proteins are autophagy modulators as well. Furthermore, LRRK2 variants have been associated with Crohn's disease (CD), an inflammatory bowel disease [94]. As other CD-associated risk genes are also linked to autophagy triggered as an antibacterial response, the disease may result from ineffective control of bacterial infection and resultant chronic inflammation [95]. Similarly, recent data suggest that LRRK2 dysfunction in PD may involve the immune system [96], and the involvement of aberrant autophagy in such process warrants further investigation. Whilst the link between LRRK2 and autophagy is becoming solid, the precise underlying mechanism(s) remain unknown. Both direct and indirect scenarios can be envisioned, and evidence for both is emerging. Rab proteins and calcium seem to play potentially important and not mutually exclusive roles. Calcium is known to both positively and negatively regulate autophagy, and these dual effects may depend on the precise intraorganellar location at which it is required for autophagosome-lysosome or endosome-lysosome fusion, respectively [49, 72]. Many questions remain to be addressed, such as whether TPCs (or NAADP binding proteins) are LRRK2 targets, whether LRRK2 causes indeed measurable changes in intracellular calcium levels, or how LRRK2 regulates the activity or localization of distinct rab proteins. Additional work is needed toward delineating the precise molecular links between LRRK2, autophagy, and NAADP-mediated events.

Acknowledgments

This work is supported by Grants from the Spanish Ministry of Economy and Competitiveness (BFU2011-29899), the Junta de Andalucía (CTS 6816), and the Michael J. Fox Foundation.

References

[1] G. Halliday, A. Lees, and M. Stern, "Milestones in Parkinson's disease-Clinical and pathologic features," *Movement Disorders*, vol. 26, no. 6, pp. 1015–1021, 2011.

[2] A. Zimprich, S. Biskup, P. Leitner et al., "Mutations in LRRK2 cause autosomal-dominant parkinsonism with pleomorphic pathology," *Neuron*, vol. 44, no. 4, pp. 601–607, 2004.

[3] C. Paisán-Ruíz, S. Jain, E. W. Evans et al., "Cloning of the gene containing mutations that cause PARK8-linked Parkinson's disease," *Neuron*, vol. 44, no. 4, pp. 595–600, 2004.

[4] M. J. Farrer, "Genetics of Parkinson disease: paradigm shifts and future prospects," *Nature Reviews Genetics*, vol. 7, no. 4, pp. 306–318, 2006.

[5] J. Hardy, "Genetic analysis of pathways to parkinson disease," *Neuron*, vol. 68, no. 2, pp. 201–206, 2010.

[6] K. Haugarvoll and Z. K. Wszolek, "Clinical features of LRRK2 parkinsonism," *Parkinsonism and Related Disorders*, vol. 15, no. 3, pp. S205–S208, 2009.

[7] W. Satake, Y. Nakabayashi, I. Mizuta et al., "Genome-wide association study identifies common variants at four loci as genetic risk factors for Parkinson's disease," *Nature Genetics*, vol. 41, no. 12, pp. 1303–1307, 2009.

[8] J. Simón-Sánchez, C. Schulte, J. M. Bras et al., "Genome-wide association study reveals genetic risk underlying Parkinson's disease," *Nature Genetics*, vol. 41, no. 12, pp. 1308–1312, 2009.

[9] M. A. Nalls, V. Plagnol, D. G. Hernandez et al., "Imputation of sequence variants for identification of genetic risks for Parkinson's disease: a meta-analysis of genome-wide association studies," *The Lancet*, vol. 377, no. 9766, pp. 641–649, 2011.

[10] M. R. Cookson, W. Dauer, T. Dawson, E. A. Fon, M. Guo, and J. Shen, "The roles of kinases in familial Parkinson's disease," *Journal of Neuroscience*, vol. 27, no. 44, pp. 11865–11868, 2007.

[11] I. N. Rudenko, R. Chia, and M. R. Cookson, "Is inhibition of kinase activity the only therapeutic strategy for LRRK2-associated Parkinson's disease?" *BMC Medicine*, vol. 10, article 20, 2012.

[12] L. Bosgraaf and P. J. M. Van Haastert, "Roc, a Ras/GTPase domain in complex proteins," *Biochimica et Biophysica Acta*, vol. 1643, no. 1–3, pp. 5–10, 2003.

[13] S. Biskup and A. B. West, "Zeroing in on LRRK2-linked pathogenic mechanisms in Parkinson's disease," *Biochimica et Biophysica Acta*, vol. 1792, no. 7, pp. 625–633, 2009.

[14] E. Greggio and M. R. Cookson, "Leucine-rich repeat kinase 2 mutations and Parkinson's disease: three questions," *ASN Neuro*, vol. 1, no. 1, Article ID e00002, 2009.

[15] I. N. Rudenko, A. Kaganovich, D. N. Hauser et al., "The G2385R variant of leucine-rich repeat kinase 2 associated with Parkinson's disease is a partial loss-of-function mutation," *Biochemical Journal*, vol. 446, no. 1, pp. 99–111, 2012.

[16] L. Guo, P. N. Gandhi, W. Wang, R. B. Petersen, A. L. Wilson-Delfosse, and S. G. Chen, "The Parkinson's disease-associated protein, leucine-rich repeat kinase 2 (LRRK2), is an authentic GTPase thatstimulates kinase activity," *Experimental Cell Research*, vol. 313, no. 16, pp. 3658–3670, 2007.

[17] P. A. Lewis, E. Greggio, A. Beilina, S. Jain, A. Baker, and M. R. Cookson, "The R1441C mutation of LRRK2 disrupts GTP hydrolysis," *Biochemical and Biophysical Research Communications*, vol. 357, no. 3, pp. 668–671, 2007.

[18] D. C. Berwick and K. Harvey, "LRRK2 signaling pathways: the key to unlocking neurodegeneration?" *Trends in Cell Biology*, vol. 21, no. 5, pp. 257–265, 2011.

[19] P. A. Lewis and C. Manzoni, "LRRK2 and human disease: a complicated question or a question of complexes?" *Science Signaling*, vol. 5, no. 207, article 2, 2012.

[20] E. Greggio, I. Zambrano, A. Kaganovich et al., "The Parkinson disease-associated leucine-rich repeat kinase 2 (LRRK2) is a dimer that undergoes intramolecular autophosphorylation," *Journal of Biological Chemistry*, vol. 283, no. 24, pp. 16906–16914, 2008.

[21] J. Deng, P. A. Lewis, E. Greggio, E. Sluch, A. Beilina, and M. R. Cookson, "Structure of the ROC domain from the

Parkinson's disease-associated leucine-rich repeat kinase 2 reveals a dimeric GTPase," *Proceedings of the National Academy of Sciences of the United States of America*, vol. 105, no. 5, pp. 1499–1504, 2008.

[22] S. Sen, P. J. Webber, and A. B. West, "Dependence of leucine-rich repeat kinase 2 (LRRK2) kinase activity on dimerization," *Journal of Biological Chemistry*, vol. 284, no. 52, pp. 36346–36356, 2009.

[23] Z. Berger, K. A. Smith, and M. J. Lavoie, "Membrane localization of LRRK2 is associated with increased formation of the highly active lrrk2 dimer and changes in its phosphorylation," *Biochemistry*, vol. 49, no. 26, pp. 5511–5523, 2010.

[24] G. Ito and T. Iwatsubo, "Re-examination of the dimerization state of leucine-rich repeat kinase 2: predominance of the monomeric form," *Biochemical Journal*, vol. 441, pp. 987–994, 2012.

[25] J. Alegre-Abarrategui, H. Christian, M. M. P. Lufino et al., "LRRK2 regulates autophagic activity and localizes to specific membrane microdomains in a novel human genomic reporter cellular model," *Human Molecular Genetics*, vol. 18, no. 21, pp. 4022–4034, 2009.

[26] S. Biskup, D. J. Moore, F. Celsi et al., "Localization of LRRK2 to membranous and vesicular structures in mammalian brain," *Annals of Neurology*, vol. 60, no. 5, pp. 557–569, 2006.

[27] S. Higashi, D. J. Moore, R. Yamamoto et al., "Abnormal localization of leucine-rich repeat kinase 2 to the endosomal-lysosomal compartment in lewy body disease," *Journal of Neuropathology and Experimental Neurology*, vol. 68, no. 9, pp. 994–1005, 2009.

[28] E. Greggio, S. Jain, A. Kingsbury et al., "Kinase activity is required for the toxic effects of mutant LRRK2/dardarin," *Neurobiology of Disease*, vol. 23, no. 2, pp. 329–341, 2006.

[29] W. W. Smith, Z. Pei, H. Jiang, V. L. Dawson, T. M. Dawson, and C. A. Ross, "Kinase activity of mutant LRRK2 mediates neuronal toxicity," *Nature Neuroscience*, vol. 9, no. 10, pp. 1231–1233, 2006.

[30] A. B. West, D. J. Moore, C. Choi et al., "Parkinson's disease-associated mutations in LRRK2 link enhanced GTP-binding and kinase activities to neuronal toxicity," *Human Molecular Genetics*, vol. 16, no. 2, pp. 223–232, 2007.

[31] C. Laccarino, C. Crosio, C. Vitale, G. Sanna, M. T. Carrì, and P. Barone, "Apoptotic mechanisms in mutant LRRK2-mediated cell death," *Human Molecular Genetics*, vol. 16, no. 11, pp. 1319–1326, 2007.

[32] B. D. Lee, J. H. Shin, J. Vankampen et al., "Inhibitors of leucine-rich repeat kinase-2 protect against models of Parkinson's disease," *Nature Medicine*, vol. 16, no. 9, pp. 998–1000, 2010.

[33] J. Dusonchet, O. Kochubey, K. Stafa et al., "A rat model of progressive nigral neurodegeneration induced by the Parkinson's disease-associated G2019S mutation in LRRK2," *Journal of Neuroscience*, vol. 31, no. 3, pp. 907–912, 2011.

[34] D. MacLeod, J. Dowman, R. Hammond, T. Leete, K. Inoue, and A. Abeliovich, "The familial Parkinsonism gene LRRK2 regulates neurite process morphology," *Neuron*, vol. 52, no. 4, pp. 587–593, 2006.

[35] E. D. Plowey, S. J. Cherra, Y. J. Liu, and C. T. Chu, "Role of autophagy in G2019S-LRRK2-associated neurite shortening in differentiated SH-SY5Y cells," *Journal of Neurochemistry*, vol. 105, no. 3, pp. 1048–1056, 2008.

[36] J. Sämann, J. Hegermann, E. von Gromoff, S. Eimer, R. Baumeister, and E. Schmidt, "Caenorhabditits elegans LRK-1 and PINK-1 act antagonistically in stress response and neurite outgrowth," *Journal of Biological Chemistry*, vol. 284, no. 24, pp. 16482–16491, 2009.

[37] C. H. Lin, P. I. Tsai, R. M. Wu, and C. T. Chien, "LRRK2 G2019S mutation induces dendrite degeneration through mislocalization and phosphorylation of tau by recruiting autoactivated GSK3β," *Journal of Neuroscience*, vol. 30, no. 39, pp. 13138–13149, 2010.

[38] B. Winner, H. L. Melrose, C. Zhao et al., "Adult neurogenesis and neurite outgrowth are impaired in LRRK2 G2019S mice," *Neurobiology of Disease*, vol. 41, no. 3, pp. 706–716, 2011.

[39] D. Chan, A. Citro, J. M. Cordy, G. C. Shen, and B. Wolozin, "Rac1 protein rescues neurite retraction caused by G2019s leucine-rich repeat kinase 2 (LRRK2)," *Journal of Biological Chemistry*, vol. 286, no. 18, pp. 16140–16149, 2011.

[40] D. Ramonet, J. P. L. Daher, B. M. Lin et al., "Dopaminergic neuronal loss, reduced neurite complexity and autophagic abnormalities in transgenic mice expressing G2019S mutant LRRK2," *PLoS ONE*, vol. 6, no. 4, Article ID e18568, 2011.

[41] K. Stafa, A. Trancikova, P. J. Webber et al., "GTPase activity and neuronal toxicity of Parkinson's disease-associated LRRK2 is regulated by ArfGAP1," *PLoS Genetics*, vol. 8, Article ID e1002526, 2012.

[42] A. Sánchez-Danés, Y. Richaud-Patin, and I. Carballo-Carbajal, "Disease-specific phenotypes in dopamine neurons from human iPS-based models of genetic and sporadic Parkinson's disease," *EMBO Molecular Medicine*, vol. 4, pp. 380–395, 2012.

[43] C. T. Chu, E. D. Plowey, R. K. Dagda, R. W. Hickey, S. J. Cherra, and R. S. B. Clark, "Autophagy in neurite injury and neurodegeneration. In vitro and in vivo models," *Methods in Enzymology*, vol. 453, pp. 217–249, 2009.

[44] F. M. Menzies, K. Moreau, and D. C. Rubinsztein, "Protein misfolding disorders and macroautophagy," *Current Opinion in Cell Biology*, vol. 23, no. 2, pp. 190–197, 2011.

[45] E. Wong and A. M. Cuervo, "Autophagy gone awry in neurodegenerative diseases," *Nature Neuroscience*, vol. 13, no. 7, pp. 805–811, 2010.

[46] P. Anglade, S. Vyas, F. Javoy-Agid et al., "Apoptosis and autophagy in nigral neurons of patients with Parkinson's disease," *Histology and Histopathology*, vol. 12, no. 1, pp. 25–31, 1997.

[47] Z. Yang and D. J. Klionsky, "Eaten alive: a history of macroautophagy," *Nature Cell Biology*, vol. 12, no. 9, pp. 814–822, 2010.

[48] P. Codogno, M. Mehrpour, and T. Proikas-Cezanne, "Canonical and non-canonical autophagy: variations on a common theme of self-eating?" *Nature Reviews Molecular Cell Biology*, vol. 13, pp. 7–12, 2012.

[49] J. P. Luzio, S. R. Gray, and N. A. Bright, "Endosome-lysosome fusion," *Biochemical Society Transactions*, vol. 38, no. 6, pp. 1413–1416, 2010.

[50] Y. Tong, H. Yamaguchi, E. Giaime et al., "Loss of leucine-rich repeat kinase 2 causes impairment of protein degradation pathways, accumulation of α-synuclein, and apoptotic cell death in aged mice," *Proceedings of the National Academy of Sciences of the United States of America*, vol. 107, no. 21, pp. 9879–9884, 2010.

[51] Y. Tong, E. Giaime, and H. Yamaguchi, "Loss of leucine-rich repeat kinase 2 causes age-dependent bi-phasic alterations of the autophagy pathway," *Molecular Neurodegeneration*, vol. 7, article 2, 2012.

[52] M. C. Herzig, C. Kolly, E. Persohn et al., "LRRK2 protein levels are determined by kinase function and are crucial for kidney and lung homeostasis in mice," *Human Molecular Genetics*, vol. 20, pp. 4209–4223, 2011.

[53] D. J. Klionsky, H. Abeliovich, P. Agostinis et al., "Guidelines for the use and interpretation of assays for monitoring autophagy in higher eukaryotes," *Autophagy*, vol. 4, pp. 151–175, 2008.

[54] P. Gómez-Suaga, B. Luzón-Toro, D. Churamani et al., "Leucine-rich repeat kinase 2 regulates autophagy through a calcium-dependent pathway involving NAADP," *Human Molecular Genetics*, vol. 21, pp. 511–525, 2012.

[55] P. Gómez-Suaga and S. Hilfiker, "LRRK2 as a modulator of lysosomal calcium homeostasis with downstream effects on autophagy," *Autophagy*, vol. 8, pp. 692–693, 2012.

[56] M. Westerlund, A. C. Belin, A. Anvret, P. Bickford, L. Olson, and D. Galter, "Developmental regulation of leucine-rich repeat kinase 1 and 2 expression in the brain and other rodent and human organs: implications for Parkinson's disease," *Neuroscience*, vol. 152, no. 2, pp. 429–436, 2008.

[57] S. Biskup, D. J. Moore, A. Rea et al., "Dynamic and redundant regulation of LRRK2 and LRRK1 expression," *BMC Neuroscience*, vol. 8, article no. 102, 2007.

[58] J. C. Dachsel, K. Nishioka, C. Vilariño-Güell et al., "Heterodimerization of Lrrk1-Lrrk2: implications for LRRK2-associated Parkinson disease," *Mechanisms of Ageing and Development*, vol. 131, no. 3, pp. 210–214, 2010.

[59] C. L. Klein, G. Rovelli, W. Springer, C. Schall, T. Gasser, and P. J. Kahle, "Homo- and heterodimerization of ROCO kinases: LRRK2 kinase inhibition by the LRRK2 ROCO fragment," *Journal of Neurochemistry*, vol. 111, no. 3, pp. 703–715, 2009.

[60] H. Hanafusa, K. Ishikawa, S. Kedashiro et al., "Leucine-rich repeat kinase LRRK1 regulates endosomal trafficking of the EGF receptor," *Nature Communications*, vol. 2, no. 1, p. 158, 2011.

[61] K. Ishikawa, A. Nara, K. Matsumoto et al., "EGFR-dependent phosphorylation of leucine-rich repeat kinase LRRK1 is important for proper endosomal trafficking of EGFR," *Molecular Biology of the Cell*, vol. 23, pp. 1294–1306, 2012.

[62] J. M. Bravo-San Pedro, M. Niso-Santano, R. Rómez-Sánchez et al., "The LRRK2 G2019S mutant exacerbates basal autophagy through activation of the MEK/ERK pathway," *Cellular Molecular Life Sciences*. In press.

[63] M. Hakimi, T. Selvanantham, E. Swinton et al., "Parkinson's disease-linked LRRK2 is expressed in circulating and tissue immune cells and upregulated following recognition of microbial structures," *Journal of Neural Transmission*, vol. 118, no. 5, pp. 795–808, 2011.

[64] A. Orsi, H. E. J. Polson, and S. A. Tooze, "Membrane trafficking events that partake in autophagy," *Current Opinion in Cell Biology*, vol. 22, no. 2, pp. 150–156, 2010.

[65] C. M. Fader and M. I. Colombo, "Autophagy and multivesicular bodies: two closely related partners," *Cell Death and Differentiation*, vol. 16, no. 1, pp. 70–78, 2009.

[66] N. Shin, H. Jeong, J. Kwon et al., "LRRK2 regulates synaptic vesicle endocytosis," *Experimental Cell Research*, vol. 314, no. 10, pp. 2055–2065, 2008.

[67] Y. Xiong, C. E. Coombes, A. Kilaru et al., "GTPase activity plays a key role in the pathobiology of LRRK2," *PLoS Genetics*, vol. 6, no. 4, Article ID e1000902, 2010.

[68] G. Piccoli, S. B. Condliffe, M. Bauer et al., "LRRK2 controls synaptic vesicle storage and mobilization within the recycling pool," *Journal of Neuroscience*, vol. 31, no. 6, pp. 2225–2237, 2011.

[69] C. Bucci, R. G. Parton, I. H. Mather et al., "The small GTPase rab5 functions as a regulatory factor in the early endocytic pathway," *Cell*, vol. 70, no. 5, pp. 715–728, 1992.

[70] B. Ravikumar, S. Imarisio, S. Sarkar, C. J. O'Kane, and D. C. Rubinsztein, "Rab5 modulates aggregation and toxicity of mutant huntingtin through macroautophagy in cell and fly models of Huntington disease," *Journal of Cell Science*, vol. 121, no. 10, pp. 1649–1660, 2008.

[71] H. W. Platta and H. Stenmark, "Endocytosis and signaling," *Current Opinion in Cell Biology*, vol. 23, no. 4, pp. 393–403, 2011.

[72] I. G. Ganley, P. M. Wong, N. Gammoh, and X. Jiang, "Distinct autophagosomal-lysosomal fusion mechanism revealed by thapsigargin-induced autophagy arrest," *Molecular Cell*, vol. 42, no. 6, pp. 731–743, 2011.

[73] P. R. Pryor, B. M. Mullock, N. A. Bright, S. R. Gray, and J. P. Luzio, "The role of intraorganellar Ca^{2+} in late endosome-lysosome heterotypic fusion and in the reformation of lysosomes from hybrid organelles," *Journal of Cell Biology*, vol. 149, no. 5, pp. 1053–1062, 2000.

[74] L. Yu, C. K. McPhee, L. Zheng et al., "Termination of autophagy and reformation of lysosomes regulated by mTOR," *Nature*, vol. 465, no. 7300, pp. 942–946, 2010.

[75] M. W. Dodson, T. Zhang, C. Jiang et al., "Roles of the Drosophila LRRK2 homolog in rab7-dependent lysosomal positioning," *Human Molecular Genetics*, vol. 21, pp. 1350–1363, 2012.

[76] F. Di Domenico, R. Sultana, A. Ferree et al., "Redox proteomics analyses of the influence of co-expression of wild-type or mutated LRRK2 and Tau on C. elegans protein expression and oxidative modification: relevance to Parkinson disease," *Antioxidants and Redox Signaling*, vol. 17, no. 11, pp. 1490–1506, 2012.

[77] A. Ferree, M. Guillily, H. Li et al., "Regulation of physiologic actions of LRRK2: focus on autophagy," *Neurodegenerative Disease*, vol. 10, pp. 238–241, 2012.

[78] A. H. Guse and H. C. Lee, "NAADP: a universal Ca^{2+} trigger," *Science Signaling*, vol. 1, no. 44, p. re10, 2008.

[79] A. J. Morgan and A. Galione, "NAADP induces pH changes in the lumen of acidic Ca^{2+} stores," *Biochemical Journal*, vol. 402, no. 2, pp. 301–310, 2007.

[80] E. Lloyd-Evans, A. J. Morgan, X. He et al., "Niemann-Pick disease type C1 is a sphingosine storage disease that causes deregulation of lysosomal calcium," *Nature Medicine*, vol. 14, no. 11, pp. 1247–1255, 2008.

[81] S. Patel and R. Docampo, "Acidic calcium stores open for business: expanding the potential for intracellular Ca^{2+} signaling," *Trends in Cell Biology*, vol. 20, no. 5, pp. 277–286, 2010.

[82] G. C. Churchill, Y. Okada, J. M. Thomas, A. A. Genazzani, S. Patel, and A. Galione, "NAADP mobilizes Ca^{2+} from reserve granules, lysosome-related organelles, in sea urchin eggs," *Cell*, vol. 111, no. 5, pp. 703–708, 2002.

[83] A. J. Morgan, F. M. Platt, E. Lloyd-Evans et al., "Molecular mechanisms of endolysosomal Ca^{2+} signalling in health and disease," *Biochemical Journal*, vol. 439, pp. 349–374, 2011.

[84] E. Brailoiu, D. Churamani, X. Cai et al., "Essential requirement for two-pore channel 1 in NAADP-mediated calcium signaling," *Journal of Cell Biology*, vol. 186, no. 2, pp. 201–209, 2009.

[85] P. J. Calcraft, M. Ruas, Z. Pan et al., "NAADP mobilizes calcium from acidic organelles through two-pore channels," *Nature*, vol. 459, no. 7246, pp. 596–600, 2009.

[86] S. Patel, L. Ramakrishnan, T. Rahman et al., "The endo-lysosomal system as an NAADP-sensitive acidic Ca^{2+} store: role for the two-pore channels," *Cell Calcium*, vol. 50, no. 2, pp. 157–167, 2011.

[87] Y. Lin-Moshier, T. F. Walseth, D. Churamani et al., "Photoaffinity labeling of nicotinic acid adenine dinucleotide

phosphate (NAADP) targets in mammalian cells," *Journal of Biological Chemistry*, vol. 287, pp. 2296–2307, 2012.

[88] C. C. Scott and J. Gruenberg, "Ion flux and the function of endosomes and lysosomes: PH is just the start: the flux of ions across endosomal membranes influences endosome function not only through regulation of the luminal pH," *BioEssays*, vol. 33, no. 2, pp. 103–110, 2011.

[89] R. Parkesh, A. M. Lewis, P. K. Aley et al., "Cell-permeant NAADP: a novel chemical tool enabling the study of Ca^{2+} signalling in intact cells," *Cell Calcium*, vol. 43, no. 6, pp. 531–538, 2008.

[90] E. Naylor, A. Arredouani, S. R. Vasudevan et al., "Identification of a chemical probe for NAADP by virtual screening," *Nature Chemical Biology*, vol. 5, no. 4, pp. 220–226, 2009.

[91] E. Brailoiu, T. Rahman, D. Churamani et al., "An NAADP-gated two-pore channel targeted to the plasma membrane uncouples triggering from amplifying Ca^{2+} signals," *Journal of Biological Chemistry*, vol. 285, no. 49, pp. 38511–38516, 2010.

[92] V. Rybalchenko, M. Ahuja, J. Coblentz et al., "Membrane potential regulates NAADP dependence of the pH and Ca^{2+} sensitive organellar two-pore channel TPC1," *Journal of Biological Chemistry*, vol. 287, pp. 20407–20416, 2012.

[93] S. Bialik and A. Kimchi, "Lethal weapons: DAP-kinase, autophagy and cell death. DAP-kinase regulates autophagy," *Current Opinion in Cell Biology*, vol. 22, no. 2, pp. 199–205, 2010.

[94] J. C. Barrett, S. Hansoul, and D. L. Nicolae, "Genome-wide association defines more than 30 distinct susceptibility loci for Crohn's disease," *Nature Genetics*, vol. 40, pp. 955–962, 2008.

[95] A. Kabi, K. P. Nickerson, and C. R. Homer, "Digesting the genetics of inflammatory bowel disease: insights from study of autophagy risk genes," *Inflammatory Bowel Diseases*, vol. 18, pp. 782–792, 2012.

[96] E. Greggio, L. Civiero, M. Bisaglia et al., "Parkinson's disease and immune system: is the culprit LRRKing in the periphery?" *Journal of Neuroinflammation*, vol. 9, article 94, 2012.

5. Pathogenic LRRK2 modulates degradative receptor trafficking by regulation of late endosomal budding

In the present study, we evaluated effects of wildtype and pathogenic LRRK2 on endocytic trafficking of the epidermal growth factor receptor (EGFR). The trafficking route of the EGFR is purely degradative [370] and distinct from other receptors such as the transferrin receptor, which is recycled back to the cell surface via a recycling compartment, or the mannose 6-phosphate receptor, which undergoes retromer-mediated retrieval back to the Golgi from a late endosomal compartment. Upon binding EGF, the EGFR is internalized by clathrin-mediated endocytosis, and subsequently sorted to the lysosome for degradation. Such trafficking seems dependent on CIN85, which interacts with the late endosomal GTPase Rab7 to recruit dynamin 2 (dyn2), a large GTPase which deforms lipid bilayers causing vesicle scission. Action of the CIN85-dyn2 complex results in post-endosomal budding necessary for EGFR trafficking from a late endosomal to lysosomal compartment for subsequent degradation [330], as mentioned previously.

Pathogenic LRRK2 delays EGFR degradation

To investigate the role of LRRK2 in EGFR internalization and degradation, we expressed epitope-tagged LRRK2 constructs in HeLa cells and assessed binding and degradation of fluorescently labelled EGF (Alexa555-EGF). Binding of Alexa555-EGF at 4°C was reduced in the presence of wildtype LRRK2, and this effect was more pronounced in the presence of pathogenic G2019S or R1441C-mutants (Fig. 9A,B). To monitor endocytic movement in cells overexpressing wildtype or mutant LRRK2, cells were incubated with Alexa555-EGF at 4°C, followed by washing to remove labeled EGF from the medium, and endocytosed Alexa555-EGF was quantified 10 and 30 min upon incubation of cells at 37°C. Under these conditions, we observed a delay in Alexa555-EGF clearance in wildtype LRRK2, which was very pronounced in G2019S- and R1441C-mutant LRRK2-expressing cells (Fig. 9C). Such delay was not observed with the kinase-inactive K1906M LRRK2 mutant, which was expressed to similar levels as wildtype or mutant LRRK2, indicating that the observed effects are LRRK2 kinase activity-dependent (Fig. 9C, Fig.S1).

As the CIN85-dyn2 complex is important for trafficking of the EGFR out of a late endosomal compartment, we next expressed dominant-negative versions of either CIN85 (CIN85-dn) or dyn2 (dyn2-dn) unable to bind to each other [332]. Overexpression of either CIN85-dn or dyn2-dn mimicked the effects of mutant LRRK2,

both in terms of Alexa555-EGF surface binding and delayed clearance (Fig. S1). To determine whether the changes in intracellular fluorescent EGF were due to altered EGFR degradation, we performed biochemical EGFR degradation assays in transfected HEK293T cells expressing wildtype or mutant LRRK2. Indeed, cells expressing mutant LRRK2 showed a delay in EGFR degradation compared to mock-transfected cells (Fig. 9D), similarly to what has been previously described when overexpressing CIN85-dn or dyn2-dn binding mutants [332].

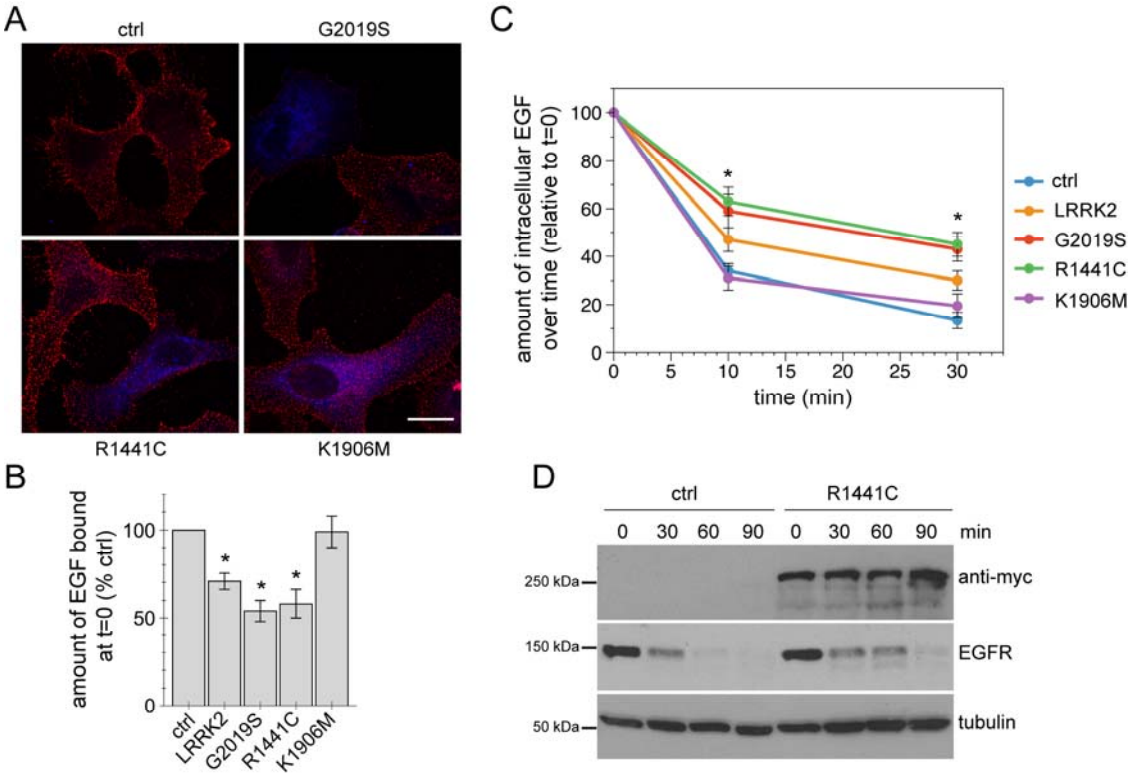

Figure 9. LRRK2 delays EGFR degradation (A) HeLa cells were transfected with empty pCMV vector (ctrl) or the indicated myc-tagged LRRK2 constructs, and processed for immunocytochemistry with an anti-myc antibody (blue) after binding of Alexa555-EGF for 30 min at 4 ºC. Scale bar, 15 µm. **(B)** The amount of surface-bound fluorescent EGF was quantified using ImageJ from 20 transfected cells per condition per experiment. N=8 experiments (ctrl versus LRRK2), 7 (ctrl versus R1441C), 4 (ctrl versus G2019S) and 2 (ctrl versus K1906M) (*, $p < 0.05$). **(C)** Upon binding of fluorescent EGF at 4 ºC, cells were washed to remove unbound EGF, and shifted to 37ºC to allow internalization of bound EGF. Quantification of internalized Alexa555-EGF was performed at 0 min, and after 10 min and 30 min of internalization. Values are normalized to the amount of Alexa555-EGF binding at t=0. N=8 experiments (ctrl versus LRRK2), 7 (ctrl versus R1441C), 4 (ctrl versus G2019S) and 2

(ctrl versus K1906M) (*, $p < 0.05$). **(D)** HEK293T cells were transfected with empty pCMV (ctrl) or mutant LRRK2 construct. Cells were serum-starved for 1 h in the presence of cycloheximide to block novel protein synthesis, and EGFR internalization stimulated with non-labelled EGF for the indicated time points. Cell extracts (40 µg) were analyzed by Western blot for EGFR levels and tubulin as loading control, as well as for levels of LRRK2 protein using an anti-myc antibody. The experiment was repeated twice with similar results.

LRRK2 regulates late endosomal EGFR trafficking

Rab5 and Rab7 primarily associate with early and late endosomes, respectively. We next asked whether LRRK2 affects the switch from Rab5 to Rab7 during early-to-late endosomal transition. For this purpose, we coexpressed GFP-tagged versions of Rab5 or Rab7 with LRRK2, and visualized trafficking of fluorescent EGF through these compartments. Previously, we assured that overexpression of GFP-tagged Rab5 or Rab7 did not alter EGFR trafficking in either the absence or presence of mutant LRRK2 (Fig. 10A,B).

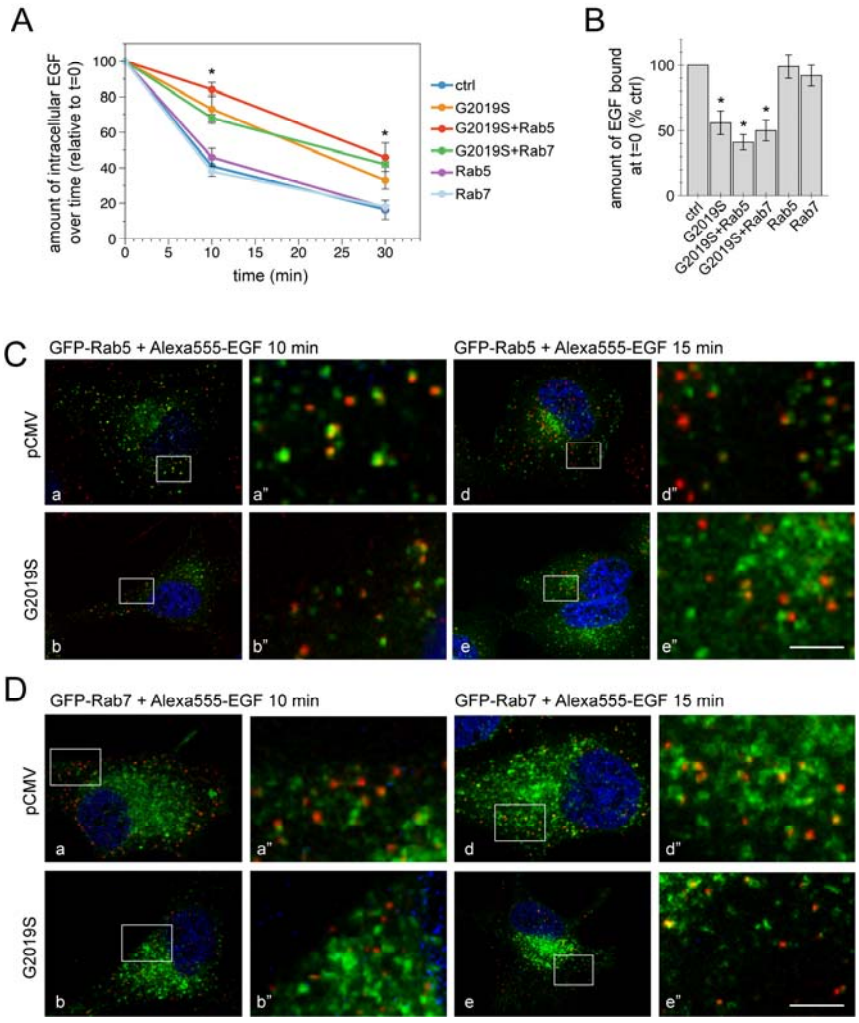

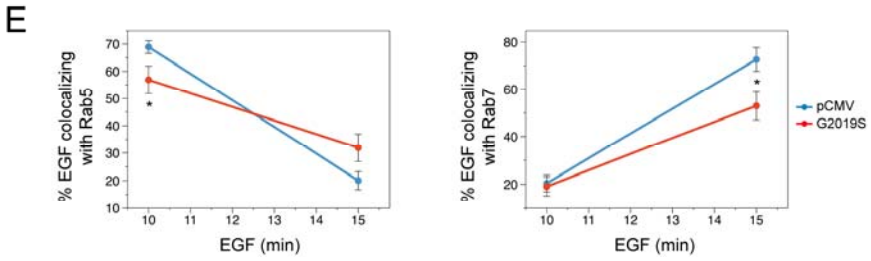

Figure 10. Mutant LRRK2 causes a delay in the Rab5/Rab7 switch (A,B) HeLa cells were transfected either with empty pCMV vector (ctrl), or co-transfected with mutant LRRK2 and the indicated constructs, and Alexa555-EGF binding and uptake experiments performed as described in legend to Figure 9. N=3 experiments (*, $p < 0.05$). **(C,D)** Hela cells were co-transfected with empty vector (pCMV) or mutant LRRK2, and either GFP-Rab5 or GFP-Rab7, and Alexa555-EGF uptake performed for either 10 min or 15 min. Colocalization of Alexa555-EGF with either GFP-Rab5 or GFP-Rab7 was quantified as described in Materials and Methods. Scale bar, 20 μm. **(E)** The average percentage of colocalization of Alexa555-EGF with GFP-Rab5 (left) or GFP-Rab7 (right) 10 min and 15 min after shifting cells to 37ºC was quantified from 10-15 cells per experiment. N=3 experiments (*, $p < 0.05$).

Most Rab5-positive endosomes were distributed in the cell periphery, whilst Rab7-positive late endosomes were more commonly observed in a perinuclear region (Fig. 10C,D). In mock-transfected cells, at 10 min after a brief pulse of Alexa555-EGF stimulation, most of the fluorescent EGF was found in early endosomes, as evidenced by its colocalization with Rab5 (Fig. 10C, E). After 15 min, most EGF had disappeared out of early endosomes, as evidenced by decreased co-localization with Rab5, and this decrease was accompanied by an increase in the colocalization with Rab7, indicative of the progression of the EGFR to late endosomal compartments (Fig. 10D, E). In mutant LRRK2-transfected cells, there was a slight decrease in the co-localization of fluorescent EGF with Rab5 after 10 min, and a slight but non-significant increase after 15 min. Importantly, there was a pronounced decrease in the colocalization of fluorescent EGF with Rab7 after 15 min in LRRK2-transfected cells as compared to mock-transfected cells, suggesting impaired entry of the EGFR into the Rab7-positive compartment (Fig. 10E).

Together, these data indicate that transition of EGFR from early to late endosomes is affected in mutant LRRK2-expressing cells, a process which is dependent on the rab5/7 switch.

Pathogenic LRRK2 impairs vesiculation of late endosomes

We next wondered whether LRRK2 may be recruited onto late endosomes upon EGF stimulation. Whilst overexpressed wildtype and pathogenic mutant LRRK2 were largely cytosolic (not shown), addition of non-fluorescent EGF allowed occasional detection of pathogenic LRRK2 on GFP-Rab7-positive late endosomal structures (Fig. 11A). Careful analysis showed that at times pathogenic LRRK2 could be detected on the outer membrane of GFP-Rab7-positive structures (Fig. 11B).

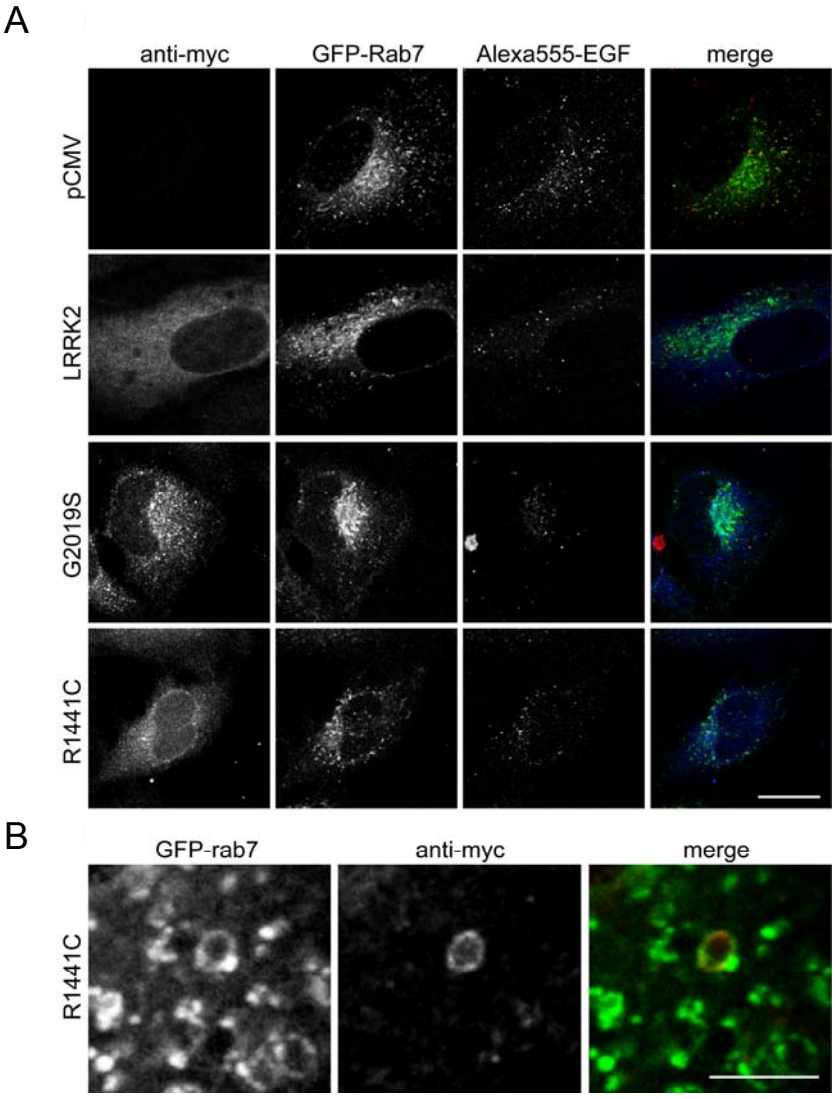

Figure 11. Mutant LRRK2 can localize to late endosomes**. (A)** HeLa cells were co-transfected with GFP-Rab7 and the indicated constructs, starved overnight, and RhEGF uptake performed for 60 min, followed by staining for LRRK2 with an anti-LRRK2 antibody. Scale bar, 15 μm. **(B)** For higher resolution images of mutant LRRK2 localization to individual GFP-rab7-labelled late endosomes, cells were co-transfected as indicated, EGF uptake experiments performed with non-fluorescent ligand, and staining for LRRK2 performed using an Alexa594-coupled secondary antibody. Scale bar, 4 μm.

To gain insight into how mutant LRRK2 may regulate trafficking events from the late endosome, we performed time-lapse microscopy of Rhodamine-EGF (RhEGF)-stimulated HeLa cells co-expressing GFP-Rab7. Expression of wildtype, and to a larger degree G2019S- or R1441C-mutant LRRK2 caused a striking difference in the morphology of GFP-Rab7-positive structures (Fig. 12A,B). Whereas mock-transfected or kinase-inactive K1906M LRRK2-transfected cells showed mainly punctate GFP-rab7-positive structures and few, short tubules (≤ 1.5 μm), the LRRK2-expressing cells displayed an increased number of tubules, and an increased number of long tubules (> 1.5 μm) which were positive for RhEGF (Fig. 12A,B). Such phenotype was identical to that observed when overexpressing CIN85-dn mutant (Fig. 12B), as previously described [332], indicating that the vesiculation process was attenuated.

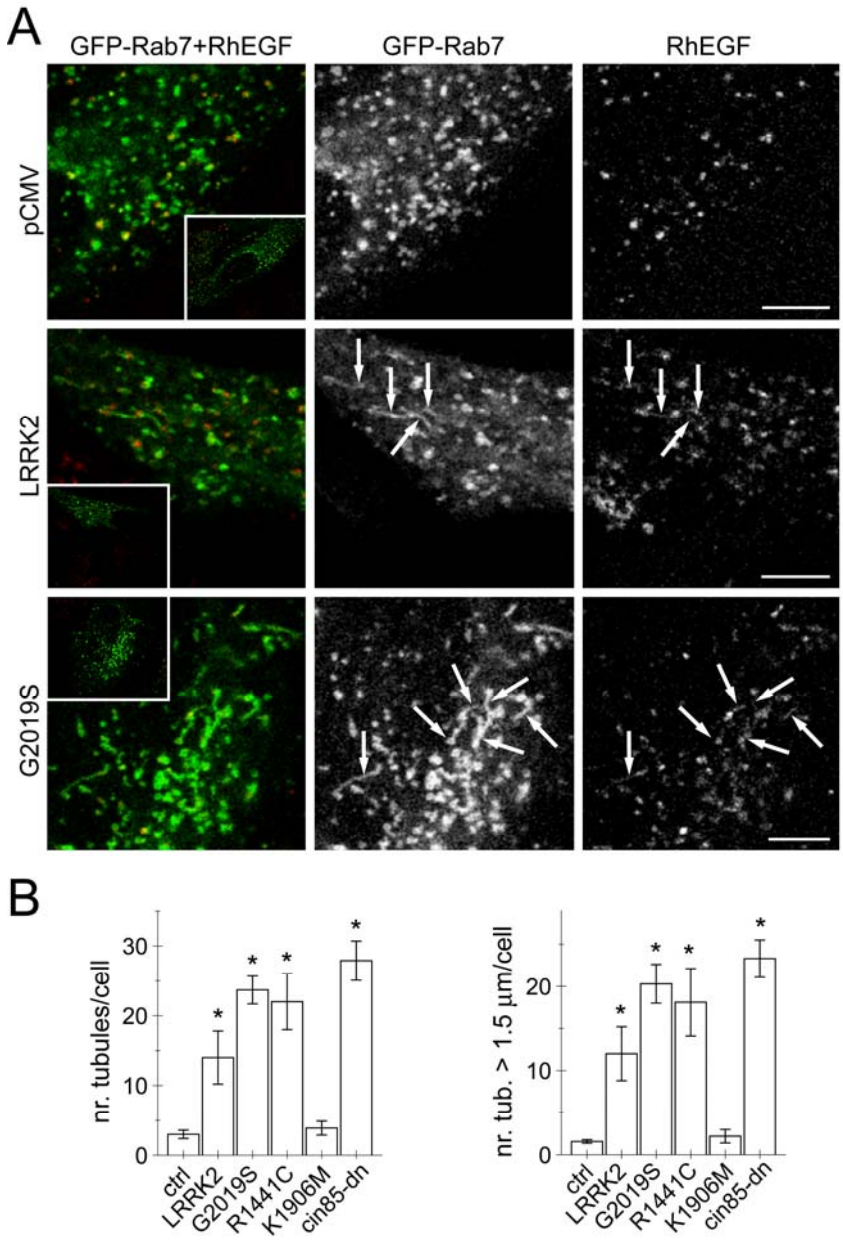

Figure 12. Mutant LRRK2 prevents late endosomal budding and increases GFP-Rab7 tubule length. **(A)** Movie stills of HeLa cells co-expressing GFP-Rab7 and indicated constructs and stimulated with RhEGF. Arrows point to long Rab7-positive tubules containing RhEGF. Scale bar, 8 µm. **(B)** Quantification of the total number of GFP-Rab7 tubules (left), and the number of long tubules (> 1.5 µm) (right). GFP-Rab7 tubules containing RhEGF were quantified over the entire imaging period. 7-15 cells were quantified per condition in each experiment. N=4 experiments (except 3 experiments for R1441C, 2 for K1906M), *, $p < 0.05$.

.

We asked whether such phenotype may also be observed in cells expressing endogenous levels of mutant LRRK2. For this purpose, we analyzed Rab7 staining in primary dermal fibroblasts from PD patients carrying the G2019S LRRK2 mutation and age- and sex-matched healthy controls. Rab7 staining was largely punctate in control fibroblasts, and no changes in the amount of Rab7 punctae per area could be observed in the G2019S LRRK2 mutant fibroblasts (Fig. 13A,B). However, most G2019S mutant fibroblasts displayed at least one Rab7-positive tubule > 5 μm (Fig. 13C). These data indicate that pathogenic mutant LRRK2 interferes with the formation of carriers emanating from the late endosome, resulting in a delay in EGFR degradation.

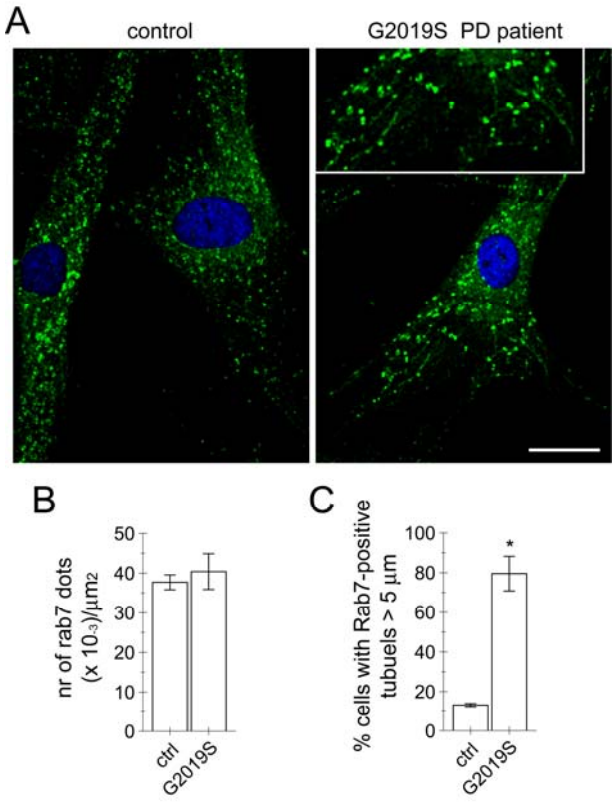

Figure 13. Fibroblasts from G2019S LRRK2 PD patients display increased amount of rab7-positive tubular endosomes. (A) Fibroblasts from healthy control or G2019S LRRK2 PD patients were stained for endogenous rab7. As rab7-positive late endosomal tubules are very sensitive to fixation and detergent conditions, a specific protocol was necessary as described in Materials and Methods. Scale bar, 30 μm**. (B)** Individual cells were scored for the amount of rab7-positive structures, and fluoresent signal normalized to cell size. **(C)** The percentage of cells containing at least one Rab7-positive tubular structure > 5 μm was

determined by analyzing between 30-50 cells per fibroblast line (n=5 control lines, n=5 G2019S LRRK2 PD lines). *, $p < 0.05$.

The CIN85/dyn2/Rab7 pathway is involved in the LRRK2-mediated late endosomal trafficking defects

We sought to determine whether the LRRK2-mediated defects at the late endosome may be rescued by modulating the CIN85/dyn2 complex [332]. Overexpressed CIN85 and dyn2 were found to localize to Rab7-positive structures (Fig. S1), as previously described [332]. Whilst overexpression of CIN85 or dyn2 had not effect on EGFR downregulation compared to mock-treated cells, they largely rescued the LRRK2-mediated delay in EGFR degradation (Fig. 14A,B). CIN85 was more efficient in rescuing the trafficking deficit as compared to dyn2 (Fig. 14A,B). As CIN85 is thought to interact with Rab7 on late endosomes, followed by recruitment of dyn2 to vesiculate late endosomal membranes [332], we wondered whether active Rab7 may be implicated in this process. Overexpression of active, GTP-bound GFP-Rab7-Q67L did not affect EGFR trafficking in mock-transfected cells, but suppressed the delay in EGFR degradation induced by LRRK2 (Fig. 14C,D). This was not observed when expressing wildtype Rab7, even though both wildtype and active mutant Rab7 were expressed to similar degrees (Fig. 14E). The LRRK2-mediated delay in EGFR degradation was also suppressed when expressing GFP-Rab7L1, a Rab protein largely localized to the Golgi and to tubular structures emerging from the Golgi [372]. However, 60 min upon fluorescent EGF internalization, some colocalization of RhEGF with GFP-Rab7L1 could be observed in both mock-transfected and mutant LRRK2-transfected cells (Fig. 14F), indicating that at least a fraction of overexpressed GFP-Rab7L1 may directly contribute to late endosomal trafficking of the EGFR.

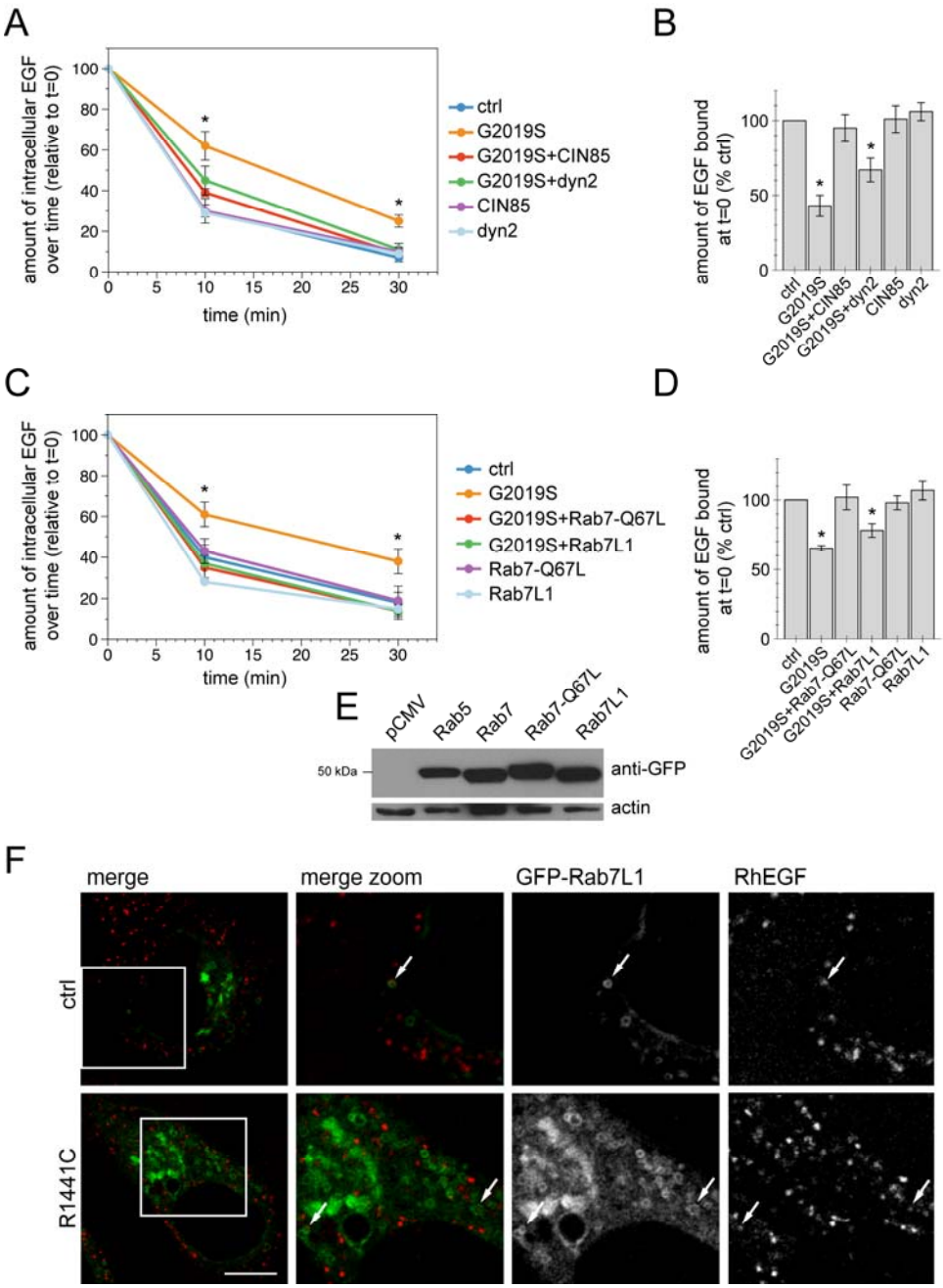

Figure 14. The CIN85/dyn2/rab7 pathway regulates the LRRK2-mediated delay in EGFR degradation. . (**A,B**) HeLa cells were transfected either with empty pCMV vector (ctrl), or co-transfected with mutant LRRK2 and the indicated constructs, and Alexa555-EGF binding and uptake experiments performed as described in legend to Figure 9. N=3 experiments (*, $p < 0.05$). (**C,D**) HeLa cells were transfected either with empty pCMV vector (ctrl), or co-transfected with mutant LRRK2 and the indicated constructs, and Alexa555-EGF binding and uptake experiments performed as described in legend to Figure 9. N=3 experiments (*, $p < 0.05$). (**E**) Transfected cell extracts were analyzed by Western blotting to assure similar levels of overexpression of the various GFP-tagged Rab contructs. (**F**) Movie stills of HeLa cells

cotransfected with GFP-Rab7L1 and either with empty pCMV vector (ctrl) or mutant LRRK2, and loaded with RhEGF for 1 h. Arrows indicate colocalization of RhEGF with GFP-Rab7L1. Scale bar, 10 μm.

Pathogenic LRRK2 downregulates the activation state of Rab7

Given the above-mentioned data, we reasoned that LRRK2 may regulate the levels and/or activity of Rab7. No change in Rab7 protein levels were observed in cells overexpressing mutant LRRK2 as compared to mock-transfected cells, fibroblasts from G2019S LRRK2 patients, or postmortem brain extracts from G2019S LRRK2 patients versus healthy controls (Figs. 15A,B). We thus focused on determining effects of LRRK2 on Rab7 activity. Rab protein activity is regulated by guanine nucleotide exchange factors (GEFs), which activate Rabs by facilitating the exchange of GDP for GTP, and GTPase-activating proteins (GAPs), which inactivate Rabs by accelerating the hydrolysis of the bound GTP to GDP [373, 374]. Rab proteins only associate with their effector proteins when GTP-bound, and this produces a downstream response associated with GTPase activation of the given Rab protein. Whilst the identity of the mammalian Rab7 GEF remains controversial, TBC1D15 seems to act as a GAP for Rab7 [375, 376]. Interestingly, TBC1D15 overexpression delayed EGFR degradation (Fig. 15B,C). Such delay could be rescued when expressing catalytically active, GTP-bound Rab7-Q67L or Rab7L1, but not wildtype Rab7 (Fig. 15B,C), identical to what was observed with mutant LRRK2 expression. These eperiments confirm that Rab7-Q67L is functionally active in cells, and indicate that Rab7L1 may impact upon the same EGFR trafficking pathway as Rab7.

Several effector proteins for Rab7 have been identified [318, 322, 377]. RILP (Rab interacting lysosomal protein) is the best-studied Rab7 effector, and binds selectively to Rab7-GTP to recruit the dynein-dynactin motor complex and facilitate vesicle movement toward the minus end of microtubules [318, 377]. The N terminus of RILP recruits dynein motors, but does not bind GTP-Rab7, such that an N-terminally truncated RILP construct functions as dominant-negative mutant to inhibit Rab7-dependent endolysosomal fusion reactions [318, 377]. Consistent with the possibility that pathogenic LRRK2 may deregulate Rab7 activity, overexpression of dn-RILP, but not wt-RILP, mimicked the effects of pathogenic LRRK2 on delayed EGFR degradation (Fig. 15D,E).

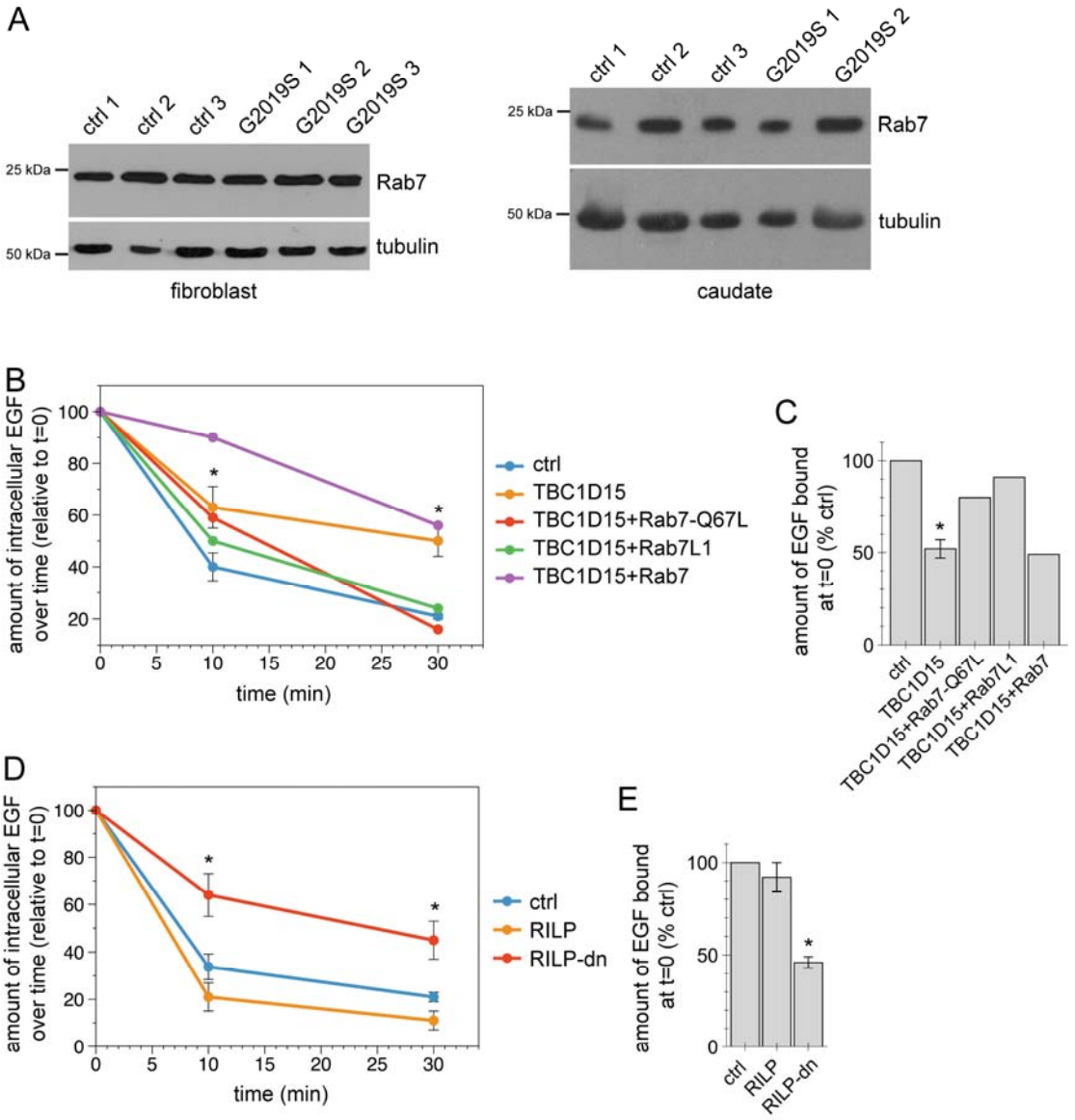

Figure 15. Mutant LRRK2 alters the Rab7 cycle. (**A**) Western blots of dermal fibroblast extracts (40 µg per lane) from three healthy control and three G2019S LRRK2 PD (left), or extracts from postmortem caudate brain (50µg per lane) from healthy control and two G2019S LRRK2 PD patients (right) display no drastic changes Rab7 protein levels. (**B,C**) HeLa cells were transfected either with empty pCMV vector (ctrl), or co-transfected with the Rab7 GAP TBC1D15 and the indicated constructs or empty pCMV vector, and Alexa555-EGF binding and uptake experiments performed as described in legend to Figure 9. N=3 experiments (*, $p < 0.05$). (**D,E**) HeLa cells were transfected either with empty pCMV vector (ctrl), or with the Rab7 effector RILP or a dominant-negative version thereof (RILP-dn), and Alexa555-EGF binding and uptake experiments performed as described in legend to Figure 9. N=3 experiments (*, $p < 0.05$).

To gain more direct evidence for a LRRK2-induced change in Rab7 activity, we employed an effector pull-down assay using the Rab7 binding domain of RILP to selectively isolate Rab7-GTP from cell lysates [376]. Pull-down assays from cells expressing Rab7, or mutants that are predominantly GTP-bound (Rab7-Q67L) confirmed that Rab7-GTP was selectively isolated by GST-RILP (Fig. 16A). The fraction of endogenous Rab7 bound to GTP was reduced in cells expressing TBC1D15, further confirming that TBC1D15 functions as a GAP for Rab7 *in vivo* (data not shown). When overexpressing pathogenic mutant LRRK2, a striking decrease in the levels of endogenous Rab7-GTP was observed (Fig. 16B), indicating that LRRK2 decreases endogenous active Rab7 levels.

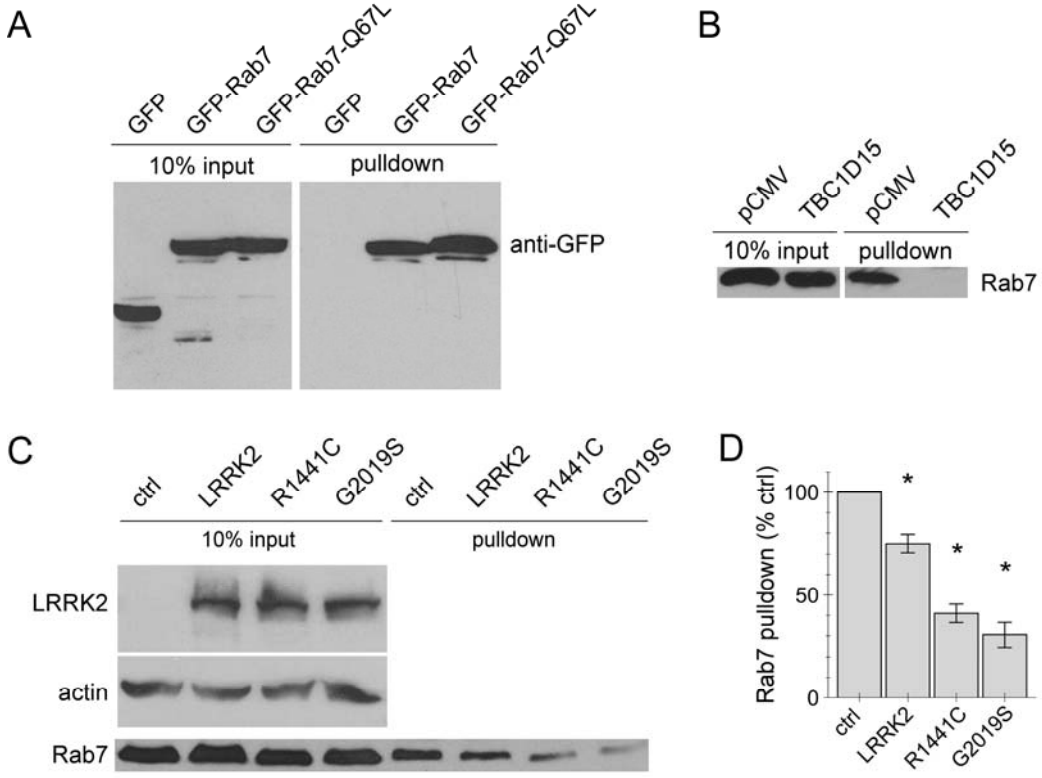

Figure 16. Mutant LRRK2 causes a decrease in Rab7 activity. Mutant LRRK2 causes a decrease in Rab7 activity. **(A)** HEK293T cells were transfected with the indicated constructs, and the Rab7 binding domain of RILP coupled to GST was used to pulldown the GTP-bound form of Rab7 from cell lysates. No signal was detected when eluates from beads coupled to GST alone were evaluated (not shown). **(B)** HEK293T cells were transfected with either emtpy pCMV vector (ctrl), or with TBC1D15, and the amount of endogenous active Rab7 isolated by GST-RILP pulldown. **(C)** HEK293T cells were transfected with either empty pCMV vector (ctrl) or indicated constructs, and endogenous active Rab7 isolated by GST-RILP pulldown.

Input (10%) was run alongside pulldowns to demonstrate equal levels of total Rab7 protein in control and LRRK2-expressing cells, and overexpression levels of various LRRK2 constructs analyzed on separate gels. **(D)** Experiments of the type described in **(C)** were quantified, and the amount of Rab7 isolated by GST-RILP expressed relative to total amount in sample (input), and normalized to amount of Rab7-GTP detected in pCMV-transfected cells. N=3 independent experiments, *, $p < 0.05$.

Supplementary Material

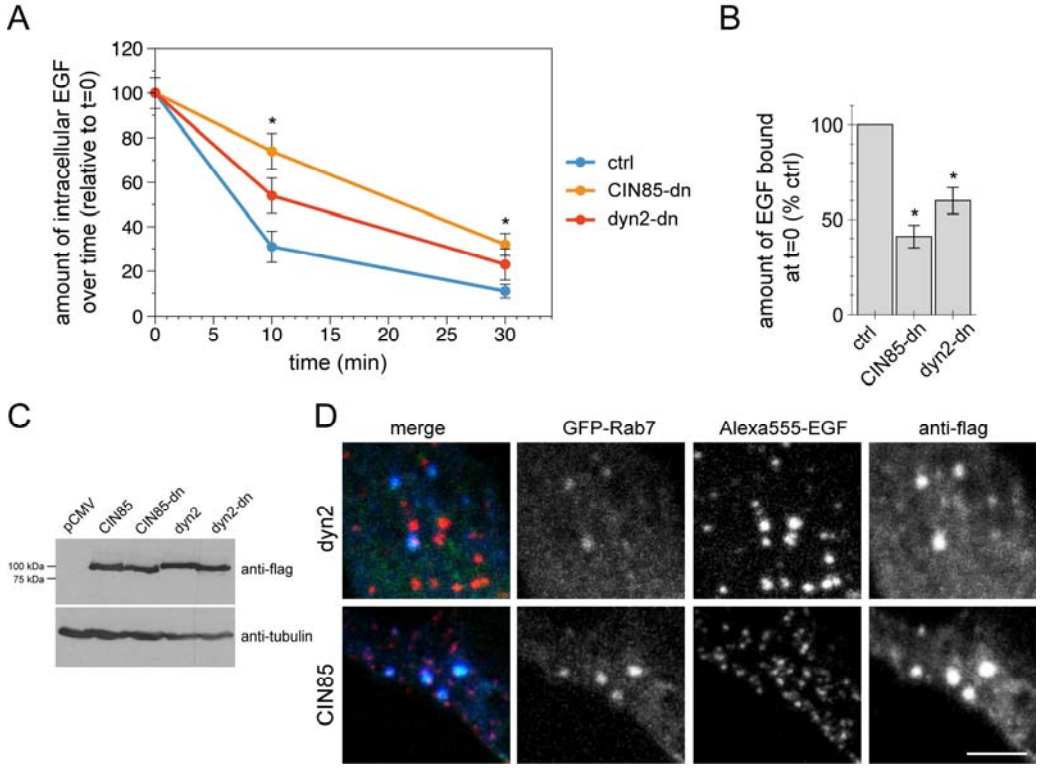

Supplementary Figure 1. CIN85-dn and dyn2-dn mimick effects of LRRK2 on EGFR degradation. (**A,B**) HeLa cells were transfected either with empty pCMV vector (ctrl), or with mutant constructs as indicated, and Alexa555-EGF binding and uptake experiments performed as described in legend to Figure 9. N=3 experiments, *, $p < 0.05$. (**C**) Transfected HEK293T cell extracts were analyzed by Western blotting to assure similar levels of overexpression of wildtype and mutant constructs. (**D**) HeLa cells were cotransfected with GFP-Rab7 and either CIN85 or dyn2, Alexa555-EGF binding and uptake performed for 20 min, and cells stained with an anti-flag antibody to demonstrate colocalization of CIN85 and dyn2 with GFP-rab7-positive, fluorescent EGF-loaded late endosomes. Scale bar, 3 μm.

VII. DISCUSSION

In the present study we show an increase in autophagosome numbers upon transient overexpression of wildtype and G2019S-mutant, but not kinase-dead LRRK2, in various cell lines including DA neuroendocrine cells [192]. Several previous studies have also indicated that LRRK2 regulates autophagy [37, 84, 85, 124, 177, 191, 194, 196], suggesting that deregulation of LRRK2 activity may be damaging to the proper functioning of the autophagy pathway [37, 84, 85, 124, 177, 191, 194, 196]. Despite these findings, the exact mechanisms underlying such deregulation have been largely unknown.

To get evidence for the molecular mechanism(s) of action for LRRK2-mediated autophagosome formation, we employed several cellular and biochemical approaches and reported a TORC1-independent, but AMPK-dependent induction of autophagy. Even though TORC1-mediated autophagy is best studied, an important role for AMPK in basal autophagy [378] regulation has emerged during the last few years [379]. We also found that such increase in basal autophagy was insensitive to 3-MA and wortmanin, as previously shown [194] pointing towards a mechanistic difference between canonical and LRRK2-mediated autophagy.

3-MA and wortmanin block starvation-induced autophagy by inhibiting Vps34, (and thus the *de novo* production of PI_3P) [380, 381]. Localized high concentrations of PI_3P are required for the formation of a membrane platform for subsequent autophagosome nucleation (see Introduction) [382]. However, there is evidence for Vps34-independent induction of autophagy [383-385]. Autophagosome formation in a Vps34-independent manner may be dependent on the membrane source for autophagosome biogenesis, as pre-existing PI_3P-enriched regions are common in the endocytic pathway, which may be sufficient for autophagosome formation. Alternatively other lipid signals may be implicated in the LRRK2-mediated autophagy induction [386].

AMPK is activated upon mitochondrial dysfunction and a decrease in ATP levels, with concomitant increase in AMP [387]. In addition, AMPK can be activated by several upstream kinases, which in turn are subject to regulation [387]. We found that LRRK2-mediated autophagy induction occurred through activation of the CaMKKβ/AMPK pathway, and could be inhibited when genetically depleting ER

calcium stores or by adding a calcium chelator. These results indicate that active LRRK2 may increase cytosolic calcium levels by inducing calcium release from the ER, and thereby activate autophagy induction through the CaMKKβ/AMPK pathway. Calcium is an important regulator of autophagy, even though contradictory data have emerged suggesting both stimulatory [267, 268] and inhibitory [269, 270] effects. It may be that the precise effects depend on characteristics of the calcium signal, its origin, and on cellular state/type (see Introduction). Luminal calcium is also important for homotypic and heterotypic fusion events between organelles within the endo-lysosomal system [341]. A decrease in lysosomal calcium levels would thus be predicted to cause a block in autophagosome-lysosome fusion and a concomitant accumulation of autophagosomes. Hence, it is important to note that an increase in autophagosome numbers may be due to autophagy induction and/or a block in autophagosome degradation.

We thus performed experiments aimed at determining if LRRK2-mediated induction of autophagy is productive, causing an increase in autophagic flux, or a block in flux and accumulation of autophagosomes due to a possible defect in lysosomal homeostasis. We found that whilst autophagosome formation is enhanced in a kinase-dependent manner, autophagic flux was decreased, and these effects were accompanied by an increase in the pH of a population of lysosomes. Even whilst such change in pH was not sufficient to cause a complete lysosomal proteolysis phenotype, it correlated with an increase in lipid doplet numbers, indicating a defect in autophagic degradation.

Our data with respect to lysosomal alterations are consistent with recent reports indicating that mutant LRRK2 alters lysosomal localization [169] or the number and/or size of lysosomes *in vitro* and *in vivo* [37, 84, 85, 187]. Such observed expansion and/or clustering of lysosomes may reflect a compensatory response of the cells to an altered upstream event, or highlight the primary mechanism of mutant LRRK2 action. Lysosomal dysfunction may further enhance exosome release and thus transmissibility of α-synuclein [326], (see figure 17). Mutant LRRK2 has recently been shown to interfere with chaperone-mediated autophagy by inhibiting the proper formation of the LAMP-2A translocation complex, thus inducing accumulation of α-synuclein and

increasing cell toxicity [37]. In that model, the LRRK2-mediated effects on lysosomal functioning are direct, but other scenarios are possible as well.

We further aimed to determine the exact mechanism by which LRRK2 causes a calcium-mediated autophagy induction and a partial alkalinization of a subpopulation of lysosomes with a concomitant decrease in degradative capacity. Interestingly, that phenotype closely matched the one triggered by NAADP, which evokes cytosolic calcium signals that can be amplified by ER calcium stores [343, 349, 388]. Accordingly, we found that elevating intracellular NAADP levels mimicked the effects observed upon LRRK2 overexpression. Conversely, an NAADP antagonist reverted the effects of LRRK2, pointing to a link between LRRK2 and NAADP-receptors.

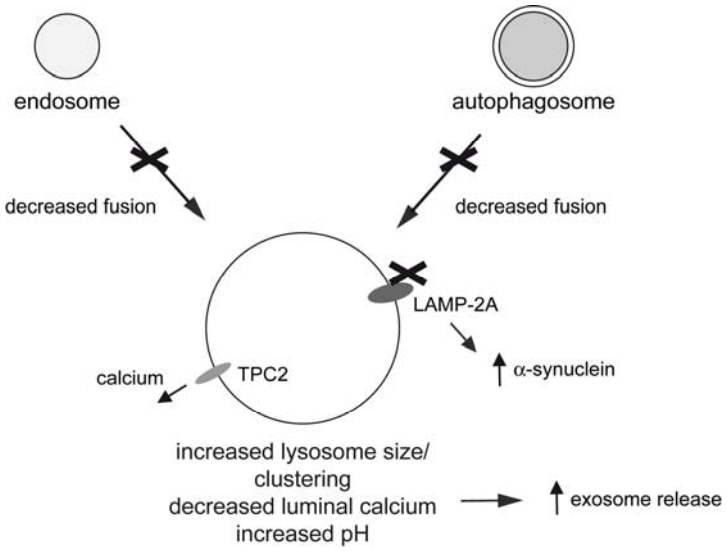

Figure 17. Lysosome-centric model for pathogenic LRRK2 action. Mutant LRRK2 may function at the lysosome to increase lysosome size/induce lysosome clustering, and may cause calcium efflux from this acidic organelle, concomitant with increased lysosomal pH. This would cause a block in efficient trafficking from both endomembrane and autophagy systems, with concomitant aberrant increase in receptor signalling and decrease in autophagic clearance. Lysosomal dysfunction may then enhance exosome release and thus transmissibility of α-synuclein. Furthermore, mutant LRRK2 has been shown to interfere with chaperone-mediated autophagy by inhibiting proper formation of the LAMP-2A translocation complex, thus inducing accumulation of α-synuclein and increasing cell toxicity.

Targets for NAADP have initially been proposed to be the endolysosomal two-pore channels TPC1 and TPC2 [338]. We found that the LRRK2-mediated increase in

autophagosome numbers could be blocked by co-overexpression of inactive mutant TPC2 which abolishes calcium conductance and displays dominant-negative effects with respect to NAADP-mediated calcium signaling [362]. In addition, TPC2 and LRRK2 were found to interact upon co-expression and immunoprecipitation. Together, these data uncover a hitherto unknown link between NAADP and LRRK2 (see figure 17).

Recent studies indicate that NAADP does not directly bind to TPCs, but rather indirectly through currently unidentified associated low-molecular weight binding proteins [389]. These proteins then may associate with TPCs to change their channel properties. Furthermore, controversy has recently been raised as to the ionic specificity of the TPCs, which have been suggested to behave as a sodium-selective channels activated by $PI(3,5)P_2$, rather than by NAADP (see Introduction). Whilst further studies will be necessary to resolve those discrepancies, at present, the vast majority of studies indicate that TPCs can conduct calcium. In addition, an attractive but highly speculative hypothesis is that the small molecular-weight proteins may be related to Rab proteins, which may link NAADP-mediated calcium release from endolysosomal compartments to fusion events, but further studies are required to address this possibility.

Finally, the link between LRRK2, NAADP-mediated release of calcium from acidic stores, and concomitant alterations in cytosolic calcium levels remains to be further validated. Whilst some data have emerged that LRRK2 may alter intracellular calcium levels [190], precise calcium imaging experiments will be needed to establish a link between changes in lysosomal, ER, mitochondrial and cytosolic calcium levels and mutant LRRK2.

Even though neurite length and neurite complexity seem robust readouts for the cellular effects of LRRK2, a series of studies have established a link between enhanced sensitivity to cellular stressors, cell death and the presence of mutant LRRK2 [186, 188, 191] and this readout also seems informative for our understanding of LRRK2 function in cells. Indeed, we found that mutant LRRK2 overexpression was not sufficient to cause cell death within 48 hours after transfection, but increased the susceptibility of cells to further insults related to protein degradation-mediated stress. Such increased cell

death could be blocked by an NAADP antagonist, suggesting that the NAADP pathway is implicated in this process.

Blocking proteasome-mediated degradation causes a concomitant increase in autophagy, a cellular response likely tailored towards clearing an increased amount of protein aggregates observed under these conditions [390]. Thus, if LRRK2 impairs autophagic flux, this should become damaging to the cell under stress conditions which require increased autophagic clearance. Interestingly, application of rapamycin, a TORC1 inhibitor, reverted the LRRK2-mediated effects on cell death, whilst a TORC1-independent autophagy-enhancing compound was unable to do so. This again suggests that mutant LRRK2 does not irreversibly block autophagic flux, but dampens flux in a reversible manner. Rapamycin has been shown to have beneficial effects for cell survival in the context of several neurodegenerative diseases [391] and seems to act on various pathways. Thus, the rapamycin-mediated reversal may be due to an increase in degradative capacity as autophagic flux is enhanced, a decrease in protein synthesis, an effect on lysosomal homeostasis or a combination thereof. Indeed, evidence for all three events were found with rapamycin [392].

In the above-mentioned studies, wildtype LRRK2 had a significant effect, similar to pathogenic G2019S-mutant LRRK2. As mutations in LRRK2 cause PD in an autosomal-dominant manner, we overexpressed the protein to mimic a gain-of-function phenotype. It is feasible that the pathogenic mechanism of LRRK2 depends on exceeding a threshold level of activity, also supported by the finding that homo- and heterozygous carriers of LRRK2 mutations are clinically indistinguishable [40]. Thus, under our experimental conditions, overexpression of both wild-type or G2019S-mutant LRRK2 may reach the threshold level required for LRRK2 function and/or activity to become pathogenic. Furthermore, it remains possible that the effects described here are a wild-type function of LRRK2 unrelated to PD, even though other studies describing an impaired autophagic balance with G2019S-mutant, but not wild-type LRRK2 [90, 124, 177, 194, 196] are consistent with the idea of a threshold effect. Alternatively, we may have missed a small but biologically important difference in effect, which nevertheless may have important consequences when present over many years.

Our studies describe a mechanism by which LRRK2 may alter autophagy, which involves late steps in the auto-lysosomal trafficking pathway. Importantly, the lysosome is the common end-point between autophagy and endocytosis (see figure 17) and, as previously mentioned in the Introduction, LRRK2 has been recently shown to regulate endocytosis and to interact with various proteins involved in endocytic vesicle recycling. Thus, we investigated the role of LRRK2 in receptor-mediated endocytosis and receptor degradation. For this purpose, we employed a well-known system, which is the trafficking of the EGFR. We performed a morphological analysis using marker proteins for early and late endosomes and described a decrease in EGFR trafficking out of late compartments upon transient overexpression of wild-type, but more so when overexpressing G2019S-mutant and R1441C-mutant, but not kinase-active LRRK2. Such delayed trafficking was associated with a decrease in EGFR degradation.

To further study LRRK2-mediated changes in the trafficking out of the late endosomal compartment, we performed time-lapse microscopy of cells overexpressing Rab7-GFP, localized to late endosomes and lysosomes. These data showed that mutant LRRK2 interfered with the vesiculation of late endosomes, causing the appearance of aberrantly elongated and distended tubules which were positive for fluoresently-labeled EGF. Such increase in tubular late endosomal structures was also observed in fibroblasts from PD patients containing the G2019S LRRK2 mutation compared to healthy controls, as indicated by staining for endogenous Rab7. Thus, the alterations in the late endosome also occur under conditions of endogenous mutant LRRK2.

Exit of the EGFR from the late endosomal compartment has previously been shown to involve CIN85/dyn2, two proteins which bind to the EGFR and link it with Rab7 on the late endosomal membrane. Consistently, a dominant-negative CIN85 mutant showed the same tubular extensions of late endosomes as observed with mutant LRRK2. In addition, overexpression of wildtype CIN85 or dyn2 rescued the LRRK2-mediated endocytic phenotype.

Given the link between CIN85/dyn2 and Rab7, we wondered whether the rab protein may be implicated in the LRRK2-mediated phenotype. Rab proteins can cycle between an active, GTP-bound state, and an inactive GDP bound state. Overexpression of the GAP (GTPase activating protein) of Rab7, which inactivates Rab7, mimicked the

effects of LRRK2 on delayed endocytic trafficking and EGFR degradation, as did overexpression of a dominant-negative Rab7 effector protein (RILP). Furthermore, overexpression of catalytically active Rab7, but not wildtype Rab7, rescued the LRRK2-mediated phenotype on EGFR trafficking. Such rescue was also observed when overexpressing Rab7L1, a rab protein implicated in Golgi trafficking. Under our experimental conditions, we could see some colocalization of Rab7L1 with fluorescent EGF, indicating that Rab7L1 may contribute to trafficking out of a late endosomal compartment.

We next wondered whether mutant LRRK2 may alter either levels or activity of Rab7. Protein levels of Rab7 were found unchanged upon mutant LRRK2 overexpression, in G2019S LRRK2 mutant versus control fibroblasts, or in postmortem brain from G2019S patients versus healthy controls. To study whether LRRK2 modulates Rab7 activity, we performed effector pull-down assays [376] and found that mutant LRRK2 decreases Rab7 activity.

Rab7 is a master regulator of late endocytic membrane transport, protein sorting, endosomal maturation and autophagy, and altering Rab7 function may impact upon all of those events. Decreased Rab7 activity can explain a delay in EGFR trafficking out of the late endosomal compartment via deficient vesiculation, leading to enlarged endosomal tubules. Interestingly, fission of tubular endosomes has previously been shown to trigger endosomal acidification [314] and thus may explain the effects on lysosomal acidification we observed previously. How altered Rab7 activity is linked to NAADP-mediated signaling in this context remains to be determined. Altered Rab7 activity may also explain the decreased autophagic flux we observed, as autophagosomes fuse with late endosomes for delivery to the lysosome.

It will be interesting to determine precisely how LRRK2 decreases Rab7 activity. LRRK2 may alter the action of GAPs or GEFs for Rab7. Interestingly, LRRK2 has been shown to regulate a GAP protein [91] and thus a similar scenario may apply to Rab7 GAP/GEF. LRRK2 itself has been shown to be regulated by GAPs and GEFs [91, 92, 393] and this may indirectly impact upon Rab7 activity. Other indirect scenarios (eg. alterations in lipid composition of the late endosomal membrane, which alter

membrane association and GTP status of Rab7) are possible as well. Future studies are needed to address the precise mechanism of LRRK2 action on Rab7 activity.

Interestingly, a recent study has reported that LRRK2 regulates retromer-mediated retrieval of the mannose 6-phosphate receptor in a Rab7L1-mediated manner [152]. However, Rab7L1 is largely localized to the Golgi apparatus, rather than the late endosome, and Rab7 has been previously shown to be required for membrane recruitment of the cargo-selective retromer complex on late endosomes [323, 394]. Thus, it seems possible that overexpressed Rab7L1 can functionally complement Rab7 at the late endosome, even though under endogenous conditions, it is largely Golgi-associated. In addition, the previous findings for LRRK2 regulating retromer-mediated retrieval are consistent with our hypothesis that LRRK2 decreases Rab7 activity, which would cause a concomitant decrease in retromer function, (see figure 18).

However, our data are in contrast to another very recent study, indicating that LRRK2 interacts with Rab7L1 on the Golgi to cause Golgi fragmentation and clearance [395]. Further studies in our model system, by analyzing the effects of rab overexpression, in the presence or absence of LRRK2, on Golgi structure and clearance, are required. It is possible that such Golgi-related events occur, but that they do not alter EGFR degradation, which is the phenotype we analysed here. Alternatively, Rab7L1-mediated events on Golgi may be dependent on the levels of overexpression, or on cell type.

Alltogether, our data highlight mechanism(s) underlying LRRK2-mediated deficits in autophagy-lysosomal and endosomal-lysosomal trafficking important towards gaining an understanding as to how pathogenic LRRK2 may cause cellular demise associated with PD.

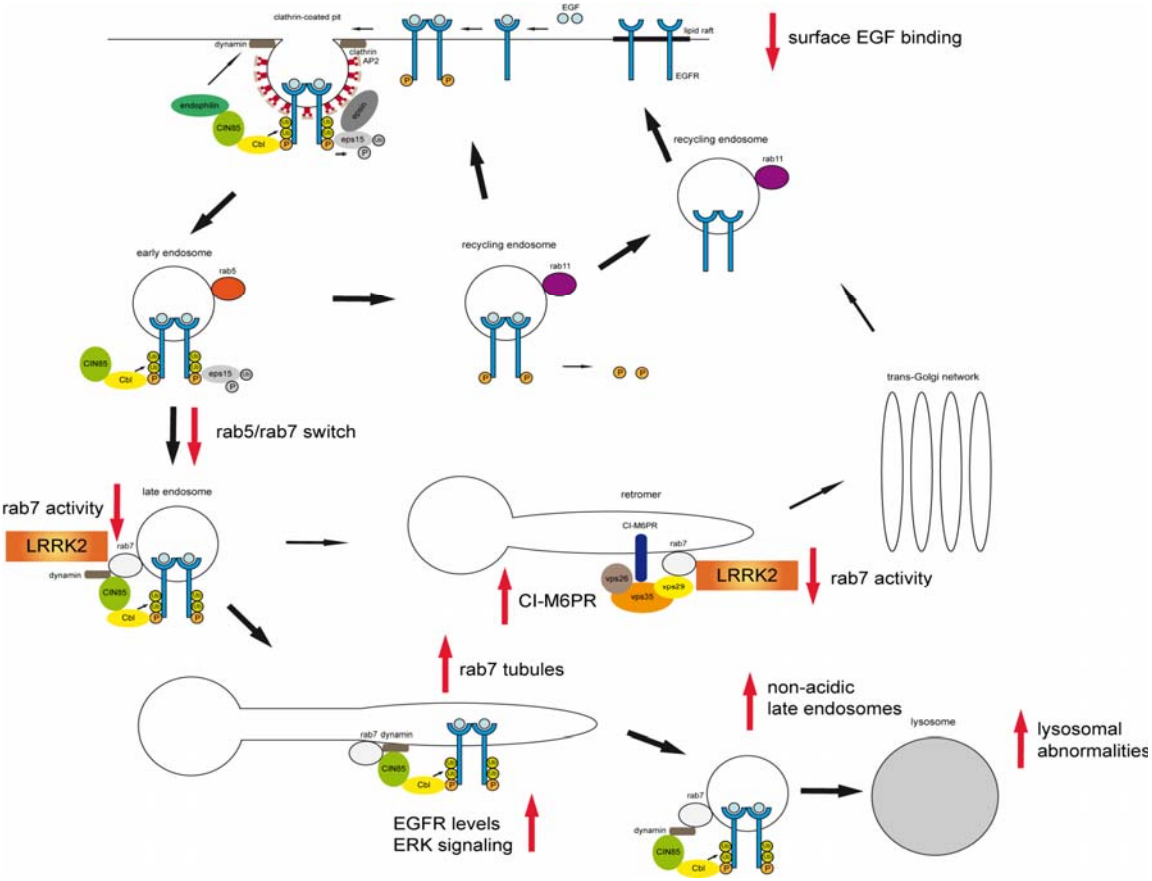

Figure 18. Model for the LRRK2-mediated events throughout the endolysosomal pathway. The LRRK2-mediated decrease in Rab7 activity may lead to a delay in the rab5-Rab7 switch and a delay in receptor trafficking out of late endosomes. This causes an accumulation of internalized EGFR in late endosomes which are aberrantly elongated into distended tubules. Inefficient pinching off from these tubules would lead to an increase in non-acidic late endosomes and lysosomal abnormalities, which we have previously observed. Rab7 activity may affect retromer-mediated retrieval of the M6PR to the TGN as well.

VIII. CONCLUSIONS/CONCLUSIONES

1. Pathogenic LRRK2 overexpression causes induction of autophagy through activation of the calcium/CaMKKβ/AMPK pathway in an mTOR-independent manner.

2. Mutant LRRK2 alkalinizes a subpopulation of lysosomes and causes accumulation of lipid droplets.

3. Mutant LRRK2 increases sensitivity of cells to stressors associated with abnormal protein degradation.
4. LRRK2 acts through NAADP (nicotinic acid adenine dinucleotide phosphate) receptors, as effects can be mimicked by the lysosomal calcium-mobilizing messenger NAADP, and reverted by an NAADP antagonist or overexpression of dominant-negative receptor constructs.

5. Mutant LRRK2 causes a delay in endocytosis and degradation of the EGFR (epidermal growth factor receptor).

6. Mutant LRRK2 causes a delay in the rab5-Rab7 switch of early-to-late endosomal trafficking, and a delay in receptor trafficking out of late endosomes.

7. Mutant LRRK2 causes an accumulation of internalized EGFR in late endosomes which are aberrantly elongated into distended tubules. Rab7-positive tubular late endosomal structures are also observed in fibroblasts from mutant LRRK2 patients.

8. The effects on EGFR degradation can be rescued when overexpressing CIN85 (cbl-interacting protein of 85 kDa) or dynamin 2, proteins known to mediate vesiculation of late endosomes, and to interact with Rab7 on late endosomes.

9. Overexpression of catalytically active Rab7, or Rab7L1, rescue the endocytosis deficits mediated by mutant LRRK2. Mutant LRRK2 causes a decrease in Rab7 activity, which may underlie the effects on endocytic trafficking reported here.

1. La sobreexpresión de mutaciones patogénicas en LRRK2 provoca un aumento de la autofagia a través de la ruta de señalización calcio/CaMKKβ/AMPK, independiente de mTOR.

2. Mutaciones patogénicas en LRRK2 provocan la alcalinización de una subpoblación de lisosomas y la acumulación de gotas lipídicas.

3. Mutaciones patogénicas en LRRK2 aumentan la sensibilidad a muerte celular en la presencia de estrés debido a agregación proteíca.
4. LRRK2 actúa a través de una ruta que implica canales sensibles a NAADP (nicotinic acid adenine dinucleotide phosphate). Los efectos de la sobreexpresión de mutaciones patogénicas de LRRK2 son mimetizados por NAADP y revertidos por el antagonista de éste o la sobrexpresión de la forma dominante negativa de su receptor.
5. Mutaciones patogénicas en LRRK2 provocan un retraso en la endocitosis y degradación del EGFR (epidermal growth factor receptor).

6. Mutaciones patogénicas en LRRK2 causan un retraso en el tráfico del EGFR entre estructuras endosomales tempranas, rab5, y tardías, Rab7, además de un retraso en la salida del receptor desde el endosoma tardío.

7. Mutaciones patogénicas en LRRK2 provocan la acumulación de EGFR internealizado en endosomas tardíos, provocando estructuras anormalmente alargadas. Estas estructuras tubulares anormalmente alargadas de Rab7 también están presentes en fibroblastos de pacientes con mutaciones en LRRK2.

8. Los efectos sobre la degradación del EGFR pudieron ser revertidos por la sobreexpresión de CIN85 (cbl-interacting protein of 85 kDa) o dynamin 2, proteínas que participan en la vesiculación de los endosomas tardíos e interaccionan con Rab7 sobre estas estructuras.

9. La sobreexpresión de la forma catalíticamente activa de Rab7, o de Rab7L1, revertieron las deficiencias en endocitosis provocadas por la sobreexpresión de LRRK2 patogénica. Mutaciones patogénicas en LRRK2 provocan una

disminución en la actividad de Rab7, lo que podría explicar todos los efectos en endocitosis previamente descritos.

IX. REFERENCES

1. Jankovic, J., *Parkinson's disease: clinical features and diagnosis.* J Neurol Neurosurg Psychiatry, 2008. **79**(4): p. 368-76.
2. Dauer, W. and S. Przedborski, *Parkinson's disease: mechanisms and models.* Neuron, 2003. **39**(6): p. 889-909.
3. de Lau, L.M. and M.M. Breteler, *Epidemiology of Parkinson's disease.* Lancet Neurol, 2006. **5**(6): p. 525-35.
4. Dorsey, E.R., et al., *Projected number of people with Parkinson disease in the most populous nations, 2005 through 2030.* Neurology, 2007. **68**(5): p. 384-6.
5. Halliday, G., A. Lees, and M. Stern, *Milestones in Parkinson's disease--clinical and pathologic features.* Mov Disord, 2011. **26**(6): p. 1015-21.
6. Langston, J.W., *The Parkinson's complex: parkinsonism is just the tip of the iceberg.* Ann Neurol, 2006. **59**(4): p. 591-6.
7. Goetz, C.G., et al., *Movement Disorder Society-sponsored revision of the Unified Parkinson's Disease Rating Scale (MDS-UPDRS): scale presentation and clinimetric testing results.* Mov Disord, 2008. **23**(15): p. 2129-70.
8. Hoehn, M.M. and M.D. Yahr, *Parkinsonism: onset, progression and mortality.* Neurology, 1967. **17**(5): p. 427-42.
9. Farrer, M.J., *Genetics of Parkinson disease: paradigm shifts and future prospects.* Nat Rev Genet, 2006. **7**(4): p. 306-18.
10. Goedert, M., et al., *Parkinson's Disease, Dementia with Lewy Bodies, and Multiple System Atrophy as alpha-Synucleinopathies.* Methods Mol Med, 2001. **62**: p. 33-59.
11. Forno, L.S., *Neuropathology of Parkinson's disease.* J Neuropathol Exp Neurol, 1996. **55**(3): p. 259-72.
12. Greenfield, J.G. and F.D. Bosanquet, *The brain-stem lesions in Parkinsonism.* J Neurol Neurosurg Psychiatry, 1953. **16**(4): p. 213-26.
13. Isacson, O. and I. Mendez, *Being too inclusive about synuclein inclusions.* Nat Med, 2010. **16**(9): p. 960-1; author reply 961.
14. Segura-Aguilar, J., et al., *Protective and Toxic roles of dopamine in Parkinson's Disease.* J Neurochem.
15. Smith, Y., et al., *Parkinson's disease therapeutics: new developments and challenges since the introduction of levodopa.* Neuropsychopharmacology, 2012. **37**(1): p. 213-46.
16. Langston, J.W., et al., *Chronic Parkinsonism in humans due to a product of meperidine-analog synthesis.* Science, 1983. **219**(4587): p. 979-80.
17. Betarbet, R., et al., *Chronic systemic pesticide exposure reproduces features of Parkinson's disease.* Nat Neurosci, 2000. **3**(12): p. 1301-6.
18. Maraganore, D.M., et al., *UCHL1 is a Parkinson's disease susceptibility gene.* Ann Neurol, 2004. **55**(4): p. 512-21.
19. Gasser, T., J. Hardy, and Y. Mizuno, *Milestones in PD genetics.* Mov Disord. **26**(6): p. 1042-8.
20. Scholz, S.W., et al., *Genomics and bioinformatics of Parkinson's disease.* Cold Spring Harb Perspect Med. **2**(7): p. a009449.
21. Wang, C., et al., *Penetrance of LRRK2 G2385R and R1628P is modified by common PD-associated genetic variants.* Parkinsonism Relat Disord. **18**(8): p. 958-63.
22. Sidransky, E., et al., *Multicenter analysis of glucocerebrosidase mutations in Parkinson's disease.* N Engl J Med, 2009. **361**(17): p. 1651-61.

23. Puschmann, A., *Monogenic Parkinson's disease and parkinsonism: clinical phenotypes and frequencies of known mutations.* Parkinsonism Relat Disord. **19**(4): p. 407-15.
24. Ahmed, I., et al., *Association between Parkinson's disease and the HLA-DRB1 locus.* Mov Disord. **27**(9): p. 1104-10.
25. Gobel, A., et al., *Genetic risk factors in Parkinson's disease: single gene effects and interactions of genotypes.* J Neurol. **259**(11): p. 2503-5.
26. Wang, K.S., J.E. Mullersman, and X.F. Liu, *Family-based association analysis of the MAPT gene in Parkinson disease.* J Appl Genet. **51**(4): p. 509-14.
27. Vefring, H., et al., *The role of APOE alleles in incident Parkinson's disease. The Norwegian ParkWest Study.* Acta Neurol Scand. **122**(6): p. 438-41.
28. Golub, Y., et al., *Genetic factors influencing age at onset in LRRK2-linked Parkinson disease.* Parkinsonism Relat Disord, 2009. **15**(7): p. 539-41.
29. Polymeropoulos, M.H., et al., *Mutation in the alpha-synuclein gene identified in families with Parkinson's disease.* Science, 1997. **276**(5321): p. 2045-7.
30. Farrer, M., et al., *Low frequency of alpha-synuclein mutations in familial Parkinson's disease.* Ann Neurol, 1998. **43**(3): p. 394-7.
31. Ross, O.A., et al., *Genomic investigation of alpha-synuclein multiplication and parkinsonism.* Ann Neurol, 2008. **63**(6): p. 743-50.
32. Cookson, M.R., J. Hardy, and P.A. Lewis, *Genetic neuropathology of Parkinson's disease.* Int J Clin Exp Pathol, 2008. **1**(3): p. 217-31.
33. Fortin, D.L., et al., *Lipid rafts mediate the synaptic localization of alpha-synuclein.* J Neurosci, 2004. **24**(30): p. 6715-23.
34. el-Agnaf, O.M. and G.B. Irvine, *Aggregation and neurotoxicity of alpha-synuclein and related peptides.* Biochem Soc Trans, 2002. **30**(4): p. 559-65.
35. !!! INVALID CITATION !!!
36. Breydo, L., J.W. Wu, and V.N. Uversky, *Alpha-synuclein misfolding and Parkinson's disease.* Biochim Biophys Acta. **1822**(2): p. 261-85.
37. Orenstein, S.J., et al., *Interplay of LRRK2 with chaperone-mediated autophagy.* Nat Neurosci. **16**(4): p. 394-406.
38. Zimprich, A., et al., *Mutations in LRRK2 cause autosomal-dominant parkinsonism with pleomorphic pathology.* Neuron, 2004. **44**(4): p. 601-7.
39. Paisan-Ruiz, C., et al., *Cloning of the gene containing mutations that cause PARK8-linked Parkinson's disease.* Neuron, 2004. **44**(4): p. 595-600.
40. Hardy, J., *Genetic analysis of pathways to Parkinson disease.* Neuron, 2010. **68**(2): p. 201-6.
41. Satake, W., et al., *Genome-wide association study identifies common variants at four loci as genetic risk factors for Parkinson's disease.* Nat Genet, 2009. **41**(12): p. 1303-7.
42. Simon-Sanchez, J., et al., *Genome-wide association study reveals genetic risk underlying Parkinson's disease.* Nat Genet, 2009. **41**(12): p. 1308-12.
43. Nalls, M.A., et al., *Imputation of sequence variants for identification of genetic risks for Parkinson's disease: a meta-analysis of genome-wide association studies.* Lancet, 2011. **377**(9766): p. 641-9.
44. Singleton, A. and J. Hardy, *A generalizable hypothesis for the genetic architecture of disease: pleomorphic risk loci.* Hum Mol Genet. **20**(R2): p. R158-62.

45. Long-Smith, C.M., A.M. Sullivan, and Y.M. Nolan, *The influence of microglia on the pathogenesis of Parkinson's disease.* Prog Neurobiol, 2009. **89**(3): p. 277-87.
46. Nichols, W.C., et al., *Genetic screening for a single common LRRK2 mutation in familial Parkinson's disease.* Lancet, 2005. **365**(9457): p. 410-2.
47. Khan, N.L., et al., *Mutations in the gene LRRK2 encoding dardarin (PARK8) cause familial Parkinson's disease: clinical, pathological, olfactory and functional imaging and genetic data.* Brain, 2005. **128**(Pt 12): p. 2786-96.
48. Gaig, C., et al., *G2019S LRRK2 mutation causing Parkinson's disease without Lewy bodies.* J Neurol Neurosurg Psychiatry, 2007. **78**(6): p. 626-8.
49. Kitada, T., et al., *Mutations in the parkin gene cause autosomal recessive juvenile parkinsonism.* Nature, 1998. **392**(6676): p. 605-8.
50. Kay, D.M., et al., *Heterozygous parkin point mutations are as common in control subjects as in Parkinson's patients.* Ann Neurol, 2007. **61**(1): p. 47-54.
51. Rubio de la Torre, E., et al., *Posttranslational modifications as versatile regulators of parkin function.* Curr Med Chem, 2011. **18**(16): p. 2477-85.
52. Gegg, M.E., et al., *Mitofusin 1 and mitofusin 2 are ubiquitinated in a PINK1/parkin-dependent manner upon induction of mitophagy.* Hum Mol Genet. **19**(24): p. 4861-70.
53. Moore, D.J., *Parkin: a multifaceted ubiquitin ligase.* Biochem Soc Trans, 2006. **34**(Pt 5): p. 749-53.
54. Olzmann, J.A., et al., *Parkin-mediated K63-linked polyubiquitination targets misfolded DJ-1 to aggresomes via binding to HDAC6.* J Cell Biol, 2007. **178**(6): p. 1025-38.
55. Narendra, D., et al., *Parkin is recruited selectively to impaired mitochondria and promotes their autophagy.* J Cell Biol, 2008. **183**(5): p. 795-803.
56. Geisler, S., et al., *The PINK1/Parkin-mediated mitophagy is compromised by PD-associated mutations.* Autophagy. **6**(7): p. 871-8.
57. Tanaka, A., et al., *Proteasome and p97 mediate mitophagy and degradation of mitofusins induced by Parkin.* J Cell Biol. **191**(7): p. 1367-80.
58. Valente, E.M., et al., *PINK1 mutations are associated with sporadic early-onset parkinsonism.* Ann Neurol, 2004. **56**(3): p. 336-41.
59. Leutenegger, A.L., et al., *Juvenile-onset Parkinsonism as a result of the first mutation in the adenosine triphosphate orientation domain of PINK1.* Arch Neurol, 2006. **63**(9): p. 1257-61.
60. Beilina, A., et al., *Mutations in PTEN-induced putative kinase 1 associated with recessive parkinsonism have differential effects on protein stability.* Proc Natl Acad Sci U S A, 2005. **102**(16): p. 5703-8.
61. Mills, R.D., et al., *Biochemical aspects of the neuroprotective mechanism of PTEN-induced kinase-1 (PINK1).* J Neurochem, 2008. **105**(1): p. 18-33.
62. Dagda, R.K., et al., *Loss of PINK1 function promotes mitophagy through effects on oxidative stress and mitochondrial fission.* J Biol Chem, 2009. **284**(20): p. 13843-55.
63. Lutz, A.K., et al., *Loss of parkin or PINK1 function increases Drp1-dependent mitochondrial fragmentation.* J Biol Chem, 2009. **284**(34): p. 22938-51.
64. Heeman, B., et al., *Depletion of PINK1 affects mitochondrial metabolism, calcium homeostasis and energy maintenance.* J Cell Sci, 2011. **124**(Pt 7): p. 1115-25.

65. Park, J., et al., *Mitochondrial dysfunction in Drosophila PINK1 mutants is complemented by parkin.* Nature, 2006. **441**(7097): p. 1157-61.
66. Clark, I.E., et al., *Drosophila pink1 is required for mitochondrial function and interacts genetically with parkin.* Nature, 2006. **441**(7097): p. 1162-6.
67. Yang, Y., et al., *Mitochondrial pathology and muscle and dopaminergic neuron degeneration caused by inactivation of Drosophila Pink1 is rescued by Parkin.* Proc Natl Acad Sci U S A, 2006. **103**(28): p. 10793-8.
68. Exner, N., et al., *Loss-of-function of human PINK1 results in mitochondrial pathology and can be rescued by parkin.* J Neurosci, 2007. **27**(45): p. 12413-8.
69. Marin, I., W.N. van Egmond, and P.J. van Haastert, *The Roco protein family: a functional perspective.* FASEB J, 2008. **22**(9): p. 3103-10.
70. Bosgraaf, L. and P.J. Van Haastert, *Roc, a Ras/GTPase domain in complex proteins.* Biochim Biophys Acta, 2003. **1643**(1-3): p. 5-10.
71. Brown, M.D. and D.B. Sacks, *Protein scaffolds in MAP kinase signalling.* Cell Signal, 2009. **21**(4): p. 462-9.
72. Gomez-Suaga, P., et al., *A Link between Autophagy and the Pathophysiology of LRRK2 in Parkinson's Disease.* Parkinsons Dis, 2012. **2012**: p. 324521.
73. Greggio, E., et al., *Kinase activity is required for the toxic effects of mutant LRRK2/dardarin.* Neurobiol Dis, 2006. **23**(2): p. 329-41.
74. Smith, W.W., et al., *Kinase activity of mutant LRRK2 mediates neuronal toxicity.* Nat Neurosci, 2006. **9**(10): p. 1231-3.
75. Lee, B.D., et al., *Inhibitors of leucine-rich repeat kinase-2 protect against models of Parkinson's disease.* Nat Med, 2010. **16**(9): p. 998-1000.
76. Marin, I., *The Parkinson disease gene LRRK2: evolutionary and structural insights.* Mol Biol Evol, 2006. **23**(12): p. 2423-33.
77. Gloeckner, C.J., et al., *The Parkinson disease causing LRRK2 mutation I2020T is associated with increased kinase activity.* Hum Mol Genet, 2006. **15**(2): p. 223-32.
78. West, A.B., et al., *Parkinson's disease-associated mutations in LRRK2 link enhanced GTP-binding and kinase activities to neuronal toxicity.* Hum Mol Genet, 2007. **16**(2): p. 223-32.
79. Lee, B.D., V.L. Dawson, and T.M. Dawson, *Leucine-rich repeat kinase 2 (LRRK2) as a potential therapeutic target in Parkinson's disease.* Trends Pharmacol Sci. **33**(7): p. 365-73.
80. Deng, X., et al., *Characterization of a selective inhibitor of the Parkinson's disease kinase LRRK2.* Nat Chem Biol. **7**(4): p. 203-5.
81. Ramsden, N., et al., *Chemoproteomics-based design of potent LRRK2-selective lead compounds that attenuate Parkinson's disease-related toxicity in human neurons.* ACS Chem Biol. **6**(10): p. 1021-8.
82. Covy, J.P. and B.I. Giasson, *Identification of compounds that inhibit the kinase activity of leucine-rich repeat kinase 2.* Biochem Biophys Res Commun, 2009. **378**(3): p. 473-7.
83. Nichols, R.J., et al., *Substrate specificity and inhibitors of LRRK2, a protein kinase mutated in Parkinson's disease.* Biochem J, 2009. **424**(1): p. 47-60.
84. Tong, Y., et al., *Loss of leucine-rich repeat kinase 2 causes age-dependent bi-phasic alterations of the autophagy pathway.* Mol Neurodegener, 2012. **7**: p. 2.
85. Tong, Y., et al., *Loss of leucine-rich repeat kinase 2 causes impairment of protein degradation pathways, accumulation of alpha-synuclein, and apoptotic cell death in aged mice.* Proc Natl Acad Sci U S A, 2010. **107**(21): p. 9879-84.

86. Li, X., et al., *Leucine-rich repeat kinase 2 (LRRK2)/PARK8 possesses GTPase activity that is altered in familial Parkinson's disease R1441C/G mutants.* J Neurochem, 2007. **103**(1): p. 238-47.
87. Lewis, P.A., et al., *The R1441C mutation of LRRK2 disrupts GTP hydrolysis.* Biochem Biophys Res Commun, 2007. **357**(3): p. 668-71.
88. Deng, J., et al., *Structure of the ROC domain from the Parkinson's disease-associated leucine-rich repeat kinase 2 reveals a dimeric GTPase.* Proc Natl Acad Sci U S A, 2008. **105**(5): p. 1499-504.
89. Ito, G., et al., *GTP binding is essential to the protein kinase activity of LRRK2, a causative gene product for familial Parkinson's disease.* Biochemistry, 2007. **46**(5): p. 1380-8.
90. Xiong, Y., et al., *GTPase activity plays a key role in the pathobiology of LRRK2.* PLoS Genet, 2010. **6**(4): p. e1000902.
91. Xiong, Y., et al., *ArfGAP1 is a GTPase activating protein for LRRK2: reciprocal regulation of ArfGAP1 by LRRK2.* J Neurosci, 2012. **32**(11): p. 3877-86.
92. Stafa, K., et al., *GTPase activity and neuronal toxicity of Parkinson's disease-associated LRRK2 is regulated by ArfGAP1.* PLoS Genet, 2012. **8**(2): p. e1002526.
93. Haebig, K., et al., *ARHGEF7 (Beta-PIX) acts as guanine nucleotide exchange factor for leucine-rich repeat kinase 2.* PLoS One, 2010. **5**(10): p. e13762.
94. Gotthardt, K., et al., *Structure of the Roc-COR domain tandem of C. tepidum, a prokaryotic homologue of the human LRRK2 Parkinson kinase.* EMBO J, 2008. **27**(16): p. 2239-49.
95. Gasper, R., et al., *It takes two to tango: regulation of G proteins by dimerization.* Nat Rev Mol Cell Biol, 2009. **10**(6): p. 423-9.
96. Klein, C.L., et al., *Homo- and heterodimerization of ROCO kinases: LRRK2 kinase inhibition by the LRRK2 ROCO fragment.* J Neurochem, 2009. **111**(3): p. 703-15.
97. Sen, S., P.J. Webber, and A.B. West, *Dependence of leucine-rich repeat kinase 2 (LRRK2) kinase activity on dimerization.* J Biol Chem, 2009. **284**(52): p. 36346-56.
98. Dzamko, N., et al., *Inhibition of LRRK2 kinase activity leads to dephosphorylation of Ser(910)/Ser(935), disruption of 14-3-3 binding and altered cytoplasmic localization.* Biochem J, 2010. **430**(3): p. 405-13.
99. Berger, Z., K.A. Smith, and M.J. Lavoie, *Membrane localization of LRRK2 is associated with increased formation of the highly active LRRK2 dimer and changes in its phosphorylation.* Biochemistry, 2010. **49**(26): p. 5511-23.
100. Greggio, E., et al., *The Parkinson's disease kinase LRRK2 autophosphorylates its GTPase domain at multiple sites.* Biochem Biophys Res Commun, 2009. **389**(3): p. 449-54.
101. Webber, P.J., et al., *Autophosphorylation in the leucine-rich repeat kinase 2 (LRRK2) GTPase domain modifies kinase and GTP-binding activities.* J Mol Biol, 2011. **412**(1): p. 94-110.
102. Kamikawaji, S., G. Ito, and T. Iwatsubo, *Identification of the autophosphorylation sites of LRRK2.* Biochemistry, 2009. **48**(46): p. 10963-75.
103. Pungaliya, P.P., et al., *Identification and characterization of a leucine-rich repeat kinase 2 (LRRK2) consensus phosphorylation motif.* PLoS One, 2010. **5**(10): p. e13672.

104. Cookson, M.R., *The role of leucine-rich repeat kinase 2 (LRRK2) in Parkinson's disease.* Nat Rev Neurosci, 2010. **11**(12): p. 791-7.
105. Liu, M., et al., *Kinetic mechanistic studies of wild-type leucine-rich repeat kinase 2: characterization of the kinase and GTPase activities.* Biochemistry, 2010. **49**(9): p. 2008-17.
106. Taymans, J.M., et al., *LRRK2 kinase activity is dependent on LRRK2 GTP binding capacity but independent of LRRK2 GTP binding.* PLoS One, 2011. **6**(8): p. e23207.
107. Greggio, E., et al., *The Parkinson disease-associated leucine-rich repeat kinase 2 (LRRK2) is a dimer that undergoes intramolecular autophosphorylation.* J Biol Chem, 2008. **283**(24): p. 16906-14.
108. Kett, L.R. and W.T. Dauer, *Leucine-rich repeat kinase 2 for beginners: six key questions.* Cold Spring Harb Perspect Med, 2012. **2**(3): p. a009407.
109. Houlden, H. and A.B. Singleton, *The genetics and neuropathology of Parkinson's disease.* Acta Neuropathol. **124**(3): p. 325-38.
110. Kruger, R., *LRRK2 in Parkinson's disease - drawing the curtain of penetrance: a commentary.* BMC Med, 2008. **6**: p. 33.
111. Greggio, E. and M.R. Cookson, *Leucine-rich repeat kinase 2 mutations and Parkinson's disease: three questions.* ASN Neuro, 2009. **1**(1).
112. Luzon-Toro, B., et al., *Mechanistic insight into the dominant mode of the Parkinson's disease-associated G2019S LRRK2 mutation.* Hum Mol Genet, 2007. **16**(17): p. 2031-9.
113. Gorostidi, A., et al., *LRRK2 G2019S and R1441G mutations associated with Parkinson's disease are common in the Basque Country, but relative prevalence is determined by ethnicity.* Neurogenetics, 2009. **10**(2): p. 157-9.
114. Simon-Sanchez, J., et al., *Parkinson's disease due to the R1441G mutation in Dardarin: a founder effect in the Basques.* Mov Disord, 2006. **21**(11): p. 1954-9.
115. Mata, I.F., et al., *Lrrk2 R1441G-related Parkinson's disease: evidence of a common founding event in the seventh century in Northern Spain.* Neurogenetics, 2009. **10**(4): p. 347-53.
116. Ross, O.A., et al., *Haplotype analysis of Lrrk2 R1441H carriers with parkinsonism.* Parkinsonism Relat Disord, 2009. **15**(6): p. 466-7.
117. Daniels, V., et al., *Insight into the mode of action of the LRRK2 Y1699C pathogenic mutant.* J Neurochem, 2011. **116**(2): p. 304-15.
118. Li, Y., et al., *The R1441C mutation alters the folding properties of the ROC domain of LRRK2.* Biochim Biophys Acta, 2009. **1792**(12): p. 1194-7.
119. Liao, J., et al., *Parkinson disease-associated mutation R1441H in LRRK2 prolongs the "active state" of its GTPase domain.* Proc Natl Acad Sci U S A, 2014.
120. Miklossy, J., et al., *LRRK2 expression in normal and pathologic human brain and in human cell lines.* J Neuropathol Exp Neurol, 2006. **65**(10): p. 953-63.
121. Higashi, S., et al., *Localization of Parkinson's disease-associated LRRK2 in normal and pathological human brain.* Brain Res, 2007. **1155**: p. 208-19.
122. Zhu, X., et al., *LRRK2 protein is a component of Lewy bodies.* Ann Neurol, 2006. **60**(5): p. 617-8; author reply 618-9.
123. Giasson, B.I., et al., *Biochemical and pathological characterization of Lrrk2.* Ann Neurol, 2006. **59**(2): p. 315-22.

124. Alegre-Abarrategui, J., et al., *LRRK2 regulates autophagic activity and localizes to specific membrane microdomains in a novel human genomic reporter cellular model.* Hum Mol Genet, 2009. **18**(21): p. 4022-34.
125. Biskup, S., et al., *Localization of LRRK2 to membranous and vesicular structures in mammalian brain.* Ann Neurol, 2006. **60**(5): p. 557-69.
126. Higashi, S., et al., *Abnormal localization of leucine-rich repeat kinase 2 to the endosomal-lysosomal compartment in lewy body disease.* J Neuropathol Exp Neurol, 2009. **68**(9): p. 994-1005.
127. Hatano, T., et al., *Leucine-rich repeat kinase 2 associates with lipid rafts.* Hum Mol Genet, 2007. **16**(6): p. 678-90.
128. Nichols, R.J., et al., *14-3-3 binding to LRRK2 is disrupted by multiple Parkinson's disease-associated mutations and regulates cytoplasmic localization.* Biochem J, 2010. **430**(3): p. 393-404.
129. Muda, K., et al., *Parkinson-related LRRK2 mutation R1441C/G/H impairs PKA phosphorylation of LRRK2 and disrupts its interaction with 14-3-3.* Proc Natl Acad Sci U S A. **111**(1): p. E34-43.
130. West, A.B., et al., *Parkinson's disease-associated mutations in leucine-rich repeat kinase 2 augment kinase activity.* Proc Natl Acad Sci U S A, 2005. **102**(46): p. 16842-7.
131. Jaleel, M., et al., *LRRK2 phosphorylates moesin at threonine-558: characterization of how Parkinson's disease mutants affect kinase activity.* Biochem J, 2007. **405**(2): p. 307-17.
132. Li, X., et al., *Phosphorylation-dependent 14-3-3 binding to LRRK2 is impaired by common mutations of familial Parkinson's disease.* PLoS One. **6**(3): p. e17153.
133. Dzamko, N., et al., *The IkappaB kinase family phosphorylates the Parkinson's disease kinase LRRK2 at Ser935 and Ser910 during Toll-like receptor signaling.* PLoS One. **7**(6): p. e39132.
134. Matta, S., et al., *LRRK2 controls an EndoA phosphorylation cycle in synaptic endocytosis.* Neuron. **75**(6): p. 1008-21.
135. Gillardon, F., *Leucine-rich repeat kinase 2 phosphorylates brain tubulin-beta isoforms and modulates microtubule stability--a point of convergence in parkinsonian neurodegeneration?* J Neurochem, 2009. **110**(5): p. 1514-22.
136. Kawakami, F., et al., *LRRK2 phosphorylates tubulin-associated tau but not the free molecule: LRRK2-mediated regulation of the tau-tubulin association and neurite outgrowth.* PLoS One, 2012. **7**(1): p. e30834.
137. Qing, H., et al., *Lrrk2 phosphorylates alpha synuclein at serine 129: Parkinson disease implications.* Biochem Biophys Res Commun, 2009. **387**(1): p. 149-52.
138. Gloeckner, C.J., et al., *The Parkinson disease-associated protein kinase LRRK2 exhibits MAPKKK activity and phosphorylates MKK3/6 and MKK4/7, in vitro.* J Neurochem, 2009. **109**(4): p. 959-68.
139. Imai, Y., et al., *Phosphorylation of 4E-BP by LRRK2 affects the maintenance of dopaminergic neurons in Drosophila.* EMBO J, 2008. **27**(18): p. 2432-43.
140. Kumar, A., et al., *The Parkinson's disease associated LRRK2 exhibits weaker in vitro phosphorylation of 4E-BP compared to autophosphorylation.* PLoS One. **5**(1): p. e8730.
141. Caesar, M., et al., *Leucine-rich repeat kinase 2 functionally interacts with microtubules and kinase-dependently modulates cell migration.* Neurobiol Dis, 2013.

142. Gandhi, P.N., et al., *The Roc domain of leucine-rich repeat kinase 2 is sufficient for interaction with microtubules.* J Neurosci Res, 2008. **86**(8): p. 1711-20.
143. Rudenko, I.N. and M.R. Cookson, *14-3-3 proteins are promising LRRK2 interactors.* Biochem J, 2010. **430**(3): p. e5-6.
144. Yacoubian, T.A., et al., *Differential neuroprotective effects of 14-3-3 proteins in models of Parkinson's disease.* Cell Death Dis, 2010. **1**: p. e2.
145. Paul, A.L., P.C. Sehnke, and R.J. Ferl, *Isoform-specific subcellular localization among 14-3-3 proteins in Arabidopsis seems to be driven by client interactions.* Mol Biol Cell, 2005. **16**(4): p. 1735-43.
146. Wang, L., et al., *The chaperone activity of heat shock protein 90 is critical for maintaining the stability of leucine-rich repeat kinase 2.* J Neurosci, 2008. **28**(13): p. 3384-91.
147. Dachsel, J.C., et al., *Identification of potential protein interactors of Lrrk2.* Parkinsonism Relat Disord, 2007. **13**(7): p. 382-5.
148. Ko, H.S., et al., *CHIP regulates leucine-rich repeat kinase-2 ubiquitination, degradation, and toxicity.* Proc Natl Acad Sci U S A, 2009. **106**(8): p. 2897-902.
149. Hsu, C.H., et al., *MKK6 binds and regulates expression of Parkinson's disease-related protein LRRK2.* J Neurochem. **112**(6): p. 1593-604.
150. Hsu, C.H., D. Chan, and B. Wolozin, *LRRK2 and the stress response: interaction with MKKs and JNK-interacting proteins.* Neurodegener Dis. **7**(1-3): p. 68-75.
151. Piccoli, G., et al., *LRRK2 controls synaptic vesicle storage and mobilization within the recycling pool.* J Neurosci, 2011. **31**(6): p. 2225-37.
152. Macleod, D.A., et al., *RAB7L1 Interacts with LRRK2 to Modify Intraneuronal Protein Sorting and Parkinson's Disease Risk.* Neuron, 2013. **77**(3): p. 425-39.
153. Civiero, L., et al., *Biochemical characterization of highly purified leucine-rich repeat kinases 1 and 2 demonstrates formation of homodimers.* PLoS One, 2012. **7**(8): p. e43472.
154. Shin, N., et al., *LRRK2 regulates synaptic vesicle endocytosis.* Exp Cell Res, 2008. **314**(10): p. 2055-65.
155. Chan, D., et al., *Rac1 protein rescues neurite retraction caused by G2019S leucine-rich repeat kinase 2 (LRRK2).* J Biol Chem, 2011. **286**(18): p. 16140-9.
156. Sakaguchi-Nakashima, A., et al., *LRK-1, a C. elegans PARK8-related kinase, regulates axonal-dendritic polarity of SV proteins.* Curr Biol, 2007. **17**(7): p. 592-8.
157. Samann, J., et al., *Caenorhabditits elegans LRK-1 and PINK-1 act antagonistically in stress response and neurite outgrowth.* J Biol Chem, 2009. **284**(24): p. 16482-91.
158. Yao, C., et al., *Kinase inhibitors arrest neurodegeneration in cell and C. elegans models of LRRK2 toxicity.* Hum Mol Genet. **22**(2): p. 328-44.
159. Liu, Z., et al., *Inhibitors of LRRK2 kinase attenuate neurodegeneration and Parkinson-like phenotypes in Caenorhabditis elegans and Drosophila Parkinson's disease models.* Hum Mol Genet. **20**(20): p. 3933-42.
160. Marin, I., *Ancient origin of the Parkinson disease gene LRRK2.* J Mol Evol, 2008. **67**(1): p. 41-50.
161. Reiter, L.T., et al., *A systematic analysis of human disease-associated gene sequences in Drosophila melanogaster.* Genome Res, 2001. **11**(6): p. 1114-25.

162. Lee, S., et al., *LRRK2 kinase regulates synaptic morphology through distinct substrates at the presynaptic and postsynaptic compartments of the Drosophila neuromuscular junction.* J Neurosci, 2010. **30**(50): p. 16959-69.
163. Lee, S.B., et al., *Loss of LRRK2/PARK8 induces degeneration of dopaminergic neurons in Drosophila.* Biochem Biophys Res Commun, 2007. **358**(2): p. 534-9.
164. Venderova, K., et al., *Leucine-Rich Repeat Kinase 2 interacts with Parkin, DJ-1 and PINK-1 in a Drosophila melanogaster model of Parkinson's disease.* Hum Mol Genet, 2009. **18**(22): p. 4390-404.
165. Ng, C.H., et al., *Parkin protects against LRRK2 G2019S mutant-induced dopaminergic neurodegeneration in Drosophila.* J Neurosci, 2009. **29**(36): p. 11257-62.
166. Liu, Z., et al., *A Drosophila model for LRRK2-linked parkinsonism.* Proc Natl Acad Sci U S A, 2008. **105**(7): p. 2693-8.
167. Li, T., et al., *Models for LRRK2-Linked Parkinsonism.* Parkinsons Dis, 2011. **2011**: p. 942412.
168. Hindle, S., et al., *Dopaminergic expression of the Parkinsonian gene LRRK2-G2019S leads to non-autonomous visual neurodegeneration, accelerated by increased neural demands for energy.* Hum Mol Genet. **22**(11): p. 2129-40.
169. Dodson, M.W., et al., *Roles of the Drosophila LRRK2 homolog in Rab7-dependent lysosomal positioning.* Hum Mol Genet. **21**(6): p. 1350-63.
170. Lee, Y., V.L. Dawson, and T.M. Dawson, *Animal models of Parkinson's disease: vertebrate genetics.* Cold Spring Harb Perspect Med. **2**(10).
171. Li, Y., et al., *Mutant LRRK2(R1441G) BAC transgenic mice recapitulate cardinal features of Parkinson's disease.* Nat Neurosci, 2009. **12**(7): p. 826-8.
172. Tong, Y., et al., *R1441C mutation in LRRK2 impairs dopaminergic neurotransmission in mice.* Proc Natl Acad Sci U S A, 2009. **106**(34): p. 14622-7.
173. Melrose, H.L., et al., *Impaired dopaminergic neurotransmission and microtubule-associated protein tau alterations in human LRRK2 transgenic mice.* Neurobiol Dis, 2010. **40**(3): p. 503-17.
174. Winner, B., et al., *Adult neurogenesis and neurite outgrowth are impaired in LRRK2 G2019S mice.* Neurobiol Dis, 2011. **41**(3): p. 706-16.
175. Li, X., et al., *Enhanced striatal dopamine transmission and motor performance with LRRK2 overexpression in mice is eliminated by familial Parkinson's disease mutation G2019S.* J Neurosci, 2010. **30**(5): p. 1788-97.
176. Chen, C.Y., et al., *(G2019S) LRRK2 activates MKK4-JNK pathway and causes degeneration of SN dopaminergic neurons in a transgenic mouse model of PD.* Cell Death Differ, 2012. **19**(10): p. 1623-33.
177. Ramonet, D., et al., *Dopaminergic neuronal loss, reduced neurite complexity and autophagic abnormalities in transgenic mice expressing G2019S mutant LRRK2.* PLoS One, 2011. **6**(4): p. e18568.
178. Ness, D., et al., *Leucine-rich repeat kinase 2 (LRRK2)-deficient rats exhibit renal tubule injury and perturbations in metabolic and immunological homeostasis.* PLoS One. **8**(6): p. e66164.
179. Hinkle, K.M., et al., *LRRK2 knockout mice have an intact dopaminergic system but display alterations in exploratory and motor co-ordination behaviors.* Mol Neurodegener. **7**: p. 25.

180. Andres-Mateos, E., et al., *Unexpected lack of hypersensitivity in LRRK2 knock-out mice to MPTP (1-methyl-4-phenyl-1,2,3,6-tetrahydropyridine).* J Neurosci, 2009. **29**(50): p. 15846-50.
181. Deng, X., et al., *Characterization of a selective inhibitor of the Parkinson's disease kinase LRRK2.* Nat Chem Biol, 2011. **7**(4): p. 203-5.
182. Doggett, E.A., et al., *Phosphorylation of LRRK2 serines 955 and 973 is disrupted by Parkinson's disease mutations and LRRK2 pharmacological inhibition.* J Neurochem, 2012. **120**(1): p. 37-45.
183. Stafa, K., et al., *Functional interaction of Parkinson's disease-associated LRRK2 with members of the dynamin GTPase superfamily.* Hum Mol Genet.
184. Collier, T.J., et al., *Cellular models to study dopaminergic injury responses.* Ann N Y Acad Sci, 2003. **991**: p. 140-51.
185. Hartfield, E.M., et al., *Cellular reprogramming: a new approach to modelling Parkinson's disease.* Biochem Soc Trans. **40**(5): p. 1152-7.
186. Nguyen, H.N., et al., *LRRK2 mutant iPSC-derived DA neurons demonstrate increased susceptibility to oxidative stress.* Cell Stem Cell, 2011. **8**(3): p. 267-80.
187. Sanchez-Danes, A., et al., *Disease-specific phenotypes in dopamine neurons from human iPS-based models of genetic and sporadic Parkinson's disease.* EMBO Mol Med. **4**(5): p. 380-95.
188. Cooper, O., et al., *Pharmacological rescue of mitochondrial deficits in iPSC-derived neural cells from patients with familial Parkinson's disease.* Sci Transl Med, 2012. **4**(141): p. 141ra90.
189. Sanders, L.H., et al., *LRRK2 mutations cause mitochondrial DNA damage in iPSC-derived neural cells from Parkinson's disease patients: reversal by gene correction.* Neurobiol Dis. **62**: p. 381-6.
190. Cherra, S.J., 3rd, et al., *Mutant LRRK2 Elicits Calcium Imbalance and Depletion of Dendritic Mitochondria in Neurons.* Am J Pathol, 2013. **182**(2): p. 474-84.
191. Bravo-San Pedro, J.M., et al., *The LRRK2 G2019S mutant exacerbates basal autophagy through activation of the MEK/ERK pathway.* Cell Mol Life Sci, 2013. **70**(1): p. 121-36.
192. Gomez-Suaga, P., et al., *Leucine-rich repeat kinase 2 regulates autophagy through a calcium-dependent pathway involving NAADP.* Hum Mol Genet, 2012. **21**(3): p. 511-25.
193. Hakimi, M., et al., *Parkinson's disease-linked LRRK2 is expressed in circulating and tissue immune cells and upregulated following recognition of microbial structures.* J Neural Transm, 2011. **118**(5): p. 795-808.
194. Plowey, E.D., et al., *Role of autophagy in G2019S-LRRK2-associated neurite shortening in differentiated SH-SY5Y cells.* J Neurochem, 2008. **105**(3): p. 1048-56.
195. Iaccarino, C., et al., *Apoptotic mechanisms in mutant LRRK2-mediated cell death.* Hum Mol Genet, 2007. **16**(11): p. 1319-26.
196. MacLeod, D., et al., *The familial Parkinsonism gene LRRK2 regulates neurite process morphology.* Neuron, 2006. **52**(4): p. 587-93.
197. Dusonchet, J., et al., *A rat model of progressive nigral neurodegeneration induced by the Parkinson's disease-associated G2019S mutation in LRRK2.* J Neurosci, 2011. **31**(3): p. 907-12.
198. Liu, G.H., et al., *Progressive degeneration of human neural stem cells caused by pathogenic LRRK2.* Nature. **491**(7425): p. 603-7.

199. Cooper, O., et al., *Pharmacological rescue of mitochondrial deficits in iPSC-derived neural cells from patients with familial Parkinson's disease.* Sci Transl Med. **4**(141): p. 141ra90.
200. Nguyen, H.N., et al., *LRRK2 mutant iPSC-derived DA neurons demonstrate increased susceptibility to oxidative stress.* Cell Stem Cell. **8**(3): p. 267-80.
201. Ho, C.C., et al., *The Parkinson disease protein leucine-rich repeat kinase 2 transduces death signals via Fas-associated protein with death domain and caspase-8 in a cellular model of neurodegeneration.* J Neurosci, 2009. **29**(4): p. 1011-6.
202. Bezard, E., et al., *Animal models of Parkinson's disease: limits and relevance to neuroprotection studies.* Mov Disord. **28**(1): p. 61-70.
203. Lin, C.H., et al., *LRRK2 G2019S mutation induces dendrite degeneration through mislocalization and phosphorylation of tau by recruiting autoactivated GSK3ss.* J Neurosci, 2010. **30**(39): p. 13138-49.
204. Meixner, A., et al., *A QUICK screen for Lrrk2 interaction partners--leucine-rich repeat kinase 2 is involved in actin cytoskeleton dynamics.* Mol Cell Proteomics, 2011. **10**(1): p. M110 001172.
205. Paus, M., et al., *Enhanced dendritogenesis and axogenesis in hippocampal neuroblasts of LRRK2 knockout mice.* Brain Res, 2013. **1497**: p. 85-100.
206. Piccoli, G., et al., *LRRK2 controls synaptic vesicle storage and mobilization within the recycling pool.* J Neurosci. **31**(6): p. 2225-37.
207. Lee, S., et al., *The synaptic function of LRRK2.* Biochem Soc Trans. **40**(5): p. 1047-51.
208. Yun, H.J., et al., *LRRK2 phosphorylates Snapin and inhibits interaction of Snapin with SNAP-25.* Exp Mol Med. **45**: p. e36.
209. Yao, C., et al., *LRRK2-mediated neurodegeneration and dysfunction of dopaminergic neurons in a Caenorhabditis elegans model of Parkinson's disease.* Neurobiol Dis, 2010. **40**(1): p. 73-81.
210. Lee, S., et al., *LRRK2 kinase regulates synaptic morphology through distinct substrates at the presynaptic and postsynaptic compartments of the Drosophila neuromuscular junction.* J Neurosci. **30**(50): p. 16959-69.
211. Sakakibara, A., et al., *Microtubule dynamics in neuronal morphogenesis.* Open Biol. **3**(7): p. 130061.
212. Bjorklund, A. and S.B. Dunnett, *Dopamine neuron systems in the brain: an update.* Trends Neurosci, 2007. **30**(5): p. 194-202.
213. Parisiadou, L. and H. Cai, *LRRK2 function on actin and microtubule dynamics in Parkinson disease.* Commun Integr Biol, 2010. **3**(5): p. 396-400.
214. Parisiadou, L., et al., *Phosphorylation of ezrin/radixin/moesin proteins by LRRK2 promotes the rearrangement of actin cytoskeleton in neuronal morphogenesis.* J Neurosci, 2009. **29**(44): p. 13971-80.
215. Lin, X., et al., *Leucine-rich repeat kinase 2 regulates the progression of neuropathology induced by Parkinson's-disease-related mutant alpha-synuclein.* Neuron, 2009. **64**(6): p. 807-27.
216. Rajput, A., et al., *Parkinsonism, Lrrk2 G2019S, and tau neuropathology.* Neurology, 2006. **67**(8): p. 1506-8.
217. Cartelli, D., et al., *Microtubule destabilization is shared by genetic and idiopathic Parkinson's disease patient fibroblasts.* PLoS One, 2012. **7**(5): p. e37467.

218. Wong, E. and A.M. Cuervo, *Autophagy gone awry in neurodegenerative diseases.* Nat Neurosci, 2010. **13**(7): p. 805-11.
219. Belluzzi, E., E. Greggio, and G. Piccoli, *Presynaptic dysfunction in Parkinson's disease: a focus on LRRK2.* Biochem Soc Trans, 2012. **40**(5): p. 1111-6.
220. Takalo, M., et al., *Protein aggregation and degradation mechanisms in neurodegenerative diseases.* Am J Neurodegener Dis, 2013. **2**(1): p. 1-14.
221. Cuervo, A.M., E.S. Wong, and M. Martinez-Vicente, *Protein degradation, aggregation, and misfolding.* Mov Disord, 2010. **25 Suppl 1**: p. S49-54.
222. Olzmann, J.A., L. Li, and L.S. Chin, *Aggresome formation and neurodegenerative diseases: therapeutic implications.* Curr Med Chem, 2008. **15**(1): p. 47-60.
223. Cullen, V., et al., *Acid beta-glucosidase mutants linked to Gaucher disease, Parkinson disease, and Lewy body dementia alter alpha-synuclein processing.* Ann Neurol, 2011. **69**(6): p. 940-53.
224. Mazzulli, J.R., et al., *Gaucher disease glucocerebrosidase and alpha-synuclein form a bidirectional pathogenic loop in synucleinopathies.* Cell, 2011. **146**(1): p. 37-52.
225. Winslow, A.R., et al., *alpha-Synuclein impairs macroautophagy: implications for Parkinson's disease.* J Cell Biol, 2010. **190**(6): p. 1023-37.
226. Kabuta, T., et al., *Aberrant interaction between Parkinson disease-associated mutant UCH-L1 and the lysosomal receptor for chaperone-mediated autophagy.* J Biol Chem, 2008. **283**(35): p. 23731-8.
227. Cuervo, A.M., *Autophagy: in sickness and in health.* Trends Cell Biol, 2004. **14**(2): p. 70-7.
228. Ravikumar, B., et al., *Inhibition of mTOR induces autophagy and reduces toxicity of polyglutamine expansions in fly and mouse models of Huntington disease.* Nat Genet, 2004. **36**(6): p. 585-95.
229. Rubinsztein, D.C., *The roles of intracellular protein-degradation pathways in neurodegeneration.* Nature, 2006. **443**(7113): p. 780-6.
230. Krebiehl, G., et al., *Reduced basal autophagy and impaired mitochondrial dynamics due to loss of Parkinson's disease-associated protein DJ-1.* PLoS One. **5**(2): p. e9367.
231. Thomas, K.J., et al., *DJ-1 acts in parallel to the PINK1/parkin pathway to control mitochondrial function and autophagy.* Hum Mol Genet. **20**(1): p. 40-50.
232. Thomas, K.J., et al., *DJ-1 acts in parallel to the PINK1/parkin pathway to control mitochondrial function and autophagy.* Hum Mol Genet, 2011. **20**(1): p. 40-50.
233. Khatri, N. and H.Y. Man, *Synaptic Activity and Bioenergy Homeostasis: Implications in Brain Trauma and Neurodegenerative Diseases.* Front Neurol, 2013. **4**: p. 199.
234. Niu, J., et al., *Leucine-rich repeat kinase 2 disturbs mitochondrial dynamics via Dynamin-like protein.* J Neurochem, 2012. **122**(3): p. 650-8.
235. Devi, L., et al., *Mitochondrial import and accumulation of alpha-synuclein impair complex I in human dopaminergic neuronal cultures and Parkinson disease brain.* J Biol Chem, 2008. **283**(14): p. 9089-100.
236. Schapira, A.H., *Mitochondrial dysfunction in Parkinson's disease.* Cell Death Differ, 2007. **14**(7): p. 1261-6.

237. Zhang, J., et al., *Parkinson's disease is associated with oxidative damage to cytoplasmic DNA and RNA in substantia nigra neurons.* Am J Pathol, 1999. **154**(5): p. 1423-9.
238. Greenamyre, J.T. and T.G. Hastings, *Biomedicine. Parkinson's--divergent causes, convergent mechanisms.* Science, 2004. **304**(5674): p. 1120-2.
239. Surmeier, D.J., et al., *The role of calcium and mitochondrial oxidant stress in the loss of substantia nigra pars compacta dopaminergic neurons in Parkinson's disease.* Neuroscience, 2011. **198**: p. 221-31.
240. Chan, C.S., T.S. Gertler, and D.J. Surmeier, *Calcium homeostasis, selective vulnerability and Parkinson's disease.* Trends Neurosci, 2009. **32**(5): p. 249-56.
241. Grace, A.A. and B.S. Bunney, *Intracellular and extracellular electrophysiology of nigral dopaminergic neurons--2. Action potential generating mechanisms and morphological correlates.* Neuroscience, 1983. **10**(2): p. 317-31.
242. Chan, C.S., et al., *'Rejuvenation' protects neurons in mouse models of Parkinson's disease.* Nature, 2007. **447**(7148): p. 1081-6.
243. Lloyd-Evans, E. and F.M. Platt, *Lysosomal Ca(2+) homeostasis: role in pathogenesis of lysosomal storage diseases.* Cell Calcium. **50**(2): p. 200-5.
244. Berridge, M.J., *The endoplasmic reticulum: a multifunctional signaling organelle.* Cell Calcium, 2002. **32**(5-6): p. 235-49.
245. Guzman, J.N., et al., *Oxidant stress evoked by pacemaking in dopaminergic neurons is attenuated by DJ-1.* Nature. **468**(7324): p. 696-700.
246. Block, M.L., L. Zecca, and J.S. Hong, *Microglia-mediated neurotoxicity: uncovering the molecular mechanisms.* Nat Rev Neurosci, 2007. **8**(1): p. 57-69.
247. Nakajima, K. and S. Kohsaka, *Microglia: neuroprotective and neurotrophic cells in the central nervous system.* Curr Drug Targets Cardiovasc Haematol Disord, 2004. **4**(1): p. 65-84.
248. Fader, C.M. and M.I. Colombo, *Autophagy and multivesicular bodies: two closely related partners.* Cell Death Differ, 2009. **16**(1): p. 70-8.
249. Levine, B. and G. Kroemer, *Autophagy in the pathogenesis of disease.* Cell, 2008. **132**(1): p. 27-42.
250. Yang, Z. and D.J. Klionsky, *Eaten alive: a history of macroautophagy.* Nat Cell Biol, 2010. **12**(9): p. 814-22.
251. Hara, T., et al., *Suppression of basal autophagy in neural cells causes neurodegenerative disease in mice.* Nature, 2006. **441**(7095): p. 885-9.
252. Komatsu, M., et al., *Loss of autophagy in the central nervous system causes neurodegeneration in mice.* Nature, 2006. **441**(7095): p. 880-4.
253. Singh, R. and A.M. Cuervo, *Autophagy in the cellular energetic balance.* Cell Metab. **13**(5): p. 495-504.
254. Yorimitsu, T. and D.J. Klionsky, *Autophagy: molecular machinery for self-eating.* Cell Death Differ, 2005. **12 Suppl 2**: p. 1542-52.
255. Cuervo, A.M., *Autophagy: many paths to the same end.* Mol Cell Biochem, 2004. **263**(1-2): p. 55-72.
256. Boya, P., F. Reggiori, and P. Codogno, *Emerging regulation and functions of autophagy.* Nat Cell Biol. **15**(7): p. 713-20.
257. Lipinski, M.M., et al., *A genome-wide siRNA screen reveals multiple mTORC1 independent signaling pathways regulating autophagy under normal nutritional conditions.* Dev Cell, 2010. **18**(6): p. 1041-52.
258. Ravikumar, B., et al., *Regulation of mammalian autophagy in physiology and pathophysiology.* Physiol Rev, 2010. **90**(4): p. 1383-435.

259. Girardi, J.P., L. Pereira, and M. Bakovic, *De novo synthesis of phospholipids is coupled with autophagosome formation.* Med Hypotheses. **77**(6): p. 1083-7.
260. Korolchuk, V.I., et al., *Lysosomal positioning coordinates cellular nutrient responses.* Nat Cell Biol, 2011. **13**(4): p. 453-60.
261. Jung, C.H., et al., *ULK-Atg13-FIP200 complexes mediate mTOR signaling to the autophagy machinery.* Mol Biol Cell, 2009. **20**(7): p. 1992-2003.
262. Kim, J., et al., *AMPK and mTOR regulate autophagy through direct phosphorylation of Ulk1.* Nat Cell Biol. **13**(2): p. 132-41.
263. Woods, A., et al., *LKB1 is the upstream kinase in the AMP-activated protein kinase cascade.* Curr Biol, 2003. **13**(22): p. 2004-8.
264. Hawley, S.A., et al., *5'-AMP activates the AMP-activated protein kinase cascade, and Ca2+/calmodulin activates the calmodulin-dependent protein kinase I cascade, via three independent mechanisms.* J Biol Chem, 1995. **270**(45): p. 27186-91.
265. Loffler, A.S., et al., *Ulk1-mediated phosphorylation of AMPK constitutes a negative regulatory feedback loop.* Autophagy. **7**(7): p. 696-706.
266. Egan, D., et al., *The autophagy initiating kinase ULK1 is regulated via opposing phosphorylation by AMPK and mTOR.* Autophagy. **7**(6): p. 643-4.
267. Ghislat, G., et al., *Withdrawal of essential amino acids increases autophagy by a pathway involving Ca2+/calmodulin-dependent kinase kinase-beta (CaMKK-beta).* J Biol Chem. **287**(46): p. 38625-36.
268. Hoyer-Hansen, M., et al., *Control of macroautophagy by calcium, calmodulin-dependent kinase kinase-beta, and Bcl-2.* Mol Cell, 2007. **25**(2): p. 193-205.
269. Ganley, I.G., et al., *Distinct autophagosomal-lysosomal fusion mechanism revealed by thapsigargin-induced autophagy arrest.* Mol Cell. **42**(6): p. 731-43.
270. Williams, A., et al., *Novel targets for Huntington's disease in an mTOR-independent autophagy pathway.* Nat Chem Biol, 2008. **4**(5): p. 295-305.
271. Cardenas, C., et al., *Essential regulation of cell bioenergetics by constitutive InsP3 receptor Ca2+ transfer to mitochondria.* Cell, 2010. **142**(2): p. 270-83.
272. Luzio, J.P., S.R. Gray, and N.A. Bright, *Endosome-lysosome fusion.* Biochem Soc Trans, 2010. **38**(6): p. 1413-6.
273. Mack, H.I., et al., *AMPK-dependent phosphorylation of ULK1 regulates ATG9 localization.* Autophagy. **8**(8): p. 1197-214.
274. Chan, E.Y., *mTORC1 phosphorylates the ULK1-mAtg13-FIP200 autophagy regulatory complex.* Sci Signal, 2009. **2**(84): p. pe51.
275. Backer, J.M., *The regulation and function of Class III PI3Ks: novel roles for Vps34.* Biochem J, 2008. **410**(1): p. 1-17.
276. Di Bartolomeo, S., et al., *The dynamic interaction of AMBRA1 with the dynein motor complex regulates mammalian autophagy.* J Cell Biol, 2010. **191**(1): p. 155-68.
277. Liang, C., et al., *Autophagic and tumour suppressor activity of a novel Beclin1-binding protein UVRAG.* Nat Cell Biol, 2006. **8**(7): p. 688-99.
278. Fimia, G.M., et al., *Ambra1 regulates autophagy and development of the nervous system.* Nature, 2007. **447**(7148): p. 1121-5.
279. Matsunaga, K., et al., *Two Beclin 1-binding proteins, Atg14L and Rubicon, reciprocally regulate autophagy at different stages.* Nat Cell Biol, 2009. **11**(4): p. 385-96.
280. Pattingre, S., et al., *Bcl-2 antiapoptotic proteins inhibit Beclin 1-dependent autophagy.* Cell, 2005. **122**(6): p. 927-39.

281. Mizushima, N., *Autophagy: process and function.* Genes Dev, 2007. **21**(22): p. 2861-73.
282. Yla-Anttila, P., et al., *3D tomography reveals connections between the phagophore and endoplasmic reticulum.* Autophagy, 2009. **5**(8): p. 1180-5.
283. Hayashi-Nishino, M., et al., *A subdomain of the endoplasmic reticulum forms a cradle for autophagosome formation.* Nat Cell Biol, 2009. **11**(12): p. 1433-7.
284. Hailey, D.W., et al., *Mitochondria supply membranes for autophagosome biogenesis during starvation.* Cell. **141**(4): p. 656-67.
285. Hamasaki, M., et al., *Autophagosomes form at ER-mitochondria contact sites.* Nature. **495**(7441): p. 389-93.
286. Ravikumar, B., et al., *Plasma membrane contributes to the formation of pre-autophagosomal structures.* Nat Cell Biol. **12**(8): p. 747-57.
287. Puri, C., et al., *Diverse autophagosome membrane sources coalesce in recycling endosomes.* Cell. **154**(6): p. 1285-99.
288. Guo, Y., et al., *AP1 is essential for generation of autophagosomes from the trans-Golgi network.* J Cell Sci. **125**(Pt 7): p. 1706-15.
289. Ohashi, Y. and S. Munro, *Membrane delivery to the yeast autophagosome from the Golgi-endosomal system.* Mol Biol Cell. **21**(22): p. 3998-4008.
290. Singh, R. and A.M. Cuervo, *Autophagy in the cellular energetic balance.* Cell Metab, 2011. **13**(5): p. 495-504.
291. Gaullier, J.M., et al., *FYVE fingers bind PtdIns(3)P.* Nature, 1998. **394**(6692): p. 432-3.
292. Mizushima, N., et al., *Dissection of autophagosome formation using Apg5-deficient mouse embryonic stem cells.* J Cell Biol, 2001. **152**(4): p. 657-68.
293. Eskelinen, E.L., *New insights into the mechanisms of macroautophagy in mammalian cells.* Int Rev Cell Mol Biol, 2008. **266**: p. 207-47.
294. Jahreiss, L., F.M. Menzies, and D.C. Rubinsztein, *The itinerary of autophagosomes: from peripheral formation to kiss-and-run fusion with lysosomes.* Traffic, 2008. **9**(4): p. 574-87.
295. Mizushima, N., et al., *Autophagy fights disease through cellular self-digestion.* Nature, 2008. **451**(7182): p. 1069-75.
296. Yu, L., et al., *Termination of autophagy and reformation of lysosomes regulated by mTOR.* Nature, 2010. **465**(7300): p. 942-6.
297. Mayor, S. and R.E. Pagano, *Pathways of clathrin-independent endocytosis.* Nat Rev Mol Cell Biol, 2007. **8**(8): p. 603-12.
298. Huotari, J. and A. Helenius, *Endosome maturation.* EMBO J, 2011. **30**(17): p. 3481-500.
299. Doherty, G.J. and H.T. McMahon, *Mechanisms of endocytosis.* Annu Rev Biochem, 2009. **78**: p. 857-902.
300. Hinners, I. and S.A. Tooze, *Changing directions: clathrin-mediated transport between the Golgi and endosomes.* J Cell Sci, 2003. **116**(Pt 5): p. 763-71.
301. Jovic, M., et al., *The early endosome: a busy sorting station for proteins at the crossroads.* Histol Histopathol. **25**(1): p. 99-112.
302. Trischler, M., W. Stoorvogel, and O. Ullrich, *Biochemical analysis of distinct Rab5- and Rab11-positive endosomes along the transferrin pathway.* J Cell Sci, 1999. **112 (Pt 24)**: p. 4773-83.
303. van der Sluijs, P., et al., *The small GTP-binding protein rab4 controls an early sorting event on the endocytic pathway.* Cell, 1992. **70**(5): p. 729-40.

304. Mellman, I., *Endocytosis and molecular sorting.* Annu Rev Cell Dev Biol, 1996. **12**: p. 575-625.
305. Zerial, M. and H. McBride, *Rab proteins as membrane organizers.* Nat Rev Mol Cell Biol, 2001. **2**(2): p. 107-17.
306. Taymans, J.M., *The GTPase function of LRRK2.* Biochem Soc Trans, 2012. **40**(5): p. 1063-9.
307. Bucci, C. and M. Chiariello, *Signal transduction gRABs attention.* Cell Signal, 2006. **18**(1): p. 1-8.
308. Stenmark, H., *Rab GTPases as coordinators of vesicle traffic.* Nat Rev Mol Cell Biol, 2009. **10**(8): p. 513-25.
309. Yamashiro, D.J. and F.R. Maxfield, *Acidification of morphologically distinct endosomes in mutant and wild-type Chinese hamster ovary cells.* J Cell Biol, 1987. **105**(6 Pt 1): p. 2723-33.
310. Knaevelsrud, H. and A. Simonsen, *Lipids in autophagy: constituents, signaling molecules and cargo with relevance to disease.* Biochim Biophys Acta, 2012. **1821**(8): p. 1133-45.
311. van Dam, E.M. and W. Stoorvogel, *Dynamin-dependent transferrin receptor recycling by endosome-derived clathrin-coated vesicles.* Mol Biol Cell, 2002. **13**(1): p. 169-82.
312. Schmidt, M.R. and V. Haucke, *Recycling endosomes in neuronal membrane traffic.* Biol Cell, 2007. **99**(6): p. 333-42.
313. Clague, M.J., et al., *Vacuolar ATPase activity is required for endosomal carrier vesicle formation.* J Biol Chem, 1994. **269**(1): p. 21-4.
314. Mesaki, K., et al., *Fission of tubular endosomes triggers endosomal acidification and movement.* PLoS One, 2011. **6**(5): p. e19764.
315. Hyttinen, J.M., et al., *Maturation of autophagosomes and endosomes: A key role for Rab7.* Biochim Biophys Acta, 2013. **1833**(3): p. 503-10.
316. Dong, J., et al., *The proteasome alpha-subunit XAPC7 interacts specifically with Rab7 and late endosomes.* J Biol Chem, 2004. **279**(20): p. 21334-42.
317. Mizuno, K., A. Kitamura, and T. Sasaki, *Rabring7, a novel Rab7 target protein with a RING finger motif.* Mol Biol Cell, 2003. **14**(9): p. 3741-52.
318. Cantalupo, G., et al., *Rab-interacting lysosomal protein (RILP): the Rab7 effector required for transport to lysosomes.* EMBO J, 2001. **20**(4): p. 683-93.
319. Pankiv, S., et al., *FYCO1 is a Rab7 effector that binds to LC3 and PI3P to mediate microtubule plus end-directed vesicle transport.* J Cell Biol. **188**(2): p. 253-69.
320. Johansson, M., et al., *The oxysterol-binding protein homologue ORP1L interacts with Rab7 and alters functional properties of late endocytic compartments.* Mol Biol Cell, 2005. **16**(12): p. 5480-92.
321. Johansson, M., et al., *Activation of endosomal dynein motors by stepwise assembly of Rab7-RILP-p150Glued, ORP1L, and the receptor betalll spectrin.* J Cell Biol, 2007. **176**(4): p. 459-71.
322. Wang, T., et al., *Rab7: role of its protein interaction cascades in endo-lysosomal traffic.* Cell Signal, 2011. **23**(3): p. 516-21.
323. Rojas, R., et al., *Regulation of retromer recruitment to endosomes by sequential action of Rab5 and Rab7.* J Cell Biol, 2008. **183**(3): p. 513-26.
324. Bonifacino, J.S. and J.H. Hurley, *Retromer.* Curr Opin Cell Biol, 2008. **20**(4): p. 427-36.

325. Seaman, M.N., *The retromer complex - endosomal protein recycling and beyond.* J Cell Sci, 2012. **125**(Pt 20): p. 4693-702.
326. Alvarez-Erviti, L., et al., *Lysosomal dysfunction increases exosome-mediated alpha-synuclein release and transmission.* Neurobiol Dis. **42**(3): p. 360-7.
327. Gaborik, Z. and L. Hunyady, *Intracellular trafficking of hormone receptors.* Trends Endocrinol Metab, 2004. **15**(6): p. 286-93.
328. Sorkin, A. and L.K. Goh, *Endocytosis and intracellular trafficking of ErbBs.* Exp Cell Res, 2009. **315**(4): p. 683-96.
329. Le Roy, C. and J.L. Wrana, *Clathrin- and non-clathrin-mediated endocytic regulation of cell signalling.* Nat Rev Mol Cell Biol, 2005. **6**(2): p. 112-26.
330. Fujita, N., et al., *[Molecular mechanism of autophagosome formation in mammalian cells]*. Tanpakushitsu Kakusan Koso, 2008. **53**(16 Suppl): p. 2106-10.
331. He, P., et al., *High-throughput functional screening for autophagy-related genes and identification of TM9SF1 as an autophagosome-inducing gene.* Autophagy, 2009. **5**(1): p. 52-60.
332. Schroeder, B., et al., *A Dyn2-CIN85 complex mediates degradative traffic of the EGFR by regulation of late endosomal budding.* EMBO J. **29**(18): p. 3039-53.
333. Murphy, J.E., et al., *Endosomes: a legitimate platform for the signaling train.* Proc Natl Acad Sci U S A, 2009. **106**(42): p. 17615-22.
334. Eden, E.R., et al., *The relationship between ER-multivesicular body membrane contacts and the ESCRT machinery.* Biochem Soc Trans, 2012. **40**(2): p. 464-8.
335. Kiviluoto, S., et al., *Regulation of inositol 1,4,5-trisphosphate receptors during endoplasmic reticulum stress.* Biochim Biophys Acta. **1833**(7): p. 1612-24.
336. Lanner, J.T., et al., *Ryanodine receptors: structure, expression, molecular details, and function in calcium release.* Cold Spring Harb Perspect Biol. **2**(11): p. a003996.
337. Marchi, S., S. Patergnani, and P. Pinton, *The endoplasmic reticulum-mitochondria connection: One touch, multiple functions.* Biochim Biophys Acta. **1837**(4): p. 461-469.
338. Patel, S. and R. Docampo, *Acidic calcium stores open for business: expanding the potential for intracellular Ca2+ signaling.* Trends Cell Biol, 2010. **20**(5): p. 277-86.
339. Gerasimenko, J.V., et al., *Calcium uptake via endocytosis with rapid release from acidifying endosomes.* Curr Biol, 1998. **8**(24): p. 1335-8.
340. Miyawaki, A., et al., *Fluorescent indicators for Ca2+ based on green fluorescent proteins and calmodulin.* Nature, 1997. **388**(6645): p. 882-7.
341. Pryor, P.R., et al., *The role of intraorganellar Ca(2+) in late endosome-lysosome heterotypic fusion and in the reformation of lysosomes from hybrid organelles.* J Cell Biol, 2000. **149**(5): p. 1053-62.
342. Fernandez-Chacon, R., et al., *Synaptotagmin I functions as a calcium regulator of release probability.* Nature, 2001. **410**(6824): p. 41-9.
343. Lloyd-Evans, E., et al., *Niemann-Pick disease type C1 is a sphingosine storage disease that causes deregulation of lysosomal calcium.* Nat Med, 2008. **14**(11): p. 1247-55.
344. Hay, J.C., *Calcium: a fundamental regulator of intracellular membrane fusion?* EMBO Rep, 2007. **8**(3): p. 236-40.

345. Pinton, P., T. Pozzan, and R. Rizzuto, *The Golgi apparatus is an inositol 1,4,5-trisphosphate-sensitive Ca2+ store, with functional properties distinct from those of the endoplasmic reticulum.* EMBO J, 1998. **17**(18): p. 5298-308.
346. Mahapatra, N.R., et al., *A dynamic pool of calcium in catecholamine storage vesicles. Exploration in living cells by a novel vesicle-targeted chromogranin A-aequorin chimeric photoprotein.* J Biol Chem, 2004. **279**(49): p. 51107-21.
347. Mitchell, K.J., et al., *Dense core secretory vesicles revealed as a dynamic Ca(2+) store in neuroendocrine cells with a vesicle-associated membrane protein aequorin chimaera.* J Cell Biol, 2001. **155**(1): p. 41-51.
348. Gerasimenko, J.V., et al., *Pancreatic protease activation by alcohol metabolite depends on Ca2+ release via acid store IP3 receptors.* Proc Natl Acad Sci U S A, 2009. **106**(26): p. 10758-63.
349. Morgan, A.J. and A. Galione, *NAADP induces pH changes in the lumen of acidic Ca2+ stores.* Biochem J, 2007. **402**(2): p. 301-10.
350. Calcraft, P.J., et al., *NAADP mobilizes calcium from acidic organelles through two-pore channels.* Nature, 2009. **459**(7246): p. 596-600.
351. Patel, S., G.C. Churchill, and A. Galione, *Coordination of Ca2+ signalling by NAADP.* Trends Biochem Sci, 2001. **26**(8): p. 482-9.
352. Cheng, X., et al., *Mucolipins: Intracellular TRPML1-3 channels.* FEBS Lett, 2010. **584**(10): p. 2013-21.
353. Zhang, F., et al., *TRP-ML1 functions as a lysosomal NAADP-sensitive Ca2+ release channel in coronary arterial myocytes.* J Cell Mol Med, 2009. **13**(9B): p. 3174-85.
354. Morgan, A.J., et al., *Molecular mechanisms of endolysosomal Ca2+ signalling in health and disease.* Biochem J, 2011. **439**(3): p. 349-74.
355. Feng, X., et al., *Drosophila TRPML Forms PI(3,5)P2-activated Cation Channels in Both Endolysosomes and Plasma Membrane.* J Biol Chem. **289**(7): p. 4262-72.
356. Yamaguchi, S., et al., *Transient receptor potential mucolipin 1 (TRPML1) and two-pore channels are functionally independent organellar ion channels.* J Biol Chem, 2011. **286**(26): p. 22934-42.
357. Cang, C., et al., *mTOR regulates lysosomal ATP-sensitive two-pore Na(+) channels to adapt to metabolic state.* Cell. **152**(4): p. 778-90.
358. Wang, X., et al., *TPC proteins are phosphoinositide- activated sodium-selective ion channels in endosomes and lysosomes.* Cell. **151**(2): p. 372-83.
359. Jha, A., et al., *Convergent regulation of the lysosomal two-pore channel-2 by Mg2+, NAADP, PI(3,5)P2 and multiple protein kinases.* EMBO J. **33**(5): p. 501-11.
360. Patel, S. and E. Brailoiu, *Triggering of Ca2+ signals by NAADP-gated two-pore channels: a role for membrane contact sites?* Biochem Soc Trans, 2012. **40**(1): p. 153-7.
361. Hooper, R. and S. Patel, *NAADP on target.* Adv Exp Med Biol. **740**: p. 325-47.
362. Brailoiu, E., et al., *An NAADP-gated two-pore channel targeted to the plasma membrane uncouples triggering from amplifying Ca2+ signals.* J Biol Chem. **285**(49): p. 38511-6.
363. Naylor, E., et al., *Identification of a chemical probe for NAADP by virtual screening.* Nat Chem Biol, 2009. **5**(4): p. 220-6.

364. Berg, T.O., et al., *Use of glycyl-L-phenylalanine 2-naphthylamide, a lysosome-disrupting cathepsin C substrate, to distinguish between lysosomes and prelysosomal endocytic vacuoles.* Biochem J, 1994. **300 (Pt 1)**: p. 229-36.
365. Bowman, E.J., A. Siebers, and K. Altendorf, *Bafilomycins: a class of inhibitors of membrane ATPases from microorganisms, animal cells, and plant cells.* Proc Natl Acad Sci U S A, 1988. **85**(21): p. 7972-6.
366. Zhu, M.X., et al., *Calcium signaling via two-pore channels: local or global, that is the question.* Am J Physiol Cell Physiol. **298**(3): p. C430-41.
367. Patel, S., et al., *The endo-lysosomal system as an NAADP-sensitive acidic Ca(2+) store: role for the two-pore channels.* Cell Calcium. **50**(2): p. 157-67.
368. Pereira, G.J., et al., *Nicotinic acid adenine dinucleotide phosphate (NAADP) regulates autophagy in cultured astrocytes.* J Biol Chem, 2011. **286**(32): p. 27875-81.
369. Fdez, E., et al., *Transmembrane-domain determinants for SNARE-mediated membrane fusion.* J Cell Sci. **123**(Pt 14): p. 2473-80.
370. Madden, E.A. and B. Storrie, *Effect of acidotropic amines on the accumulation of newly synthesized membrane and luminal proteins in Chinese-hamster ovary (CHO) cell lysosomes.* Biochem J, 1989. **258**(3): p. 843-51.
371. Sigoillot, F.D., et al., *A time-series method for automated measurement of changes in mitotic and interphase duration from time-lapse movies.* PLoS One. **6**(9): p. e25511.
372. Spano, S., X. Liu, and J.E. Galan, *Proteolytic targeting of Rab29 by an effector protein distinguishes the intracellular compartments of human-adapted and broad-host Salmonella.* Proc Natl Acad Sci U S A. **108**(45): p. 18418-23.
373. Barr, F. and D.G. Lambright, *Rab GEFs and GAPs.* Curr Opin Cell Biol. **22**(4): p. 461-70.
374. Mizuno-Yamasaki, E., F. Rivera-Molina, and P. Novick, *GTPase networks in membrane traffic.* Annu Rev Biochem. **81**: p. 637-59.
375. Zhang, X.M., et al., *TBC domain family, member 15 is a novel mammalian Rab GTPase-activating protein with substrate preference for Rab7.* Biochem Biophys Res Commun, 2005. **335**(1): p. 154-61.
376. Peralta, E.R., B.C. Martin, and A.L. Edinger, *Differential effects of TBC1D15 and mammalian Vps39 on Rab7 activation state, lysosomal morphology, and growth factor dependence.* J Biol Chem. **285**(22): p. 16814-21.
377. Jordens, I., et al., *The Rab7 effector protein RILP controls lysosomal transport by inducing the recruitment of dynein-dynactin motors.* Curr Biol, 2001. **11**(21): p. 1680-5.
378. Behrends, C., et al., *Network organization of the human autophagy system.* Nature. **466**(7302): p. 68-76.
379. Alers, S., et al., *Role of AMPK-mTOR-Ulk1/2 in the regulation of autophagy: cross talk, shortcuts, and feedbacks.* Mol Cell Biol. **32**(1): p. 2-11.
380. Powis, G., et al., *Wortmannin, a potent and selective inhibitor of phosphatidylinositol-3-kinase.* Cancer Res, 1994. **54**(9): p. 2419-23.
381. Wu, Y.T., et al., *Dual role of 3-methyladenine in modulation of autophagy via different temporal patterns of inhibition on class I and III phosphoinositide 3-kinase.* J Biol Chem. **285**(14): p. 10850-61.
382. Vergne, I. and V. Deretic, *The role of PI3P phosphatases in the regulation of autophagy.* FEBS Lett. **584**(7): p. 1313-8.

383. Zhang, L., et al., *Small molecule regulators of autophagy identified by an image-based high-throughput screen.* Proc Natl Acad Sci U S A, 2007. **104**(48): p. 19023-8.
384. Zhou, X., et al., *Deletion of PIK3C3/Vps34 in sensory neurons causes rapid neurodegeneration by disrupting the endosomal but not the autophagic pathway.* Proc Natl Acad Sci U S A. **107**(20): p. 9424-9.
385. Chu, C.T., J. Zhu, and R. Dagda, *Beclin 1-independent pathway of damage-induced mitophagy and autophagic stress: implications for neurodegeneration and cell death.* Autophagy, 2007. **3**(6): p. 663-6.
386. Dall'Armi, C., K.A. Devereaux, and G. Di Paolo, *The role of lipids in the control of autophagy.* Curr Biol. **23**(1): p. R33-45.
387. Carling, D., *The AMP-activated protein kinase cascade--a unifying system for energy control.* Trends Biochem Sci, 2004. **29**(1): p. 18-24.
388. Guse, A.H. and H.C. Lee, *NAADP: a universal Ca2+ trigger.* Sci Signal, 2008. **1**(44): p. re10.
389. Lin-Moshier, Y., et al., *Photoaffinity labeling of nicotinic acid adenine dinucleotide phosphate (NAADP) targets in mammalian cells.* J Biol Chem. **287**(4): p. 2296-307.
390. Korolchuk, V.I., F.M. Menzies, and D.C. Rubinsztein, *Mechanisms of cross-talk between the ubiquitin-proteasome and autophagy-lysosome systems.* FEBS Lett. **584**(7): p. 1393-8.
391. Rubinsztein, D.C., P. Codogno, and B. Levine, *Autophagy modulation as a potential therapeutic target for diverse diseases.* Nat Rev Drug Discov. **11**(9): p. 709-30.
392. Li, J., S.G. Kim, and J. Blenis, *Rapamycin: One Drug, Many Effects.* Cell Metab. **19**(3): p. 373-379.
393. Haebig, K., et al., *ARHGEF7 (Beta-PIX) acts as guanine nucleotide exchange factor for leucine-rich repeat kinase 2.* PLoS One. **5**(10): p. e13762.
394. Seaman, M.N., et al., *Membrane recruitment of the cargo-selective retromer subcomplex is catalysed by the small GTPase Rab7 and inhibited by the Rab-GAP TBC1D5.* J Cell Sci, 2009. **122**(Pt 14): p. 2371-82.
395. Beilina, A., et al., *Unbiased screen for interactors of leucine-rich repeat kinase 2 supports a common pathway for sporadic and familial Parkinson disease.* Proc Natl Acad Sci U S A. **111**(7): p. 2626-31.

X. List of Papers

1. Leucine-rich repeat kinase 2 regulates autophagy through a calcium-dependent pathway involving NAADP.

Gómez-Suaga P, Luzón-Toro B, Churamani D, Zhang L, Bloor-Young D, Patel S, Woodman PG, Churchill GC, Hilfiker S.

Hum Mol Genet. 2012 Feb 1;21(3):511-25

Factor de Impacto: 7.692 Quartil: Q1

2. LRRK2 as a modulator of lysosomal calcium homeostasis with downstream effects on autophagy.

Gómez-Suaga P, Hilfiker S.

Autophagy. 2012 Apr;8(4):692-3.

Factor de Impacto:12.042 Quartil: Q1

3. A link between LRRK2, autophagy and NAADP-mediated endolysosomal calcium signalling.

Gómez-Suaga P, Churchill GC, Patel S, Hilfiker S.

Biochem Soc Trans. 2012 Oct;40(5):1140-6.

Factor de Impacto: 2.587 Quartil: Q2

4. A Link between Autophagy and the Pathophysiology of LRRK2 in Parkinson's Disease.

Gómez-Suaga P, Fdez E, Blanca Ramírez M, Hilfiker S.

Parkinsons Dis. 2012;2012:324521

Revista de nueva edición, factor de impacto por determinar.

5. Pathogenic LRRK2 modulates degradative receptor trafficking by regulation of late endosomal budding (en preparación).

Gómez-Suaga P, el al.